MECHANISM OF ACTION STUDIES ON

NEW LIGANDS FOR SOLUBLE GUANYLATE CYCLASE.

by

Patricia Alonso Fernandez

A thesis submitted for the degree of

Doctor of Philosophy

at the

UNIVERSITY OF LONDON

Supervised by

Dr. David. L. Selwood and Dr. David. J. Madge

Department of Medicinal Chemistry   December 2001

Wolfson Institute for Biomedical Research

University College London

ProQuest Number: U643190

All rights reserved

INFORMATION TO ALL USERS
The quality of this reproduction is dependent upon the quality of the copy submitted.

In the unlikely event that the author did not send a complete manuscript
and there are missing pages, these will be noted. Also, if material had to be removed,
a note will indicate the deletion.
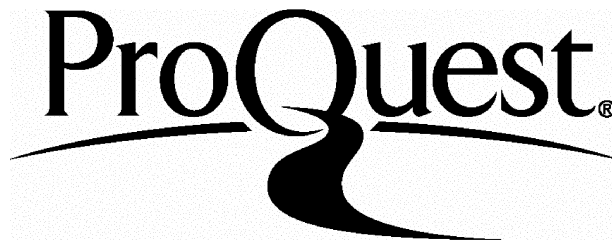
ProQuest U643190

Published by ProQuest LLC(2016). Copyright of the Dissertation is held by the Author.

ProQuest LLC
789 East Eisenhower Parkway
P.O. Box 1346
Ann Arbor, MI 48106-1346

To my parents and my grandmother

"Begin at the beginning," the king said gravely, "and go on till you come to the end: then stop."

Lewis Carroll, *Alice's adventures in Wonderland*

Abstract

This thesis will comprise two topics.

The first part relates to the application of photoaffinity labelling to soluble guanylate cyclase (sGC), which belongs to a family of enzymes that catalyse the conversion of guanosine-5'-triphosphate (GTP) to cyclic guanosine-3', 5'-monophosphate (cGMP). By formation of the intracellular signalling molecule cGMP, sGC plays a key role in smooth muscle relaxation and inhibition of platelet aggregation and in many signal transduction pathways. Although there are two types of activators of sGC, NO-dependent (nitrovasodilators such as sodium nitroprusside, DEANO, etc.) and NO-independent (YC-1, 1-benzyl-3-5'-hydroxymethyl-2'-furyl indazole), the mechanism of action of only the former is understood. This thesis describes an attempt to locate residues that make up the binding sites for these activators. This comprises the design, synthesis and biological evaluation of small molecule activators, and their photolabeled analogues, followed by photoaffinity labelling experiments using tryptic digestion and mass spectroscopy (MALDI) for the identification of peptide fragments covalently bonded to activator analogue.

The second part involves the investigation of a traceless linker designed for use in the solid phase synthesis of sGC modulators. The resulting method could also be applied in the synthesis of a variety of biologically active molecules. We wanted to design a linker which would combine the advantages of a traceless and a "safety-catch" linker. Therefore we investigated the application of a benzoisothiazol-based linker as this heterocycle is stable until activated by oxidation of the sulphur atom, allowing facile cleavage in the last step of the synthesis.

Acknowledgements

My heart-felt thanks goes to my supervisors David L. Selwood and David J. Madge for their invaluable help, support, patience, teaching and understanding. Without their help this work could not have been possible.

Thanks to everybody involved in sGC project. I would like to also thank to the medicinal chemistry group (past and present) especially, Marcel, Grant, Briggitte, Cristina, Basil and Chi-Kit ("cheeky" in another words).
Thanks to Mushtaq and Shaheda, for their prayers.

Many thanks to the different labs I passed through in the Wolfson Institute, in the Rayne Institute, and the UCL NMR, MS and microanalysis group.

Thanks again to David, David, and Bakhtiar for their help in making corrections and comments, any mistakes that remain belong solely to me.

Thanks to my family, my flatmates and friends near and far for coping with "the monk" for these past few months. To my friend and sister, Angeles for making me laugh and for her support. Thanks to all those that during all these years in one way or another helped to make this possible.

Special thanks to Bakhtiar for his excellent "paperwork".

This work was been funded by the Wolfson Institute for Biomedical Research, to whom I am very grateful.

Abbreviations

9-BBN	9-borabicyclo[3.3.1]nonane
AC	Adenylate cyclase
AET	2-aminoethylisothiouronium bromide
AIBN	azobisisobutyronitrile
APCI	Atmospheric pressure chemical ionization
BBP	bifunctional photoaffinity probe
Boc	*tert*-butyloxycarbonyl
BP	benzophenone
CC	combinatorial chemistry
cGMP	Cyclic guanosine-3',5'-monophosphate
COSY	Correlation spectroscopy
DBU	1,8-diazabicyclo[5.4.0]undec-7-ene
DCM	Dichloromethane
DEA/NO	1-(*N*,*N*-diethylamino)diazen-1-ium-1,2-diolate
DEAD	Diethyl azodicarboxylate
DIC	1,3-diisopropylcarbodiimide
DIPEA	*N*,*N*-diisopropylethylamine
DMAP	4-(*N*,*N*-dimethylamino)pyridine
DMF	*N*,*N*-dimethylformamide
dppf	1,1'-bis(diphenylphosphino)ferrocene
dppp	1,3-bis(diphenylphosphino)propane
DTT	dithiotheitol
EDC	1-ethyl-3-(3-(dimethylaminopropyl)carbodiimide
EDRF	Endothelium derived relaxation factor
EDTA	ethylenediaminetetraacetic acid
EI	Electron impact
ELISA	Enzyme-linked immunoabsorbent assay
FAB	Fast atom bombardment
Fmoc	9-fluorenylmethyloxycarbonyl
GTN	Nitroglycerin
GTP	Guanosine-5'-triphosphate

HATU	N-[(dimethylamino)-1H-1,2,3-triazolo[4,5b]pyridin-1-ylmethylene]-N-methylmethanaminium
HMBC	Heteronuclear Multiple Bond Correlation
HMQC	Heteronuclear Multiple-Quantum Coherence
HOBT	1-hydroxybenzotriazole
HOSA	Hydroxylamine-*O*-sulfonic acid
HPLC	High performance liquid chromatography
IBMX	3-isobutyl-1-methylxanthine
IBMX	3-isobutyl-1-methylxanthine
LFA-1	Lymphocyte function-associated antigen-1
MALDI	Matrix-assisted laser desorption/ionization
m-CPBA	3-chloroperoxybenzoic acid
MOM	methoxymethyl
MTS	2,4,6-trimethylbenzenesulfonyl or mesitylenesulfonyl
NBS	N-bromosuccinimide
NMP	*N*-methylpyrrolidone
NMR	nuclear magnetic resonance
NOE	nuclear Overhauser effect
NOESY	nuclear overhauser effect spectroscopy
ODQ	[1,2,4]oxadiazolo[4,3-a]quinoxalin-1-one
PAL	Photoaffinity labelling
PEG	Poly(ethylene glycol)
PPi	Pyrophosphate
PPIX	Protoporphyrin IX
PS	polystyrene
p-TSA	*p*-toluene sulfonic acid
REM	Regenerated resin and Michael addition
SAR	Structure activity relationship
SDS-PAGE	Sodium dodecyl sulphate polyacrylamide gel
sGC	Soluble guanylate cyclase
SIN-1	3-morpholino sydnomine hydrochloride
SPOS	solid phase organic synthesis
TBAF	*tetra*-n-butylammonium fluoride

TEA	Triethylamine
TEMED	*N,N,N',N'*-tetramethylethylenediamine
TFA	trifluoroacetic acid
TFPA	tetrafluorophthalic anhydride
THF	tetrahydrofuran
THP	tetrahydropyranyl
TMAD	*N,N,N'N'*-tetramethylazodicarboxamide
TOF	Time of flight
TPD	3-trifluoromethyl-3-phenyldiazirine
TPP	triphenylphosphine
YC-1	[5-(1-benzyl-1H-indazol-3-yl)-furyl]methanol

Contents

CHAPTER 1
REVIEW
Traceless Linkers

CHAPTER 2
Application of photoaffinity labelling to soluble guanylate cyclase

CHAPTER 3

Investigation on a benzoisothiazol derivative as apossible traceless linker

CHAPTER 4
EXPERIMENTAL

CHAPTER ONE

REVIEW

Traceless linkers

1.1 Introduction

Since Woehler's urea synthesis in the early 19th century, organic chemistry has became an art dedicated to the design and synthesis of compounds with a wide spectrum of applications. With the advent of the 21st century and the advancement of technology, this art has now taken the form of combinatorial chemistry (CC).

The origin of this elegant discipline is associated with Merrifield's pioneering work in solid phase peptide synthesis in the early 1960s. However, it was not until the last decade that attention became focused in this area of research. The discovery of novel biological targets, the development of new assays and high throughput screening (HTS) technologies have lead to a greater demand for the production of a large number of small molecules. This demand was the impetus behind the renewed interest in this field.

Combinatorial chemistry is based on parallel synthesis, in which a large number of chemical compounds can be generated within a short period of time.[1] Many groups have explored high-speed chemistry, both of mixtures and of single compounds, for biological applications such as drug discovery, or receptor-ligand studies. CC has several different uses such as, finding a lead compound with the desired properties or improving potency by analogue synthesis. CC also provides a way of rapidly exploring structure-activity relationships (SAR) to understand how the lead compound works. Thus, it is not surprising that this field has captivated both the attention and the imagination of chemists.

This field involves a variety of chemical techniques, whether in solution or on solid phase. Although both approaches offer distinct advantages, the latter is the most common method employed for the synthesis of combinatorial libraries. This is due to the benefit of being able to drive reactions to completion by using excess quantities of reagents, and then simply washing them away at the end. Finally, the easy purification of intermediates makes solid-supported strategy an attractive alternative.

Many factors have to be considered in the design of a solid phase organic synthesis (SPOS) library. Crucial decisions include the correct choice of the solid support, mode of attachment and cleavage of products from the matrix.

The solid support is generally a resin, an insoluble polymer that swells in the presence of the reaction solvent but which is inert to the reaction conditions. Resin types, and other important parameters, such as their loading and bead size fall outside the scope of this review.

The mode of connection and cleavage of small molecules from the resin depends on the adequate selection of the linker group. It tethers the compound being synthesized to the solid phase support and must survive the desired synthetic transformations without degradation. Thus, the linker group is a key component in any successful synthetic strategy on solid phase. Ideally, the linker should be stable to all reactions used in a synthesis sequence and should be cleaved quantitatively under conditions that do not degrade the desired target molecule.

Linkers are usually bifunctional spacer molecules which contain on one end an anchoring group for attachment to the solid support and on the other end a functional group used for the subsequent chemical transformations and cleavage procedures.[2] Traditionally, linkers are derived from protecting groups linked to the solid support, therefore, after cleavage, the final products contain a residual polar functional group, typically an acid or amide, which in many cases is not desirable as these vary the activity of the lead compounds. The need for more versatile linkers and cleavage strategies has led to the development of the elegant concept of traceless linkers. These are linkers which, after cleavage, afford the final molecules with no trace of the point of linkage to the solid phase as it has usually been replaced by an aliphatic or aromatic hydrogen. Thus, no element of the linker remains in the final products.

The literature commonly refers to such linkers as those which leave no memory of the immobilization in the final compounds. This definition can lead to confusion and, as Brase pointed out,[3] the immobilization influences the chemical properties of the attached molecule by mesomeric and inductive effects of the anchoring group.

The large number of publications on SPOS over the past decade shows the increase of interest in this area of chemistry. These include specialized reviews on different types of linkers.[4,5,6]

This review is intended to show a summary of the traceless linkers reported to date. The classification is based on the reaction conditions that lead to cleavage and is displayed in alphabetic order.

1.2 Cleavage conditions

1.2.1 Acidic cleavage

1.2.2 Basic cleavage

1.2.3 Cyclization as a means of linker removal

1.2.4 Deboronization as a strategy for linker removal

1.2.5 Oxidation conditions

1.2.6 Photolytic cleavage

1.2.7 Reductive cleavage

1.2.8 Thermolytic cleavage

A desired characteristic for the cleavage conditions is that they must not affect the final product functionality.

1.2.1 Acidic cleavage

Cleavage of the linker under acidic conditions is a common method used in solid-phase synthesis and many examples involving the cleavage of a traceless linker (particularly attached to an aromatic ring) in acid media can be found in the literature.

The strength of the acid required to induce cleavage is related to the electron donor substituents on the aromatic system that stabilizes the transient resin-bound cation. The mesomeric effect of the electron donor groups results in an increase in the resonance stabilization, enabling use of milder acidic conditions for cleavage.

Due to the large number of publications on silyl-based traceless linkers, and since the protodesilation requires in most of the cases acidic treatment in the cleavage step, we include a subdivision in this section that deals with silicon linkers.

- **Desilylation**

Ellman and coworkers reported one of the first traceless linkers for arenes. Their earliest publications described the synthesis of a library of 1,4-benzodiazepines using a silicon-based linker.[7] This work expanded the possibilities of solid phase synthesis, which until then was limited to peptides. The impact on the scope of combinatorial chemistry was immense. Since then a large number of small molecules and diverse drug-like structures have been synthesized by solid phase synthesis.

Improvements in the synthesis of benzodiazepines have been carried out by the same group and it was in 1997 when the authors published their investigations on a traceless linker based not just on silicon and but also on germanium linking strategies.[8]

The main difference between the two strategies is primarily in the cleavage conditions. On account of the electron-poor nature of the protonated benzodiazepine, the silicon-aryl bond remains stable to TFA and requires HF for the cleavage. These strong conditions give silylated benzodiazepines as side products and also affect certain functional groups in the final products. These problems however, are avoided by using the germanium-based linker, which lead to pure compounds after cleavage using neat TFA. Thus, due to the milder conditions required for the cleavage, germanium-containing linkers constitute a better choice versus the silyl-containing one as a wider range of functional groups are tolerated

in the cleavage. Scheme 1 illustrates the sequence of reactions that led to benzodiazepine derivatives using Ellman's metal-based linker strategies. The synthesis began with a Stille coupling reaction of resin-bound stannane **1** with both aromatic and aliphatic acid chlorides to give support-bound adduct **2**. Removal of the corresponding protecting group gives 2-aminoaryl ketones **3**. Acylation with an α-*N*-Fmoc-amino acid fluoride, and removal of the Fmoc group, affords intermediate **4**, which is cyclized in acidic media forming adduct **5**. Support-bound benzodiazepine derivative **6** is reached after deprotonation and alkylation, introducing in this way different substitutes. Finally, **6** undergoes cleavage reaction under acidic conditions to give the benzodiazepine derivative **7**. As mentioned above, while cleavage of the germanium linker takes place by using either TFA or an electrophile, such as Br_2, the silyl linker needs anhydrous HF for the cleavage.

a: M = Si, P= ((2-(4-biphenyl)isopropyl) oxy) carbonyl (Bpoc)

b: M = Ge, P= (2-(4-methylphenyl)isopropyl)carbamate (Mpc)

n=2 M=Si
n=3 M=Ge
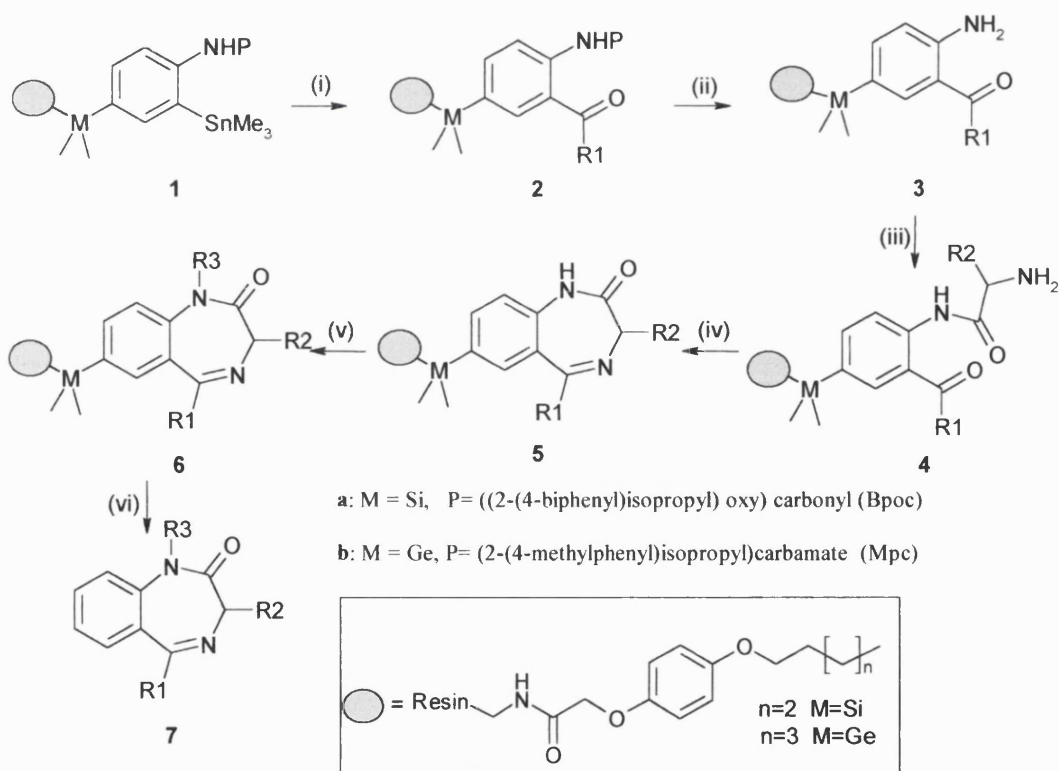
Scheme 1. (i) Acid chloride, Pd_2dba_3, $CHCl_3$, (ii) **2a**: 3% CF_3COOH, **2b**: B-chlorocatechol-borane, (iii) FMOC amino acid fluoride, 20% piperidine/DMF, (iv) 5% AcOH, 65°C, (v) lithiated oxazolidinone, R3-X, (vi) **6a**: 1. $TFA/Me_2S/H_2O$, 2. HF (anhy.), **6b**: TFA, or Br_2.

Structures **7a** and **7b** are two examples of benzodiazepine derivatives obtained using the silyl and germanium linkers respectively.

7a   **7b**
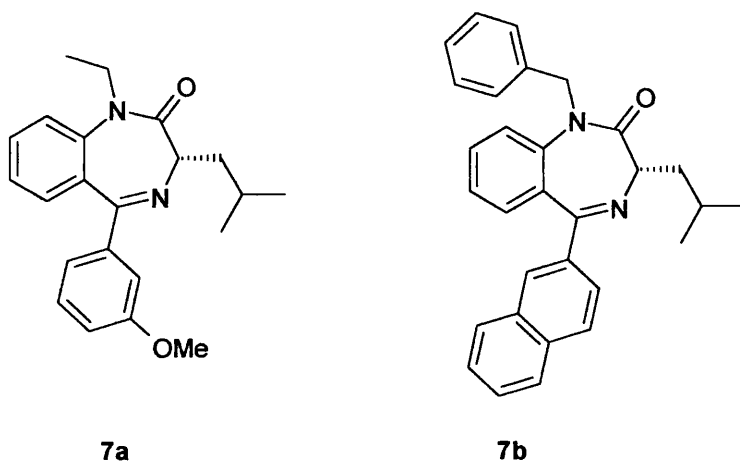
Ellman and coworkers have also published the synthesis of pyridine-based tricyclics using a silicon-based linker in which the silyl group joins to the support through a stable aliphatic tether **8** (Scheme 2).[9] This faciliates the direct loading of aromatic compounds to the support and enables the cleavage of the silyl group only from the aromatic compound.

The method starts with formation of resin-bound pyridine **9**, by reaction of the linker **8** with N-Boc-3-amino-2-chloropyridine. Then next step introduces the first point of diversity into the molecules by addition of 2-azidobenzoyl chlorides to give the amide products. The amide is alkylated, inserting the second element of diversity. Reduction of the azide affords the 2-chlorooxazolidine intermediate, subsequent treatment with acid forms the pyridine-based tricyclic. This is subjected to alkylation or acylation introducing the final element of diversity. Finally, treatment with Bu$_4$NF cleaves the final tricyclics **10** from the support. Compound **11** is an interesting example of molecules obtained by this route, which contains the key piperazine pharmacophore of pirenzepine.
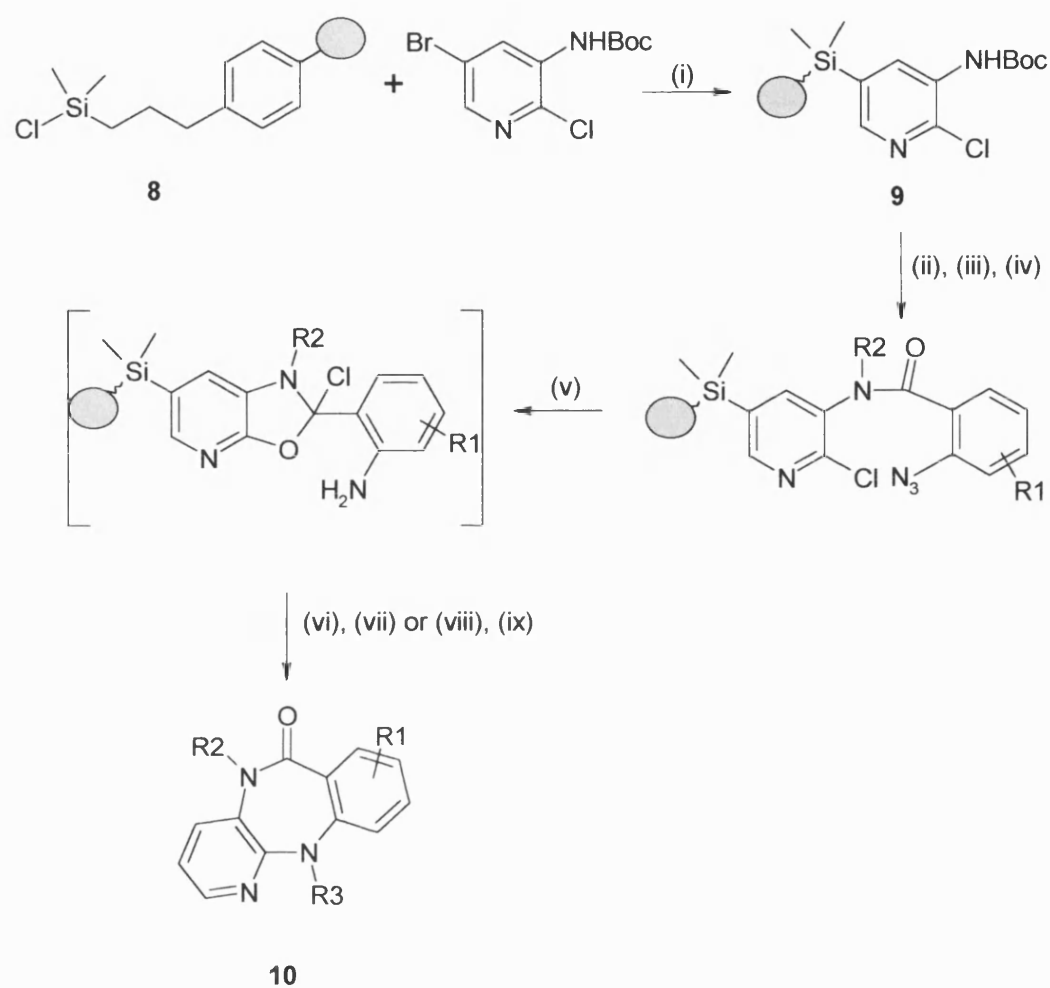
Scheme 2. (i) KH in THF, then *tert*-BuLi, (ii) 85% TFA in CH$_2$Cl$_2$, (iii) substituted 2-azidobenzoyl chloride, CH$_2$Cl$_2$/Py (9:1), (iv) lithiated acetanilide in THF, R2X, (v) SnCl$_2$/PhSH/Et$_3$N (1:4:5) in CH$_2$Cl$_2$, (vi) DMF/TFA/H$_2$O (7:2:1), (vii) lithiated N-*tert*-butylbenzamide in THF, then R3X or (RCO)$_2$O, (viii) chloroacetyl chloride, Et$_3$N in dioxane, then N-methylpyrazine, CH$_2$Cl$_2$, (ix) Bu$_4$NF, THF.
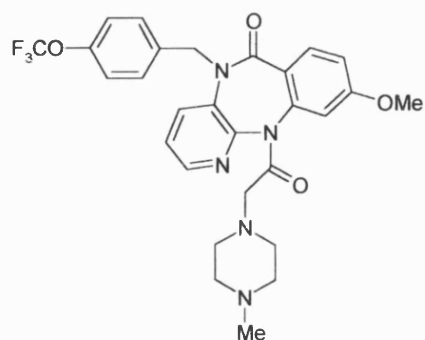
11

Veber *et al* also carried out pioneering work in the investigation of a traceless linker for arenes.[10] As shown in Scheme 3 the silicon-aryl bond in **12** is cleaved with TFA at 25°C, the presence of the oxygen enables mild acidic conditions to provide the substituted arenes **13**.
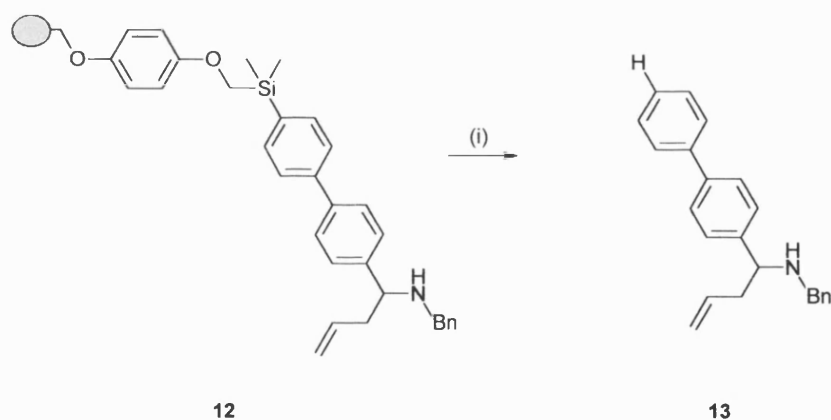
12   **13**

Scheme 3. (i) TFA, 25°C

In 1996, Boehm and Showalter reported the synthesis of a series of benzofurans using a silyl ether linker.[11] This linker has shown itself to be stable in a variety of reaction conditions as shown in Scheme 4.
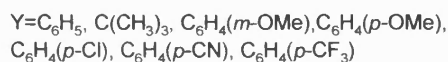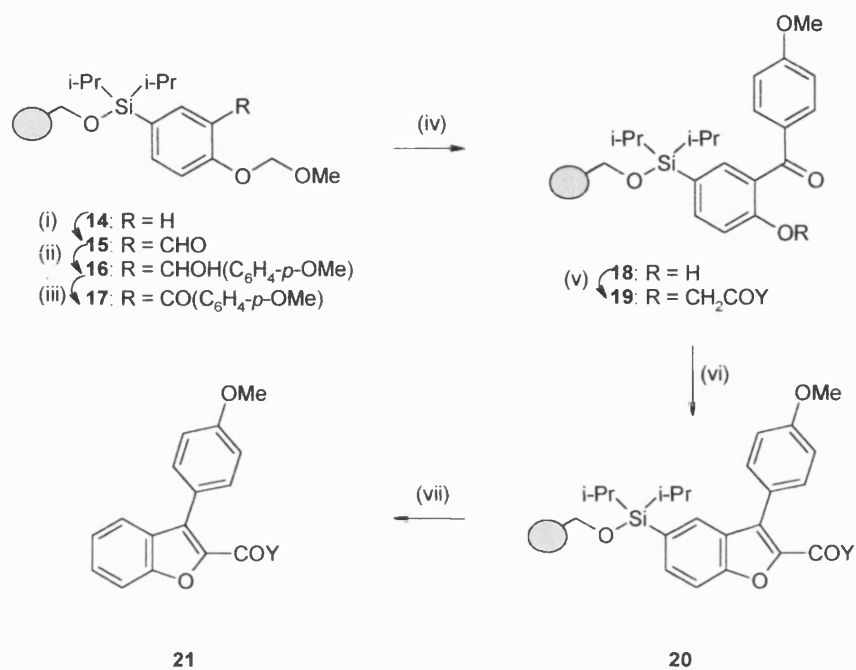
Scheme 4. (i) 1. *n*-BuLi, TMEDA, Et$_2$O, 0°C, 2. anhydrous DMF, 0°C, (ii) 4-bromoanisole, *n*-BuLi, THF, -78°C, (iii) 1-hydroxy-1,2-benziodoxol-3(1*H*)-one, DMSO/THF, rt, (iv) 5% TFA in CH$_2$Cl$_2$, 0°C, (v) BrCH$_2$COY, (*i*-Pr)$_2$NEt, NMP, 80°C, (vi) DBU, NMP, 80°C, (vii) TBAF, DMF, 65°C

Resin-bound silyl ether **14** is formed by reaction of polystyrene hydroxymethyl resin with chlorosilane and imidazole. This is subjected to *ortho*-lithiation, followed by treatment with DMF giving rise to the resin-bound aldehyde **15**, which is converted into the corresponding benzhydrol **16** by reaction with *p*-lithioanisole. Oxidation of **16** provides resin-bound MOM-ether **17**. Cleavage with TFA affords the resin-bound phenol **18**. Reaction of this phenol with a variety of α-bromoketones forms the corresponding resin-bound diketone **19**. Cyclisazion of this gives the resin-bound benzofurans **20**.

An interesting feature of this linker is the fact that under adequate conditions, the cleavage takes place selectively either in the carbon-silicon or in the silicon-oxygen bond to give the respective products. Thus, while cleavage with TBAF provides the benzofuran **21**, reaction with TFA gives the corresponding silanol resulting from cleavage of the silicon-oxygen bond.

The same authors have described the synthesis of 2,3-disubstituted benzopyran-4-ones, using the diisopropylsilyloxy traceless linker (shown previously) demonstrating the versatility of this linker in the synthesis of different heterocyclics.[12]

As depicted in Scheme 5, addition of arylmagnesium chloride to the aldehyde **15**, followed by oxidation with IBX gives the corresponding resin-bound ketone **22**. Removal of the MOM group in TFA forms the phenol **23**, which is treated with the amide acetal in THF to obtain the corresponding resin-bound benzopyranone **24**. This can be selectively cleaved to give either the benzopyranone **25** by treatment with CsF or 0.2 M TBAF in DMF, or to form the silanol **26** when 0.01 M TBAF in THF is used.
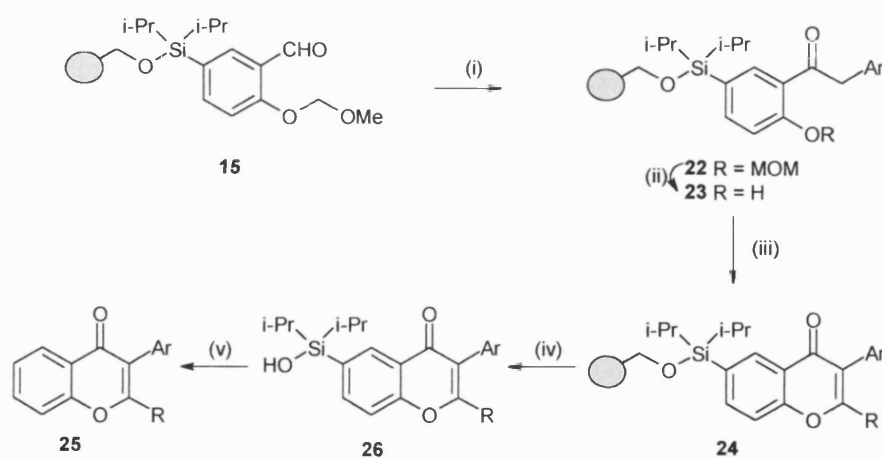
Scheme 5. (i) 1. ArCH₂MgCl, THF, 4h, 2. IBX, DMSO/THF, (ii) 4% TFA, DCM, 0°C, (iii) amide acetal, THF, 40°C, 6 h, (iv) 0.01 M TBAF, THF, 1 h, (v) saturated CsF, DMF, 60°C, 16 h, or 0.2 M TBAF, THF/DMF (1:4), 45°C, 30 min.

A group in Germany have published the synthesis of regioregular head-to-tail-coupled oligo(3-arylthiophene)s using the silyl ether traceless linker above described.[13]

The monomer, resin-bound 3-(p-tolyl)thiophene (**27**), undergoes *ortho*-lithiation and subsequent reaction with iodine to provide the substrate for a Suzuki reaction with thiophene boronic ester forming the bisthiophene **28**. Repetition of the halogenation/Suzuki coupling sequence gives the resin-bound tetrathiophene **29**. Cleavage of the linker by fluoride-mediated protodesilylation affords the oligomer **30** in 48% overall yield (Scheme 6).
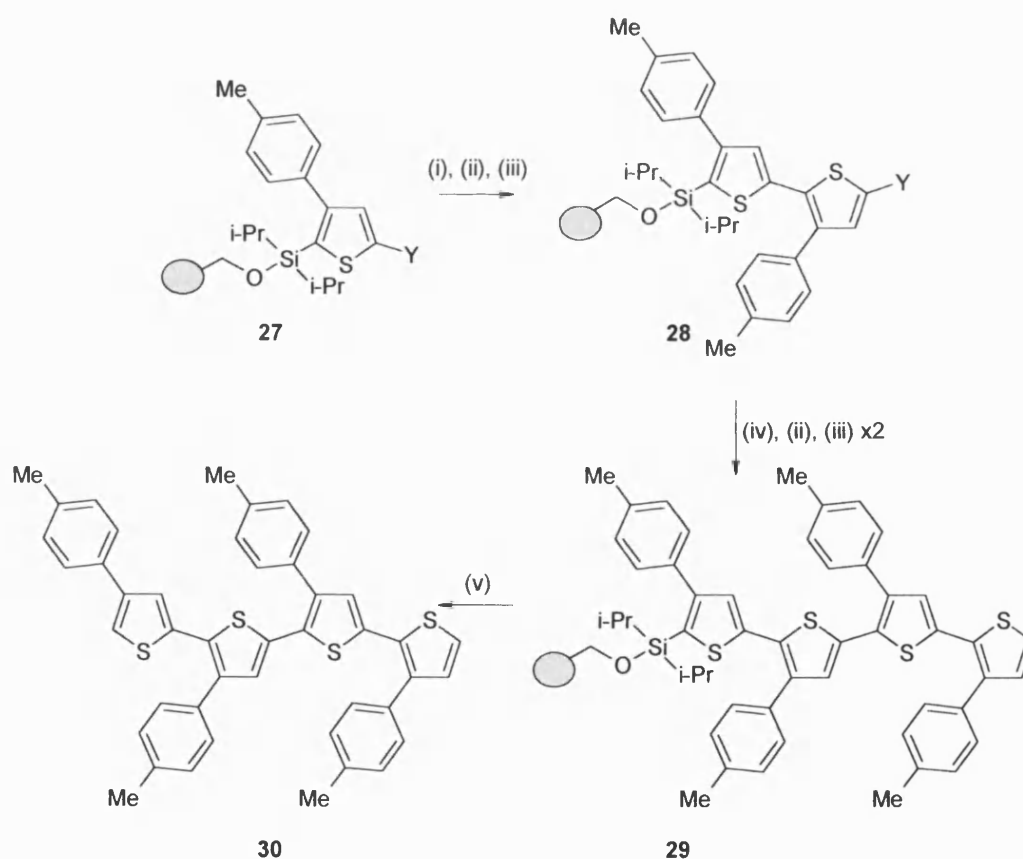
Scheme 6. (i) LDA, THF, (ii) I₂, (iii) thiophene boronic ester, Pd(PPh₃)₄ (5 mol%), NaHCO₃, THF, (iv) Hg(OCOC₅H₁₁)₂, CH₂Cl₂, (v) TBAF, THF.

Also described is the synthesis of a trialkylsilane linker, based on the hydrosilylation of resin-bound olefins with disubstituted silanes (Scheme 7).[14] This linker contains a stable Si-H group, which can be used for the loading of alcohols, aromatic, allyl or alkynyl compounds by reaction of linker **31** with alcohols or the corresponding Grignard or alkyllithium reagents. While cleavage of silyl ethers takes place with HF/Py, aromatic compounds are released after treatment with TFA/DCM for electron rich aromatic derivatives or with tetrabutylammonium fluoride for electron-deficient aromatics.
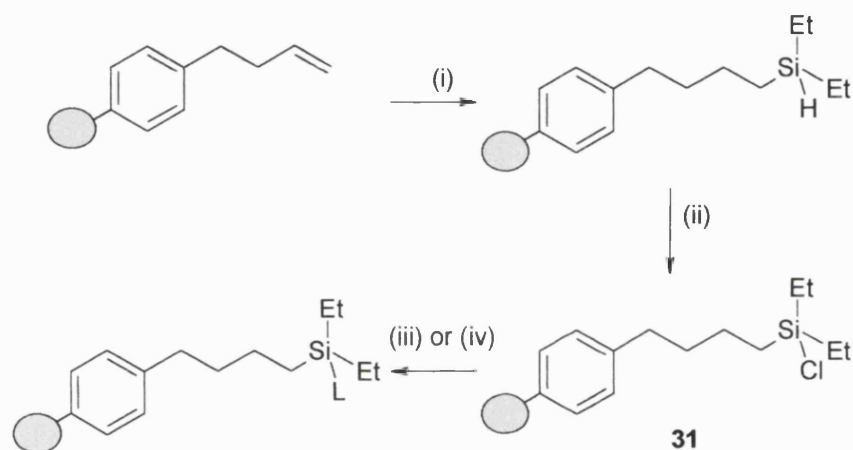
Scheme 7. (i) Et_2SiH_2 (2 equiv.) toluene, $RhCl(PPh_3)_3$ (0.4 mol%), (ii) 1,3-dichloro-5,5-dimethylhydantoin (3 equiv.), CH_2Cl_2, 1.5 h, (iii) ROH, (3 equiv.), imidazole (3.5 equiv.), CH_2Cl_2, 4 h, (L= OR) (iv) ArLi (L= Ar)or allylmagnesium chloride (L= allyl) (5 equiv.), THF, -78→0 °C.

Silverman and Lee published the application of a polymer-bound phenylalanine silyl-based linker in the synthesis of dipeptides on solid support.[15] This work demonstrated that phenylalanine-containing peptides could be obtained in any order of reaction sequence desired, from both the *N*- and *C*- termini by attachment of the amino acid side chain to the polymer. This is in contrast to conventional solid-phase peptide synthesis which allows the elongation of the amino acid backbone unidirectionally. This work is an important contribution to the synthesis of more diverse libraries of peptides and peptidomimetics (Scheme 8).
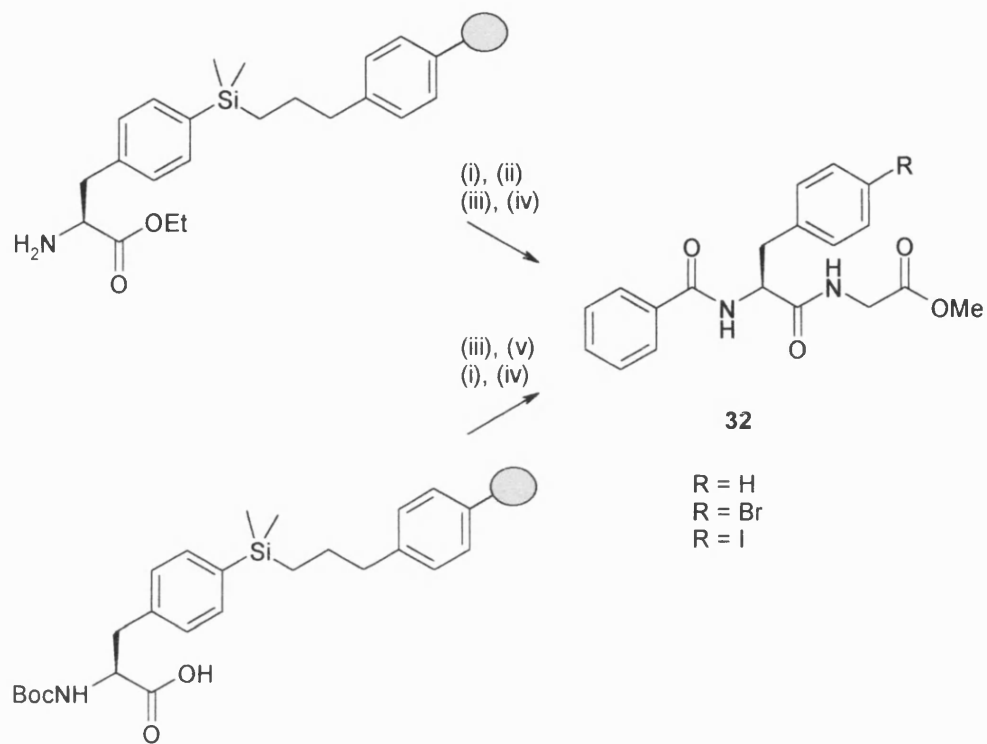
Scheme 8. (i) benzoic acid, EDC, HOBT, TEA, DMF (ii) THF/H$_2$O (8:1), LiOH, reflux, 1h (iii) Gly-OMe, EDC, HOBT, TEA, DMF (iv) TFA/CH$_2$Cl$_2$ (1:1), 24h, rt, (R=H) or Br$_2$/CH$_2$Cl$_2$ (R=Br) or ICl/CH$_2$Cl$_2$ (R=I) (v) TFA/CH$_2$Cl$_2$ (1:1), 10min, rt.

The cleavage of the dipeptide **32** from the resin takes place by proto-*ipso*desylation with TFA or alternatively by *ipso*-substitution of the silyl group with electrophiles. The later option creates a point of diversity in the molecule by allowing substitution reactions at the halide.

This group also described the asymmetric synthesis of β-amino acid analogues with a nonpolar aromatic side chain.[16] Treatment of the chiral building block **33** with TFA and subsequently reaction with bromine provides **34**. Further transformation of building block **33** was also suitable for the synthesis of 3-aryl-β-alanine-containing tripeptides **35** (Scheme 9).
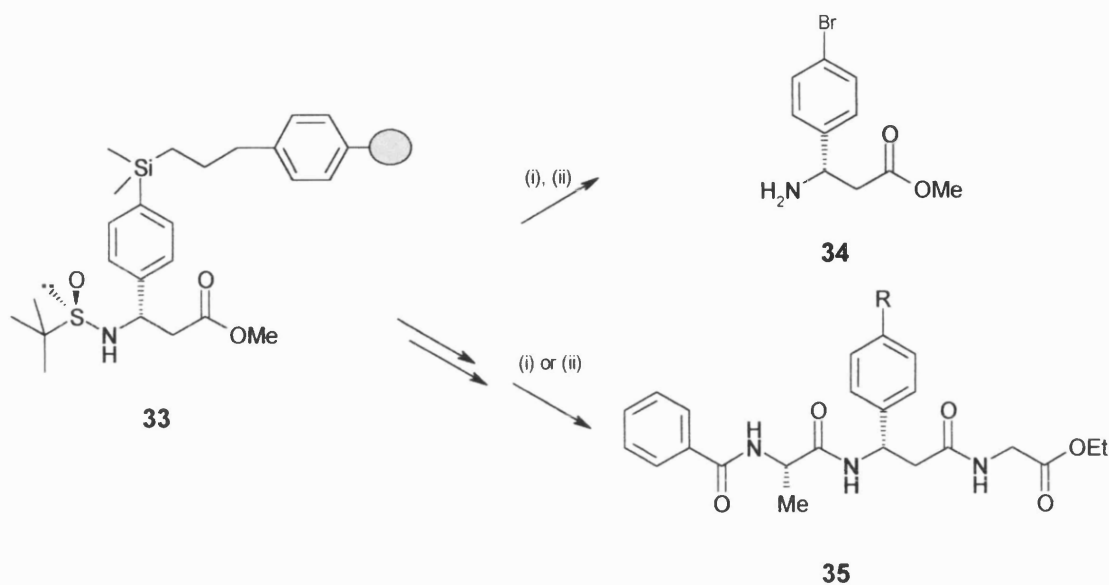
Scheme 9. (i) TFA/CH$_2$Cl$_2$ (1:1), 24h, rt (ii) Br$_2$/CH$_2$Cl$_2$

The same arylsilyl strategy was employed for the synthesis of phenylglycine-containing peptides **36** (Scheme 10). This methodology can also provide access to cyclic peptides, such as Sansalvamide (**37**) a natural product, which shows significant cancer cell cytotoxicity.[17]
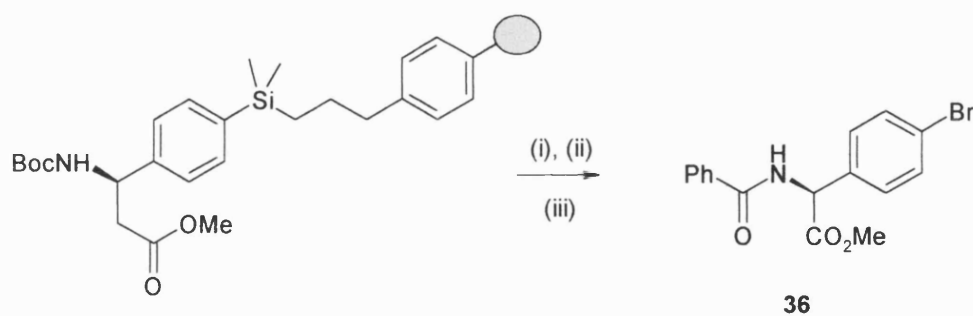
Scheme 10. (i) TFA/CH$_2$Cl$_2$ (1:1), 10min, rt (ii) benzoic acid, EDC, HOBT, TEA, DMF (iii) Br$_2$/ CH$_2$Cl$_2$
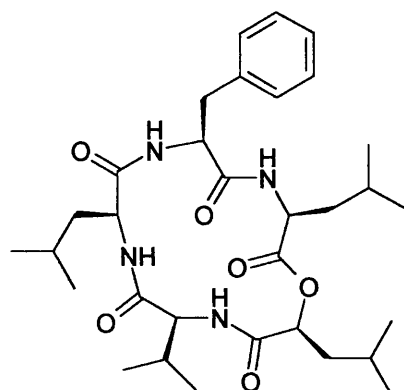
37

Recently, the same authors have published a comprehensive paper describing synthetic protocols for the construction of arylsilane-based linkers.[18] These linkers serve to prepare aromatic, polyaromatic and heteroaromatic-containing molecules. 4-Allyldimethylsilyl-1-bromobenzene is used as the starting material for the preparation of a variety of phenylsilane linkers. On one hand the starting material offers the possibility to introduce different functional groups at the bromo position, where various chemical reactions can take place. On the other hand the allyl group constitutes the point of attachment to the polymer. Chemical transformations of the starting material lead to diverse linkers that upon cleavage either with 50% TFA in CH_2Cl_2 or with Br_2, as displayed in Scheme 11, provide substituted aryl compounds such as **38**, a hydroxamic acid analogue.
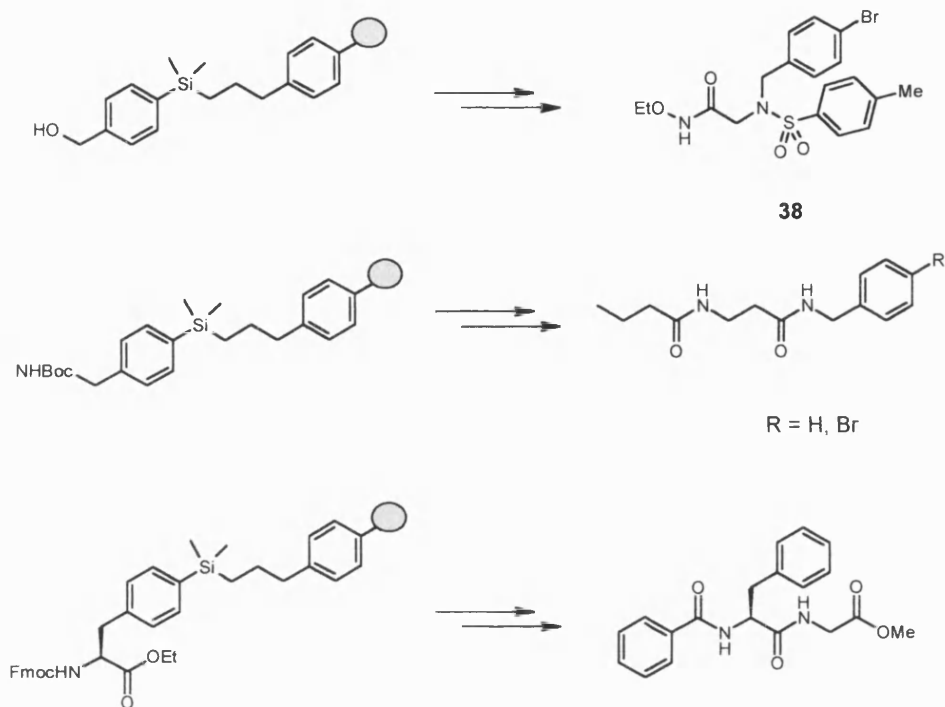
Scheme 11. Phenylsilane linkers

This methodology has been applied to other aromatic systems to give polyaromatic compounds **39** (Scheme 12) or heteroaromatic molecules **40** (Scheme 13).
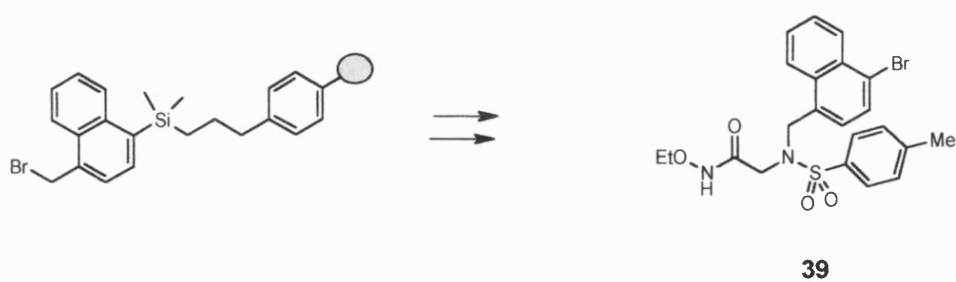
Scheme 12. Polyaromatic linkers
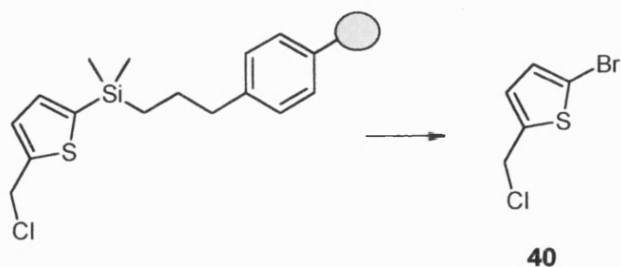
Scheme 13. Heteroaromatic linkers

The work described by Silverman and Lee is of great importance, as it provides a method for the synthesis of oligopeptides and peptidomimetics containing phenylalanine or other amino acids with nonpolar aromatic side chains as the key pharmacophore. By attachment of the phenylalanine side chain to the polymer, the residues at both the *N*- and *C*-termini can be modified, producing libraries with high diversity and biological activity.

Tacke and coworkers have described another silicon-based linker for the solid phase synthesis of aromatic compounds.[19] This work offers novel cleavage conditions for the release of the desired organic compounds. Si-C cleavage takes place by reaction with a *vic*-diol, such as 1,2-dihydroxybenzene, forming a zwitterionic pentacoordinate silicate **41** linked to the support along with methanol and methane. Realizing that the most common method used for desilylation is acidic conditions, the approach described in this paper extends the possibility to introduce functional groups which may be acid sensitive.

41
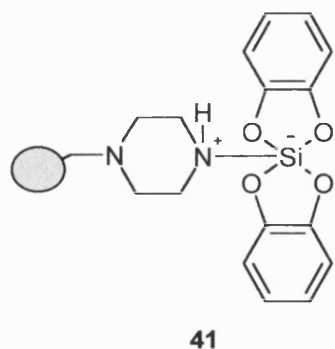
Starting from Merrifield resin and piperazine, followed by reaction with an adequate aryl substituted (chloromethyl)silane builds the scaffold **42**. As depicted in Scheme 14 this can undergo cleavage (path a), releasing the aryl compound **43** or further chemical transformations of the aryl group can be carried out by treatment with arylzinc reagents in the presence of the catalyst PdCl$_2$(dppf) to yield the resin-bound **44** (path b). Another option for aryl modification is through a Heck reaction (path c), such as by reaction of **42** with methyl acrylate, triethylamine as a base and PdCl$_2$/PPh$_3$ as catalyst to afford **45**. Both silane-containing resins **44** or **45** undergo cleavage to give the corresponding aryl compound **46** and **47** respectively.
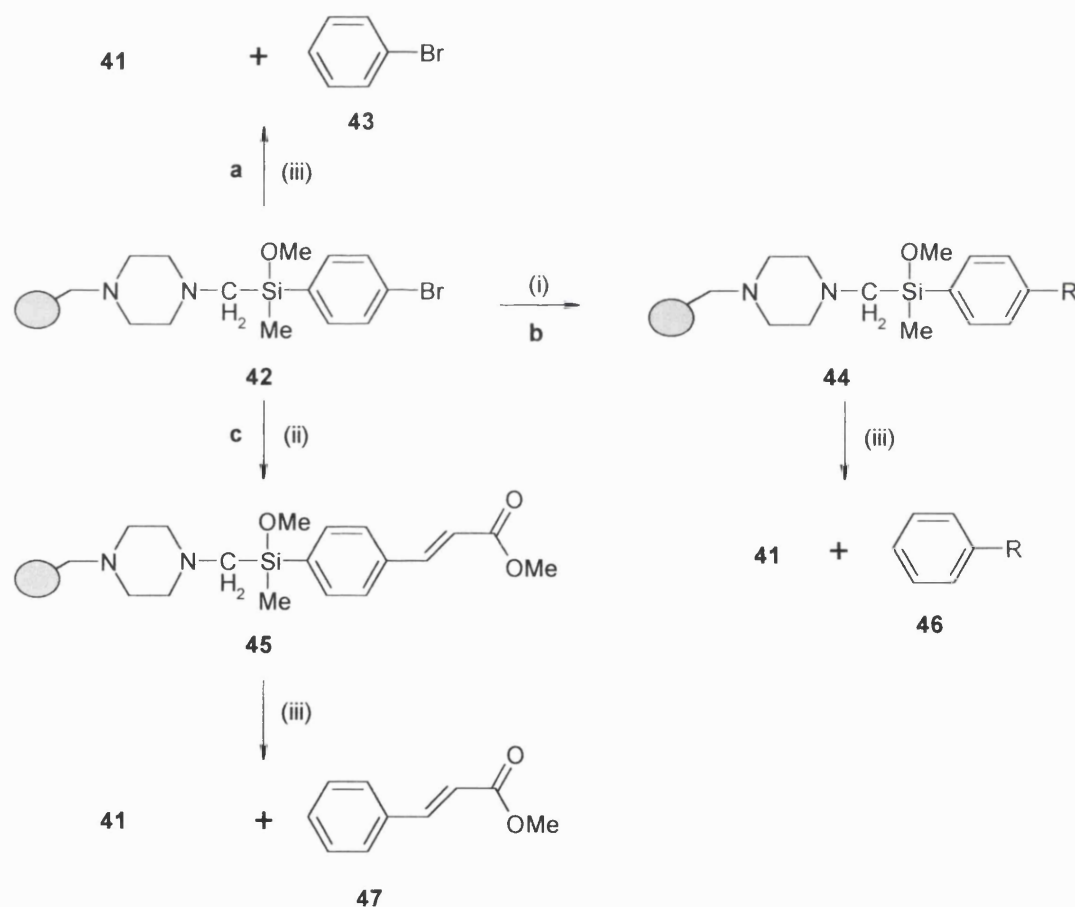
Scheme 14. (i) RZnBr, [PdCl$_2$(dppf)], (ii) methyl acrylate, NEt$_3$, [Pd Cl$_2$/PPh$_3$], (iii) 1,2-dihydroxybenzene, ACN, 50°C.

Substituted guanidines cover a wide range of pharmacological activities (e.g. anti-tumor, anti-hypertensive, and cardiotonic). Therefore interest in the production of their derivatives based on solid supported library construction have increased in recent years.

Min Li and collaborators have explored the use of traceless linker strategies. As shown in Scheme 15, one of these strategies involves the synthesis of a benzoylated isothiocyanate resin **48**, by converting the carboxypolystyrene into the corresponding acyl chloride and then, reacting it with tetrabutylammonium thiocyanate.[20] As this resin behaves like an electron-withdrawing substituent, it easily undergoes addition reactions with a variety of amines to form the corresponding acyl thioureas **49**. Reaction of the resin bound acyl thioureas with 1-(3-dimethyaminopropyl)-3-ethylcarbodiimide hydrochloride (EDC) and an amine (primary or secondary) results in the formation of the resin bound guanidine **50**. Finally cleavage of the acyl guanidine with trifluoroacetic acid in $CHCl_3$ and MeOH (1:1:1) gives rise the substituted guanidines **51**.
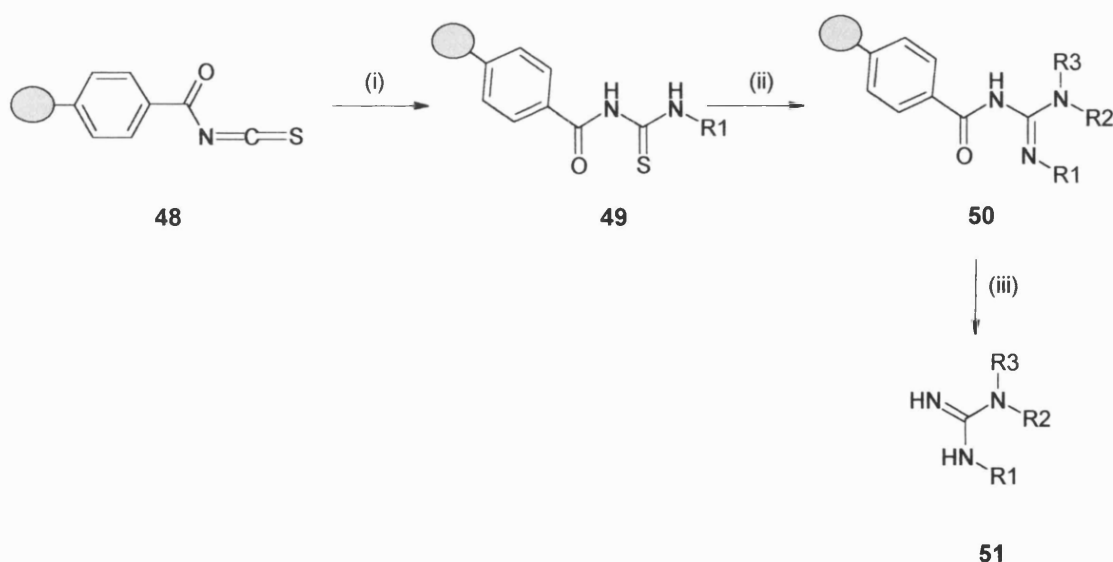
Scheme 15. (i) R1NH$_2$, DMF (ii) R2R3NH, EDC, DIPEA, CHCl$_3$ or DMF (iii) TFA:CHCl$_3$:MeOH (1:1:1), 45-60°C, 24-72 hrs.

Scheme 16 illustrates another strategy described by the same group.[21] This approach used the Rink resin as an amine component in reactions with isothiocyanates and amines to form disubstituted guanidines. Although this method is restricted to aromatic isothiocyanates and aliphatic amines, the fact that no special linker is required and the short two-step synthesis makes this procedure a simple route to access disubstituted guanidines, such as compound **52**. This is obtained in 100% yield and 83% purity.
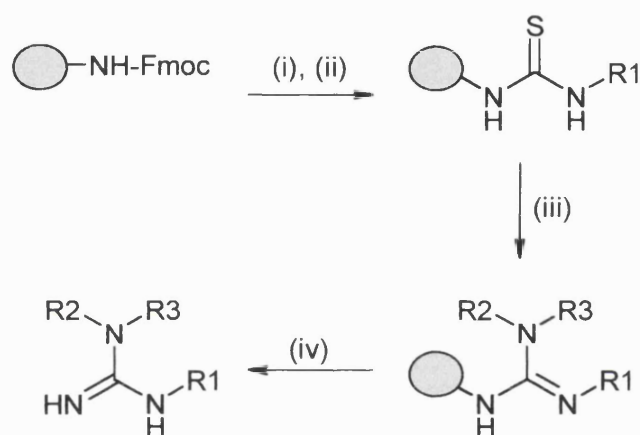
Scheme 16. (i) 25% piperidine/DMF, (ii) R1-N=C=S, CH$_2$Cl$_2$, r.t., 8h, (iii) R2R3NH, DIC, DIPEA, CHCl$_3$, 50°C, 2 days, (iv) 25% TFA/CH$_2$Cl$_2$, rt., 1h.
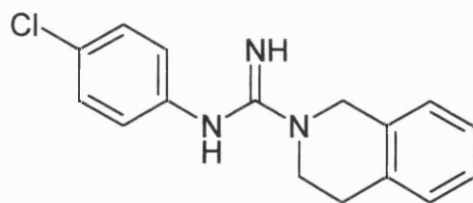
52

Based on the same methodology described in Scheme 15, Wilson reported the solid-phase synthesis of 2,4-diaminoquinazoline derivatives.[22] Scheme 17 shows the application of this approach to the synthesis of prazosin, a known α-1 antagonist, used for the treatment of hypertension in man. Resin-bound **53** is synthesized by reaction of resin **48** and 2-amino-4,5-dimethoxybenzonitrile in NMP. Treatment of **53** with 1-(2-furoyl)-piperazine and 1-(3-dimethylamino-propyl-3-ethylcarbodiimide hydrochloride) (EDC) under basic conditions gives resin-bound guanidine **54**, which under acidic conditions (TFA:H$_2$O) releases prazosin **55** as the TFA salt in 70% yield. Other 2,4-diaminoquinazolines, such as **56** (74%) can be obtained by this method when corresponding secondary amines are applied.
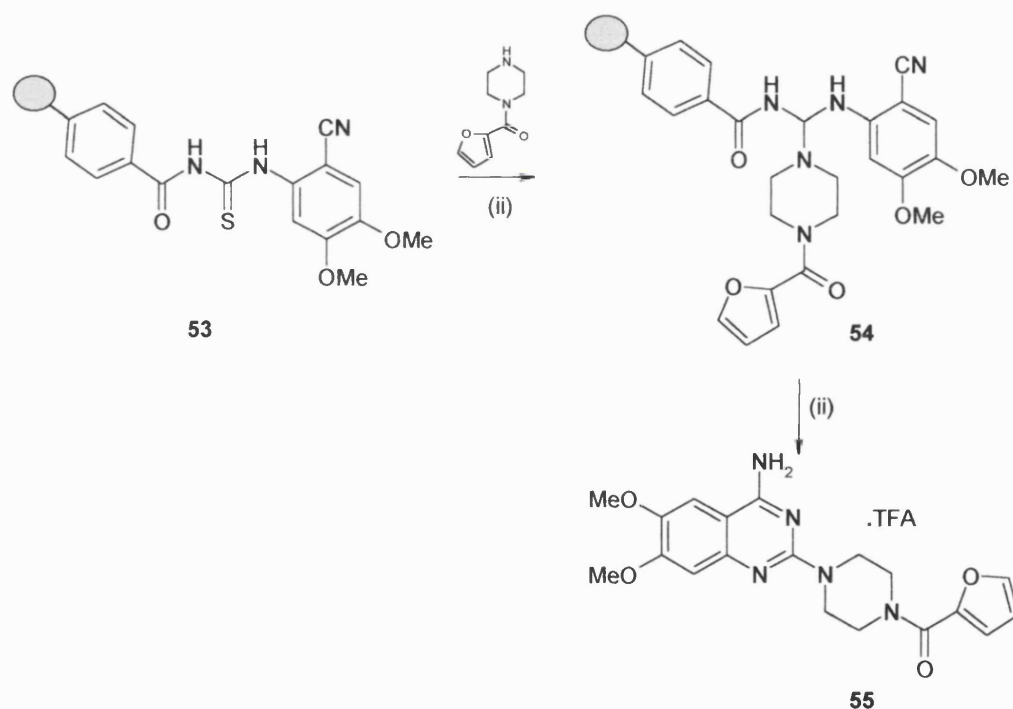
Scheme 17. (i) EDC, *i*-Pr$_2$NEt, CHCl$_3$, 24 h, (2x), (ii) TFA : H$_2$O (95:5), 80 °C, 16 h (2x)

56
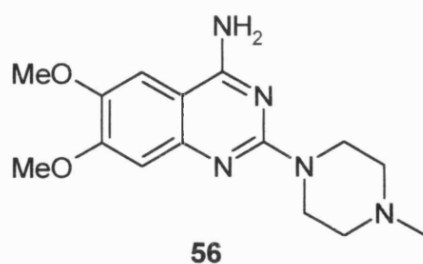
Recently, the same authors have reported a solid phase synthesis of trisubstituted 2-aminoimidazolones based on the intramolecular cyclization between a δ-guanidinium nitrogen and the resin bound amide carbonyl under acidic conditions.[23]

Their guanidine synthesis procedure provides an attractive route to obtain guanidino amides, guanidino acids, or 2-aminoimidazolones just by altering the type of amino acids bound on the resin. The resin bound amino acid moiety **57** is transformed into the resin bound thiourea **58**. This undergoes the guanylation reaction to give the resin bound guanidine **59**, which is cleaved under acidic conditions releasing the substituted 2-aminoimidazolone **60** (Scheme 18).

57   **58**

60   **59**
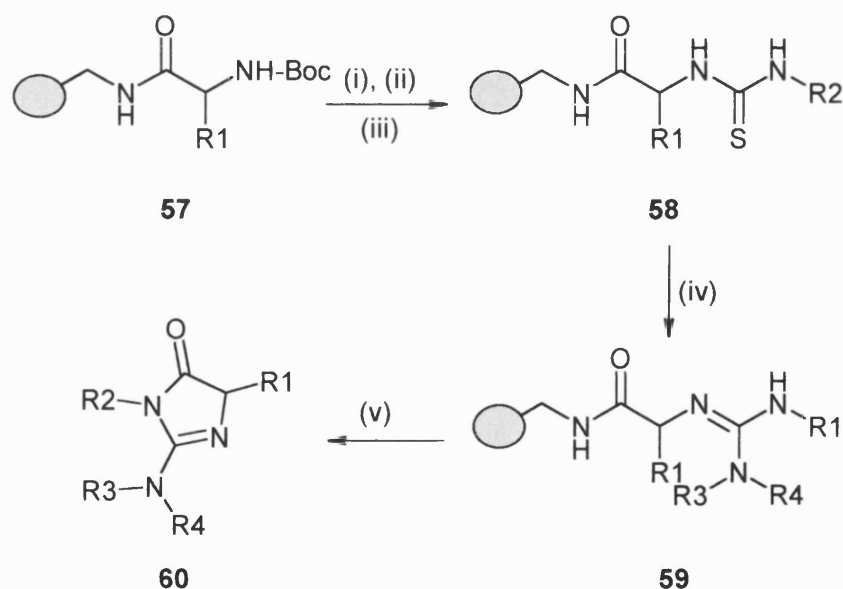
Scheme 18. (i) 30% TFA/CH$_2$Cl$_2$, (ii) 10% Et$_3$N wash, (iii) R2-N=C=S, CH$_2$Cl$_2$, r.t., 15h, (iv) R3R4NH, DIC, DIPEA, CHCl$_3$, 50°C, 2 days, (vi) 10% AcOH/CH$_2$Cl$_2$, rt, 15 h.

Another traceless linker for the preparation of *N,N*-disubstituted guanidines has been described by a group at University of California.[24] The release of the products also takes place under acidic conditions, however the resin is attached to a urethane-protected triflyl guanidine via a carbamate linkage (Scheme 19). The guanidinylating resin **61** is converted into the resin-bound guanidines **62** by reaction with primary and secondary amines. Cleavage with TFA: CH_2Cl_2 (1:1) yields the desired compounds **63**.

The traceless linker described by this group allows the preparation guanidines from cyclic and acyclic secondary amines. This constitutes an advantage as most of the described methods utilize only cyclic amines.
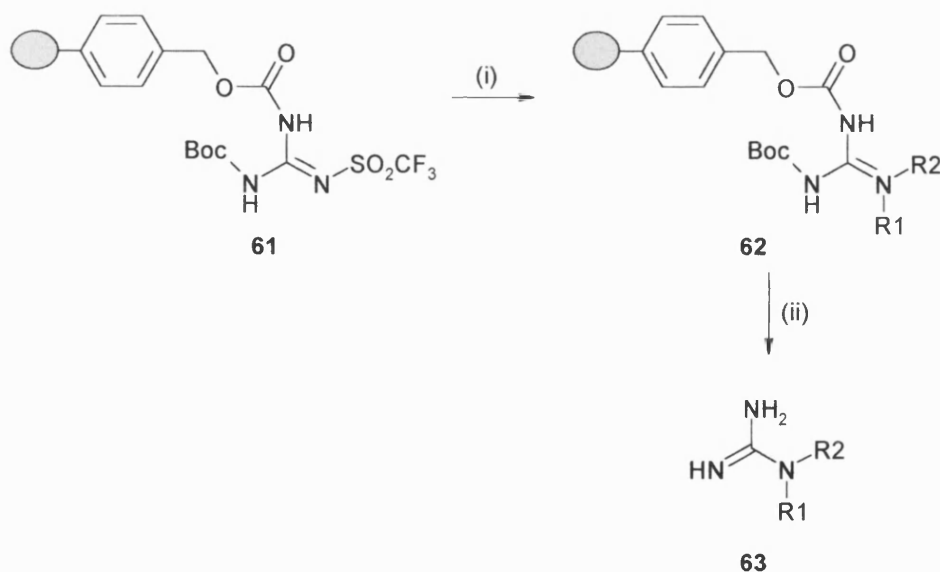
Scheme 19. (i) HNR1R2, CH_2Cl_2, (ii) TFA:CH_2Cl_2 (1:1).

This group has also developed a traceless linker that under acidic conditions releases a piperazinone containing enkephalin analogue.[25]

This elegant work begins with formation of the Wang resin bound N-alkylated glycine, which is converted into the resin bound carboxylic acid. This is transformed into the resin bound tertiary amide, by reaction with a variety of amines; introducing a point of diversity into the molecules. As illustrated in Scheme 20 the cleavage step in acidic medium induces cyclisation of the piperazinone scaffold at room temperature, providing the desired products.
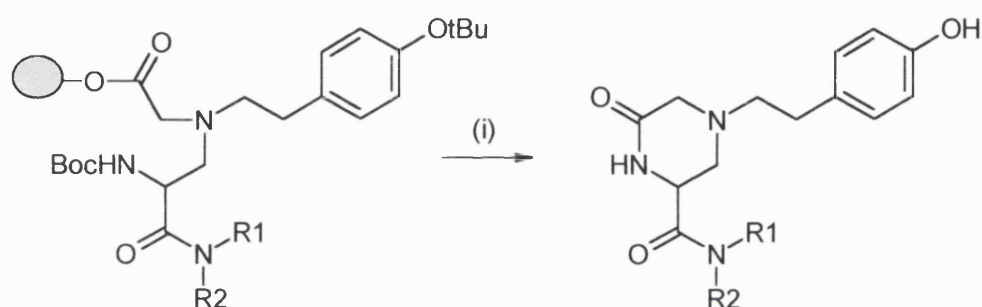
Scheme 20. (i) 5 % H_2O in TFA

Compound **64** has been obtained in this series and is found to be a potent μ-opioid receptor.

64
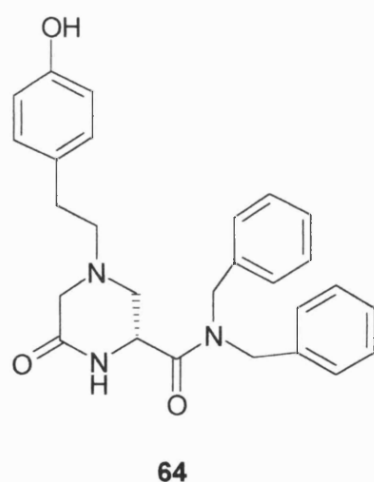
A linker, which provides ketoamides has been reported by a group at Cambridge University.[26]

Formation of a resin-bound N-benzyl tertiary amine followed by N-acylation forms resin-bound intermediate **65**. As depicted in Scheme 21 the nitrogen-benzyl carbon bond is cleaved by acid chloride to release tertiary amides **66**. Interesting in this work is that the products can readily undergo cyclization with ammonia to form 1,2,4,5-tetrasubstituted imidazoles **67**. Thus, from the same synthetic route two compound libraries can be obtained. Table 1 shows some of the substituents for the products. Yields vary from 25 to 88% for the amides and from 23 to 84% for the imidazoles.
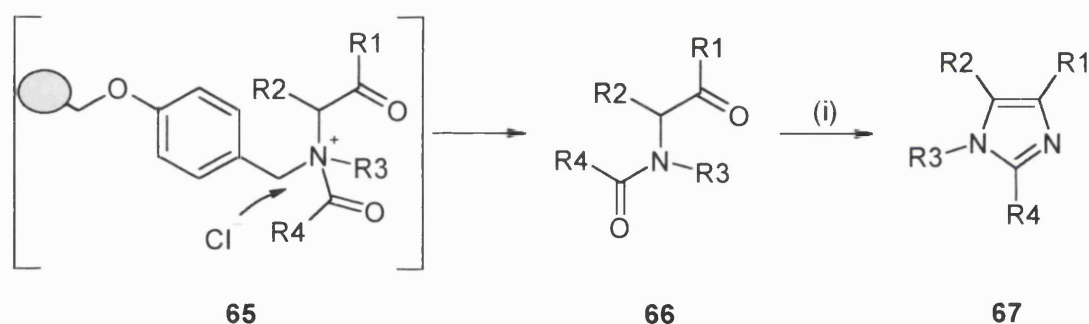
Scheme 21. (i) NH$_4$OAc, AcOH, DMF, 90°C, 24 h

Table 1. Substituents for compounds **66** and **67**

R1	R2	R3	R4
C$_6$H$_4$(4-OMe)	H	n-C$_4$H$_9$	Me
C$_6$H$_4$(4-Cl)	H	Bn	Me
Ph	Me	n-C$_4$H$_9$	Me
C$_6$H$_4$(4-Cl)	H	n-C$_4$H$_9$	CH$_2$OAc

Brase and collaborators developed a traceless linker system based on triazenes.[27] This linker leads to modified arenes and besides the easy of its accessibility,

remarkable is the fact that it presents the possibility of various chemical transformations both prior to and during the cleavage step.

Reaction of various diazonium salts (derived from available anilines) with a secondary amine resin, synthesized from Merrifield resin and benzylamine or piperazine forms the triazene systems **68** or **69**, respectively.

Scheme 22 shows possible chemical transformations for the system **68**. Heck reaction and asymmetric dihydroxylation, followed by cleavage with HCl gives the product **70** in 95% yield. Cleavage after the Heck reaction forms product **71** in 81% yield.
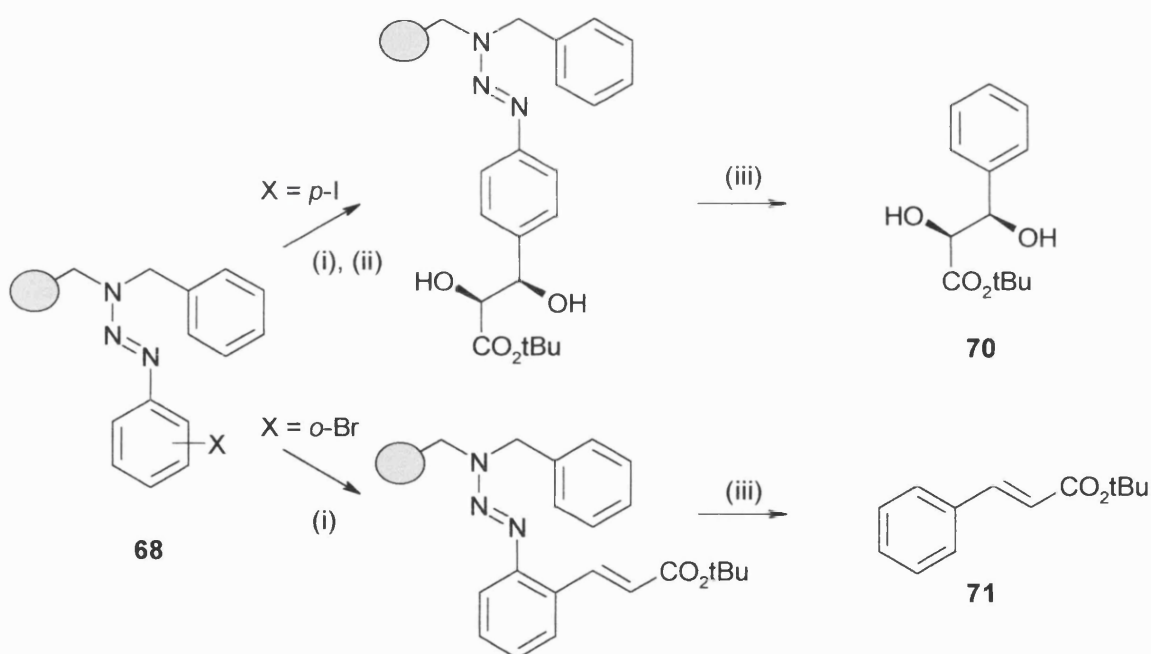
Scheme 22. (i) $H_2C=CHCO_2tBu$, $Pd(OAc)_2$, PPh_3, NEt_3, DMF, 24 h, 80°C, ultrasound (ii) AD-mixβ, acetone/H_2O(10:1), methanesulfonamide, 72 h (iii) THF/conc. HCl (10:1), 5 min, 50°C, ultrasound.

In addition to the acidic cleavage forming a C-H bond, the triazene linker offers the possibility of cleavage-cross-coupling reactions using palladium-catalysed

systems.[28] As depicted in Scheme 23, triazene **69** undergoes Heck reaction with iodobenzene. The cleavage reaction takes place by coupling with cyclopentene to give compound **72**, therefore forming a C-C bond.

69   **72**
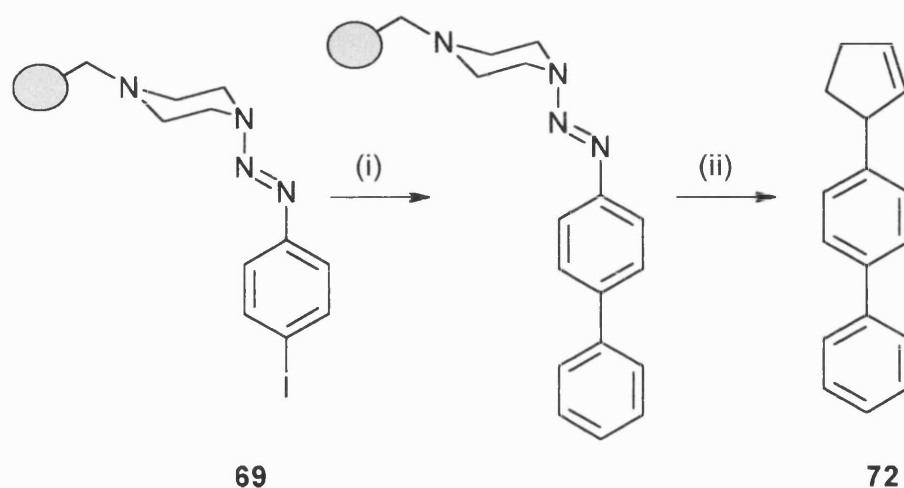
Scheme 23. (i) iodobenzene, Pd(OAc)$_2$, PPh$_3$, NEt$_3$, DMF, 24 h, 80°C, ultrasound (ii) TFA, Pd(OAc)$_2$, cyclopentene, 4 h, 40°C.

A traceless synthesis of quinoxalinones has also been described.[29] As shown in Scheme 24 dihydroquinoxalinones **73** are cleaved from the resin by TFA or gaseous HF or HCl. Products of the cleavage **73** undergo air oxidation to yield the target compounds **74**.

X= Cl, NO$_2$
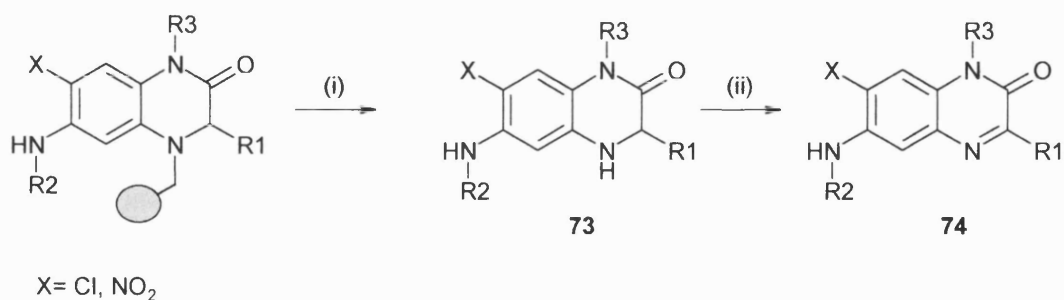
Scheme 24. (i) TFA or gaseous HF or HCl, rt (ii) air oxidation, MeOH, rt

Compounds **75** and **76** are examples of quinoxalinones obatained by this method.
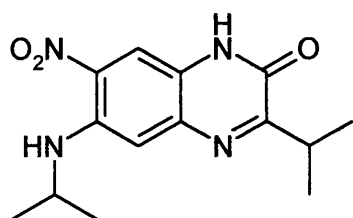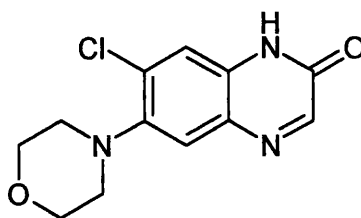
75   **76**

1.2.2 Basic cleavage

The concept of traceless linker has also been used for the synthesis of indole derivatives, based on a sulfonyl linker.[30] The indole ring is formed via intramolecular cyclization after coupling of a resin-bound aryl iodide with a terminal alkyne. The terminal alkyne constitutes one point of diversity in the molecule.

This sulfonyl based linker offers the advantage of a dual-activation process. On one hand the linker acts as an activating group to facilitate indole cyclization, on the other hand it is cleaved under mild conditions by means of reaction with tetrabutylammonium fluoride, to provide the products, such as **77**, in high yield and purity (85 and 100%) (Scheme 25).

A second point of diversity can be introduced by formation of resin bound organometallic as a precursor for the introduction of diverse substituents into the 3-position.
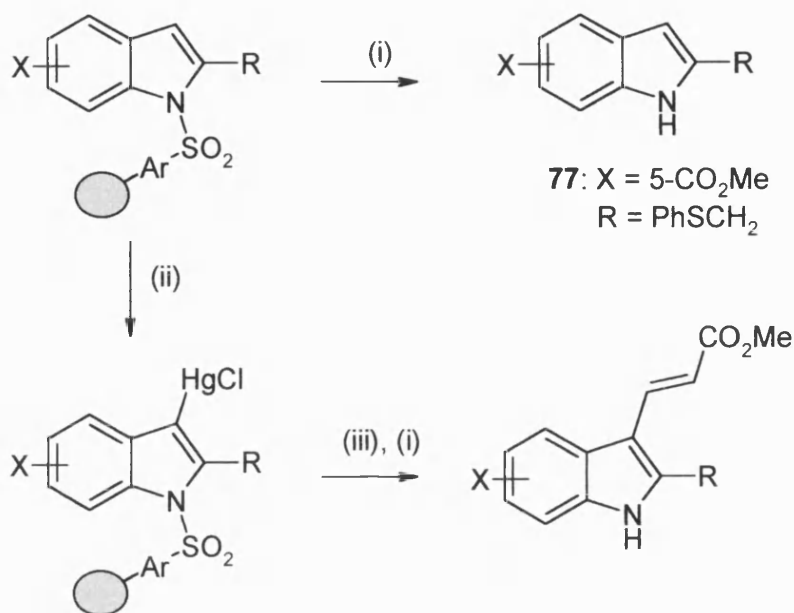
Scheme 25. (i) TBAF, THF, 70°C, 5 h, (ii) Hg(OAc)$_2$, HClO$_4$, HOAc, dioxane, NaCl, (iii) H$_2$C=CHCO$_2$Me, Pd(OAc)$_2$

Recently, Tumelty's group has described the solid-phase synthesis of substituted benzimidazoles.[31] This synthesis presents a few points of notable interest. The linker is attached to the *N*-1 in the heterocycle in contrast to others described routes of benzimidazoles where the point of attachment to the linker remains in the aromatic ring as a carboxamide bond. Thus, the products present an additional point to introduce diverse tertiary carboxamides, resulting in three points of diversity into the final compounds. Another interesting aspect is that release of the desired structures takes place under mild basic conditions and involves a final Hofmann elimination as shown in Scheme 26. Purities of final products are high, however yields are very low, shown to be dependent on the electronic characteristics of the alkylating species for the introduction of R3-aryl substituent. One of the best results is obtained with compound **78** that has been synthesised in 75% yield and 87% purity.
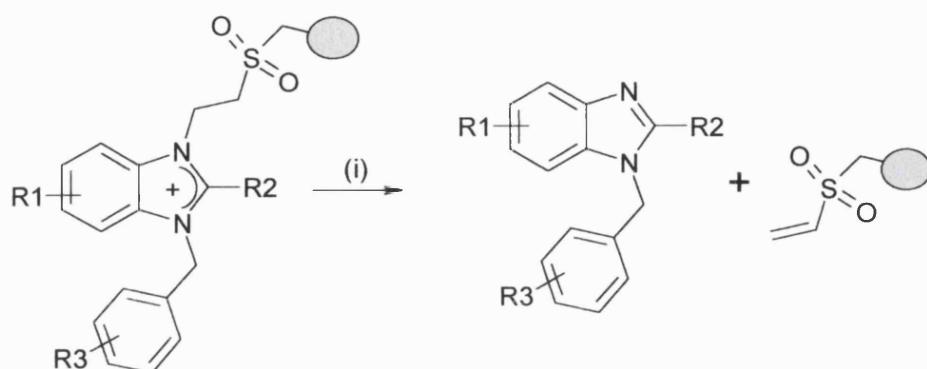
Scheme 26. (i) triethylamine, DCM (1:19), 18 h, rt.
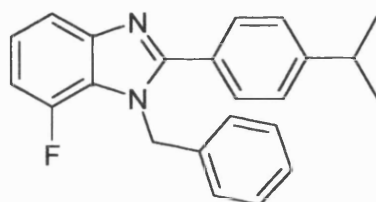
78

A traceless linker that releases substituted amines has been described by Wade and collaborators.[32] The design of such a linker capitalizes in the ability of a sulfide linker to remain stable prior to oxidative activation, acting as a "safety catch". After oxidation to the sulfone the linker is cleaved by β-elimination by secondary amines forming the desired products. (Scheme 27)
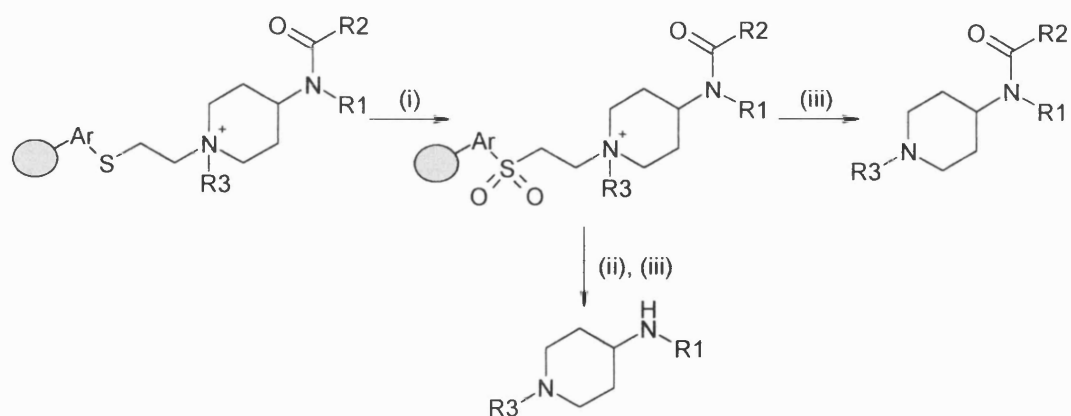
Scheme 27. (i) *m*-CPBA, (ii) TFA, (iii) Me₂NH.

A hydroxylamine-based linker has been described for the synthesis of tertiary amines, which are released from the linker under base-induced cleavage.[33]

Briefly, Boc-protected hydroxylamine linker undergoes alkylation, then deprotection and reductive alkylation to give resin-bound **79**. This is quaternised and subjected to cleavage under basic conditions to yield the products **80** (Scheme 28). It is noteworthy that this linker shows stability to strong acids.
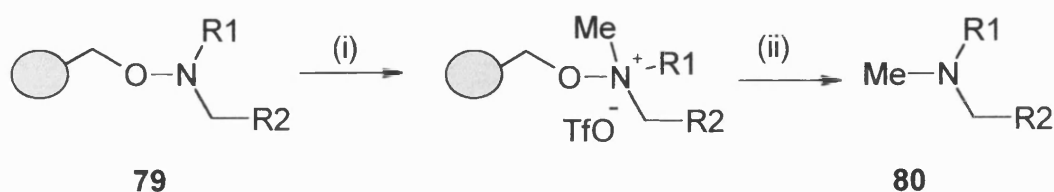
Scheme 28. (i) MeOTf/CH$_2$Cl$_2$ (ii) Et$_3$N/CH$_2$Cl$_2$

1.2.3 Cyclization as a means of linker removal

Another method for traceless cleavage is as part of a cyclization step.

Schore and collaborators prepared a variety of cyclic ethers via 3+2 cycloaddition of nitrile oxides to alkenes and dienes to give isoxazolines. These then underwent electrophile-induced cyclization. [34]

As Scheme 29 depicts, protected polymer-bound 2-nitro-1-phenylethanol **81** acts as a cycloaddition precursor to undergo 1,3-dipolar cycloaddition with 1,6-heptadiene (**82**, n=1) or with 1,7-octadiene (**82**, n=3) to form the corresponding isoxazoline **83**. This reacts with ICl or I$_2$ inducing cyclization and giving rise 2-(cyanomethyl)-6-(iodomethyl) tetrahydropyran **84** or the seven-membered ring derivative **85**, respectively.

Scheme 30 and 31 show similar procedure for the synthesis of 6-membered rings **86** and spirocyclic derivatives **87**.
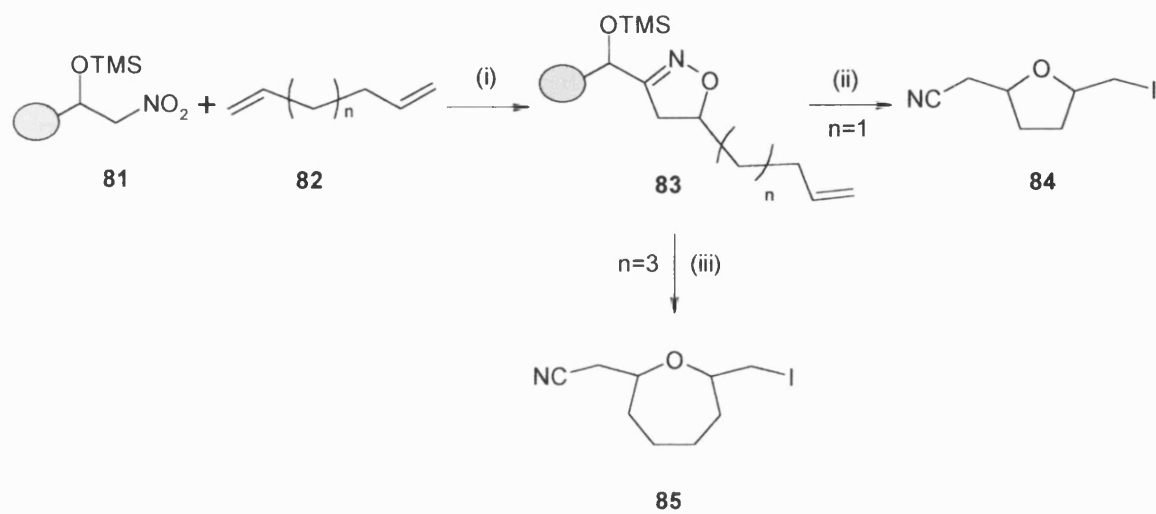
Scheme 29. (i) PhNCO, NEt₃, PhH, (ii) ICl, CH₂Cl₂, -78°C (iii) I₂, CH₂Cl₂, rt.
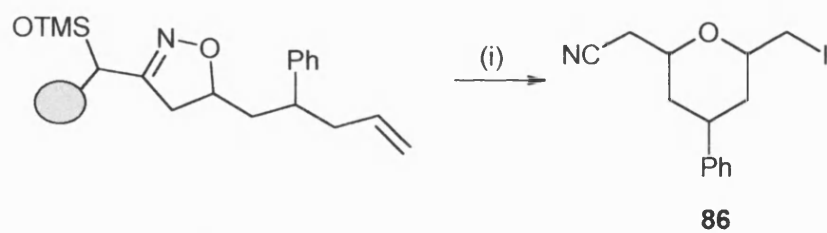
Scheme 30. (i) I₂, CH₂Cl₂, rt.
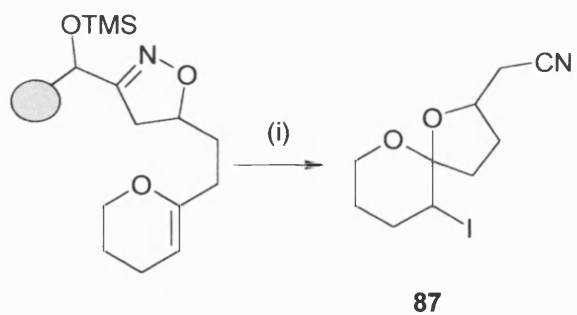
Scheme 31. (i) I₂, CH₂Cl₂, rt.

Structurally diverse 1-phenyl-pyrazolone derivatives have been synthesized in a solid phase fashion making use of cyclisation in the cleavage step.[35]
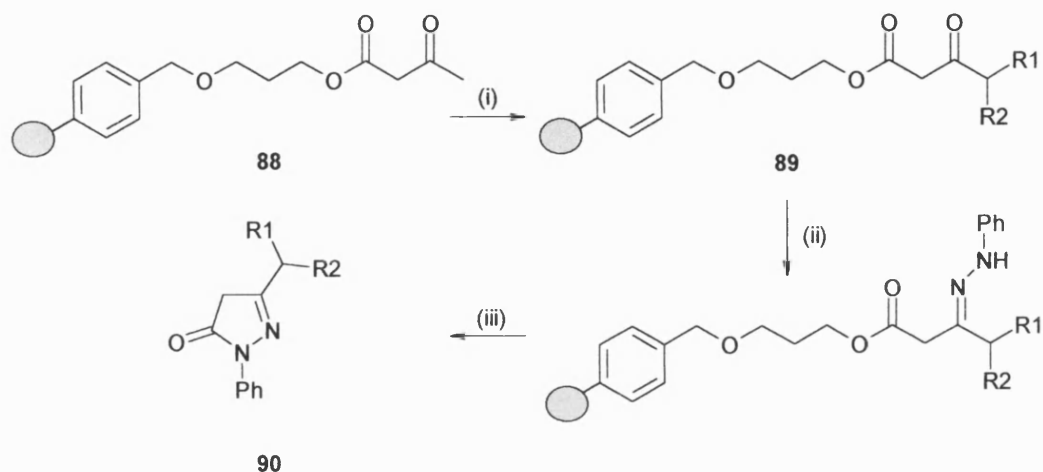
Scheme 32. (i) 1. LDA, THF, 0°C, 2. R1X, THF, 0°C, 3. n-BuLi, THF, 0°C, 4. R2X, H⁺, THF, 0→ 25°C, (ii) Ph-NH-NH2, THF, rt, (iii) 100°C, toluene.

The dianion of polymer-bound acetoacetate **88** is generated and trapped with various alkylating agents to give the corresponding γ-alkylated β-ketoesters **89**. Subsequent reaction with phenylhydrazine results in cyclisation with cleavage from the polymeric support giving the 1-phenyl-pyrazolones **90** (Scheme 32).

Due to their many pharmaceutical uses, 1,4-benzodiazepine-2,5-diones have been the target of several solid phase synthesis strategies. In work reported by Mayer *et al.*[36] 1,4-benzodiazepine-2,5-dione derivatives **94** were obtained by reduction-induced cyclisation of substituted aminoamides **93**. Scheme 33 displays the synthesis of such compounds. Two different starting materials can be used in the synthesis, permitting introduction of a diverse array of substituents. Either *o*-anthranilic acid **95** or *o*-nitrobenzoic acid **96** are coupled with the deprotected form of the Fmoc amino acid derivatized Wang resin **91** to give the corresponding polymer bound amide **92**. Fmoc deprotection of the anthranilate intermediate or

reduction of the o-nitro group gives intermediate **93**, which under the cyclisation conditions produces 1,4-benzodiazepine-2,5-diones derivatives **94**.
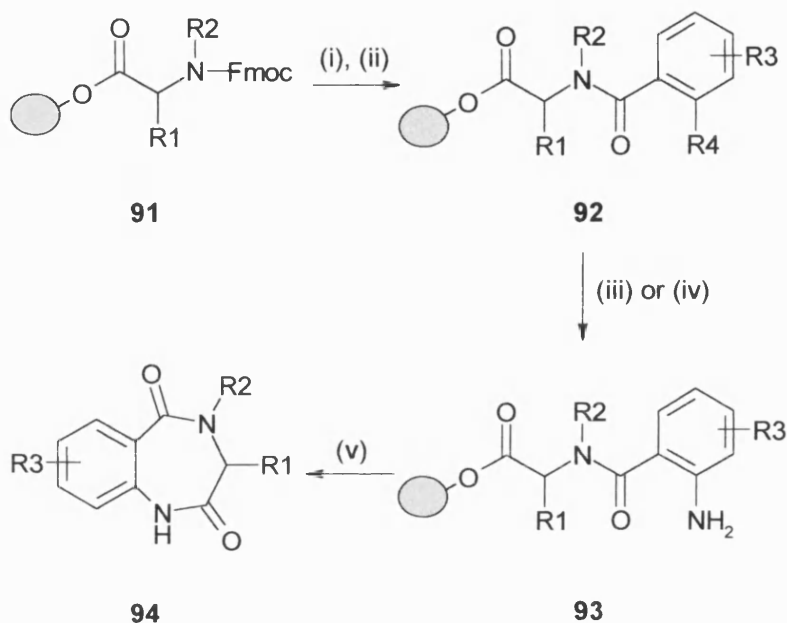
Scheme 33. (i) piperidine/DMF, (ii) *o*-Anthranilic acid **95** or *o*-nitrobenzoic acid **96**, DCC/HOBt, (R4=NHFmoc, (iii) piperidine/DMF, (R4=NO$_2$, (iv) SnCl$_2$/DMF, (v) NaOtBu/THF 60°C, 24h.

Brown and collaborators have found an elegant procedure for the synthesis of seven-membered ring-containing cyclic sulfonamides.[37] They described the cyclisative release of such sulfonamides **100** by ring-closing olefin metathesis using Grubbs catalyst.

Scheme 34 shows one of the approaches for the synthesis of such compounds. Starting with malonate alkylation of allylic chloride, followed by Krapcho dealkoxycarbonylation, the ester **97** is obtained. Removal of the THP protecting group permits coupling with the N-Boc sulfonamide **98** using a Mitsunobu reaction. The ester is then reduced and finally a carboxyethylpolystyrene resin **99** is formed by carbodiimide coupling of the alcohol.
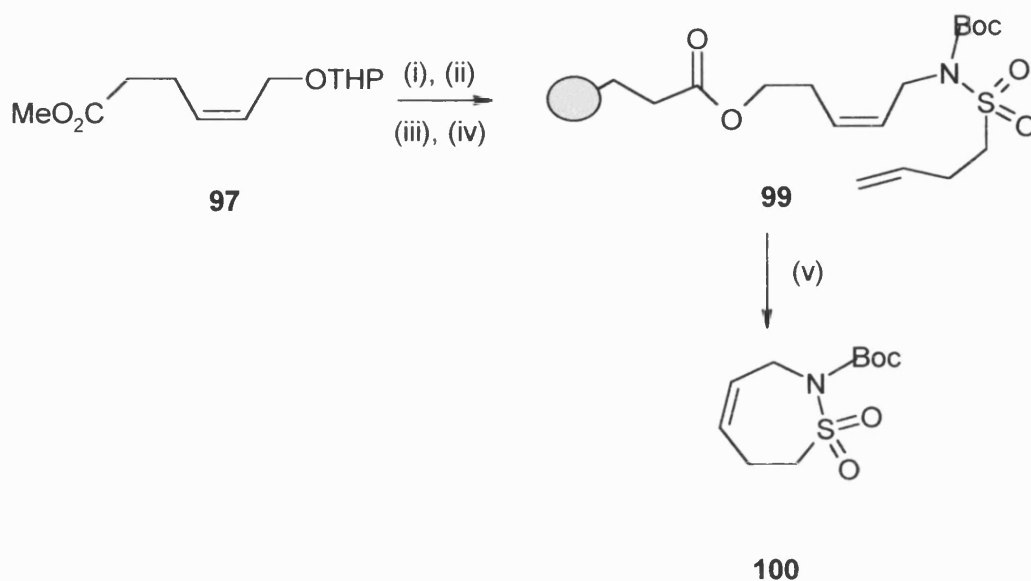
Scheme 34. (i) *p*-TSA/MeOH (ii) DEAD, PPh₃, CH₂=CH-(CH₂)₂SO₂NHBoc (**98**)/THF (iii) LiAlH₄/Et₂O (iv) 2-carboxyethylpolystyrene, DIC, DMAP/CH₂Cl₂ (v) Grubbs catalyst /reflux.

Wang, Chen and Kin investigated the application of diverse silyl linkers in solid phase synthesis.[38] Scheme 35 shows the method they applied for the synthesis of the silyl linkers. Direct lithiation of 4-bromopolystyrene resin, gives 4-lithiated polystyrene resin, which reacts with chlorodimethylvinylsilane **101** or methyl-phenyl-vinyl-chlorosilane **102** to provide the corresponding polymer-bound vinylsilane **103**. Hydroboration of the vinylsilanes with 9-BBN and subsequent oxidation, provides the polymer-bound 2-(trialkylsilyl)ethanol linker **104**.
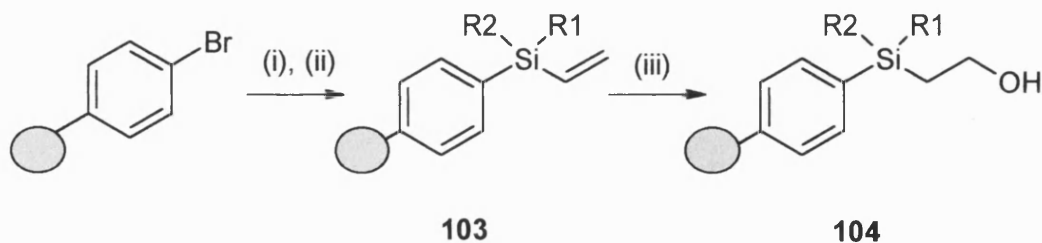
Scheme 28. (i) n-BuLi, toluene, (ii) **101** or **102**, THF, (iii) 9-BBN, H₂O₂, NaOH

The authors reported further modifications of the precursor **104** providing more diverse Si-based linkers, such as polymer-supported 2-(trialkylsilyl)ethyl bromide **105**, tosylate **106**, 4-nitrophenyl carbonate **107**, imidazolide carbamate **108** (Scheme 36).
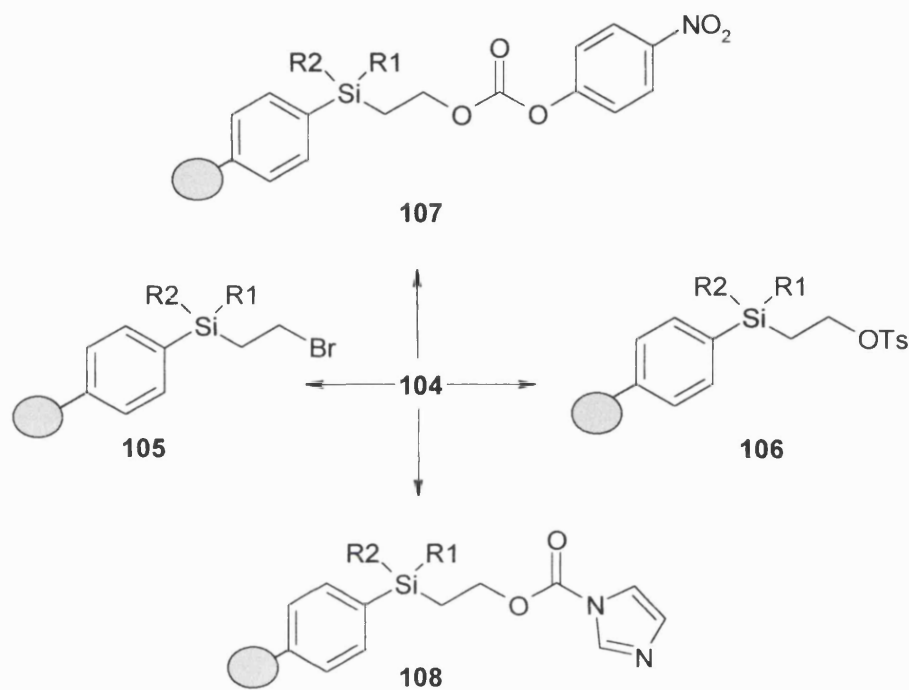
Scheme 36. Silyl-based linkers

As an example of the application of these linkers in solid phase synthesis Scheme 37 shows the synthesis of diketopipearizines **111** from the precursor linker **104**. Starting with the acylation of polymeric 2-(diphenylmethylsilyl)ethanol linker with Fmoc-Ala, followed by Fmoc deprotection gives intermediate **109**. Further Fmoc-aa coupling and Fmoc deprotection affords adduct **110**. Cyclisation in acidic media induces cleavage of the silyl linker giving rise to **111**. Tryprostatin B **112** has been synthesized utilising this strategy.
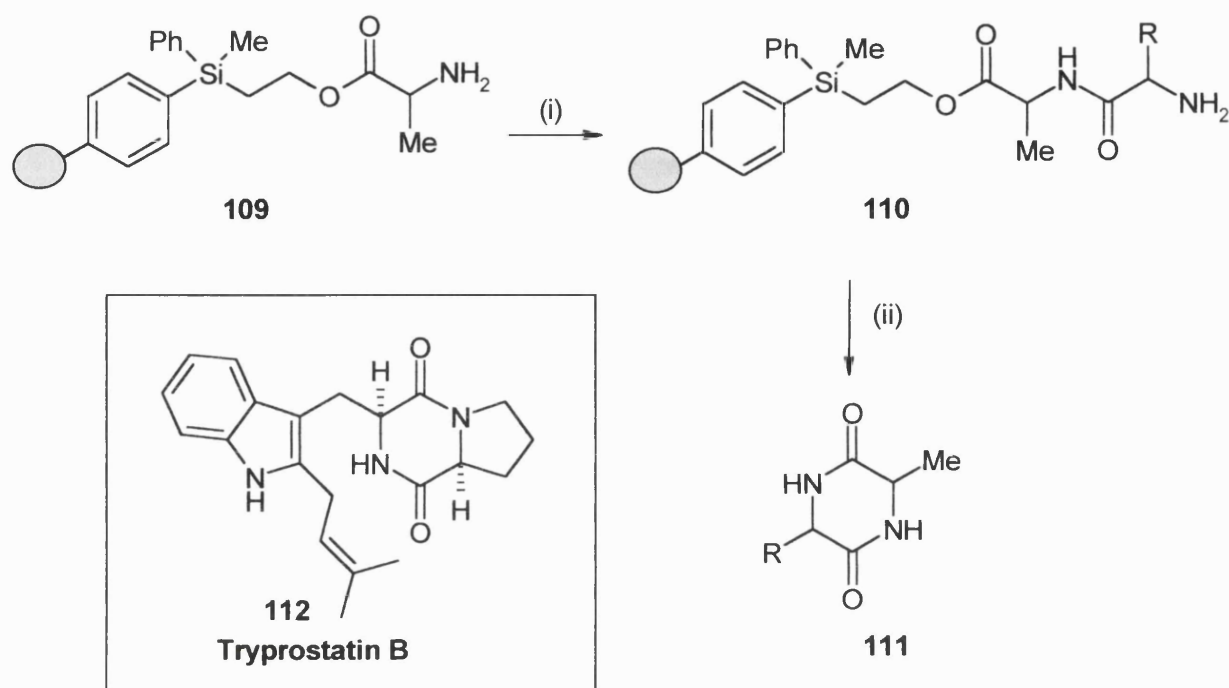
Scheme 37. (i) 1. Fmoc-aa, iPr$_2$NEt, HATU, HOBT, DMF, 2. 20% piperidine/NMP, rt, (ii) 30% AcOH/MeOH, rt

In work reported by Hong and collaborators is described the synthesis of 11-heterosteroids via fulvene hetero [6 + 3] cycloaddition.[39]

The fulvene resin **113** is formed by coupling of REM resin with formic acid and subsequent reaction with Et$_3$OBF$_4$ followed by a THF solution of sodium cyclopentadienide. As depicted in Scheme 38 the cleavage takes place by reaction of the fulvene resin with a solution of a benzoquinone or an indoaniline in benzene forming the corresponding product by cyclization **114**.

113   **114**
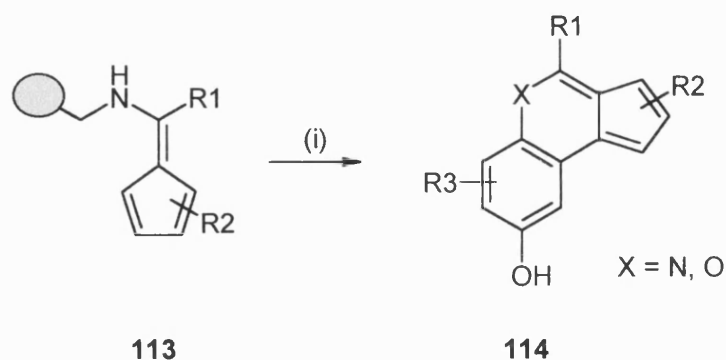
Scheme 38. (i) C_6H_6, benzoquinones or indoanilines.

1.2.4 Deboronation as a strategy for linker removal

An interesting strategy for the synthesis of aromatic compounds has been developed by a group in France.[40] The method consists of the attachment of functionalized arylboronic acids to the support **115**, followed by different solid-phase transformations. Release of the aromatic compounds takes place under reaction with $Ag(NH_3)_2NO_3$. Scheme 39 shows an example of this methodology.
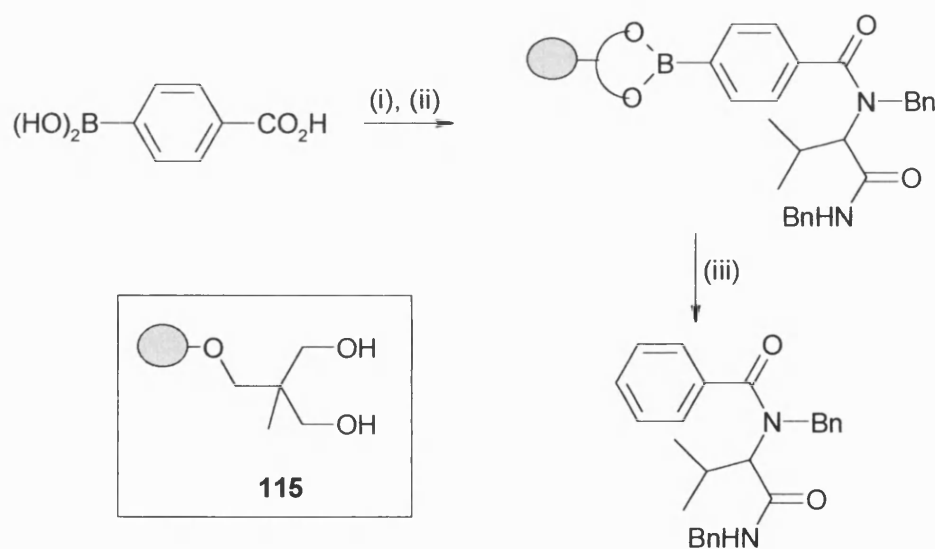
Scheme 39. (i) benzylamine, isobutyraldehyde, benzylisonitrile, MeOH, 60°C (ii) resin **115**, THF, reflux (iii) $Ag(NH_3)_2NO_3$, THF, reflux

1.2.5 Oxidation conditions

This section deals with the types of traceless linkers where the oxidation reaction either directly cleaves the linker from the desired molecule, or induces a rearrangement detaching the linker from the final product.

Sammelson and Kurth have reported an oxidation-Cope elimination cleavage procedure for the synthesis of *N*,*N*-disubstituted hydroxylamines from REM resin.[41] Michael addition of secondary amines to the REM resin **116** produces the corresponding tertiary β-amino ester **117**. This reacts with m-CPBA forming the *N*-oxide **118**, which finally undergoes Cope elimination to produce the *N*, *N*-disubstituted hydroxylamines **119** (Scheme 40).

The authors also describe an alternative approach, which allows the introduction of more diverse substituents in the final products (Scheme 41). Michael addition of a primary amine to **116** followed by reductive amination with a pyridine-borane complex in DMF/EtOH gives the tertiary amine **120**. As several different amines and aldehydes can be used a variety of products can be obtained. Examples of compounds synthesised using Scheme 40 include 1,2,3,4-tetrahydroisoquinolin-2-ol, methylbenzylhydroxylamine or 2,6-dimethylmorpholin-4-ol. Hexylpropylhydroxylamine or (4-nitrobenzyl)propylhydroxylamine are examples of products formed are outlined in Scheme 41.
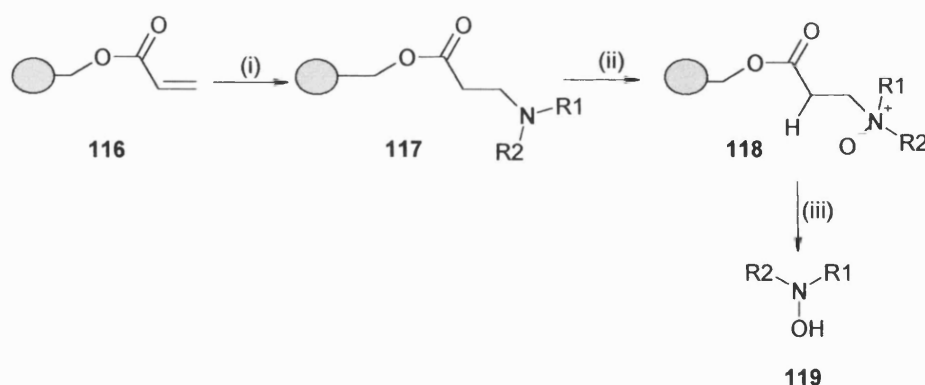
Scheme 40. (i) R1R2NH, DMF, rt (iii) m-CPBA, CHCl₃, rt
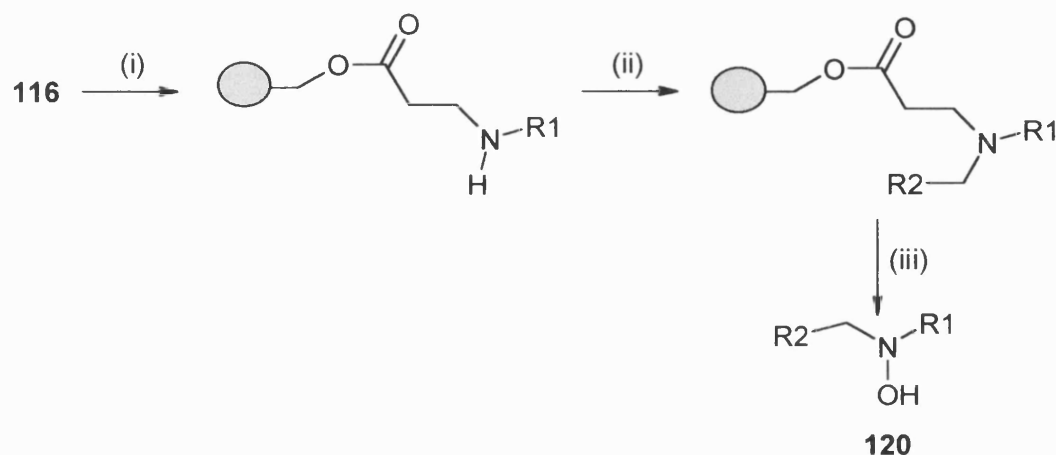
Scheme 41. (i) R_1NH_2, DMF, rt, (ii) R_2CHO, borano-pyridine complex, DMF/EtOH (4:1), rt, (iii) m-CPBA, CHCl$_3$, rt.

Timar and Gallagher described a procedure to synthesise a resin-bound 2-(thiobenzyl)ethyl carbamate **123** based on the ability of an N-vinyloxycarbonyl (VOC) derivative **121** to undergo addition of a benzylic thiyl radical **122** (Scheme 42). This provides a method for attaching secondary amines.[42] Oxidation of **123** with m-CPBA followed by treatment of the corresponding sulfone with DBU gives the amine **124**. This procedure allows one to use substrates containing amine-sensitive functionality, for example aminoketones.
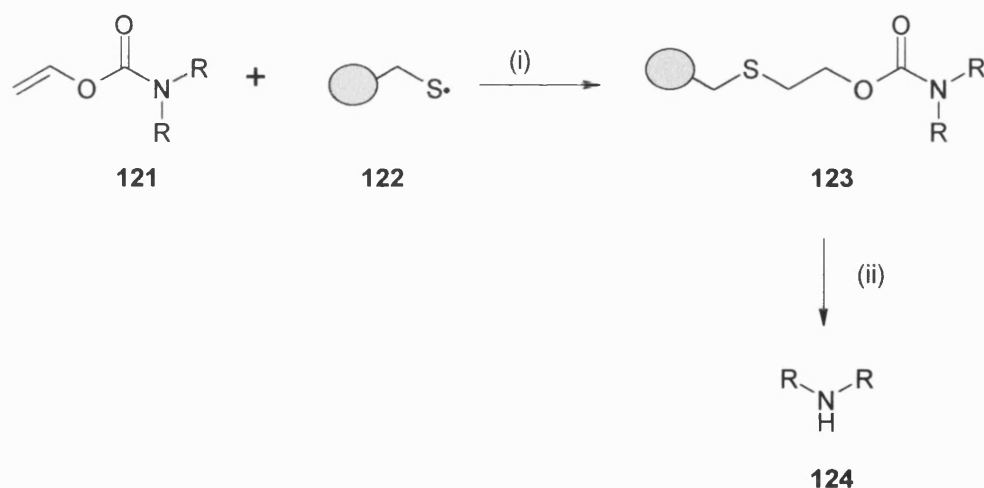
Scheme 42. (i) AIBN, DMF, 80°C, (ii) m-CPBA, CH$_2$Cl$_2$, then DBU, CH$_2$Cl$_2$, rt, 2h.

1.2.6 Photolytic cleavage

In work reported by Routledge et al. a photolabile traceless linker **127** was shown to act as an effective promoter of aliphatic C-H bond in solid-phase organic chemistry.[43]

The synthesis of linker **127** is depicted in Scheme 43. Initial alkylation of trityl protected 4-hydroxymercaptophenol with chloromethylpolystyrene gives resin bound adduct **125**. This undergoes resin deprotection, followed by reaction with 1,1-thiocarbonyldiimidazole to form **126**. Finally, displacement of imidazole with *N*-methylhydroxylamine provides resin bound linker **127**.

The authors used linker **127** to prepare 1,3-dimethylindole **129**. As illustrated in Scheme 44, attachment of N-methylindole-3-acetic acid to the linker **127** forms the adduct **128**, which cleaves under photolysis conditions at 350nm to give **129** in a low yield but high purity.
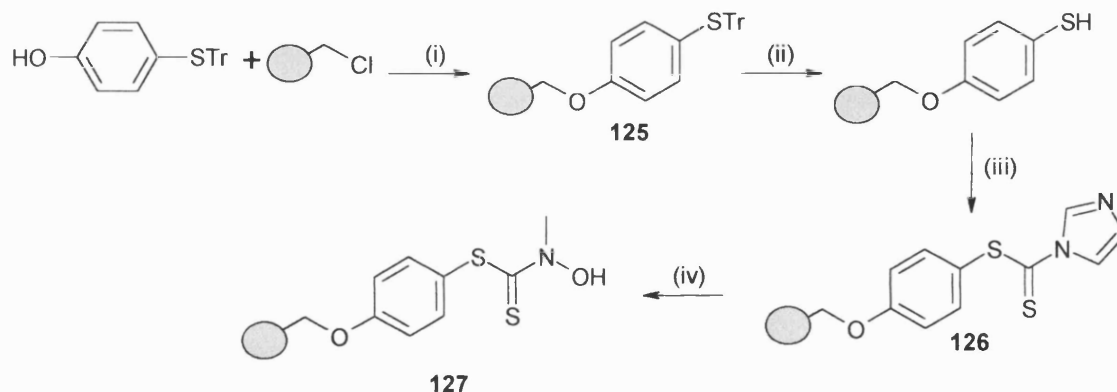
Scheme 43. (i) NaH, DMF, 60°C, 18 h, (ii) TFA:CH$_2$Cl$_2$:triethylsilane, (9:10:1), rt, 1h, (iii) 1,1-thiocarbonyldiimidazole, CH$_2$Cl$_2$, rt, 18 h, (iv) N-methylhydroxylamine hydrochloride, triethylamine, CH$_2$Cl$_2$, rt, 18 h.
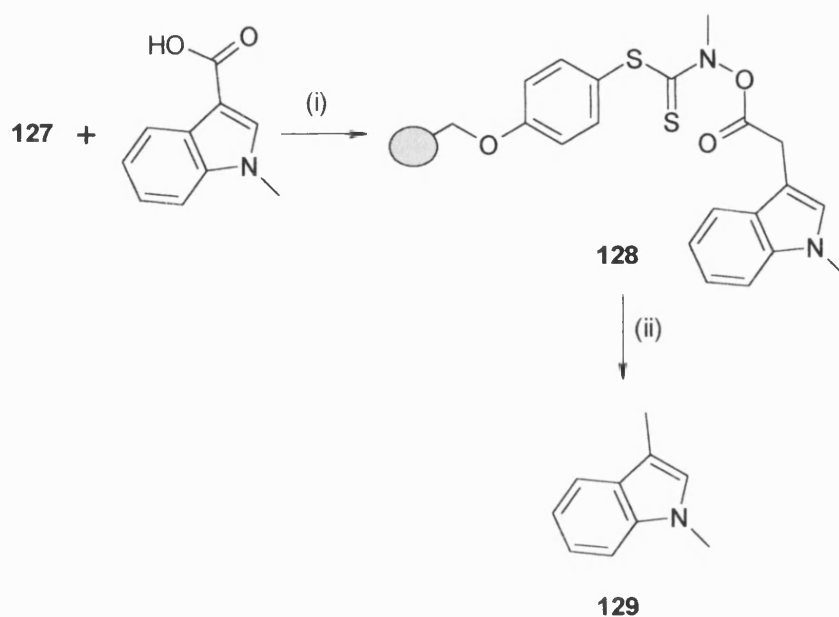
Scheme 44. (i) DIC, HOBt, DMAP, (ii) 2-methyl-2-propanethiol, 350nm.

1.2.7 Reductive cleavage

Kuster and Scheeren have published the synthesis of resin-bound nitroalkenes **132** and their applications in the production of libraries of cyclic arylethylamines **134** and bicyclic nitroso acetals **139**.[44]

They demonstrated that reduction of the ester linker with LiAlH$_4$ successfully cleaves the final products from the linker in a traceless manner.

Scheme 45 shows the two step synthesis of the resin-bound nitroalkenes **132**. Coupling of nitroacetic acid with the polystyrene based Wang resin **130** provides resin-bound nitroacetic acid **131**. This then reacts with diverse aldehydes *via* a microwave assisted Knoevenagel reaction to form **132**.
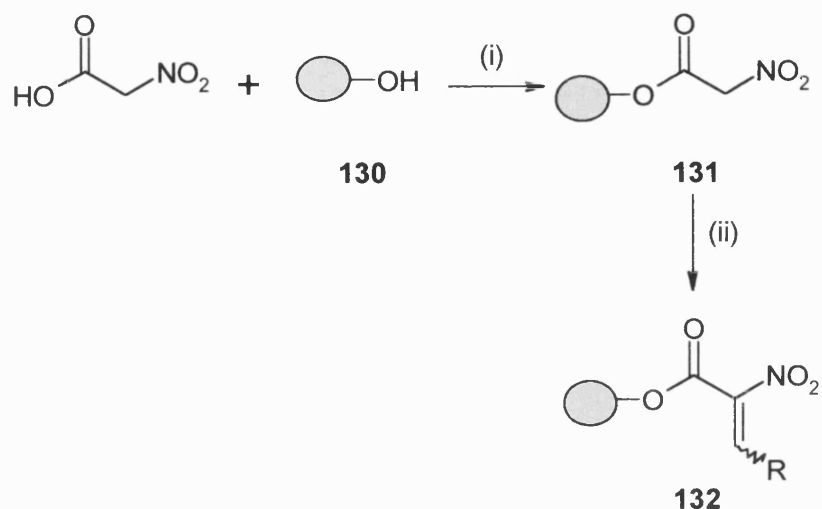
Scheme 45. (i) DIC/HOBT, (ii) RCHO, NH$_4$OAc, THF, 20 min., 350 W

This work shows a novel path for solid phase cycloaddition reactions involving nitroalkenes. Schemes 46 and 47 illustrate the conditions required for the production of cyclic arylethylamines and bicyclic nitroso acetals, respectively.

The former are synthesized by reaction of **132a** (R=Ph) with 2,3-dimethylbutadiene **133** through high pressure promoted Diels-Alder reaction. Subsequent reduction with LiAlH$_4$ gives selectively the *cis*-phenylethylamine **134**. Alternatively reduction of the nitro group to the amine with SnCl$_2$.H$_2$O, followed by reduction with LiAlH$_4$ gives cyclic phenylethylamino alcohol **135**.

In Scheme 47 one can see an attractive means of making bicyclic nitroso acetals **139**. Three component tandem [4+2]/[3+2] cycloaddition of **132a** acting as heterodiene, ethylvinyl ether **136** acting as a dienophile and styrene **137** acting as a dipolarophile yields various resin-bound adducts **138.** LiAlH$_4$ reduction gives the corresponding hydroxymethyl-substituted nitrosoacetals **139**.
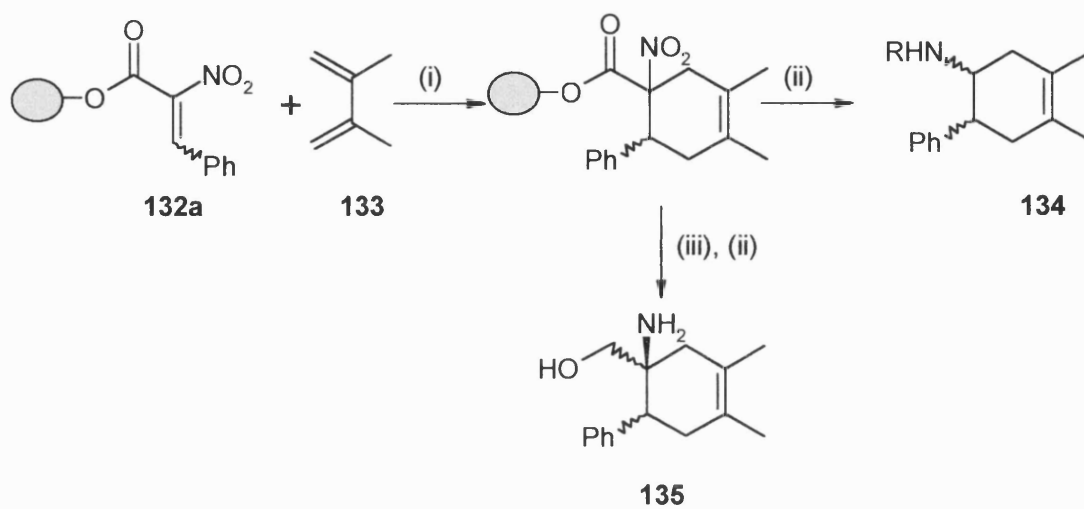
Scheme 46. (i) 15 Kbar, (ii) LiAlH$_4$, (iii) SnCl$_2$.H$_2$O.
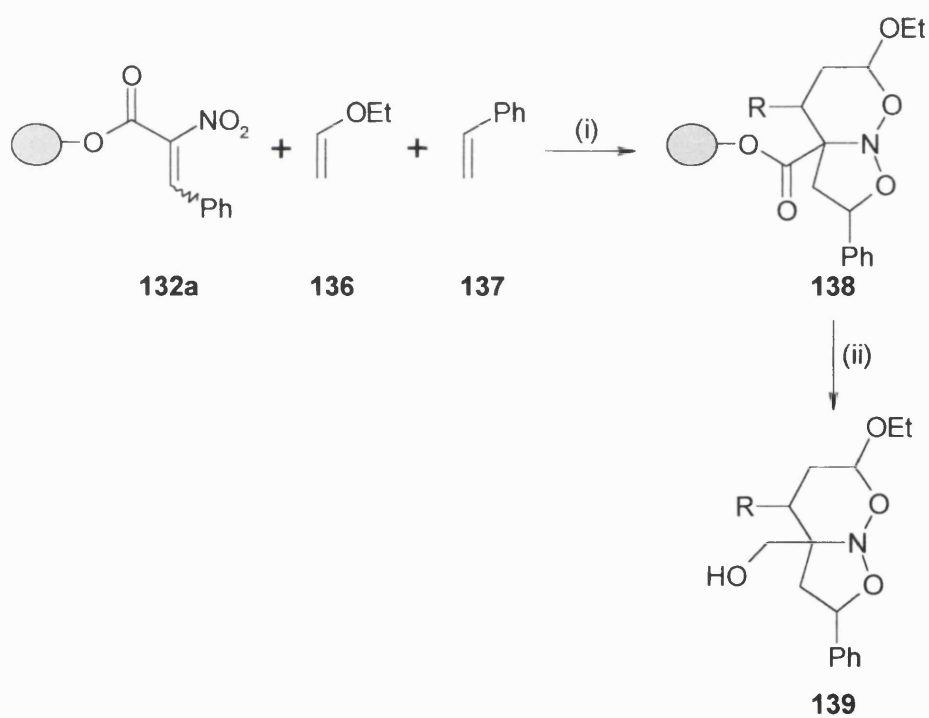
Scheme 47. (i) 15 Kbar, (ii) LiAlH$_4$

Recently, Pan and Holmes reported the synthesis of a novel perfluoroalkylsulfonyl (PFS) **140** linker and its use as a traceless linker in SPS (Scheme 48).[45]

Linker **140** allows the attachment of phenols to the solid phase via sulfonate formation and subsequent reductive cleavage of **141** to afford the parent arene **142**.

It is interesting to note that steric or electronic effects do not seem to affect the cleavage, and bulky compounds, such as arene **143** have been synthesized by this method.

140 → (i) → **141**

(ii)

Ar-H
142
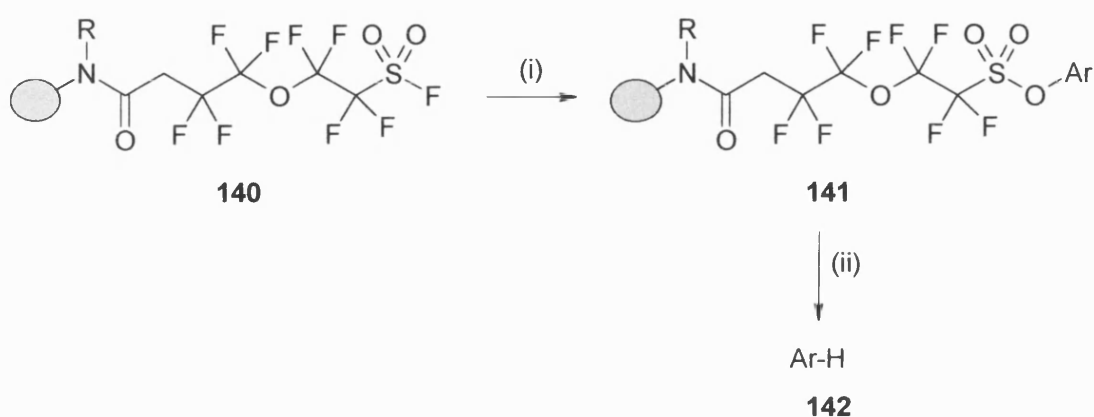
Scheme 48. (i) ArOH, K$_2$CO$_3$, DMF, (ii) Pd(OAc)$_2$, dppp, DMF, Et$_3$N, HCO$_2$H.

COCH$_3$
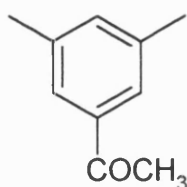
143

A group at Southampton University investigated a new method for synthesizing thioesters on a solid support and the cleavage conditions for their conversion into alcohols, ketones and lactones.[46] Merrifield resin is heated with aqueous DMF solutions of thioamides **144** in the presence of sodium iodide forming resin-bound adducts **145**. Adduct **145a** can be converted into alcohols **146** or ketones **147** either by reduction with lithium borohydride or by reaction with organocuprates,

respectively. Cleavage of an appropriate substituted thioester **145b** with boron trichloride gives the lactone **148** (Scheme 49).
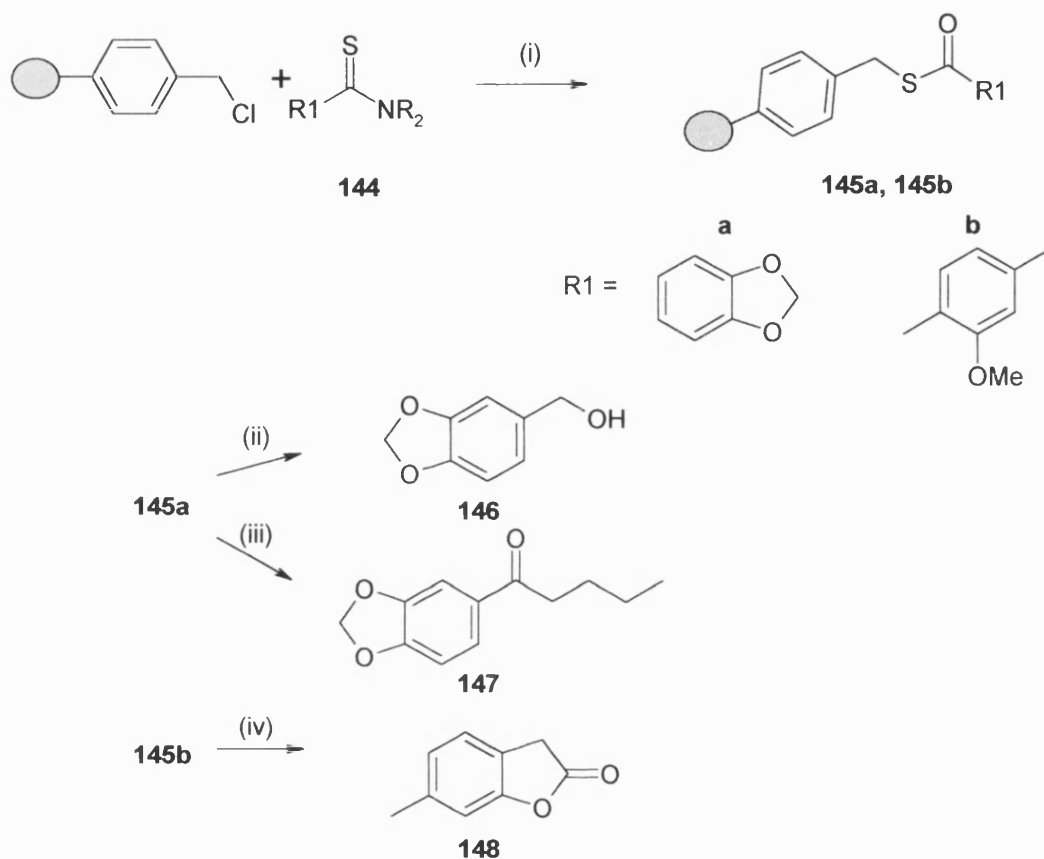
Scheme 49. (i) NaI, aq. DMF, Δ, (ii) LiBH₄, THF, rt, 5h, (iii) Bu₂CuLi, THF, -78°C, 5h, (iv) BCl₃, CH₂Cl₂, 0°C, 5h.

Formation of aliphatic C-H bonds is a topic of interest in organic chemistry that has been transferred to solid phase synthesis. In this context, Janda *et.al.* have developed new linkers and investigated their use in the production of aliphatic C-H bonds.[47]

In their earliest publication they described the synthesis of a MeO-PEG thiol linker **149**, which is obtained by the condensation of the homopolymer MeO-PEG with 2-amino-4-(trifluoromethyl) benzenethiol hydrochloride. Incorporation of alkyl molecules, such as bromide **150** takes place in the thiol position forming the alkylated MeO-PEG **151**, which is subjected to cleavage under reductive conditions

with Raney nickel affording compound **152**. Thus, through desulfurization a new C-H bond is formed (Scheme 50).
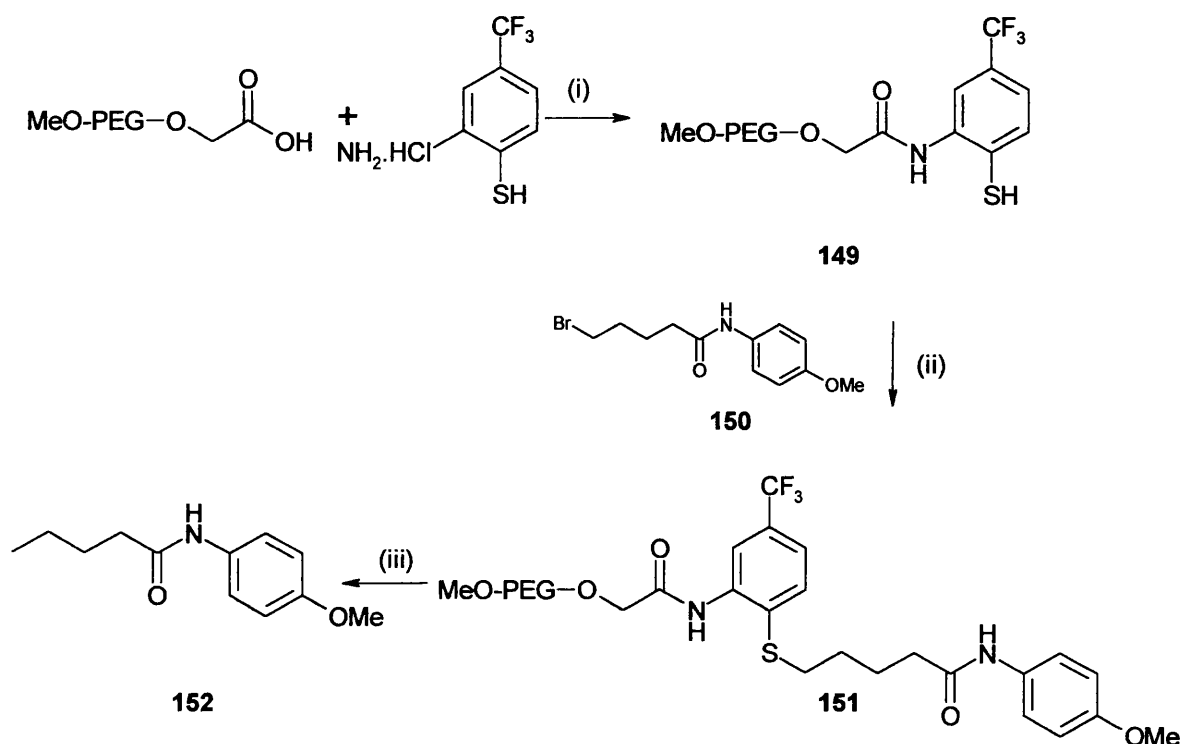
Scheme 50. (i) DIC, DMAP, THF-CH₂Cl₂ (1:1), 20°C, 16 h, (ii) Cs₂CO₃, DMF, 20°C, 4 h, (iii) H₂, Raney Ni, MeOH-EtOH (1.5:1), 20°C, 3 h.

The same group described the synthesis of linkers **155** and **158** (Scheme 51), using aromatic disulfides as starting materials instead of a thiol (this undergoes oxidation making it difficult to synthesise the desired target). Condensation of the homopolymer MeO-PEG **153** with 4-aminophenyl disulfide **154** or MeO-PEG amine **156** with 2,2'-dithiosalicylic acid **157** followed by reduction with dithiothreitol produces linkers **155** and **158**, respectively.[48]

Synthesis of compound **152** using linkers **155** and **158** is based on the same methodology shown in Scheme 50, confirming their utility as traceless linkers.
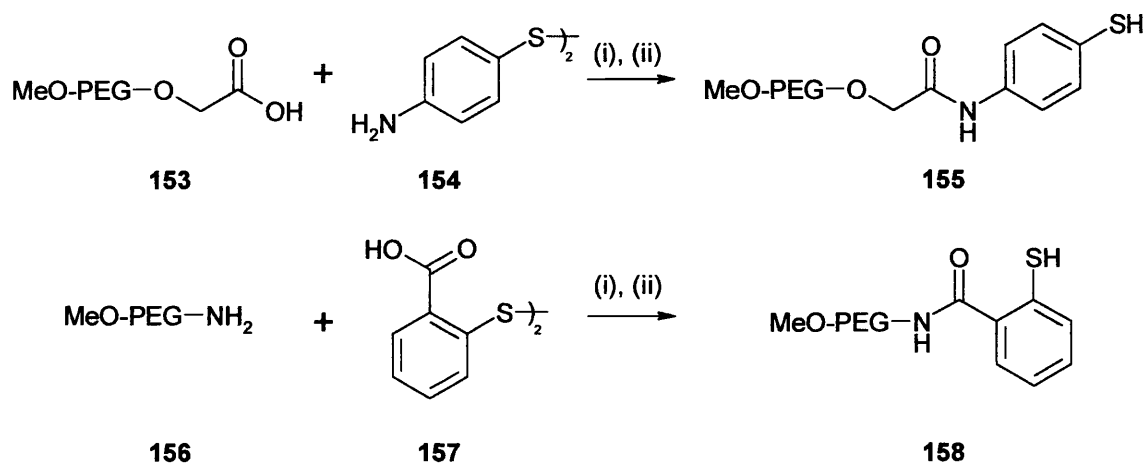
Scheme 51. (i) DIC, DMAP, CH₂Cl₂, 20 °C, 16 h, (ii) DTT, H₂O, reflux, 3h.

In a related article, they subsequently described a more extensive strategy for the formation of C-H aliphatic bonds.[49] This new approach involves oxidation of the polymeric linker sulfide to the corresponding sulfone, followed by reduction with Na/Hg. The use of the highly chemoselective oxidizing agent potassium hydrogen persulfate (KHSO₅) instead of m-CPBA and the reducing agent Na/Hg in place of Raney nickel allows the introduction of a diverse range of functional groups in the molecule, such as olefines and ketones that otherwise would be affected by the cleavage conditions.

As illustrated in Scheme 52 a benzyl amide derivative **162** is obtained by alkylation of the linker **159** with bromide **160** giving the polymeric linker sulfide **161**. This finally undergoes cleavage via the two-step oxidation-reduction sequence as shown to give **162**.
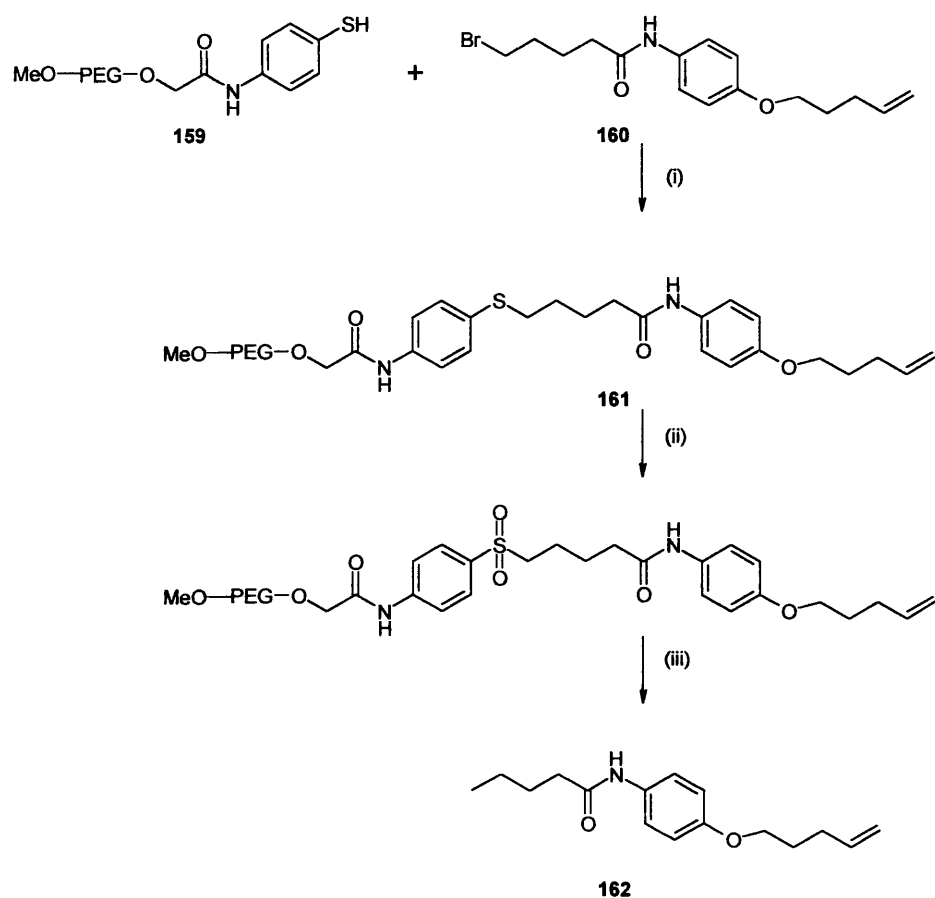
Scheme 52. (i) Cs$_2$CO$_3$, DMF, 20°C, 15h, (ii) KHSO$_5$, H$_2$O, 20°C, 3h, (iii) 5% Na-Hg, Na$_2$HPO$_4$, MeOH, -40°C→-20°C→0°C.

Replacement of the amide bond in the polymeric linker **159** with an ether moiety provides a more versatile linker **167**, as outlined in a publication by the same group.[50] Linker **167** is formed by mesylation of poly(ethylene glycol) methyl ether **163**, followed by treatment with the disulfide **164**, and finally reduction of the mixture **165** and **166** with DTT (Scheme 53).

MeO-PEG—OH $\xrightarrow{\text{(i)}}$ MeO-PEG—OMs

163

HO—⟨ ⟩—S—S—⟨ ⟩—OH
(ii)   **164**

MeO-PEG—O—⟨ ⟩—S—S—⟨ ⟩—OH **+** MeO-PEG—O—⟨ ⟩—S—)$_2$

165   **166**

(iii)

MeO-PEG—O—⟨ ⟩—SH

167
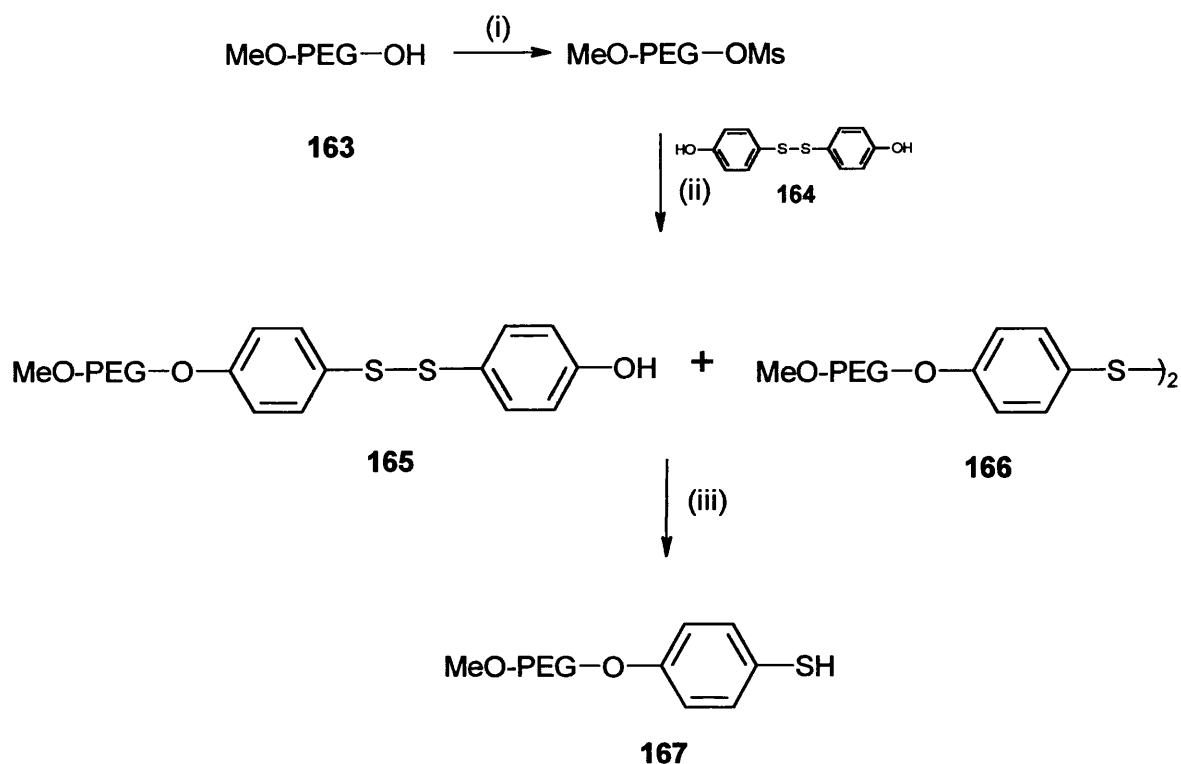
Scheme 53. (i) MsCl, Et$_3$N, rt, 12h, (ii) Cs$_2$CO$_3$, DMF, 65 °C, 6h, (iii) DTT, H$_2$O, reflux, 3 h.

Alkylation of linker **167** with symmetric dihalides **168** gives sulfide **169** that acts as a polymeric alkylating agent.

As depicted in Scheme 54, introduction of malonate into the polymer amplifies the range of transformations in the linker as this can be further alkylated. When **170** contains an aromatic ring, this undergoes oxidation of the polymeric linker sulfide to the corresponding sulfone, followed by reduction with Na/Hg to give the desired molecule **171** (Scheme 55).

However, cleavage of a non-benzylic sulfone under the same conditions does not produce satisfactory results. The cleavage conditions were examined. Results indicate that the reductive cleavage is solvent sensitive and that a combination of MeOH/DMF (1/8) is a good solvent system for desulfonylation.[51]
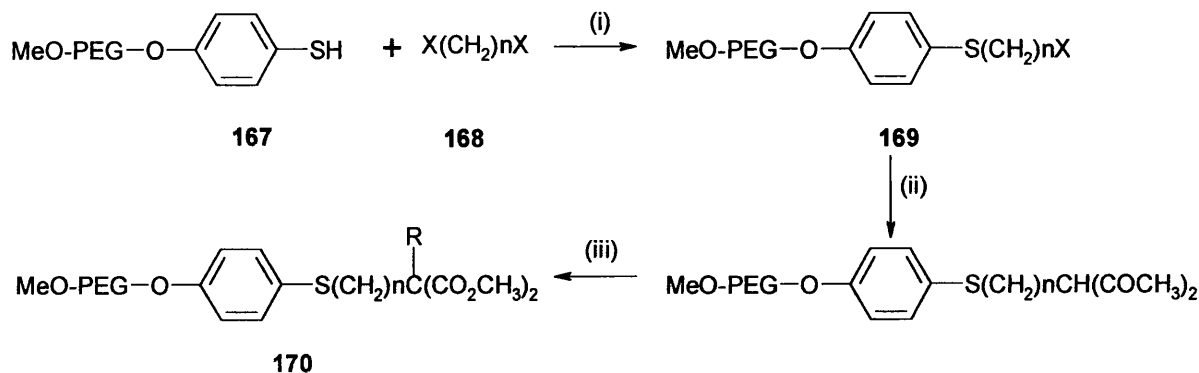
Scheme 54. (i) Cs₂CO₃, DMF, rt, 14 h, (ii) CH₂(CO₂CH₃)₂, Cs₂CO₃, DMF, rt, 18 h, (iii) RX, Cs₂CO₃, DMF, rt, 19 h.
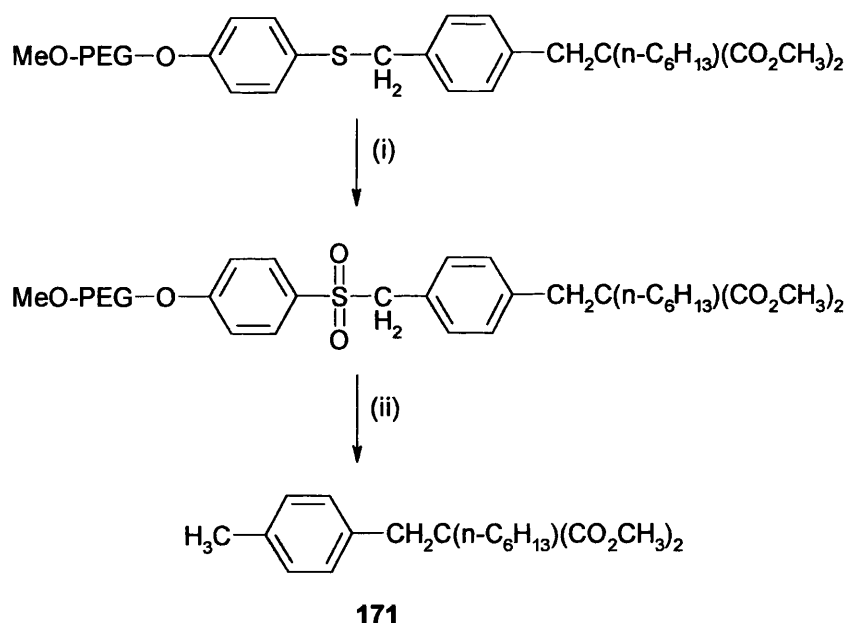
Scheme 55. (i) KHSO₅, H₂O, 20°C, 3h, (ii) 5% Na-Hg, Na₂HPO₄, THF-MeOH (1:1), -40°C→0°C.

A group at Cambridge has described the synthesis of amides and ureas using a hydroxylamine linker, which releases the products after reductive cleavage of N-O bond the using samarium (II) iodide.[52] Although the yields of the products are quite modest (30-54%), this paper offers a new methodology to cleave the N-O bond, by using SmI₂ the cleavage does not require acidic conditions.

Starting by acylation of a Wang-based hydroxylamine resin, followed by alkylation of the hydroxamic nitrogen provides the resin-bound adduct **172**. As shown in Scheme 56 reductive cleavage of **172** gives the desired products **173**. Amide **174** and urea **175** are examples of compounds obtained by this method.

172   **173**
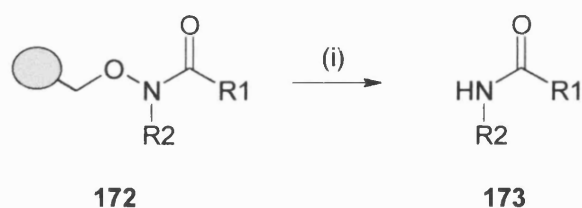
Scheme 56. SmI$_2$/THF, 25°C, 3h.

174   **175**
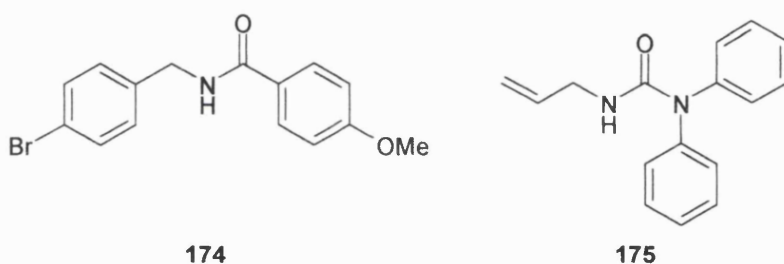
1.2.8 Thermolytic cleavage

Dithiocarbamates are known to fragment upon thermolysis into the corresponding isothiocyanate and alkylthiol in the presence of silver or mercury salts at high temperatures. Wagner and Mioskowski have developed a traceless linker for thioureas based on a modification of this methodology.[53]

Condensation of a primary amine with carbon disulfide in the presence of the Merrifield resin forms the resin-bound dithiocarbamates **176**. As illustrated in Scheme 57 thermolytic cleavage of **176** at 60°C using a primary or secondary amine as nucleophiles gives the corresponding thioureas **177**. The thiourea

formation is shown to be dependent on steric hindrance and the nucleophilicity of the amine used in the cleavage reaction.

176   **177**
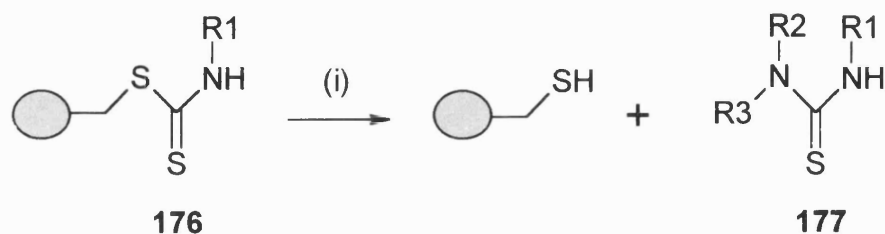
Scheme 57. (i) R1R2NH, 60 °C

It is worth noting that the mild reaction conditions required for the cleavage are compatible with diverse functional groups. Thioureas, such as **178** has been prepared by this method with a yield of 97%.

178
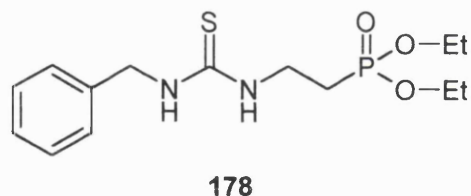
Based on the intermediate resin-bound dithiocarbamates **176**, the same authors have also described the synthesis of *N,N',N''* trisubstituted guanidines.[54] In contrast to the traceless strategies for guanidines previously described in this review, this procedure does not involve acidic cleavage of the linker, but thermolytic conditions at 100 °C in the presence of an excess of primary amine in toluene for 60 h.

The method consists of formation of supported isothiourea **179**, by reaction of **176** with an excess of oxalyl chloride, followed by an excess of primary amine in toluene. Finally, thermolytic cleavage gives the guanidines **180** as depicted in Scheme 58.
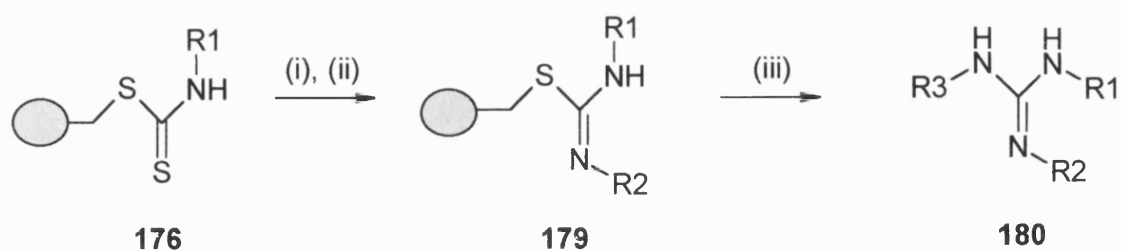
Scheme 58. (i) COCl$_2$, toluene, 60°C, 12 h, (ii) R2NH$_2$, toluene, 60°C, 12 h, (iii) R3NH$_2$, toluene, 100°C, 60 h.

The reaction conditions used in this four-step process are compatible with different functional groups, however only primary amines can be used by this method since the nucleophilic substitution of thioalkyl appears to be sensitive to steric hindrance. Trisubstituted guanidine **181** (42% yield) is an example of compounds obtained by this method.

181
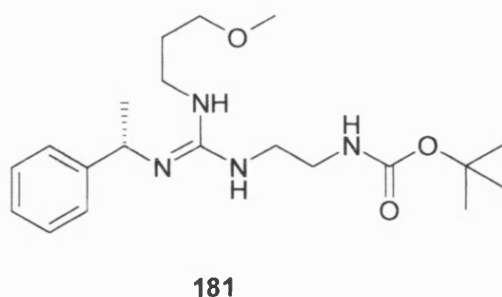
Paio and collaborators have recently reported the application of a resin-bound benzotriazole for the preparation of unsymmetrical aryl ureas.[55] The formation of the traceless linker takes place in one step by coupling of benzotriazole-5-carboxylic acid with polystyrene-polyoxyethylene-amino (AG-NH$_2$) or aminomethyl-polystyrene (AM-PS) resins, showing that the later releases the products in high purity. Besides being a single step synthesis, this approach shows the advantage that the benzotriazole nucleus does not need any protection at the reactive nitrogen, but is often needed in others method. The resin-bound benzotriazole is converted into the corresponding supported carbonyl chloride,

which reacts with arylamines to form the supported urea derivatives **183**. As Scheme 59 shows, release of the products occurs by reaction of **182** with an amine at high temperature in a suitable solvent, chlorobenzene at 100°C, provides the best results.
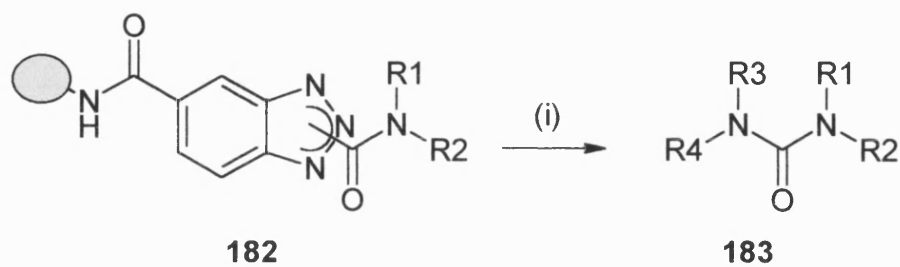
Scheme 59. (i) NHR3R4, 100°C, chlorobenzene.
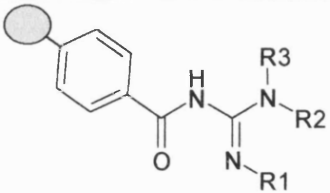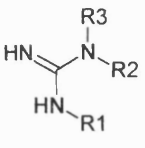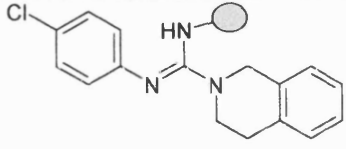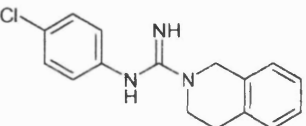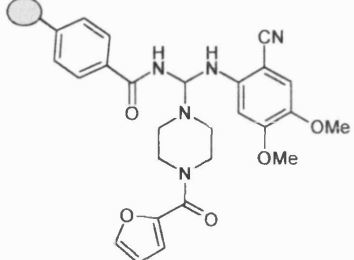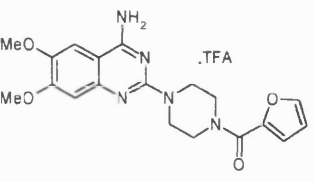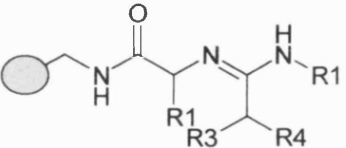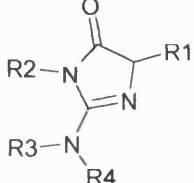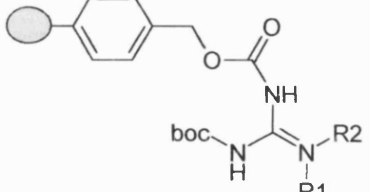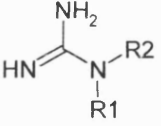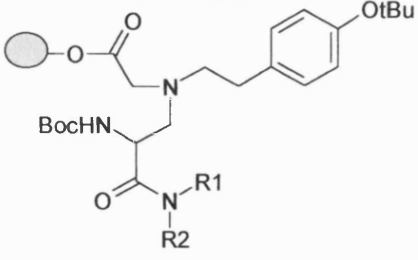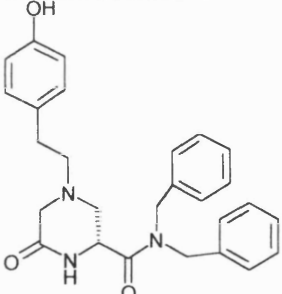
1.2 Table Summary

Table 2 displays a summary of the traceless linkers here described as well as the compounds formed after the cleavage, cleavage conditions and number of the reference.

R = Reference
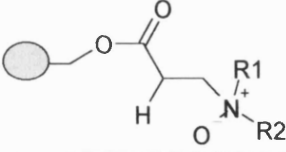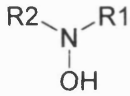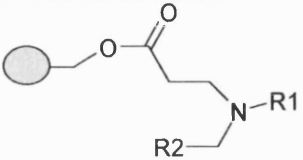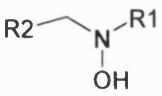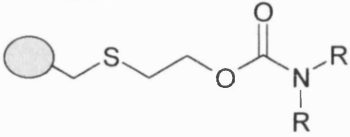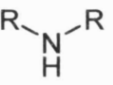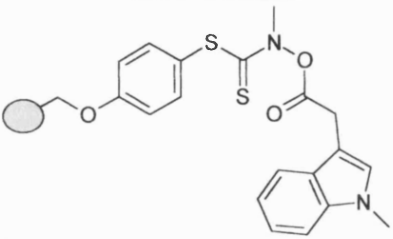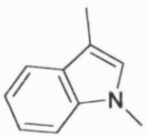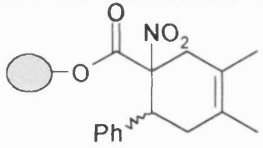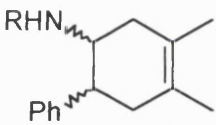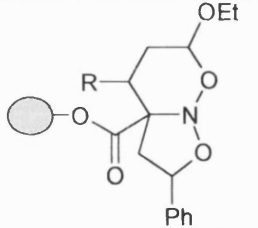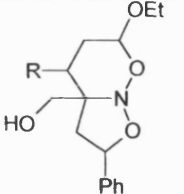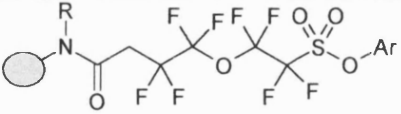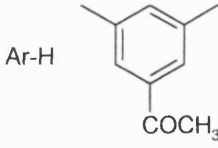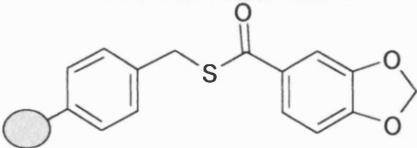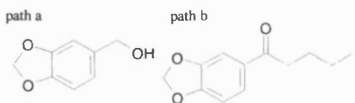
Linker	Product	Reagent	R
		M=Si HF M=Ge TFA	**8**
		Bu₄NF	**9**
		TFA, 25°C	**10**
		TBAF, 65°C	**11**

		CsF, 60°C or TBAF 45°C	**12**
		TBAF	**13**
		TFA or Br$_2$	**15**
		Br$_2$	**18**
		Br$_2$	**18**
		Br$_2$	**18**
	R= Br R= Ar R=	1,2 dihidro benzene ACN	**19**

		TFA/ CHCl₃/ MeOH	20
		TFA/ CH₂Cl₂ rt	21
		TFA/ H₂O 80°C	22
		10% AcOH/ CH₂Cl₂ rt	23
		TFA/ CH₂Cl₂	24
		TFA/5% H₂O	25

(structure with R1, R2, R3, O, N)	path a / path b structures; R1 R2 R3 R4: C$_6$H$_4$(4-OMe) H n-C$_4$H$_9$ Me; C$_6$H$_4$(4-Cl) H n-C$_4$H$_9$ CH$_2$OAc	path a: R4COCl; path b: R4COCl NH$_4$OAc AcOH 90°C	**26**
(triazene structure with R1, R2)	R1/R2 structures: CO$_2$tBu, H, HO OH CO$_2$tBu	THF/HCl 10:1	**27**
(piperazine triazene biphenyl structure)	(cyclopentene biphenyl structure)	TFA Pd(OAc)$_2$ cyclopentene 40°C	**28**
(quinoxalinone structure X, R1, R2, R3)	(quinoxalinone structure X, R1, R2, R3)	TFA, air oxidation	**29**
MeO$_2$C ... CH$_2$SPh, N–SO$_2$–Ar	MeO$_2$C ... CH$_2$SPh, N–H	TBAF 70°C	**30**
(benzimidazolium structure, F, sulfone)	(benzimidazole structure, F, benzyl)	Et$_3$N/ CH$_2$Cl$_2$	**31**

Substrate	Product	Conditions	#
		Me₂NH	32
		Et₃N/ CH₂Cl₂	33
		n=1 ICl CH₂Cl₂ -78°C n=3 I₂ CH₂Cl₂ rt	34
		100°C toluene	35
		NaO*t*Bu/ THF 60°C	36
		Grubbs catalyst/ reflux	37
		30% AcOH/ MeOH rt	38
		C₆H₆ benzoquinones or indoanilines	39
		Ag(NH₃) NO₃, THF, reflux	40

		m-CPBA CHCl₃ rt	41

Structure (bead ester betaine)	R2–N(OH)–R1	m-CPBA CHCl₃ rt	**41**
Structure (bead ester, N–R1, R2)	R2–CH₂–N(OH)–R1	m-CPBA CHCl₃ rt	**41**
Structure (bead S-ethyl carbamate N(R)R)	R–N(H)–R	m-CPBA CH₂Cl₂ DBU CH₂Cl₂ rt	**42**
Structure (bead O-phenyl dithiocarbamate, N-methyl indole)	3-methyl-1-methylindole	350nm	**43**
Structure (NO₂, Ph, dimethyl cyclohexene ester)	RHN... Ph dimethyl cyclohexene	LiAlH₄	**44**
Structure (OEt bicyclic R, Ph)	OEt R HO N O O Ph	LiAlH₄	**44**
Structure (N-R amide perfluoro sulfonate Ar)	Ar–H, 3,5-dimethyl, COCH₃	Pd(OAc)₂ ddpp, DMF, Et₃N, HCO₂H	**45**
Structure (bead phenyl methyl thioester benzodioxole)	path a / path b	path a LiBH₄ path b Bu₂CuLi	**46**

		H$_2$, Raney Ni	**47**
		5% Na-Hg Na$_2$HPO$_4$	**49**
		SmI$_2$	**52**
		R2R3NH 60°C	**53**
		R3NH$_2$ toluene 100°C	**54**
		R3R4NH 100°C	**55**

1.4 Summary

Over the last few years, various types of traceless linkers have been synthesized. These have provided different libraries of small compounds. We attempted in this review to give a general idea of those reported in the literature.

References for Review

1 Terrett, N. K.; *Combinatorial chemistry*, Oxford University Press: New York **1998**

2 Obrecht, D.; Villalgordo, J. M. *Solid-supported combinatorial and parallel synthesis of small-molecular-weight compound libraries*, Pergamon: Oxford **1998**

3 Brase, S.; Dahmen, S. *Chem. Eur. J.* **2000**, *6*, 1899-1905.

4 Eggenweiler, H-M, *DDT.* **1998**, *3* (12), 552-560.

5 Brase S. http://www.teknoarticles.com/co/2000/cosep/2brase.htm

6 Guiller, F.; Orain, D.; Bradley, M. *Chem. Rev.* **2000**, *100*, 2091-2157.

7 Plunkett, M. J.; Ellman, J. A. *J. Org. Chem.* **1995**, *60*, 6006-6007.

8 Plunkett, M. J.; Ellman, J. A. *J. Org. Chem.* **1997**, *62*, 2885-2893.

9 Woolard, F. X.; Paetsch, J.; Ellman. J.A. *J. Org. Chem.* **1997**, *62*, 6102-6103.

10 Chenera, B.; Finkelstein, J. A.; Veber, D. F. *J. Am. Chem. Soc.* **1995**, *117*, 11999-12000.

11 Boehm, T. L.; Showalter, H. D. *J. Org. Chem.* **1996**, *61*, 6498-6499

12 Harikrishnan, L. S.; Showalter, H. D. *Tetrahedron* **2000**, *56*, 515-519.

13 Briehm, C. A.; Kirschbaum, T.; Bauerle, P. *J. Org. Chem.* **2000**, *65*, 352-359.

14 Hu, Y.; Porco, J. A. Jr.; Labadie, J. W.; Gooding, O. W, Trost, B. M. *J. Org. Chem.* **1998**, *63*, 4518-4521.

15 Lee, Y.; Silverman, R. B. *J. Am. Chem. Soc.* **1999**, *121*, 8407-8408.

16 Lee, Y.; Silverman, R. B.. *Organic Letters.* **2000**, *2*(3), 303-306.

17 Lee, Y.; Silverman, R. B. http://www.unibas.ch/mdpi/ecsoc-4/b0013/b0013.htm

18 Lee, Y.; Silverman, R. B. *Tetrahedron* **2001**, 57, 5339-5352.

19 Tacke, R.; Ulmer, B.; Wagner, B.; Arlt, M. *Organometallics* **2000**, *19*, 5297-5309.

20 Wilson, L. J.; Klopfenstein, S. R.; Li M. *Tetrahedron Lett.* **1999**, *40*, 3999-4002.

21 Min, L.; Wilson, L. J.; Portlock, D.E. *Tetrahedron Lett.* **2001**, *42*, 2273-2275.

22 Wilson, L. J. *Organic Letters.* **2001**, *3*, 585-588.

23 Min. L.; Wilson, L. J. *Tetrahedron Lett.* **2001**, *42*, 1455-1458.

24 Zapf, C. W.; Creighton, C. J.; Tomioka, M.; Goodman, M. *Organic Letters.* **2001**, *3* (8), 1133-1136.

25 Shreder, K.; Zhang, L.; Gleeson, J-P.; Ericcson, J.A.; Yalamoori, V.V.; Goddman, M. *J. Comb. Chem.* **1999**, *1*, 383-387.

26 Lee, H. B.; Balasubramamian, S. *Organic Letters.* **2000**, *2* (3), 323-326.

27 Brase, S.; Enders, D.; Kobberling, J.; Avemaria, F. *Angew. Chem. Int. Ed.* **1998**, *37*, 3413-3415.

28 Brase, S.; Schroen, M. *Angew. Chem.* **1999**, *111*, 1139-1142.

29 Krchnak, V.; Szabo, L.; Vagner, J. *Tetrahedron Lett.* **2000**, *41*, 2835-2838.

30 Zhang, H-C.; Ye, H.; Moretto, A. F.; Brumfield, K. K.; Maryanoff, B. E. *Organic Letters.* **2000**, *2* (1), 89-92.

31 Tumelty, D.; Cao, K.; Holmes, C. P. *Organic Letters.* **2001**, *3*(1), 83-86.

32 Wade, W. S.; Yang, F.; Sowin, T.J. *J. Comb. Chem.* **2000**, *2*, 266-275.

33 Blaney, P.; Grigg, R.; Rankovic, Z.; Thoroughgood, M. *Tetrahedron Lett.* **2000**, *41*, 6635-6638.

34 Ockey, D. A.; Lane, D. R.; Seeley, J. A.; Schore, N. E. *Tetrahedron* **2000**, *56*, 711-717.

35 Tietze, L. F.; Steinmetz, A. *Synlett.* **1996**, 667-668.

36 Mayer, J. P.; Zhang, J.; Lenz, D. M.; Gaudino, J. J. *Tetrahedron Lett.* **1996**, *37*, 8081-8084.

37 Brown, R. C. D.; Castro, J. L.; Moriggi, J-D. *Tetrahedron Lett.* **2000**, *41*, 3681 -3685.

38 Wang, B.; Chen, L.; Kim, K. *Tetrahedron Lett*, **2001**, *42*, 1463-1466.

39 Hong, B-C.; Chen, Z-Y.; Chen, W-H. *Organic Letters.* **2000**, *2* (17), 2647 -2649.

40 Pourbaix, C.; Carreaux, F.; Carboni, B.; Deleuze, H. *Chem. Commun.* **2000**, 1275-1276.

41 Sammelson, R. E.; Kurth, M. J. *Tetrahedron Lett.* **2001**, *42*, 3419-3422.

42 Timar, Z.; Gallagher T. *Tetrahedron Lett*, **2000**, *41*, 3173-3176.

43 Horton, J. R.; Stamp, L. M.; Routledge, A. *Tetrahedron Lett,* **2000,** *41,* 9181
    -9184.

44 Kuster, G. J.; Scheeren, H. W. *Tetrahedron Lett.* **2000,** *41,* 515-519.

45 Pan, Y.; Holmes, C. P. *Organic Letters.* **2001,** 3-4.

46 May, P. J.; Bradley, M.; Harrowven, D. C.; Pallin, D. *Tetrahedron Lett.* **2000,**
    41, 1627-1630.

47 Zhao, X.; Jung, K. W.; Janda, K. D. *Tetrahedron Lett,* **1996,** *37,* (36), 6491
    -6494.

48 Zhao, X.; Jung, K. W.; Janda, K. D. *Tetrahedron* **1997,** 53, (19), 6645-6652.

49 Zhao, X.; Jung, K. W.; Janda, K. D. *Tetrahedron Lett,* **1997,** *38,* (6), 977-980.

50 Zhao, X.; Jung, K. W.; Janda, K. D. *Tetrahedron Lett,* **1997,** *38,* (31), 5437
    -5440.

51 Zhao, X.; Jung, K. W.; Janda, K. D. *Tetrahedron Lett,* **1998,** *8,* 2439-2442.

52 Myers, R. M.; Langston, S. P.; Conway, S. P.; Abell, C. *Organic Letters.* **2000,**
    2, (10), 1349-1352.

53 Gomez, L.; Gellibert, F.; Wagner, A.; Mioskowski, C. *J. Comb. Chem.* **2000,** *2,*
    75-79.

54 Gomez, L.; Gellibert, F.; Wagner, A.; Mioskowski. *Chem. Eur. J.* **2000,** *6* (21),
    4016-4020

55 Paio, A.; Crespo, R. F.; Seneci, P.; Ciraco, M. *J. Comb. Chem.* **2001,** *3,* 354-
    359.

CHAPTER TWO

Application of Photoaffinity labeling to soluble Guanylate cyclase.

2.1 Introduction

Cells in a multicellular organism need to communicate with one another in order to regulate their development and organization into tissues, control their growth and division, and coordinate their functions. Biological signal transduction pathways control the essential functions in all cells and tissues. The nitric oxide-soluble guanylate cyclase-cyclic guanosine-3′,5′-monophosphate (NO-sGC-cGMP) pathway is one fascinating example that nature has developed for this purpose. Some of its many physiological functions include inhibition of platelet aggregation, smooth muscle relaxation and neurotransmission. By gaining a better understanding of the mechanisms of this pathway at the molecular level the development of new selective medicines may be possible.

2.1.1 Soluble Guanylate Cyclase

The Guanylate Cyclases (GC) are a family of enzymes that catalyse the conversion of guanosine-5′-triphosphate (GTP) to cyclic guanosine-3′,5′-monophosphate (cGMP) with concomitant production of pyrophosphate (PPi) (Figure 1).[1] There are two general classes of the cyclase, particulate guanylate cyclase (pGC) and soluble guanylate cyclase (sGC).[2] The two systems known to generate cGMP are markedly different. Isoforms of pGC are activated by peptide ligands which bind to cell membrane receptors. These receptors have transmembrane domains contiguous with an intracellular guanylyl cyclase. sGC on the other hand is a heme-containing heterodimeric enzyme and is the major receptor for the intercellular signalling agent nitric oxide (NO).[3]
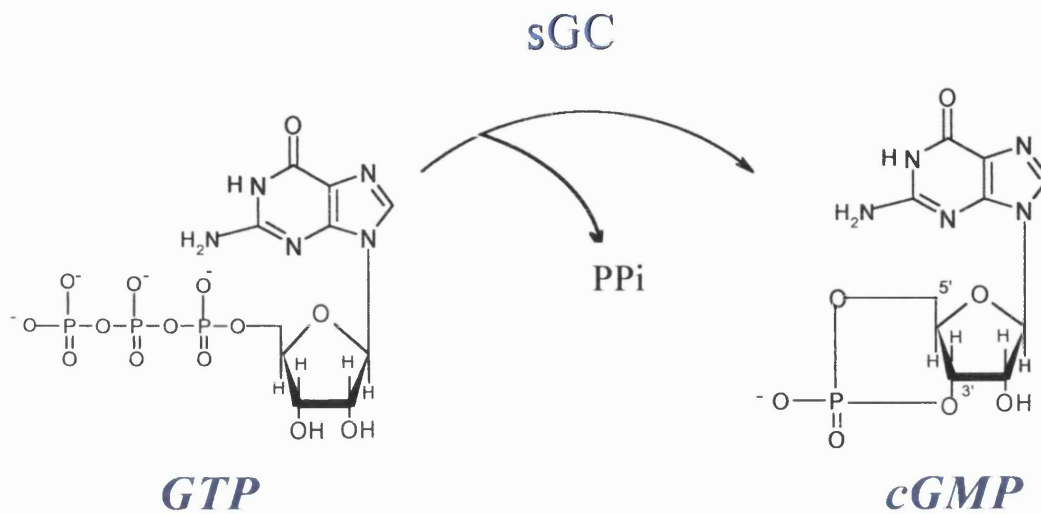
Figure 1. Synthesis of cGMP by sGC

Cyclic guanosine-3′,5′-monophosphate, a primary signalling molecule in biological systems, is capable of modulating a diverse number of cellular functions and regulates a variety of enzymes and proteins including ion channels, phosphodiesterases, and cGMP- dependent protein kinases.[4] Thus, by formation of the intracellular signalling molecule cGMP, guanylyl cyclase plays a key role in smooth muscle relaxation and inhibition of platelet agreggation.

Since the identification of the endothelial relaxation factor (EDRF) as nitric oxide,[5] interest in sGC has increased, and now we have a better insight into the interesting NO-sGC-cGMP signaling system. However, there is still much to be learnt about the mechanism by which nitric oxide and other small molecules activate sGC.

2.1.1.1 Properties and Structure of sGC

sGC exists as a heterodimeric heme protein,[6] with a total molecular mass of about 150 kDa, and is comprised of an α and a β subunit of which four types exist (α_1, β_1, α_2, β_2). The subunits show sequence homology with each other especially in the C-terminal region, where they also show homology with adenylate cyclase (AC) and particulate guanylate cyclase.

All the subtypes show various degrees of expression in different tissues. The $\alpha_1\beta_1$ isoform is widely expressed and is the first one that has been shown to exist at the protein level in animal tissues. Originally, sGC was purified from bovine and rat lung showing that the heterodimer consists of a large subunit with a molecular mass of 73 KDa (bovine)[7] or 82 KDa (rat)[8] and of a smaller one of 70 KDa,[9,10] representing the α_1 and β_1 components, respectively.

Expression experiments revealed that coexpresion of both subunits is required to form a catalytically active enzyme.[11] In addition to the $\alpha_1\beta_1$ isoform, the α_2 subunit has been shown to form an active heterodimer with the β_1[12] and in 1998 Russwurn et al. demonstrated the existence of an $\alpha_2\beta_1$ isoform in vivo in human placenta.[13] α_2 Seems to have a more restricted expression pattern than α_1, and although they have differences in the primary structure, both subunits seem to be functionally alike. The same can not be said for the interchangeability of the β subunit, with most publications indicating that β_2 is unable to generate an active heterodimer. Gupta et al. have reported that $\alpha_1\beta_2$ forms an active heterodimer, although the NO-stimulated cGMP formation is much lower than for the $\alpha_1\beta_1$ isoform.[14] The β_2 subunit shows some structural differences when compared with β_1, mainly, the former has an 86 amino acid C-terminal region that extends beyond the C-terminal of β_1 which contains a consensus sequence for isoprenylation/carboxymethylation (-CVVL).[15]

It has been accepted that subunits isolated from adult human brain, termed α_3 and β_3 represent the human forms of rat α_1 and β_1 and are not additional isoforms. This is based on sequence homology.[16]

The protein structure can be divided into three domains: catalytic, regulatory (heme binding) and dimerization (Figure 2).[17]
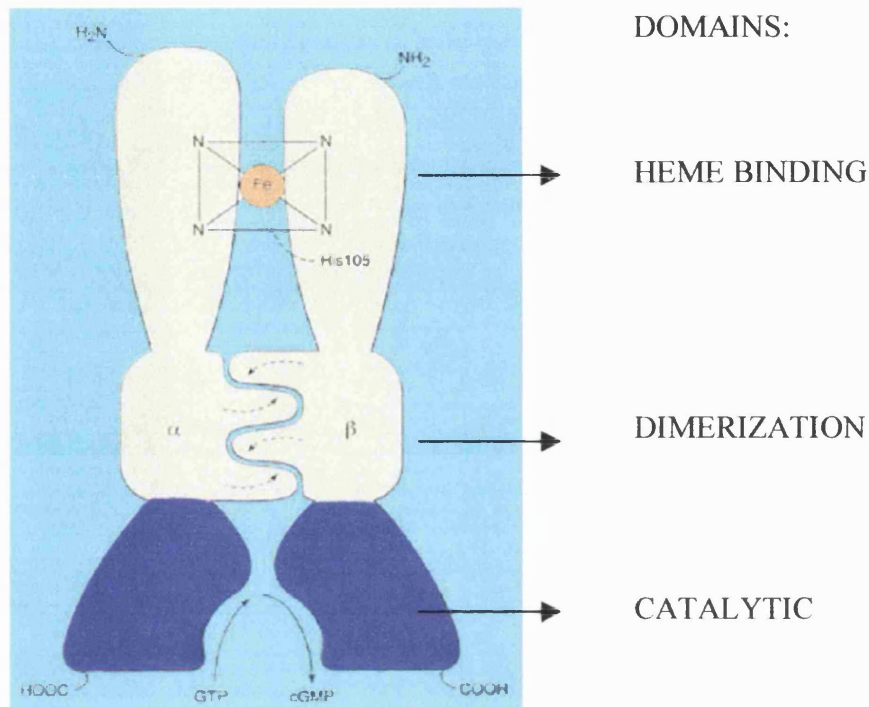
Figure 2. Schematic representation of sGC

- **Catalytic and Dimerization Domains**

The catalytic domain represents the region responsible for the basal cGMP formation. The reaction proceeds with inversion of the configuration, presumably by direct attack of the 3' hydroxyl on the α-phosphate, releasing inorganic pyrophosphate.[18] This reaction requires the presence of Mg^{2+} or Mn^{2+} as cofactor. Several studies have indicated that the catalytic domain is localized in the C-terminal region of both the α_1 and β_1 subunits.[19] In this regard, aligment of amino acid sequences between AC, pGC and sGC shows that the C-terminal region of all three enzymes exhibits a high degree of homology, suggesting that these catalytic domains are descended from a common ancestor. Furthermore, mutation of two residues within the C-terminal region of the α_1

has been shown to cause complete loss of basal activity.[20] Finally, deletion mutagenesis experiments in the amino terminus of the α_1 and β_1 subunits showed that this region is not involved in the catalytic activity.[19]

Despite the fact that both α_1 and β_1 subunits contain their own catalytic domains, catalytic activity is dependent upon coexpression of both subunits and the dimerization domain is thought to mediate the subunit association in the formation of heterodimers.[21]

- **Regulatory Domain**

sGC contains iron-protoporphyrin IX (heme b) as a cofactor[22] and it has been shown to bind one molecule of ferrous heme per heterodimer.[23] The heme binding region confers NO sensitivity to the enzyme[24] and has been localised to the N-terminal region of the β_1 subunit.[25,19] This part constitutes the least conserved region of the protein and is not homologous to any other known protein, showing that the heme is in an unique environment. Other studies have contributed to define the localisation and environment of the heme-binding region. Spectral analysis indicated that the N-terminal half of the β_1 subunit (amino acids 1-385) was sufficient to bind heme in a similar manner to the wild-type sGC.[22] In addition, molecular approaches, such as point mutation have shown that the heme moiety is bound to the enzyme *via* an imidazole axial ligand provided by H105 in the β_1 subunit.[19, 26] Thus, when H105 and other conserved histidine residues in sGC were mutated to phenylalanine and expressed in a baculovirus/SF9 system as a heterodimeric protein (α_1/β_1), only H105F lost the NO-stimulated sGC activity. These results are also consistent with those from site-directed mutagenesis of the conserved histidines in sGC β_1 (1-385) to alanine or glycine and expressed in *E.coli*, which result in a loss of NO-responsiveness. Therefore, it is concluded that the N-terminal region of the β_1 subunit is itself sufficient for heme binding, and the histidine H105 is the heme proximal ligand. Further spectral studies confirmed that the heme ligand was histidine. The electronic absorption spectrum is characteristic of a five-coordinate high-spin ferrous heme with imidazole as the axial ligand, showing a

sharp Soret band at 431nm and a single broad peak in the α/β region at 562 nm, and a porphyrin to Fe^{2+} charge transfer band at 770nm.[27,28] The heme can be oxidized using ferricyanide, yielding a ferric heme which has a Soret maximum at 392, a peak at 511nm corresponding to the β band of the heme and a peak at 642 nm from a porphyrin to Fe^{3+} charge transfer. Thus even in the ferric state, the heme is five-coordinate high spin, with the unusual property of not binding water, probably due to a hydrophobic distal pocket lacking a residue which can hydrogen bond to water and stabilize the coordination of the water by the iron.[29]

Besides the axial histidine, mutagenesis experiments have also indicated that the highly conserved cysteines (Cys 78 and Cys 214) in the β_1 subunit are also involved in the regulation of sGC activity.[30]

2.1.1.2. Activation

Soluble guanylate cyclase is an unusual hemeprotein when compared to others such as hemoglobin and myoglobin.[31] Its distinctive properties are related to the binding of small ligands suggesting an extraordinary coordination environment.[32] sGC does not bind oxygen. It has a very low affinity for carbon monoxide and nitric oxide is a powerful activator of the enzyme.

- **NO-Dependent activation.**

Synthesised from L-arginine by the enzyme NO-synthase in endothelial cells, nitric oxide (NO) functions, at low concentrations, as a signalling molecule. Although NO may participate in other physiological functions, which do not involve sGC, most of its effects are mediated *via* activation of sGC. This includes regulation of vascular smooth muscle relaxation, inhibition of platelet aggregation, and neuronal communication.[33,34]

It has been proposed that activation of sGC by NO is a direct result of both the formation of a 5-coordinate nitrosyl-heme complex by release of the axial ligand (Figure 3) and of the changes in porphyrin structure. This mediates a global conformational change in the protein, which results in activation.
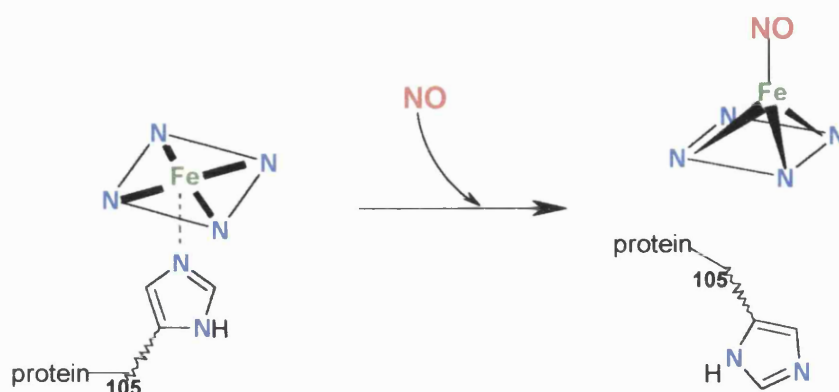
Figure 3. Activation of sGC by Nitric oxide.

Various experiments have supported the proposed mechanism. Initially, in the 1980's, several research groups demonstrated that the ability of NO to activate purified sGC is dependent on the presence of heme. Removal of the heme results in loss of the ability of NO to activate the enzyme.[35, 36] It was also found that heme-deficient enzyme is activated by NO-heme and the metal-free protoporphyrin IX (PPIX), and that free heme does not activate the enzyme.[21] Based on these findings, Ignarro suggested that the heme, once bound by NO, elicits an out-of-plane movement of the centre iron, to produce a heme core size similar to that of a free porphyrin. Thus, both NO-heme and PPIX activate the enzyme through a similar mechanism. In addition Traylor and Sharma using thermodynamic data revealed that NO binds better to the heme without proximal base, suggesting that when NO binds heme there is a tendency of breaking of the proximal base to iron bond due to the NO negative *trans* effect.[37] An interesting experiment with metalloporphyrin-substituted enzymes has been carried out suggesting that, effectively the release of the axial ligand takes place during activation of sGC by NO. In connection with this, the non-native metalloporphyrins, Mn(II)PPIX and Co(II)PPIX, were introduced into heme-deficient sGC forming five-coordinate complexes. The addition of NO produces a non activated six-coordinate complex for Mn(II)sGC, while Co(II)sGC forms an activated five-coordinate complex, implying that activation

of sGC requires the scission of the histidine ligand. This observation is due to the increasing *trans* influence across the first row transition metals from Mn(II) to Co(II) in the presence of a nitrosyl ligand.[38] Spectroscopic studies, such as resonance Raman,[39,40,41] electronic absorption[42] and electron spin resonance spectroscopy [43] support the axial ligand release mechanism since the NO-activated sGC contains five-coordinate Fe(II)-PPIX(NO) complex. As a result of these experiments, it is generally accepted that scission of the histidine-iron bond occurs during activation of sGC by NO. However, the finding that CO also activates sGC, although with much lower affinity, and that this ligand forms a 6- coordinated complex, indicates that the absence of a metal-proximal histidine bond is not sufficient criterion for activation of sGC and that activation induces a conformational change that rearranges the structure of the heme proximal pocket.

In addition to endogenous sources of NO, other nitrovasodilators activate the enzyme. Some of these compounds such as sodium 1-(*N*-*N*-diethylamino)diazen-1-ium-1,2-diolate (DEA/NO) (**1**) or 5-amino-3-morpholin-4-yl-1,2,3-oxadiazol-3-ium chloride (3-morpholino sydnonimine hydrochloride) (SIN-1) (**2**) are genuine NO donors, in that, they undergo spontaneous (or light induced) reaction at physiological pH in simple aqueous buffered media to release NO. In contrast, the stimulatory effect on sGC of others agents such as 2-aminoethyl imidothiocarbamate (*2-aminoethylisothiouronium bromide, AET*) [44] (**3**) or organic nitrates ($RONO_2$) is connected with the generation of NO during their biotransformation and the subsequent interaction of the NO with the sGC heme. The prototypical nitrate, 2,3-bis(nitrooxy)propyl nitrate or more commonly, nitroglycerin (GTN) (**4**) has been used in treatment of angina pectoris for over a century.

1

2

3

4
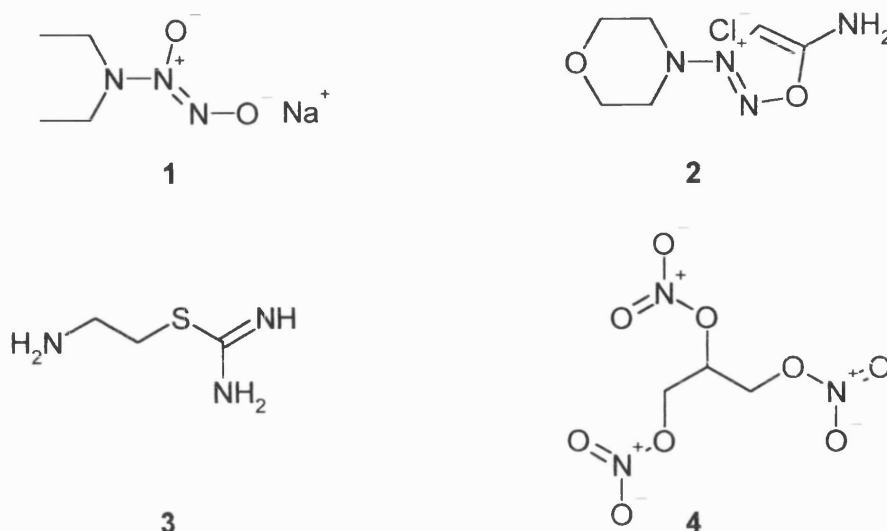
- **NO-independent activation**

In addition to the nitrogen-oxide-containing compounds it has been established that carbon monoxide (CO) is another small molecule that is involved in sGC activation, although it only leads to a 4- to 6-fold activation.[45] Spectroscopic data indicate that CO binds to the heme, forming a 6-coordinate complex, with the histidine-Fe bond intact due to the positive trans effect of this molecule (Figure 4).[46]
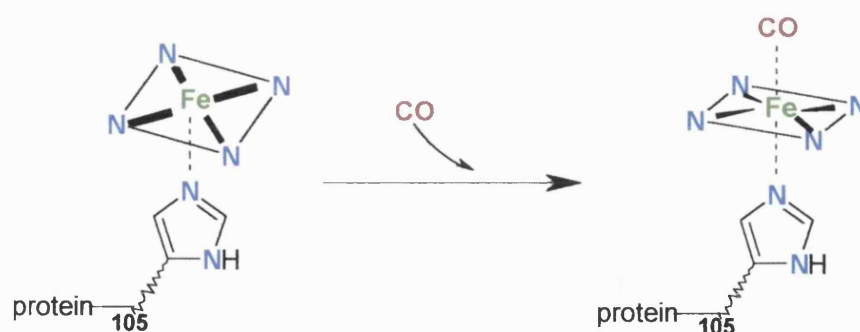
Figure 4. Activation of sGC by Carbon monoxide

It has been suggested that this complex is dissociated to form a 5-coordinate intermediate, which should be responsible for the observed stimulation. This

suggestion is confirmed by the determination of the dissociation rate, which indicates that the binding of CO to sGC is a one step process in which the off-rate of CO from the hexacoordinate complex is much faster than typically found in hemeproteins.

However, there are conflicting reports on the effect of the CO on enzyme function. Burstyn's group has reported that CO does not activate sGC at a variety of physiologically relevant concentrations of CO and at a variety of heme concentrations.[47] Nevertheless, it has been shown that activation of sGC by CO is significantly enhanced in the presence of YC-1 [5-(1-benzyl-1H-indazol-3-yl)-2-furyl]methanol (5), an NO-independent sGC activator.
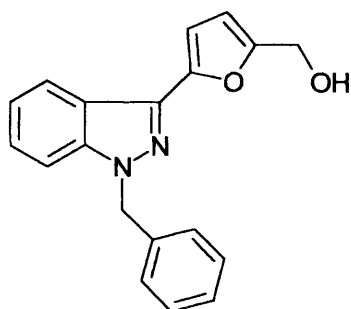
YC-1

5

YC-1 was first synthesised by a group in Taiwan.[48] Since biological studies have shown that this derivative of benzylindazole inhibits platelets aggregation[49] and smooth muscle cell proliferation, by acting as an activator of sGC, different groups have used this compound as a pharmacological tool in order to get insight into the sGC-cGMP signalling system. Initially, it was demonstrated that YC-1 acts as an NO-independent but heme-dependent activator of sGC and that it potentiates both CO and NO-induced sGC stimulation. This effect is also observed with protoporphyrin IX, which activates sGC independent of a gaseous ligand.[50] These findings have profound implications, as this synergistic action may have a therapeutic benefit; by using YC-1 it may be possible to decrease the dose of nitrovasodilators, therefore reducing the risk of adverse effects. Therefore, the importance of elucidating the mechanism of activation of this compound is clear. To address this question

different hypotheses have been proposed but the mechanism is still not fully understood.

Koesling and collaborators first suggested that YC-1 acts by stabilizing the active conformation of the enzyme independent of the mechanism of activation. This hypothesis was based on observations that, as mentioned above, YC-1 increases NO-stimulated enzyme activity and also sensitises the enzyme, decreasing the EC_{50} for NO. In addition, the authors observed that activation of sGC by CO in the presence of YC-1 is equivalent to activation by NO alone. Furthermore, YC-1 potentiated the PPIX-induced stimulation of sGC. These results indicated that YC-1 sensitizes the enzyme towards its physiological activator and that independent of the activating species YC-1 stabilizes the active conformation of the enzyme, thus induction of the active conformation is necessary for its effect. This may explain why YC-1 alone led to a lower activation (12-fold) of the enzyme compared to NO (100-fold).

The same authors reported that the lower EC_{50} observed with NO and CO in the presence of YC-1 could not be detected with PPIX. They also demonstrated that YC-1 slowed down the dissociation rates for NO and CO from the activated enzyme and that YC-1 does not interact directly with the heme as this compound did not change the Soret absorption of basal or stimulated sGC and still bound to the heme-depleted enzyme. Taking into account all these results the authors suggested that YC-1 binds to an allosteric site on sGC molecules, and proposed that the possibility exists that there is a natural allosteric modulator of sGC.[51] These results, however, do not agree with those reported by Stone and Marletta, who did not observe any shift of the EC_{50} of CO in the presence of YC-1, or any influence of this compound in the K_{off} of CO from the heme, indicating that YC-1 does not increase the affinity of CO for the heme.[52] Furthermore, these authors did not find any increase in the NO-stimulated activity with the addition of YC-1. Koesling, in a later report, not only confirms the effect of YC-1 on ligation kinetics of CO, but also suggests that the effect of YC-1 may be to replace the proximal ligand or to stretch the proximal bond. Thus, the proposal is in agreement with a model of activation that requires free or highly labile proximal base.[53] Recently, Marletta and

collaborators have reported their results on kinetics and resonance Raman (RR) studies on sGC and YC-1. They found that in absence of CO, YC-1 does not affect the RR spectrum of the ferrous β(1-385), the isolated sGC heme-binding domain, nor does it change the spectrum of the ferrous form of baculovirus/Sf9 cell expressed sGC. However, in the presence of CO, they observed a shift in the Fe-CO stretching frequency in both systems. Thus, based on these data they suggested that YC-1 binds to the heme-binding domain which leads to a conformational change in the protein and a change in the electrostatic environment of the heme pocket. In contrast to the Koesling group, they found that YC-1 binding has no effect on the heme proximal ligand.[54] Recently, Murad and collaborators have published that YC-1 activation of sGC has both heme-dependent and heme-independent mechanisms.[55] They found that the YC-1-stimulated enzyme retained at least 40% of its original activation by YC-1 in the presence of [1,2,4]oxadiazolo[4,3-a]quinoxalin-1-one (ODQ) (6), a known selective inhibitor of sGC that oxidizes the heme iron to a ferric state. This suggests that the mechanism of action of YC-1 is not completely dependent on the sGC heme moiety. They also showed that a heme-deficient mutant sGC (H105 of the β subunit was substituted by a cysteine) was partially activated by 100 μM YC-1 (3-fold stimulation versus a 10- fold of the wild-type). Therefore this work indicates that the heme moiety, although important is not necessary for activation of sGC by YC-1. It also suggests that either there is more than one binding site for YC-1 or if there is one, changes of the heme enviroment affects the affinity of YC-1 for its binding site.
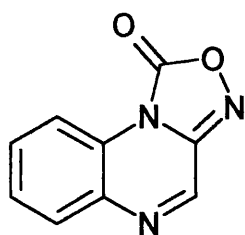
ODQ

6

Investigations into the interaction of YC-1 with sGC have been carried out by several groups during the last few years helping to gain insight into the mechanism of action of sGC. However, controversial data has generated

opposing hypotheses. Thus, knowing the molecular details of the activation of this enzyme is of critical importance; in this context knowing the binding sites of YC-1 is a crucial factor in determining the environment of the enzyme and in designing drugs which may have a therapeutic effect.

We therefore proposed investigating the binding sites on sGC by using the chemical technique of photoaffinity labeling.

2.1.2 Photoaffinity Labeling

The study of ligand-receptor interactions is one of the most challenging and fascinating aspects of pharmacological and medicinal chemistry research. X-ray crystallography, high-resolution NMR spectroscopy and site-directed mutagenesis are some of the techniques that have been used to locate binding sites for enzyme-substrate complexes. In addition chemical affinity labeling and photoaffinity labelling have been developed for this purpose. Suitable ligands for affinity labelling include enzyme substrates, allosteric effectors, haptens, neurotransmitters and hormones.

The usual goals in both photoaffinity and chemical affinity labelling are to identify a receptor in a mixture of candidates or to locate one or more of the amino acid residues that make up the binding site of a receptor.[56] In a chemical affinity labelling experiment the ligand contains a reactive group designed to react with a functional group that might be present at the binding site of the receptor that recognizes the ligand. Under unfavourable conditions reaction may occur between the ligand and groups outside the binding site, and misleading results may be obtained.[57] In a photoaffinity labelling experiment, the ligand contains a photoactivatable group, which is stable in the absence of light, eliminating much of the non-specific labelling, as labelling can be initiated after binding to the recognition site is complete (Figure 5). A second advantage of photoaffinity labelling is the considerable reactivity of photogenerated intermediates such as carbenes and nitrenes,[58] which can react with most functional groups in biological systems to form a stable covalent bond. Because of these advantages photoaffinity labelling is the most frequently

used chemical method for studying the interactions of biologically active ligands with their receptors.[59]
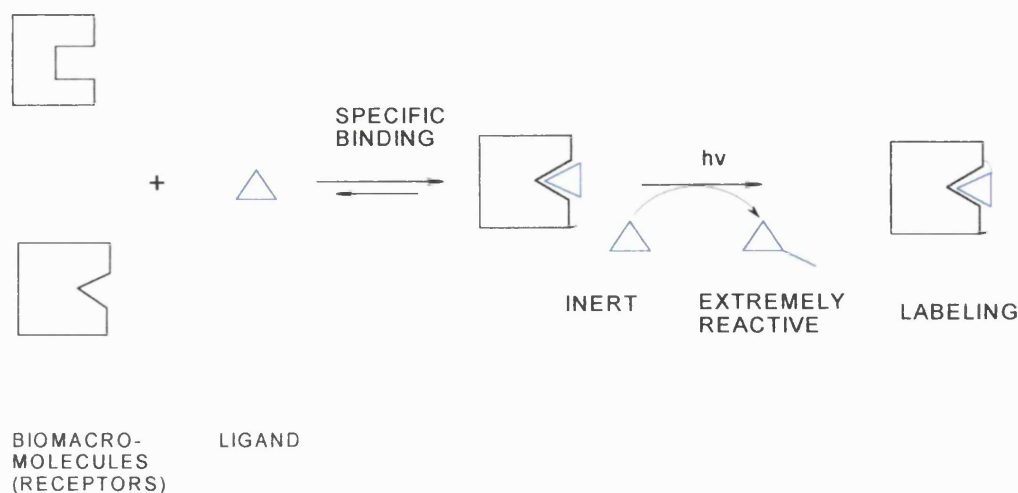
Figure 5. Schematic representation of photoaffinity labelling technique.

Since the use of photoaffinity labelling was introduced by Westheimer in 1962, several photoreactive groups have been developed for the application of this method to biological systems.[59] A photoaffinity reagent is a ligand that is chemically inert but conceals a highly reactive intermediate that is unmasked by irradiation with near ultraviolet or visible radiation.[56] The main properties desired of the photoactivatable group are: chemical stability prior to photoactivation, rapid photolysis at an appropriate wavelength and a very high reactivity of the photogenerated species.[60]
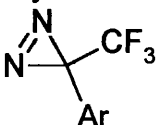
As mentioned above the main photogenerated intermediates in photoaffinity labelling are nitrenes and carbenes. Nitrene precursors, such as aryl azides, were until recently the most commonly used photoactivatable reagent due to their ease of synthesis, hence the chemistry of this group has been studied in great detail. However, low cross-linking yields in aryl azide applications are common[59] and the short-lived singlet phenylnitrenes rapidly rearrange into ketenimines, which have a significantly longer half-life and can label nucleophiles in a nonspecific maner [57] (Scheme 1).
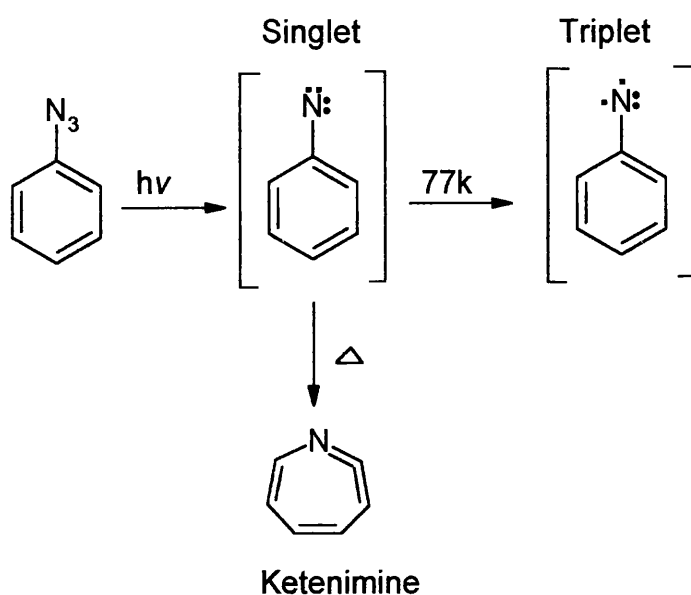
Scheme 1. Photolysis of nitrenes.

Furthermore, shorter wavelengths are required to achieve effective photodecomposition (254nm), and these photolysis conditions can cause photochemical damage to the bioactive macromolecules (Table 1).

Table 1. Chemical aspects of the photolysis of arylazide, aryldiazirine and benzophenone.

Photolabile group	Photolysis conditions	Reactive intermediate	Expected cross link
Arylazides Ar-N$_3$	≤ 300 nm	Nitrene	-N-C-, -N-X- (X=heteroatom)
Aryldiazirines	≥ 350 nm	Carbene	-C-C-, -C-X- (X=heteroatom)
Benzophenones ArCOAr	≥ 350 nm	Radicals	-C-C-

We will concentrate on the use of diazirines as photoreagents, and in particular we will make use of 3-trifluoromethyl-3-phenyldiazirine and of benzophenone, since they seem to meet most of the chemical criteria required for photoaffinity.

2.1.2.1 Diazirines

- **Properties of diazirines**

The diazirines are lipophilic, unsaturated C-N-N-three membered rings, with a chromophore that extends significantly into the 300 nm range. The strain of the small ring makes these compounds highly reactive toward loss of nitrogen on photoexcitation, acting as precursors of carbenes. However the three-membered ring shows an unexpected stability[61] toward numerous highly reactive reagents, far more so than the linear diazo isomers,[62] enabling easier chemical manipulation. These properties of diazirines make them effective reagents for photolabelling.

The diazirines contrast markedly from the isomeric diazomethanes in their physical and chemical properties (Table 2). While diazomethane is a highly reactive yellow gas (λ 412nm) diazirine absorbs in u.v region (λ 320-380nm) and is stable to phenols and acids.

Table 2. Physical Properties of C-N-N groups

	Diazirine	**Diazomethane**
electronic nature	electrophilic	nucleophilic
absorbance	λ 320-380nm	λ 412nm
stability	stable	highly reactive

- **Photolysis of diazirines**

Diazirines have a characteristic absorption pattern, with a band in the near ultraviolet (λmax 350 to 380 nm) which is resolved into a series of sharp peaks in non-polar solvents such as hexane.[60] As the N=N double bond in the diazirine system is not conjugated in aromatic derivatives, substituents on the aromatic nucleus have little effect on the absorption maximum (e.g. for 3-*H*-3-phenyldiazirines: *p*-CH$_3$O-: λmax 378; *m*-NO$_2$-: λmax 352nm).

Diazirines can be photolysed very efficiently at wavelengths around 360 nm (Scheme 2) where most biological molecules do not absorb, giving rise to carbenes as photogenerated reactive intermediates and diazo compounds as unwanted photolysis products.[56] For example, 3-*H*-3-aryldiazirines form diazo isomers to the extent of 30 to 70% when irradiated. These isomers are themselves photolysed to form carbenes, but relatively slowly at the wavelengths at which the diazirines absorb. These unwanted products can cause undesirable nonspecific labeling. However, this can be avoided by using trifluoromethyl as a sustituent, as the electron-withdrawing nature of this group strongly stabilizes the diazo-functionality and the diazo-isomer is considered to be stable under the typical experimental conditions of photoaffinity labeling.[57]

Diazo
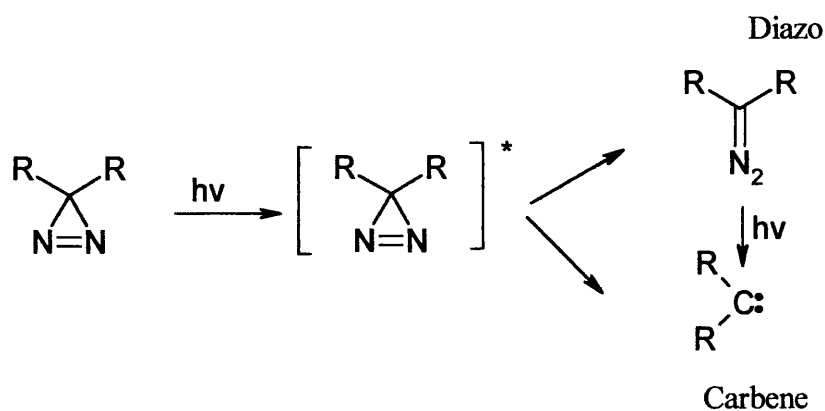
Carbene

Scheme 2. Photolysis of Diazirines

- **Carbenes**

Carbenes are neutral, divalent derivates of carbon. The two nonbonded electrons of a carbene can be either paired or unpaired. If they are paired, the species is spectrally a singlet, whereas two unpaired electrons appear as a triplet.[63] These states exhibit different reactivity (Figure 6).

SINGLET (sp^2)   TRIPLET (sp)

Figure 6. Electronic states of a carbene.

Since triplet species are diradicals, they would be expected to exhibit a reactivity similar to that of a normal radical, singlet species on the other hand should be electrophiles. A method of distinguishing between the two possibilities was developed by Skell and is based on the common reaction of addition of carbenes to double bonds to form cyclopropane derivatives. If the singlet species adds the mechanism is concerted, one step, and stereospecific since the movements of the two pairs of electrons should occur either simultaneously or in rapid succession. However, if the attack is by a triplet species, the two unpaired electrons cannot both go into a new covalent bond, since by Hund's rule they have parallel spins. So the mechanism must go through an intermediate that has two electrons of the same spin, so before ring closure one of the electrons must reverse its spin, allowing free rotation about the C-C bond, thus the reaction is not stereospecific (Scheme 3).

Reaction via singlet

Reaction via triplet
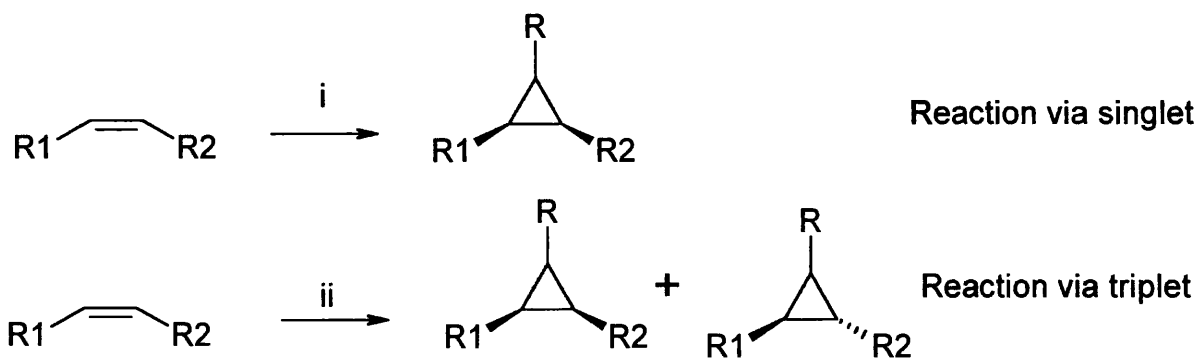
i, CH_2R, sp^2. ii, CH_2R, sp

Scheme 3. Carbene Trapping by Alkenes

Due to the electron-deficient nature of these species, they are highly reactive with practically all carbenes having lifetimes considerably under 1 sec.

Scheme 4 shows the typical reactions of a carbene.
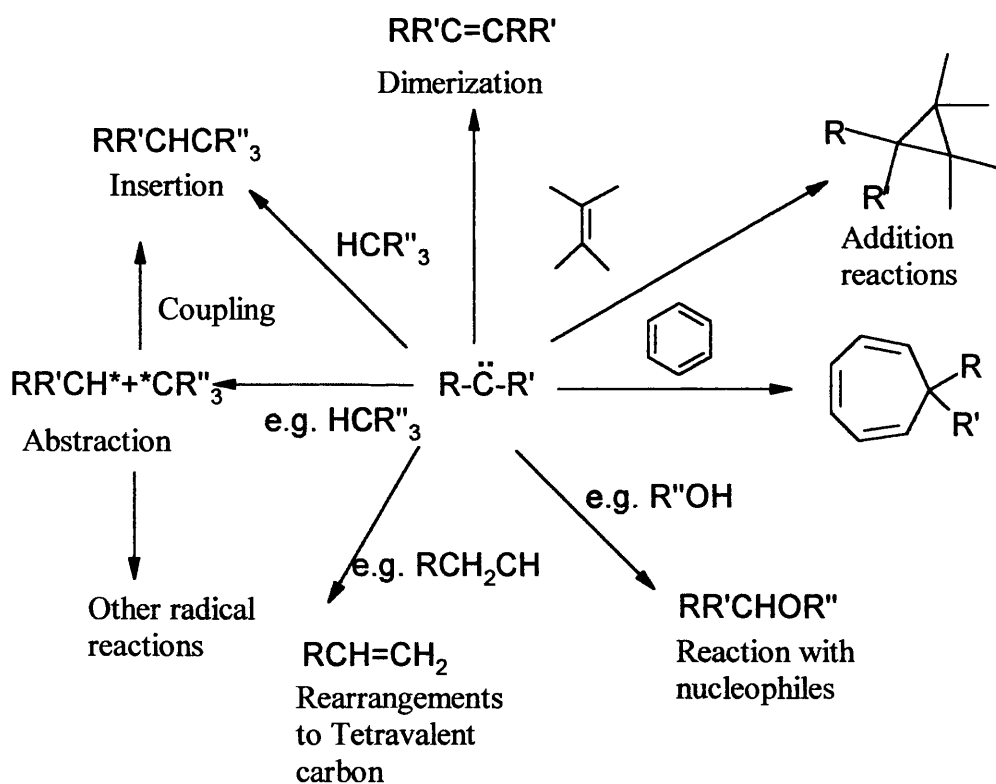
Scheme 4 Reactions of a carbene.

Besides reacting with nucleophilic groups, carbenes are capable of reacting by insertion with saturated hydrocarbons and by addition to unsaturated hydrocarbons including aromatic rings. None of the twenty different amino acid side chains is immune to attack, and hence carbenes are useful for labeling binding sites in all enzyme and receptor proteins.[64]

• 3-Trifluoromethyl-3-phenyldiazirine

Since the first synthesis of a 3-H-3-aryldiazirine several alternative aryldiazirines have been developed for photolabeling.[65,66] Most of the recent work exploits the photochemical reactivity of 3-trifluoromethyl-3-phenyldiazirine (TPD), which was first proposed as reagent for photolabeling by Brunner.[60] The TPD group is stable under a range of different chemical and physical conditions, including strong bases (KOH), oxidizing agents (N-bromosuccinimide), strong acids (trifluoroacetic acid), mild reducing agents (thiols, sodium borohydride) and heat (refluxing in dioxane, 80°C). Thus TPD is stable under a variety of conditions that enable it to be carried through synthetic steps as well as those anticipated for its use in biochemical labeling reactions.[64, 67]

The characteristic absorption of the diazirine, centered at 353 nm (ε =266), permits rapid photolysis with near uv radiation. TPD forms 35% diazo intermediate upon irradiation, and the derived carbene gives aproximately 50% C-H insertion when photolyzed in cyclohexane or 95% O-H insertion in methanol (Scheme 5). Insertion into O-H is very efficient and is reported to occur from the singlet carbene. Singlet carbenes coordinate very rapidly with the occupied p-orbitals of the oxygen to form ylids. The lifetime of the carbene in cyclohexane is much longer due to the lack of reactivity of the solvent.
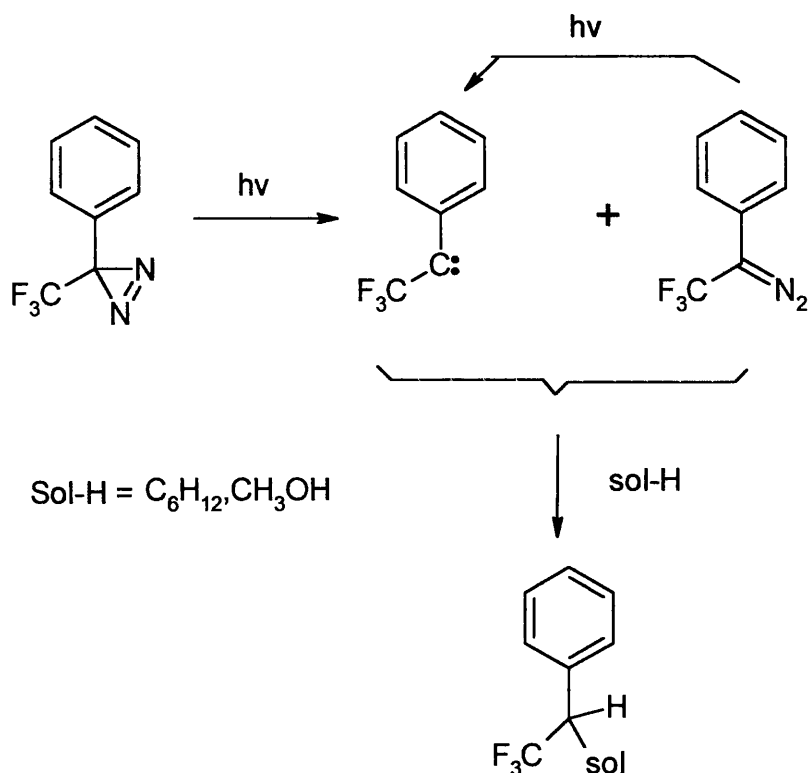
Scheme 5. Photolysis of 3-Trifluoromethyl-3-phenyldiazirine

Some complications are associated with use of the TPD group. First, the triplet carbene can react with molecular oxygen to give the corresponding ketone. Secondly it has been shown that amine groups react with this particular type of carbene, via initial N-H insertion followed by loss of HF and hydrolysis to give the corresponding ketone (Scheme 6).
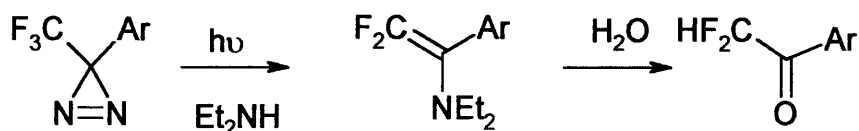
Scheme 6. Reaction of TPD with amine groups.

Despite these complications the advantages associated with this class of diazirines makes them effective reagents in photoaffinity labeling and successful applications of the TPD group have been reported. For example TPD has been incorporated into a bipolar phospholipid molecule [bis-

phosphatidylethanolamine (trifluoromethyl)phenyldiazirine] (7) designed to span the membrane through a covalently linked fatty diacyl chain and to enhace the structural information on membrane-associated regions, thus helping to identify transmembrane regions of integral membrane proteins and map the lipid-protein interface in a deep region in the membrane.[64] TPD was also used in the synthesis of (2E,4Z,6E,8E)-3,7-dimethyl-9-[3-(3-methyl-3H-diaziren-3-yl)phenyl]nona-2,4,6,8-tetraena (8), a photoactivatable analoge of 11-cis-retinal, to investigate the orientation of retinal in the visual pigment, bovine rhodopsin.[68]
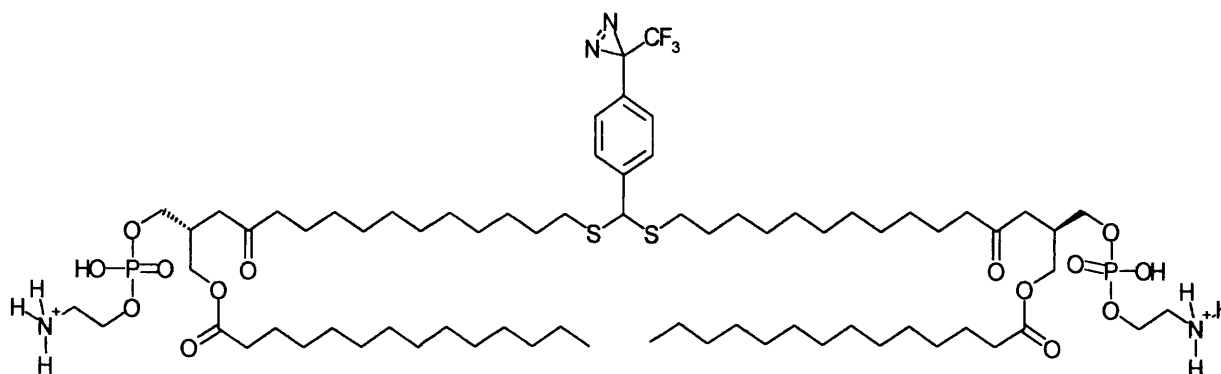
7
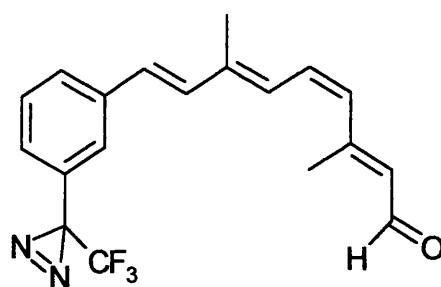
8

Yamaguchi and Saneyoshi have reported the photoaffinity labeling application of a photolabile 2',3'-dideoxyuridylate analogue (9) bearing the TPD group, when applied to HIV-1 reverse transcriptase. They found that this compound bound selectively to the dTTP binding site in the 66 kDa subunit of the p66/p51 heterodimeric enzyme.[69]
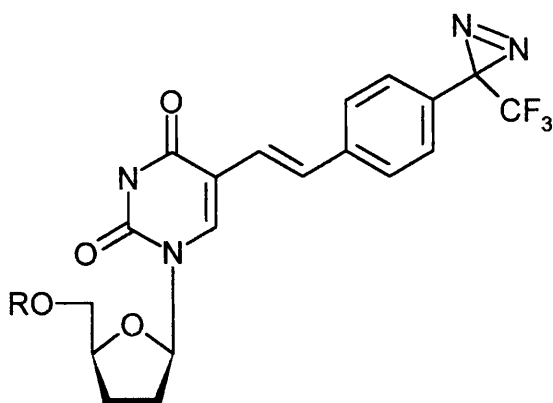
9

In some cases a low yield of incorporation of the photoprobe into the target receptor has been found, leaving a large amount of unlabeled protein in the reaction mixture. To overcome this disadvantage a combination of photoaffinity labeling and avidin-biotin technology (photoaffinity biotinylation) has been developed in recent years. This is also a powerful tool to investigate the interaction of biomolecules and substrates.

The first example of a biotinylated diazirine was reported by Hatanaka and coworkers.[70] They also described a successful application of an asparagine-linked *N*-acetylglucosamine derivative (**10**) to the photoaffinity labeling of β-1,4-galactosyltransferase.
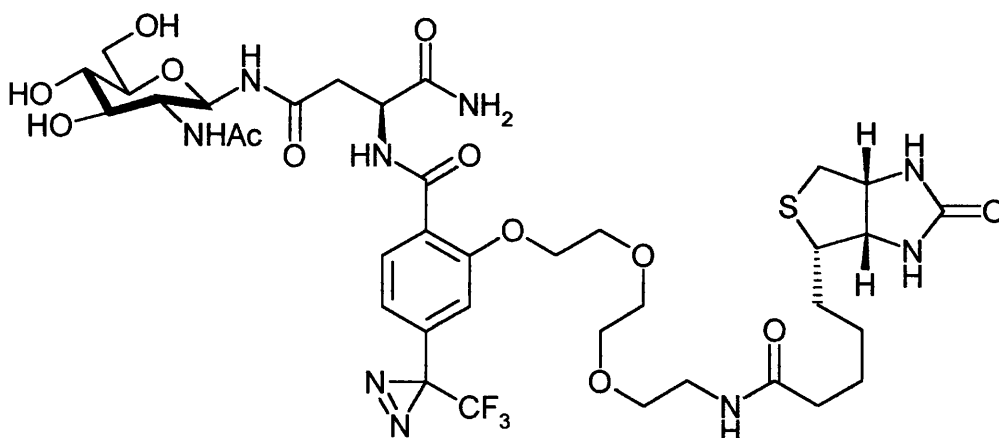
10

Briefly, the strategy consists of passing, after photolysis, the reaction mixture, which containes labeled and native enzyme through a monomeric avidin column. The native enzyme, is recovered and the biotinylated one is eluted and blotted on a polyvinylidene difluoride (PVDF) membrane for radiochemical-free detection.[71]

In order to avoid complications in MS analysis a bifunctional photoaffinity probe (BBP) of type 11 has been described.[72] This BBP group consists of a photoaffinity label (site A) and a photocleavable moiety (site B). Once the labeled peptide fragments are separated from the non-labeled ones through the avidin column, the ligand with the biotin tag is detached from the cross-linked peptides by photocleavage in site B. This allows an easier MS analysis.

11
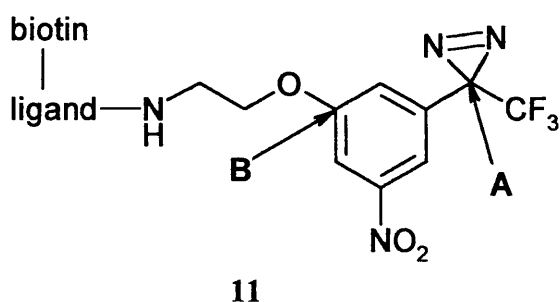
The biotin-labeling seems to be a powerful method for identifying labeled protein fragments and isolating them by affinity chromatography based on the strong interaction of biotin with either avidin or streptavidin. Several reports making use of this strategy have recently been published.[73,74,75]

With the photoaffinity biotinylation approach great progress in the photoaffinity labeling field has been reached in recent years and although we do not make use of it in this thesis, it is a direction to be look at in future work.

2.1.2.2 Benzophenones

In addition to TPD, the benzophenone (BP) group has been claimed as a very useful photoprobe in photoaffinity labeling studies. Some groups suggest that this functionality performs the best.[76]

This group is stable to common protic solvents and, as with diazirines, photolysis takes place at wavelength higher than 300nm which avoids protein damage. Photolysis gives radical intermediates, which are known to abstract hydrogen atoms.[58] Moreover, the biradicaloid triplet state of BP can be reversibly activated, and creates covalent linkage upon excitation-relaxation cycling.[77] Several examples of photolabeling with BP-peptides can be found in the literature,[78] which can be attributed to this group being stable under peptide synthesis conditions. This group not only has been incorporated into peptides, but also into small ligands. Compound **12**, for example has been shown to act as a photoaffinity label of rat liver glutathione-S-transferase.[79] The labeling site is identified as Met-112. Recently, Colman has identified the binding site of ADP in bovine liver glutamate dehydrogenase as Arg-491, though an analogue **13** containing the BP moiety as the photoreactive group.[80]

SG= glutathione-S
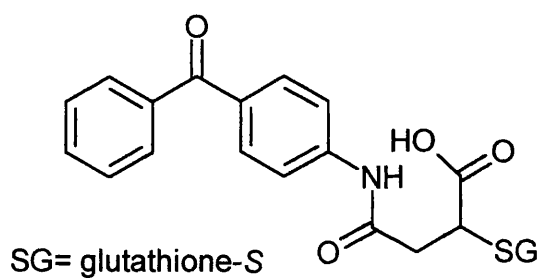
12
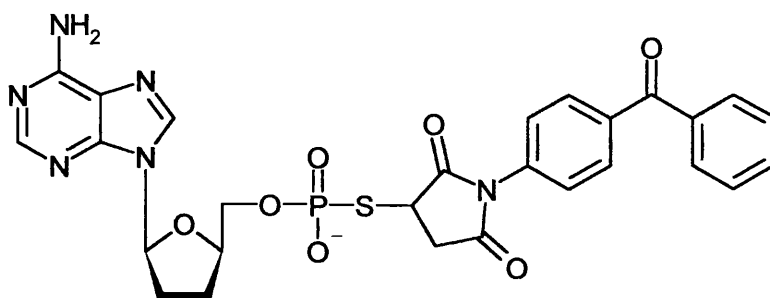
13

2.2 Hypothesis

In parallel with the photoaffinity labeling approach, modelling and sequence analysis has been used to predict possible sGC activator binding sites. A homology model of the catalytic domain of sGC is available with a proposed GTP-Mg^{2+} binding site[81] based upon a published crystal structure of type II adenylate cyclase (AC) catalytic domain.[82] Due to the almost symmetric structure of the AC and sGC catalytic domains, there exists a pocket pseudo-symmetrically related to the probable nucleotide-5'-triphosphate (NTP) binding site. For AC this pocket is known to accommodate the activator forskolin (Figure 7) and there is current speculation for a similar mode of activation for sGC (Figure 8). From the sGC homology model the pseudo-symmetric binding pocket contains a cluster of acidic residues that may complement the critical basic group of the current sGC activators (as explained in the next section). Molecular docking of a sGC activator into this pocket showed a surprising level of complementarity with the protein and consistency with the SAR data. Therefore it is possible that the sGC activators may interact with sGC in a similar manner to that of forskolin with AC. However only the catalytic domain has been considered and it may be that the activators interact with other domains of sGC. It is hoped that the photolabelling work will clarify this hypothesis.
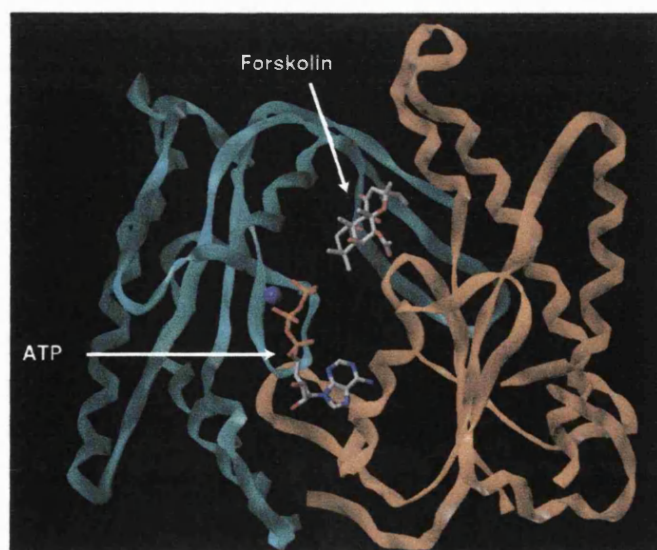
Figure7. Catalytic dimer of AC with ATP and forskolin binding site shown.
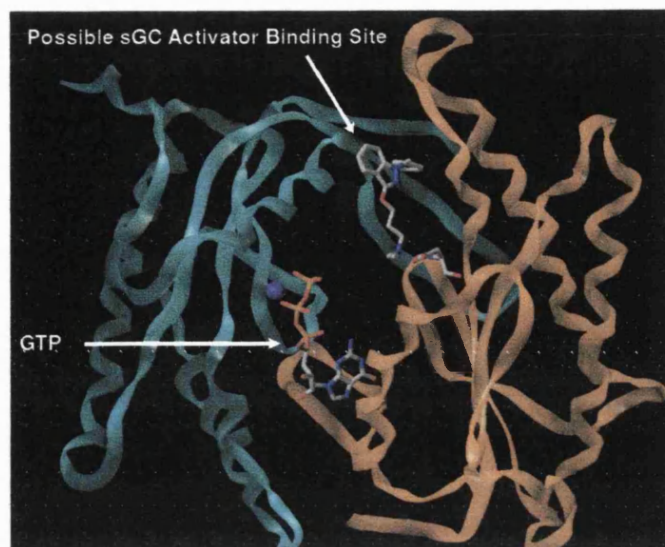
Figure 8. Catalytic dimer of sGC with GTP and possible activators binding site shown.

2.3 Design of sGC activators and its photolabile analogues

Initially, we focus our attention on YC-1, which as mentioned before, shows moderate activity on sGC and has been extensively used in the study with this enzyme. However, YC-1 has also been shown to act as a nonspecific phosphodiesterase inhibitor.[83] The fact that YC-1 is not selective for sGC makes interpretation of cell and tissue-based experiments difficult.

A medicinal chemistry program carried out by our group has identified activators of sGC with a better selectivity profile.[84] From the original lead YC-1, database searching and chemical synthesis gave compounds such as *N*-{3-[(1-benzyl-1*H*-indazol-3-yl)oxy]propyl}-*N*,*N*-dimethylamine **(14)** which is more active than YC-1 for activation of partially purified sGC. A structure-activity relationship study clearly showed that the indazole C-3 dimethylaminopropyloxy substituent was critical for enzyme activity. Based on this finding we decided to synthesize 4-chloro-*N*-[3-(dimethylamino)propyl]benzamide **(15)** as a model to investigate the possibility of incorporating a photophore and using it in the photoaffinity labelling experiments.
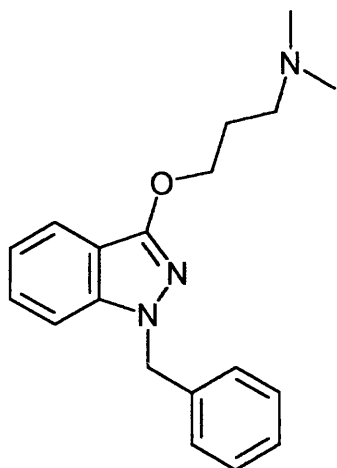
14
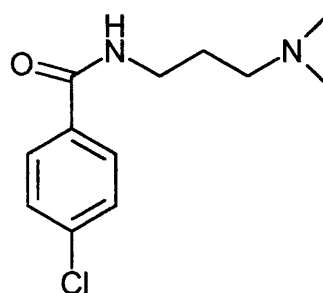
15

As reported previously, there are several photoreactive groups used in PAL. According to the literature tetrafluoro-phenyl azides, trifluoromethyl-phenyl diazirines and benzophenone are the best choice. The main criteria for the selection are:

1. The photoreactive groups should have sufficent stability under ambient light.

2. The life-time of the photochemically generated excited state should be shorter than the dissociation of the ligand-receptor complex, but long enough to spend sufficient time in a close proximity to a target site for covalent linkage.

3. The photophore should have an unambiguous photochemistry to provide a single covalent adduct.

4. The excited state or radical should react preferably with unreactive C-H groups yielding a uniform and stable covalent label rather than interact with nucleophiles including solvents.

Initially, we decided to use 3-trifluoromethyl-3-phenydiazirine as the photophore. The diazirine moiety was chosen as the photolabile group since, as noted above, it seems to meet most of the chemical criteria required for photoaffinity labelling. In this context the diazirine ring shows chemical stability towards numerous highly reactive reagents that allow chemical

manipulation. Photolysis takes place quickly at 360nm, where most biological molecules do not absorb, avoiding protein damage, and the photogenerated species, carbenes, show high reactivity with none of the twenty amino acids side chains immune to attack. As described earlier, the use of this group does present some complications. However, the advantages associated with this class of diazirines make them effective reagents in photoaffinity labeling.

In addition to the diazirine moiety, we also decided to investigate the use of benzophenone as an alternative photoreagent group to incorporate into the amide derivative in order to compare the applicability of both photophores in the system under study.

There are a few principles to take into account for the introduction of the photophores into the ligand of interest. In the design of the photolabile analogues it is necessary to carefully place the photoreactive group on the structure of the activator considering that the analogue must mimic the parent ligand as much as possible. Ideally, the ligand derivatization should be achieved with minimal modification of the total synthesis of the parent ligand. However, if a new synthesis is required, the main principle is to use a strategy that allows one to synthesize a series of photoaffinity ligands with the photophore in multiple position around the pharmacophore. This gives a better chance to find biologically active species and a definite map of the binding site.

The following approaches can be considered for the synthesis of the pholabile analogues:

Linear approach

A precursor is constructed early in the synthetic steps and in the final step is converted into the photolabile moiety, therefore during the synthesis the photophore remains intact.

Semisynthetic approach

The photoreactive group, or its precursor, can be directly attached to the parent, biologically active, ligand at a suitable functionality or complementing a structural unit already present. Thus, the photophore is generally designed to be part of the pharmacophore (*endo-photoaffinity ligands*), allowing more accurate identification of the binding site.

Tethered ligand approach

In the absence of suitable functionality for direct attachment a small linker sidearm can be introduced, which contains an appropriate functionality at the terminal position allowing the attachment of the photophore group in the final step. The photophore, connected *via* a linker of defined length is generally placed far from the pharmacophore; consequently it does not interfere with the binding but creates covalent linkages at a defined distance (*exo-photoaffinity ligands*).

With this in mind, the semisynthetic approach seems to be the most suitable for our purpose. Thus, in the case of YC-1 the 3-trifluoromethyl-3-phenyldiazirine (TPD) group was incorporated in the nitrogen at the first position (16), thus the diazirine moiety complements the benzyl group already present in the parent ligand (5). In the case of the amide derivative the diazirine was introduced at the *para* position of the benzyl group in substitution of the chloro (17). The benzophenone was introduced as a part of the structure core of the amide derivative (18). Therefore the analogues act as *endo-photoaffinity ligands*.

Figure 9 shows the structures of the parent ligands and the corresponding photolabile analogues
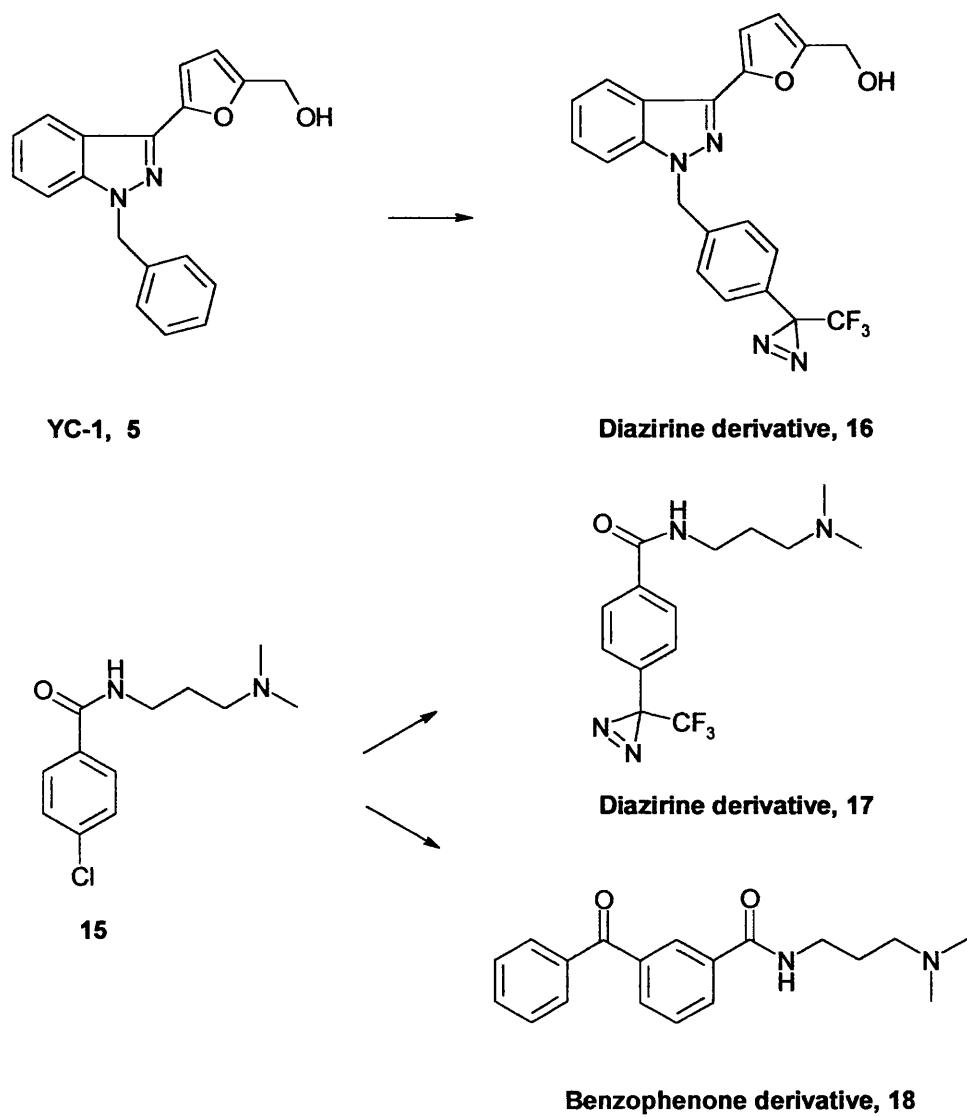
Figure 9. Structures of parent ligands and their photolabile analogues.

2.4 Chemistry

2.4.1 YC-1 and its analogue (YC-1A)

We required specific quantities of YC-1 as a pharmacological standard, as well as a method to synthesize its analogues. Other published routes use palladium coupling of an aryl tin reagent,[85] or a Suzuki type cross coupling reaction of 3-iodoindazole with 2-furylboronic acid.[86] We wished to accomplish the synthesis using readily available starting materials and reagents.

In view of the structure of the target compounds, disconnection analysis (Scheme 7) suggested two possible methods, both employing the protected furyl indazole (19) as a common intermediate:

1. Alkylation of a suitably protected furyl indazole 19 using benzyl bromide 20 for YC-1 or bromomethyl-TPD 21 for YC-1A.

2. Mitsunobu coupling of 19 with the corresponding alcohols.

Consequently, a synthesis of the furyl indazol intermediate 19, bromomethyl – TPD 21 and the corresponding hydroxymethyl-TPD 23 was required.

5, YC-1: R1= H

16,YC-1A: R1=

P: protecting group (-COOMe)

19

20, R1= H, R2= Br

21, R1=   CF3, R2= Br

22, R1= H, R2= OH

23, R1=   CF3, R2= OH
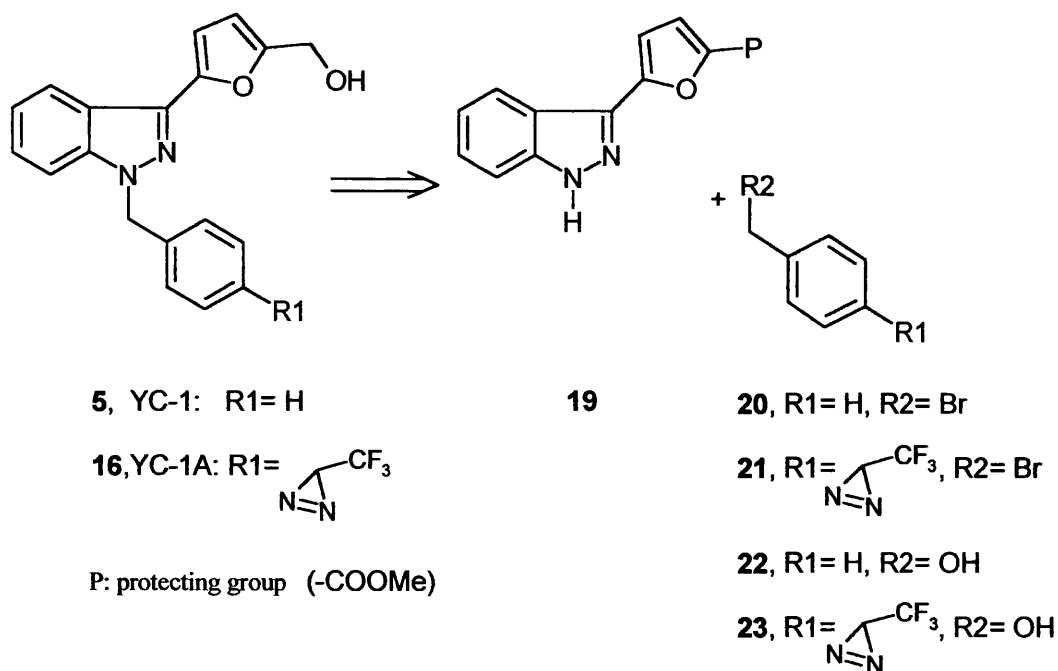
Scheme 7.   Proposed disconnection to provide YC-1 and its analogue YC-1A

- **Synthesis of the furyl indazole intermadiate 19**

We envisaged that the indazole could be accessed from diazotisation and reduction of an *ortho* amino biaryl ketone. Therefore, 2-nitrobenzoic acid **24** was used in the Friedel Crafts acylation of a protected 2-furan carboxylic acid **25** using iron (III) chloride to give the ketone **26**. Reduction of the nitro group with iron metal in acetic acid gave the amino ketone **27**. Diazotisation using sodium nitrite and hydrochloric acid followed by reduction of the diazo group with resultant cyclisation gave the key intermediate **19** (Scheme 8). This route provided compound **19** with a 60% yield for the last step and 12% overall yield.
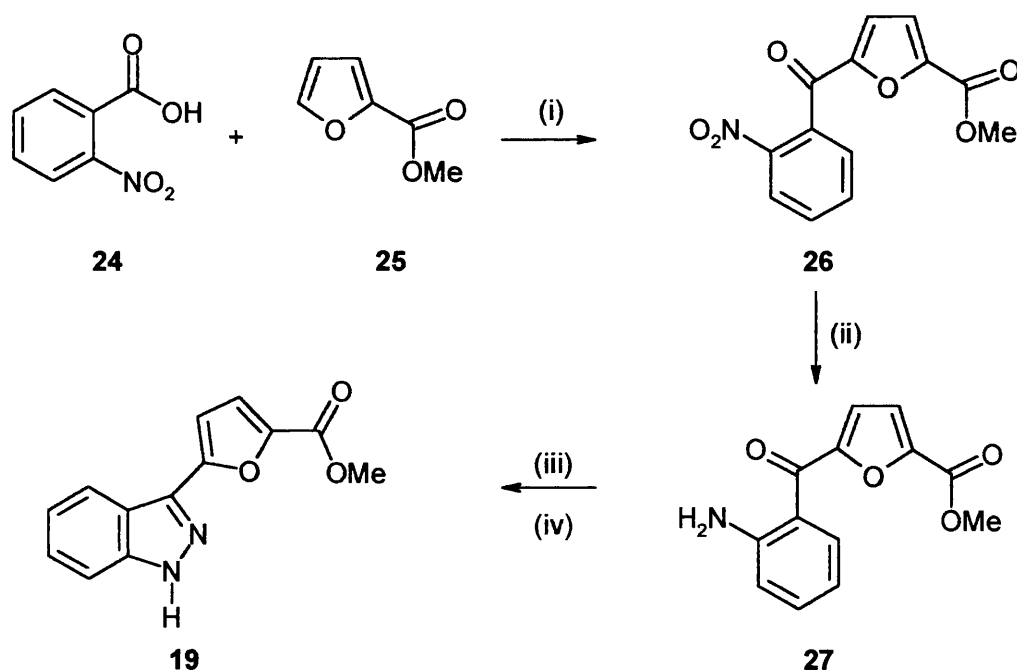
Scheme 8. (i) FeCl$_3$, CCl$_4$ (ii) Fe, AcOH/H$_2$O (iii) HCl, NaNO$_2$ (iv) SnCl$_2$.2H$_2$O

- **Synthesis of 3-(4-(bromomethyl)phenyl)-3-(trifluoromethyl)-3H-diazirine (21)**

Several routes to TPD have been reported; the route described here is an amalgamation of the best parts of several of these.[61,87,88]

Commercially available 4-(trifluoroacetyl) toluene (**28**) was converted into the corresponding oxime derivative **29** by reaction with hydroxylamine hydrochloride. The oxime was then transformed into the O-tosyl-oxime derivative **30**, which was then reacted with ammonia to give the diaziridine **31**. Initial attempts at this reaction were performed in a sealed tube with an initial temperature of -40°C, the reaction mixture was then allow to warm up to room temperature. However, the yield of this reaction increased when an excess of ammonia was added and the reaction mixture was heated at 60°C in a sealed autoclave. *p*-Toluenesulfonyl amide was isolated as a side product.

Oxidation of the diaziridine under the reported silver oxide conditions failed. Nevertheless, formation of the diazirine **32** was achieved using DMSO-oxalyl chloride in a Swern oxidation. Yields were very low (30%), probably due to the volatility of the product.[88] The diazirine compound was brominated with NBS in tetrachloromethane at 70-75°C with AIBN as initiator, giving the required product **21** although in a low yield (Scheme 9).
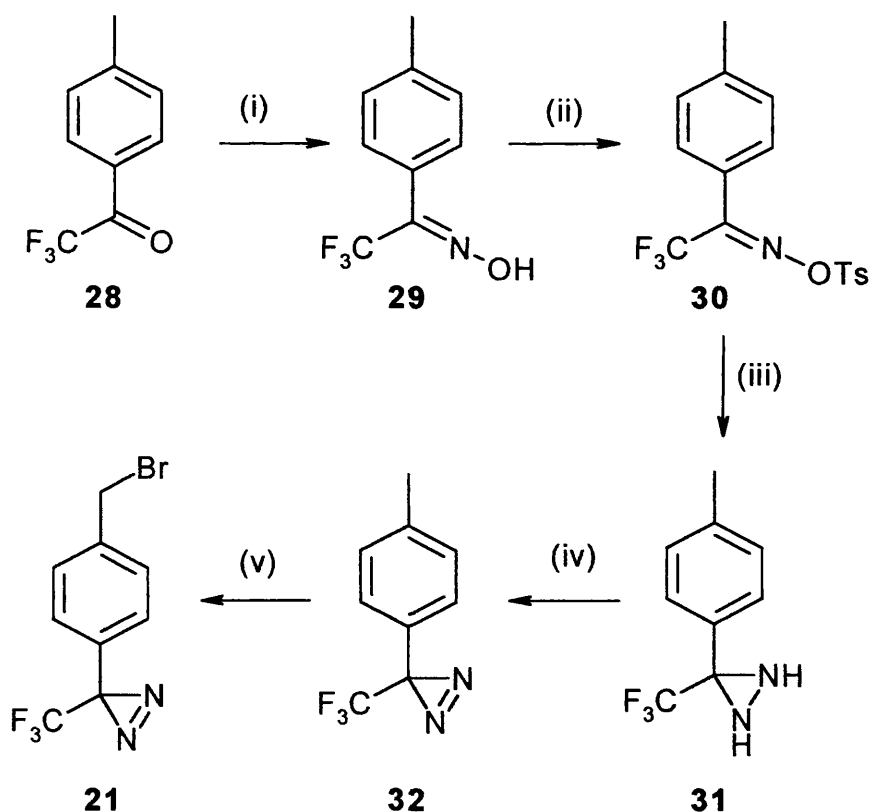
Scheme 9. (i) NH₂OH.HCl, NaOH, EtOH, reflux (ii) TsCl, pyridine, reflux (iii) NH₃ (liq), ether, heat (iv) (COCl)₂, DMSO, NEt₃, CH₂Cl₂ (v) NBS, AIBN, CCl₄, heat

- **Synthesis of [4-(3-trifluoromethyl)-3H-diaziren-3-yl]methanol (23)**

In order to apply the Mitsunobu reaction to intermediate **19**, we needed to synthesize the diazirine alcohol derivative **23**. An advantage of this route is that the required intermediate was obtained in one step (80%) by reduction of commercially available *4-[3-(trifluoromethyl)-3H-diaziridin-3-yl]* *benzoic acid* using borane (1M) in THF as the reducing agent. This reagent is selective for the reduction of carboxylic acids in the presence of other functional groups.[89]
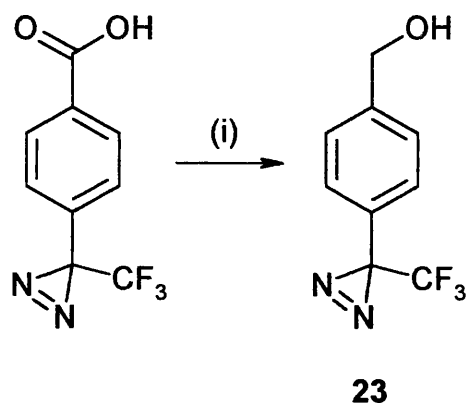
Scheme 10. (i) Borane in THF (1M)

- **Synthesis of YC-1 and YC-1A by Alkylation**

We investigated a traditional alkylation strategy (Scheme 11) for the substitution of the *N*1 position of **19**. Alkylation of **19** was achieved using sodium hydride or potassium *tert*-butoxide as a base and the required benzyl bromide **20**. Reduction of the ester **33** with calcium borohydride in refluxing THF provided YC-1 **5**, while compound **16** was achieved by reduction of **34** with the milder reducing agent diisobutylaluminiun hydride in dichloromethane.
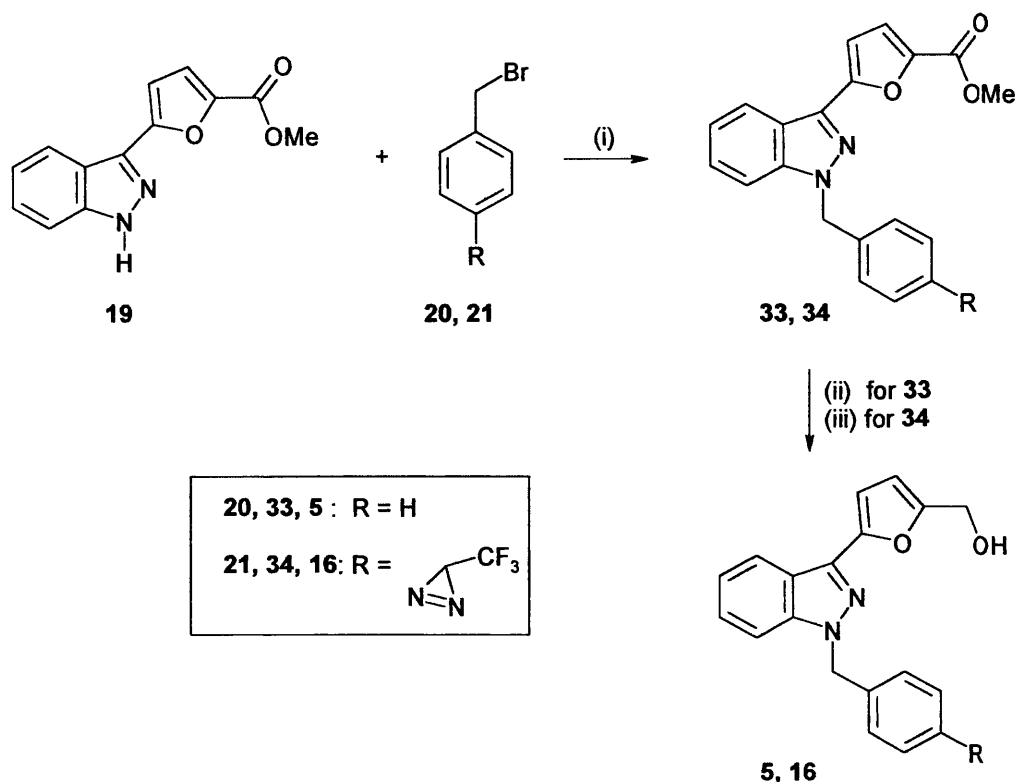
Scheme 11. (i) NaH, THF (ii) Ca (BH$_4$)$_2$, THF, reflux (iii) DIBAL-H, CH$_2$Cl$_2$

- **Synthesis of YC-1 and YC-1A by the Mitsunobu Reaction**

We also investigated an alternative route to analogues of 5 using Mitsunobu conditions (Scheme 12). It has been shown that the Mitsunobu reaction is an effective means of alkylation of indazoles and pyrazoles.[84] Since the first application of the Mitsunobu reaction in 1967, using the redox system diethyl azodicaboxylate (DEAD) and triphenylphosphine (TPP), in which carboxylic acids could be esterified with primary and secondary alcohols,[90] the reaction has been expanded to include carbon-carbon,[91] carbon-nitrogen and carbon-sulfur bond formation.[92,93,94] This reaction now represents one of the most utilized methods for the stereochemical inversion of hydroxyl groups.[95] This reaction has also been carried out on solid support, thereby becoming a useful tool in combinatorial chemistry.[96] The tributylphosphine / TMAD combination is a more reactive redox system than TPP/DEAD and generally gives improved yields for weakly acidic substrates. We used the Tsunoda modification[97] for the

synthesis of YC-1, using 1,1-*azobis*dimethyl formamide and tributylphosphine, with benzyl alcohol **22** obtaining a mixture of *N*-1 **(33)** (34%) and *N*-2 **(35)** (48%) substituted products (1:1.4). Compound **35** underwent reduction with diisobutylaluminiun hydride to give *N*-2 regioisomer **37** of YC-1 Thus with the chemistry established for YC-1 we then applied the same methodology with 4-[3-(trifluoromethyl)-3*H*-diaziridin-3-yl]benzyl alcohol **23** for the YC-1 photoaffinity analogue **16**. Under these conditions we also found a mixture of *N*-1 **(34)** and *N*-2 **(36)** (1:1.8) substituted products was obtained as shown by HPLC, LC-MS and H-NMR (Scheme 12).
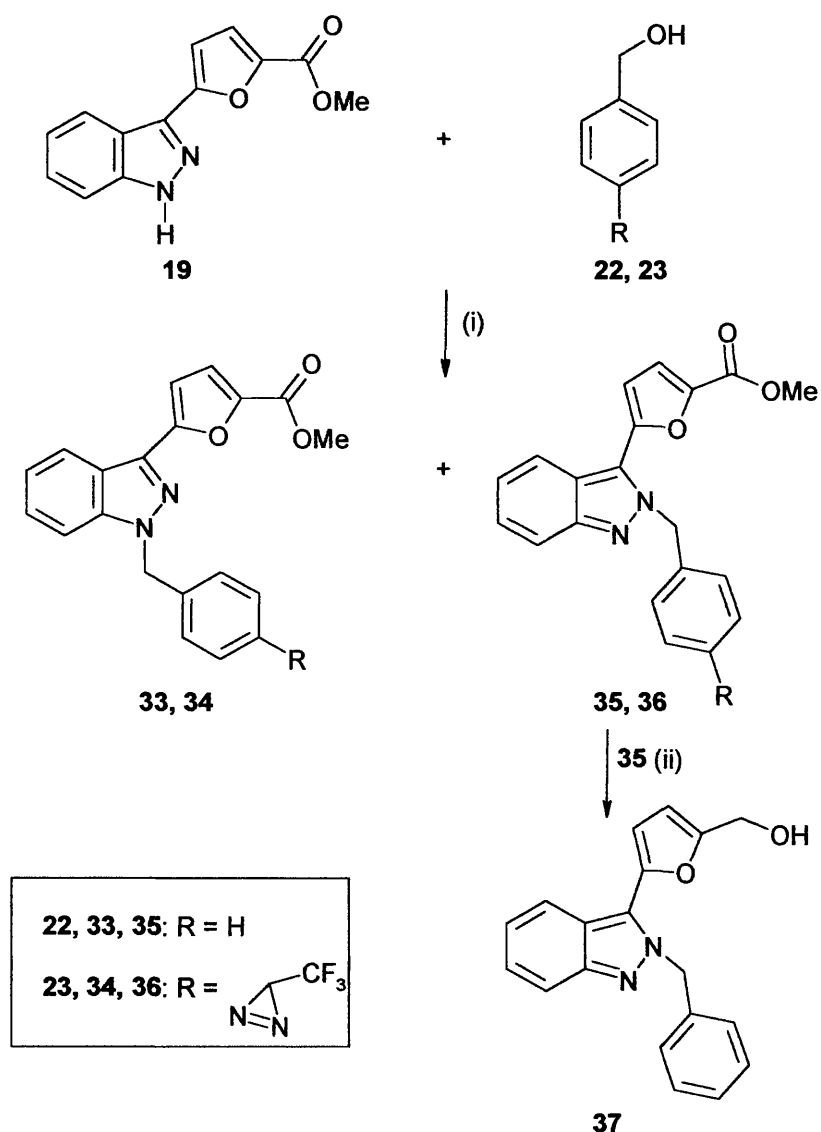
Scheme 12. (i) 1,1-azobisdimethyl formamide, tributylphosphine, toluene, 80°C (ii) DIBAL-H, CH_2Cl_2

The ^{1}H-NMR spectrum of the product after flash chromatography indicates that the reaction gave rise to two products, **33** and **35**, corresponding to the alkylation of each nitrogen of the indazole system. Both products have the same Rf in several solvent systems, such as chloroform and cyclohexane/EtOAc and it is difficult to separate them by column chromatography. In order to separate both products preparative HPLC was applied using a gradient elution of 40-80% acetonitrile in aqueous solution (0.1% TFA) over 20 min at a flow rate of 20 mL/min. Under these conditions two peaks (area%: 40.76 and 29.06) were observed corresponding to the N-2 and N-1 alkylated products, with retention times of 11.92 and 13.33 minutes, respectively.

- **Assignment of the spectra for 33 and 35**

In order to identify each product different NMR experiments were carried out. Figure 10 shows the NOESY spectrum corresponding to N-1 (Panel A) and N-2 (Panel B) alkylated products. The NOESY spectrum of the product which elutes first in the column shows space interactions between the signal at 5.9 ppm which corresponds to the methylene group and the signal at 6.65 ppm corresponding to the proton 10 (green circle, panel B) in the furyl ring. This result indicates that the compound in question is the N-2 alkylated **35**. This interaction is not observed in the NOESY spectrum of the second product, which in contrast shows interactions between the protons of the methylene group and proton 7 (violet circle, panel A) in the indazole ring and also with the protons in the ortho position of the benzyl group but not with protons in the furyl group, confirming this compound corresponds to the N-1 alkylated **33**.

The most remarkable difference between both structures in the H^1-NMR spectrum corresponds to the signal for proton 7 in the indazole, in **35** it appears at 7.8 ppm, while in **33** it is found at higher field (7.37ppm). This is due to the presence of the phenyl group near to it causing a shielding effect over it. For the same reason, proton 10 in the furyl group appears at higher field in **35** (6.75ppm) than in **33** (7 ppm).

Figure 10 Assignment of the *N*-1 and *N*-2 alkylated Regioisomers

Panel A
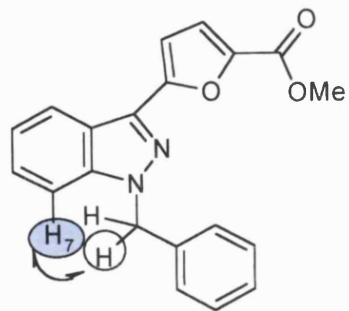
N-1 Alkylated

product

33
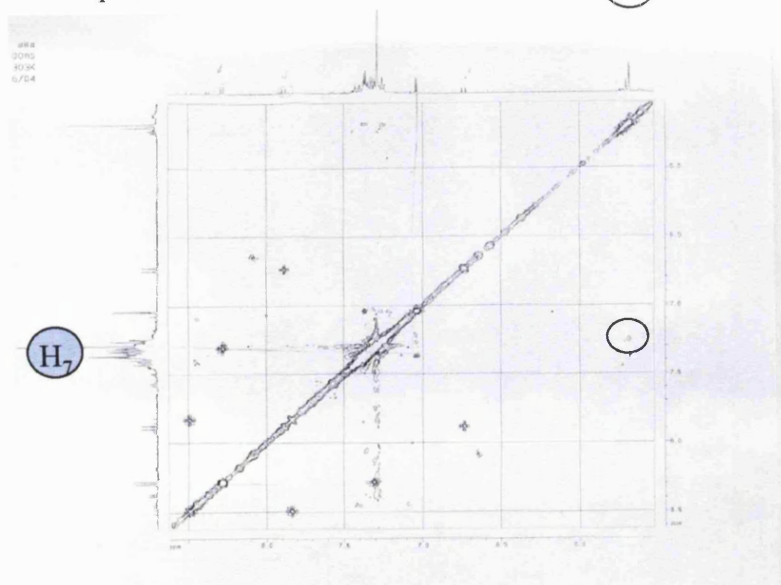
Panel B
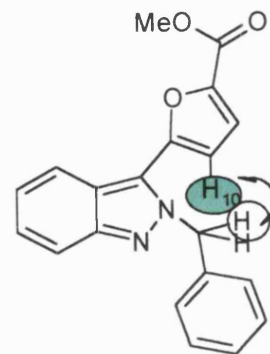
N-2 Alkylated

product

35
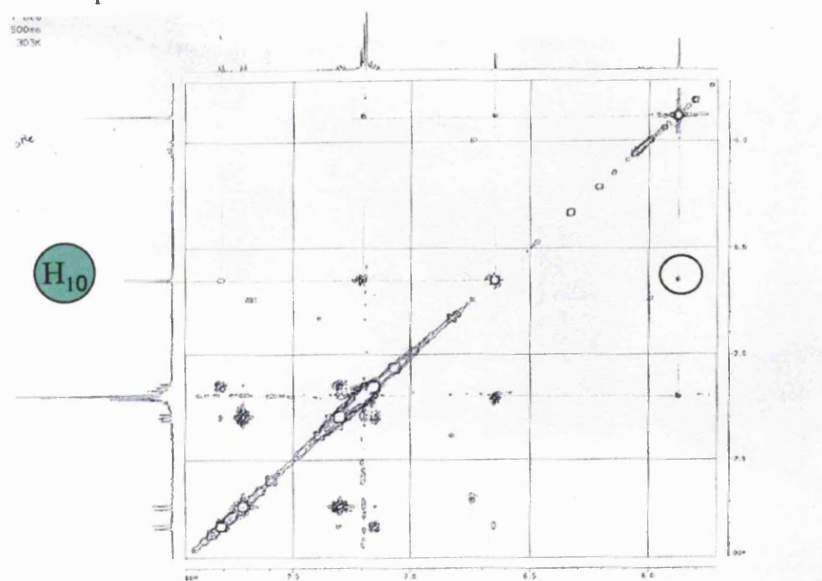
Summary

Our new method for indazole synthesis was sucessfully employed for the key YC-1 precursor **19**. Alkylation of **19** was successful by both traditional alkylation chemistry and under Mitsunobu conditions. Interestingly under the Mitsunobu conditions the major product obtained is the *N*-2 alkylated product while under typical alkylation conditions using a base and an alkylating agent, the *N*-1 alkylated compound is the sole product. It is known that alkylation of the indazole system normally gives a mixture of N-1 and N-2 alkylated products due to the tautomeric equilibrium. In our case, the 3-position substituent may have some influence in the driving force of the reaction when sodium hydride is used. We speculate that the formation of a complex between the metal of the base, the nitrogen at N-2 and the oxygen of the furyl group is possible, thus favouring alkylation in the N-1 position. Under Mitsunobu condition this coordination is absent and N-2 position can be alkylated.

2.4.2 Synthesis of amide derivatives

Transformation of a carboxylic acid into the corresponding acid chloride and subsequently reaction with an amine constitutes the classical way to form an amide bond. Other methods, more common in peptide chemistry, require the presence of a base and a coupling agent, such as HATU. The formation of the amide bond in the latter method takes place under milder conditions and in one step; this constitutes an advantage over the former route.

Commercially available *p*-chlorobenzoic acid was converted into the corresponding amide **15** by using DIPEA (diisopropylethylamine) as a basic resin and HATU (*O*-(7-azabenzotriazol-1-yl)-*N,N,N',N'*-tetramethyluronium hexafluorophosphate as a coupling reagent. Although the right product was obtained by using flash chromatography, we thought that it would be interesting to use this reaction as a model searching for other purification techniques to apply to the photolabile analogues, in order to avoid purification of the diazirine derivative on silica.

The purification strategy used is based on principles of complementary molecular recognition (CMR/R) using resins containing molecular recognition or molecular reactivity functionalities complementary to those of the solution-phase reactants, reagents and byproducts. This strategy has been used in parallel synthesis and combinatorial chemistry. The various CMR/R resins are used in sequential or simultaneous combinations to remove excess reactants, reagents and byproducts from solution-phase reaction products, which are then isolated in purified form by filtration.

In order to apply this purification technique to the required product, tetrafluorophthalic anhydride (TFPA) (38) was used as the "sequestration enabling reagent" which reacts with free amines to give compound (39).
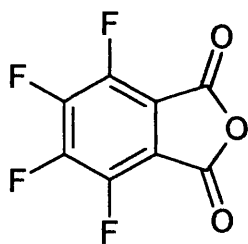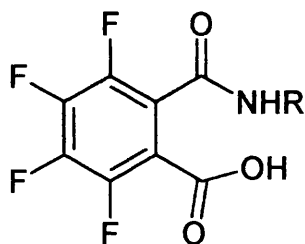
38   39

MP-carbonate resin (macroporus triethylammonium methylpolystyrene carbonate) was used in order to scavenge the free acid (starting material). However it was found that the resin reacts with the amide as well as with the acid and it was necessary to wash the filtrate with MeOH to recover the filtrate. This gave a mixture of products as indicated by LC-MS analysis, including the required one with a mass of 241. Therefore, column chromatography was the choice to purify the product.

The photolabile analogues have been synthesized following the same procedure. One of the analogues N-[3-(dimethylamino)propyl]-4-(3-methyl-3H-diaziren-3-yl)benzamide (17) (Scheme 13), contains the carbene precursor, diazirine. The

second amide 3-benzoyl-*N*-(3-dimethylamino)propyl benzamide (**18**) (Scheme 13) contains the benzophenone (a radical precursor) as the photoprobe.
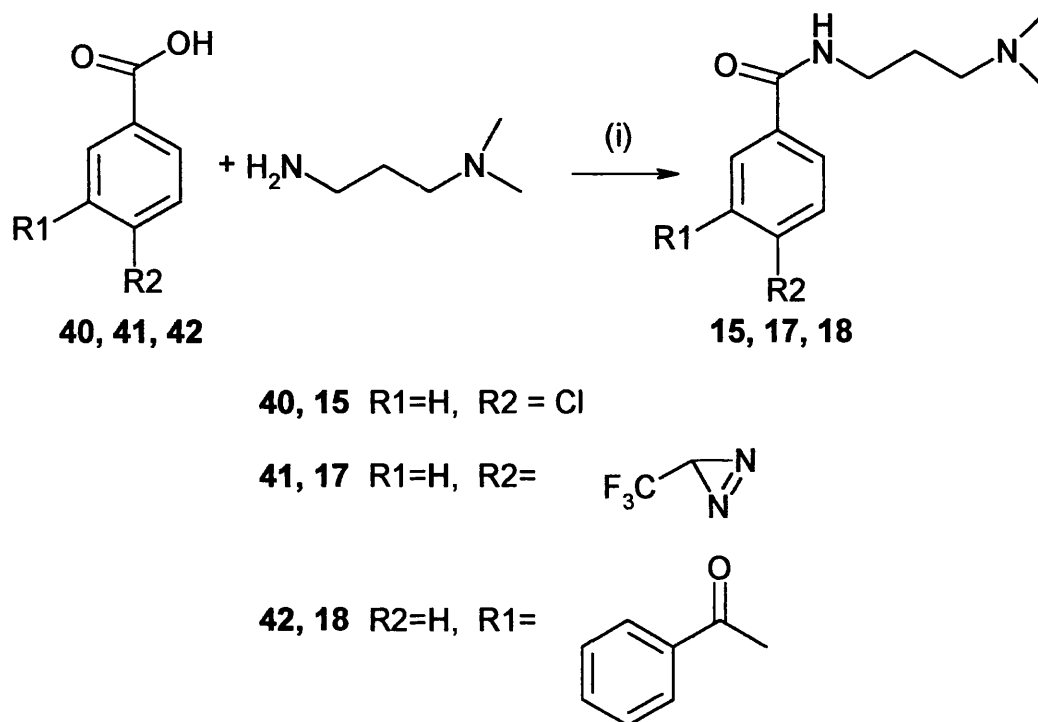
Scheme 13. (i) DIPEA, acetonitrile, HATU

- **Synthesis of 4-[1-(4-bromo-phenyl)-methanoyl]-*N*-(3-dimethylaminopropyl)-benzamide 45**

In addition we decided to synthesize an analogue that contains a bromine as well as the photoprobe. The presence of bromine is easily observed in the mass spectrum due to a series of peaks characteristic of this element, M and M+2 with the same intensity. These peaks could be used as a way of detecting the photolabeled peptides in the MALDI spectrum, as they would contain the same distribution.

We chose the benzophenone derivative for convenience as the starting material was commercially available. Thus 4-[1-(4-bromo-phenyl)-methanoyl]-benzoic acid ethyl ester **43** was converted into the corresponding carboxylic acid **44** through a saponification reaction in the presence of an aqueous solution of

NaOH in THF followed by addition of HCl. The product was then converted into the acid chloride and reacted with the 3-dimethylaminopropylamine giving the desired product **45** (Scheme 14).
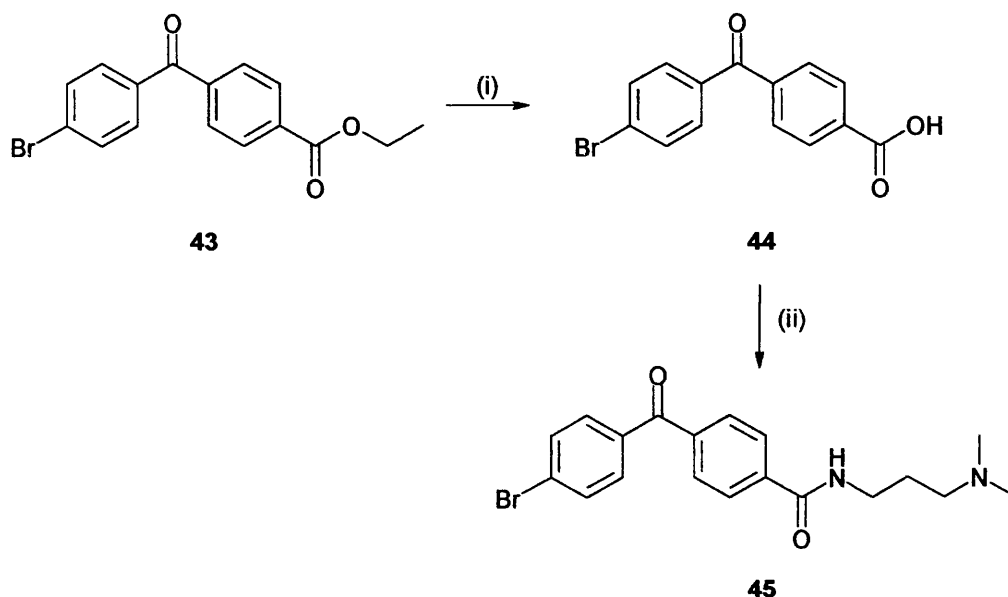
Scheme 14. (i) 10% NaOH (aq), THF (ii) $SOCl_2$, DMF, heat (iii) $H_2N(CH_2)_3N(CH_3)_2$, THF

2.5 Activation of sGC by the target compounds

The aim of this work was to use the photolabile analogues of sGC activators to locate their binding sites in sGC. For our photoaffinity analogue to give us accurate information on the binding of the parent molecule we must be confident that it occupies the same bonding site as the parent compound and in the same orientation. Thus the required structural modifications made by the introduction of the photoreagent into the corresponding compounds should not change the binding mode of the molecule. In other words, the photolabile analogue should mimic the parent ligand as much as possible. A crude way to check this is to compare the soluble guanylate cyclase activation properties of the parent and photoaffinity labelled compounds. Thus the parent ligand and its analogue must show similar activation of the enzyme.

Initially, the target compounds were assayed for sGC stimulation using baculovirus expressed, and partially purified, bovine sGC. cGMP levels were measured using a commercially available ELISA assay (*enzyme-linked immunosorbent assay*).[98] sGC was submaximally stimulated with the NO donor

compound DEA/NO **1** (300nM) and cGMP accumulation was evaluated for each compound at a range of concentrations producing the corresponding dose-response curve. The cGMP produced by each compound was expressed as a percentage of the DEA/NO response. In some cases a radioimmunoassay substituted the ELISA assay. Availability dictated the choice of assay at the time of the experiment.

ELISA assay principle

The enzyme immunoassay is based on the competition between free cGMP and a cGMP tracer (linked to a peroxidase molecule) for a limited number of cGMP-specific rabbit antiserum binding sites. The concentration of the cGMP tracer is held constant while the concentration of free cGMP varies. Thus, the amount of cGMP tracer that is able to bind to the rabbit antiserum will be inversely proportional to the concentration of free cGMP in the well. This rabbit antiserum-cGMP complex binds to the donkey monoclonal anti-rabbit antibody that has been previously attached to the well. The plate is washed to remove any unbound reagents and then the substrate to peroxidase is added to the well. The product of this enzymatic reaction has a distintive yellow colour and absorbs extrongly at 412 nm. The intensity of this colour, determined spectrophotometrically, is proportional to the amount of cGMP tracer bound to the well, which is inversely proportional to the amount of free cGMP present in the well during incubation (Figure11).
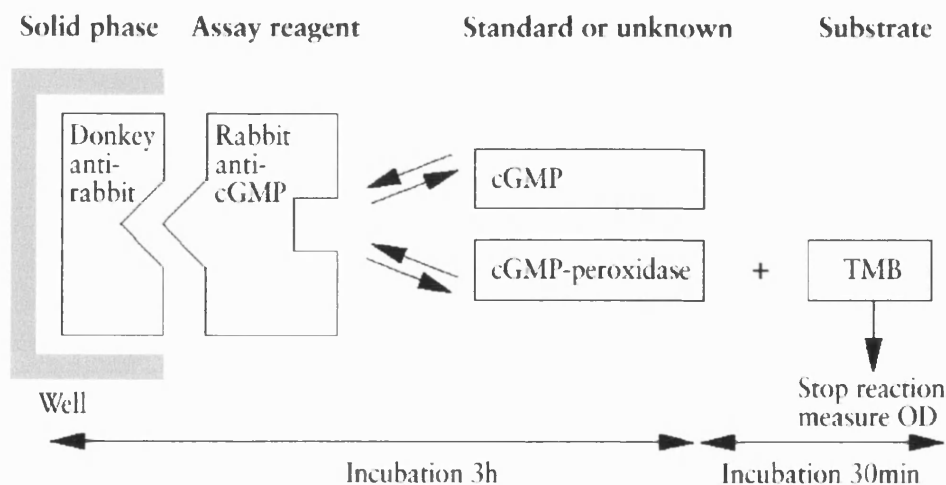
Figure 11. Schematic representation of the ELISA assay.

Radioimmunoassay principle

The assay is based on the competition between unlabelled cGMP and a fixed quantity of the tritium labelled compound for the binding to an antiserum which has a high specificity and affinity for cGMP. The amount of labelled cGMP bound to the antiserum is inversely related to the amount of cGMP present in the assay sample. Measurement of the antibody-bound radioactivity enables the amount of unlabelled cGMP in the sample to be calculated. Separation of the antibody-bound cGMP from the unbound nucleotide is achieved by ammonium sulphate precipitation, followed by centrifugation. The precipitate, which contains the antibody-bound complex, is dissolved in water and its activity determined by liquid beta-scintillation counting. The concentration of unlabelled cGMP is then determined from a linear standard curve (Figure 12).

Free   **Bound**

[³H]cGMP   [³H]cGMP-antibody

+ antibody

cGMP   cGMP-antibody
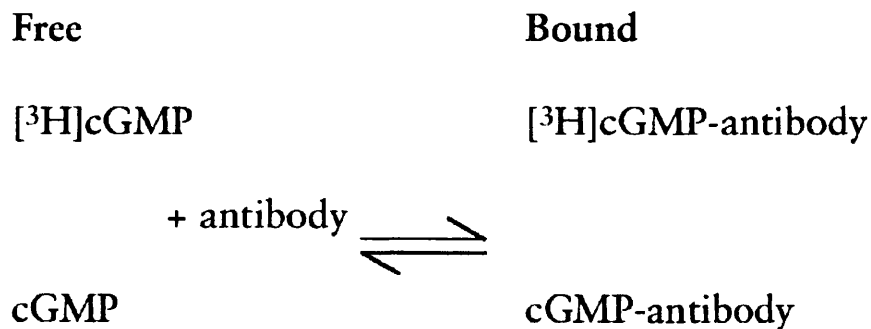
Figure 12. Schematic representation of radioimmunoassay

• **Activation of sGC by YC-1 and its Photoaffinity analogue**

In order to improve the reproducibility of the sGC assay we took advantage of the synergy between the activation of the enzyme by YC-1 and an NO donor, such as DEA/NO. With this combination of activators a significantly higher level of cGMP accumulates making the assay easier to interpret.
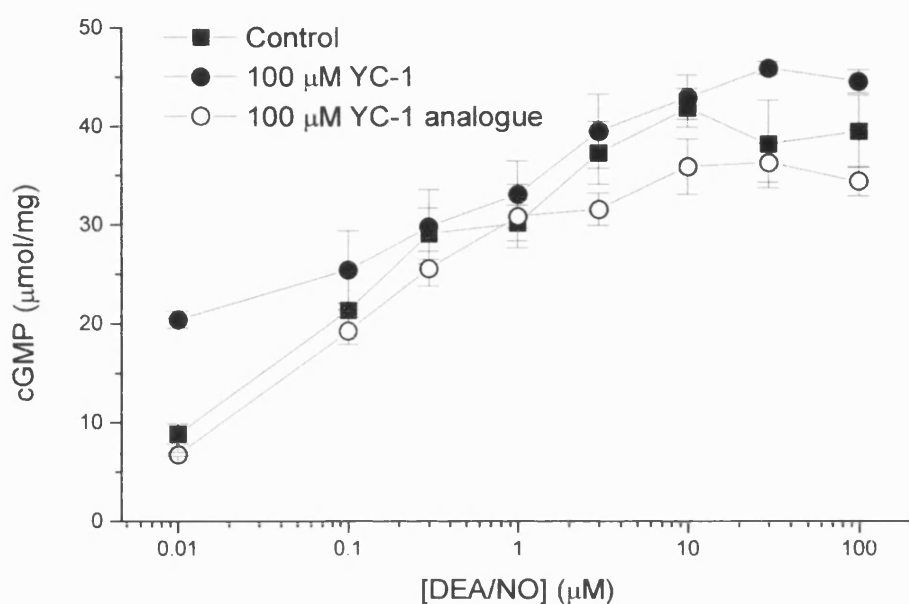
Figure 13. Effect of DEA/NO on the stimulation of sGC by YC-1 **5** and its analogue **16**.

Figure 13 shows the cGMP accumulation produced by different concentrations of DEA/NO (control, squares) and in the presence of 100 μM of YC-1 (filled circles) or YC-1A (open circles). It can be seen that YC-1 enhances NO-cGMP accumulation acting in a synergistic manner as has been reported,[50] whereas YC-1A shows an effect that is not significantly different to that produced by DEA/NO alone (the control). Thus the presence of the diazirine moiety modifies the action on sGC in relation to the parent ligand. Work published during the preparation of this thesis confirmed that substitution at the para position of the N-1 benzyl moiety of YC-1 gave compounds with lower sGC activation.[99] For this reason YC-1A is not a suitable ligand for photoaffinity labeling experiments.

We also wanted to obtain a dose-response curve for the N-2 regioisomer of YC-1 in order to observe the effect of moving the benzyl substituent to N-2.
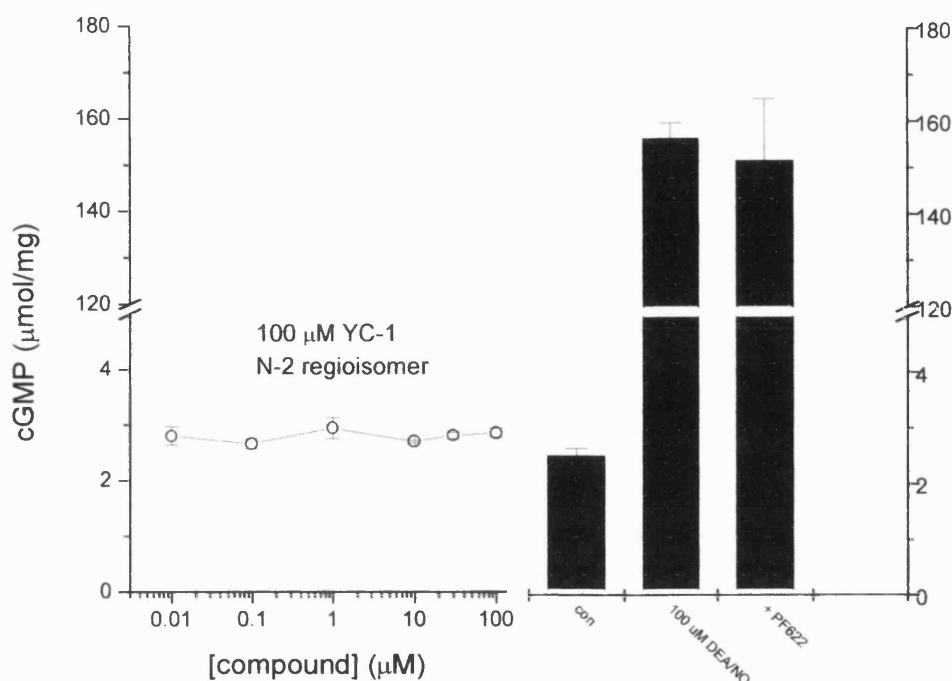
Figure 14. Stimulation of purified sGC by N-2 regioisomer **37** of YC-1 in the presence of DEA/NO

As Figure 14 illustrates, the compound under study does not show activity on sGC. In view of the structure compared to YC-1, this result may be explained by either a lack of the benzyl group in the N-1 position of the indazole or by the presence of the substituent on the N-2 position. However, a SAR study on a similar indazole system indicates that the lack of the N-1 position substituent does not affect the activity. Therefore the decrease of the activity must be due to the presence of the substituent on the N-2 position; thus it appears that the protein cannot accommodate an indazole with substitution at the N-2 position. We can speculate that this may be due to either steric interactions or electronic effects preventing the binding of some amino acid of the enzyme in that region of the molecule.

- **Activation of sGC by the amide derivatives, 15, 17, 18**
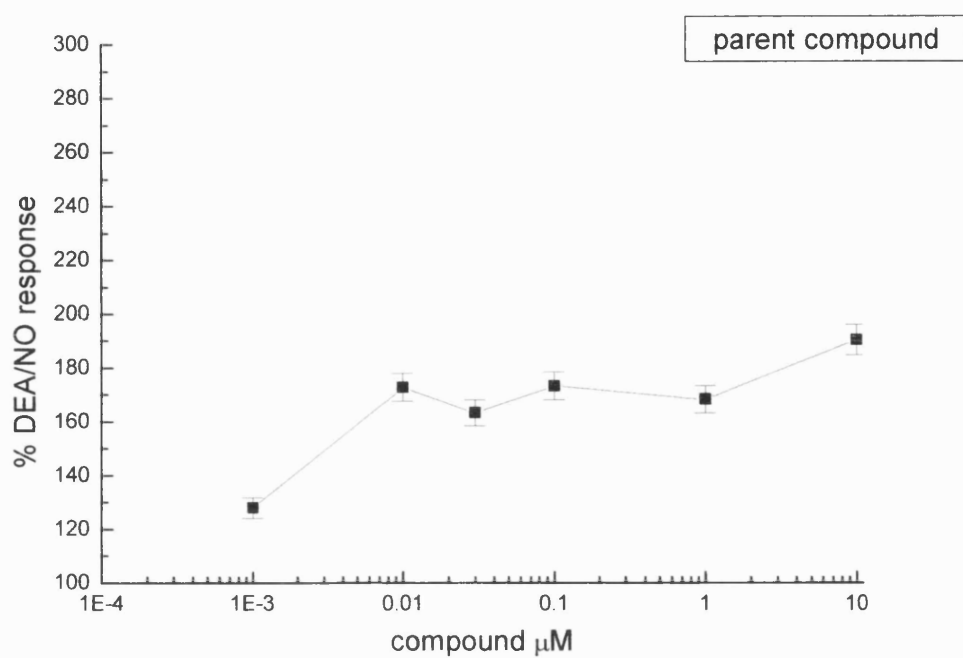
Figure 15. Stimulation of partially purified sGC by 4-chloro-N-[3-(dimethylamino)propyl]benzamide **15** at different concentrations.
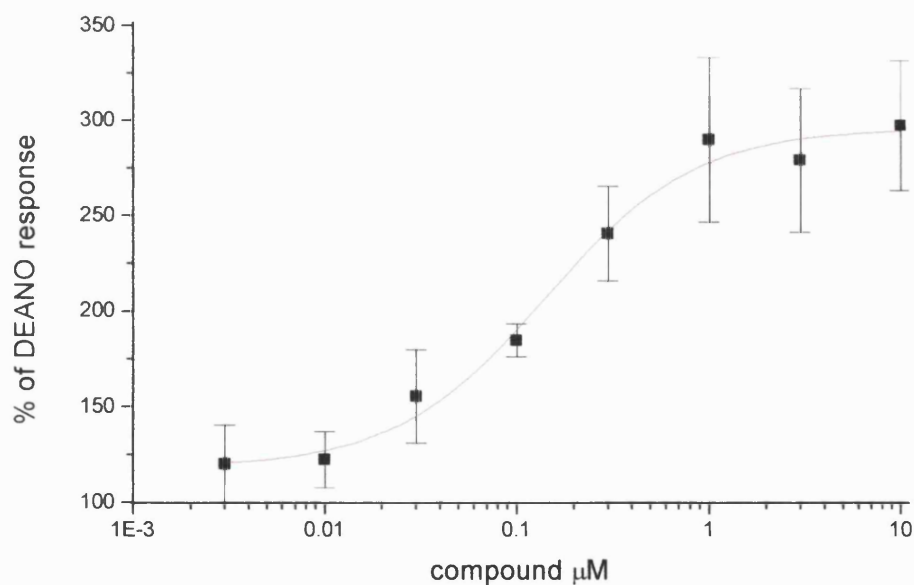
Figure 16. Stimulation of partially purified sGC by *N*-[3-(dimethylamino)propyl]-4-(3-methyl-3H-diaziren-3-yl)benzamide **17** at different concentrations.
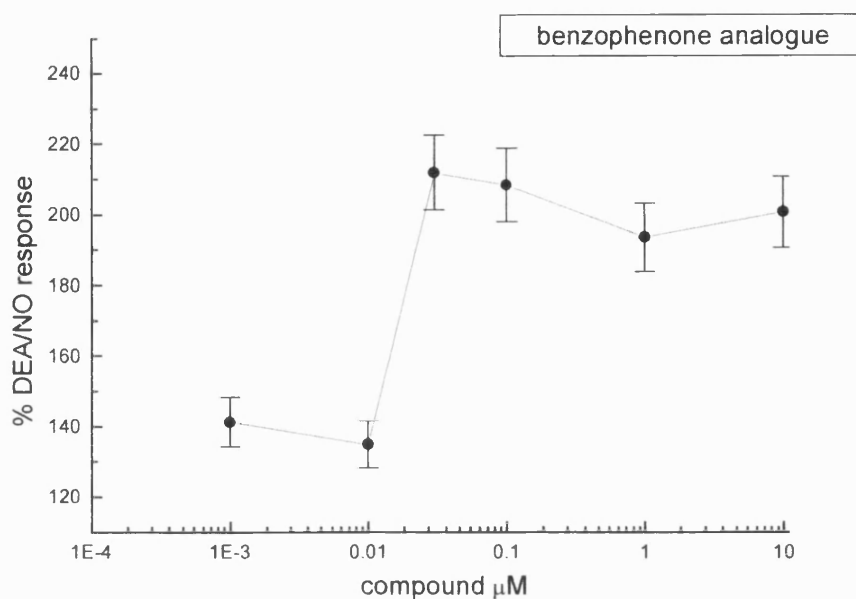
Figure 17. Stimulation of partially purified sGC by 3-benzoyl-N-[3-(dimethylamino)propyl]benzamide **18** at different concentrations.

Figures 15, 16 and 17, display the dose-response curves for the amide derivatives: parent compound, diazirine and benzophenone derivatives, respectively. All of them show some activity, the diazirine-derivative **17** having most activity for sGC. Therefore this compound was selected for further photoaffinity labelling experiments. It is noteworthy to mention that the ELISA assays were performed using partially purified enzyme. In order to decrease the variability between different experiments the cGMP elevation response of the compound of interest is compared to the response achieved with a fixed DEA/NO concentration.

- **Activation of sGC by the bromo-containing amide derivative 45**

On the other hand compound **45** shows no activity on sGC as the radioimmunoassay dictated (Figure 18). The cGMP production is similar to that of the control thus the presence of the bromine decreases the activity on sGC. As a result this compound is unsuitable for PAL experiments.
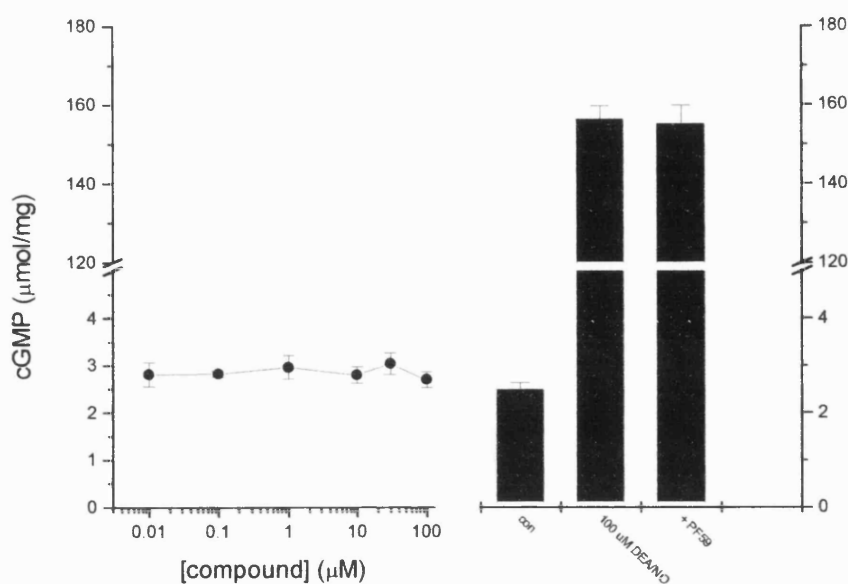
Figure 18. Stimulation of purified sGC by 4-[1-(4-bromo-phenyl)-methanoyl]-
N-(3-dimethylamino-propyl)-benzamide **45** at different concentrations

2.6 Photoaffinity labeling (PAL) experiments

Based on the results from the assays previously presented the diazirine amide
derivative **17** clearly shows the higher activation on sGC, and therefore is the
best candidate in order to use in the photoaffinity labeling experiments. At this
point we can start to imagine what needs to take place in order to initiate the
process. As Ehrlich's dictum says, "corpora non agunt nisi fixata" (a drug will
not work unless it is bound).

The major steps in a PAL experiment are:

- Incubation of the enzyme and ligand
- Removal of excess of ligand
- Photolysis
- SDS-PAGE (sodium dodecyl sulphate polyacrylamide gel)

2.6.1 Incubation

The first step in a photoaffinity labeling experiment is to allow the ligand to
bind to its receptor. The ideal outcome would be to obtain a considerable
amount of site-specific labeling and while keeping the labeling outside the

receptor site at a low level. Hence, this step is of significant importance since it will influence the success of the following steps. Not all ligands bind rapidly to their receptors and sufficient time should be allowed for equilibration before photolysis is initiated.

Time of incubation, temperature, buffer and concentration of ligand and enzyme are variables that require close monitoring. Key considerations are:

- The enzyme used in the experiments was the purified commercial available sGC which posses a specific activity of 10.000 nMol cGMP per min per mg at 37°C during 10min. We wanted to mimic the conditions used for the assays; thus the temperature and time of incubation were established in the same conditions: 37°C and 10 min respectively.

- The fact that it is not known whether binding and activation of sGC by these compounds requires the presence of the enzyme substrate, GTP. Therefore, initially, the experiments were performed both in the presence and the absence of the substrate.

- Ideally, the amount of ligand added should be equal to the amount of ligand that the enzyme requires for occupying the binding site, avoiding further non-specific labeling. To approximate to this hypothetical case, the concentration of the ligand should be as low as possible. This is possible to achieve for those enzyme-ligand complexes with low dissociation constants, however for those with high Kd, a higher concentration of the ligand may be required in order to obtain a considerable degree of labeling. Thus, the affinity of the ligand for the enzyme plays a key role in the determination of the amount of ligand to be used in the experiment. In those cases where kinetic studies are not available, the dose-response curve can be used to gain some information about the ligand concentration to be used. Due to the lack of data about the affinity of the compound under study for the enzyme we carried out a test experiment at two different values of ligand concentration, 0.5 and 10 μM.

2.6.2 Removal of the excess of ligand

After the ligand-enzyme complex has been formed in the incubation step, ideally, the next step should be the removal of the excess ligand, as free ligand can be a troublesome source of non-specific labeling.

Tight-binding ligands, which have a high affinity for their receptors, obviously present a great advantage in photoaffinity labeling experiments as the rate of dissociation from the receptor may be slow enough to allow excess ligand to be removed before the irradiation step, thus reducing non-specific labeling. Those ligands with a high dissociation constant the process is more complicated as the techniques used for removing the excess photolabile ligand, such as washing or use of antibodies, can also remove ligand which is required for reversible binding. Bearing in mind the lack of kinetic data, we briefly investigated the possibility of removing the excess ligand (prior to irradiation) by centrifugation. Therefore we carried out a test experiment with enzyme alone in order to determine if sGC precipitates on centrifugation. Initially, the solution containing enzyme and Tris buffer was centrifuged for 1 hour at 4°C and 50.000 rpm. The precipitate (pellet) was separated from the solution (supernatant) and both fractions were subjected to Gel-electrophoresis. Silver staining of the gel showed that the enzyme was present in both fractions. The same results were obtained when the speed of centrifugation was increased at 95.000 rpm or when trichloroacetic acid was used to facilitate the precipitation of the enzyme. Thus, a considerable amount of enzyme was lost into the supernatant fraction (data not shown), suggesting that centrifugation is not a good method to eliminate the excess of ligand in the system under study. In view of this result and the fact that the literature gives some examples of PAL in which purification after the binding stage is avoided, we decided to first try an experiment without purification. However, a high degree of nonspecific labeling was observed as indicated by the MALDI spectrum, which was difficult to interpret.

Therefore, we thought of the following possibilities to reduce the non-specific labelling:

1. Using equimolar concentrations of enzyme and ligand in the incubation step.

2. Using an unlabelled compound.

By using equimolar concentrations of the photolabile ligand and enzyme we attempted to saturate the binding sites of the receptor. The experiment containing the cold compound as well as the photolabile ligand was performed as a negative control. The parent ligand (unlabelled compound), present at 1000 times more concentration than the photolabile ligand, will compete for the binding site, therefore the new covalent bonds formed after irradiation would indicate sites outside of the pocket of the binding site of sGC. These experiments were carried out in parallel and repeated twice in order to compare results.

2.6.3 Photolysis

In this step the reactive intermediate, carbene, is unmasked by irradiation at 360nm, and is able to form irreversible covalent linkages ideally with the amino acids that make up the binding site. However, photochemical reactions are inherently complex and in most of the cases non-specific labelling was observed. The duration of photolysis is important. Photolysis studies of derivatives of TPD, have shown that this type of compounds readily form carbenes after irradiation from 5 to 10 minutes.

Figure 19 shows the uv-vis spectra of the amide-diazirine derivative 17 (0.6 mM) prior to irradiation (red line) and after 5 minutes of irradiation at 360nm (black line). As we can see the peak corresponding to the diazirine moiety at 360nm disappears after irradiation during the indicated period of time. Thus, we allowed a reaction time of 5 minutes and in order to obtain reproducible results the sample is irradiated at a fixed distance relative to the lamp.
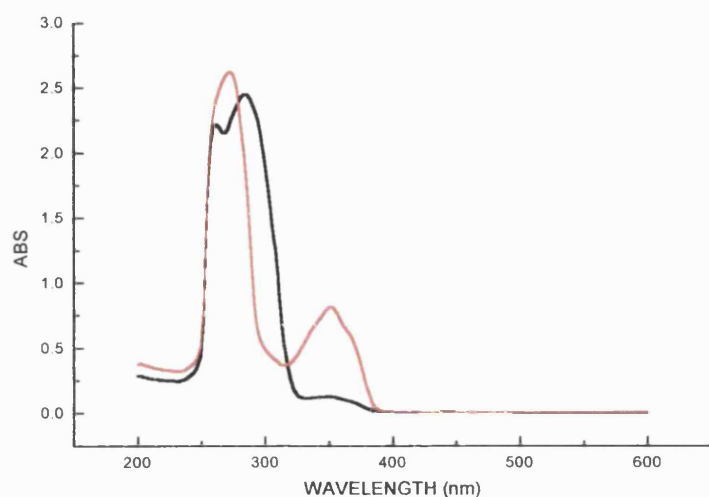
Figure 19. uv-vis spectra for compound **17** before (red line) and after (black line) exposure to irradiation for 5 min at 360nm.

Scheme 15 illustrates the formation of the photolysis product, the carbene **17a** corresponding to compound **17**.

17   **17a**
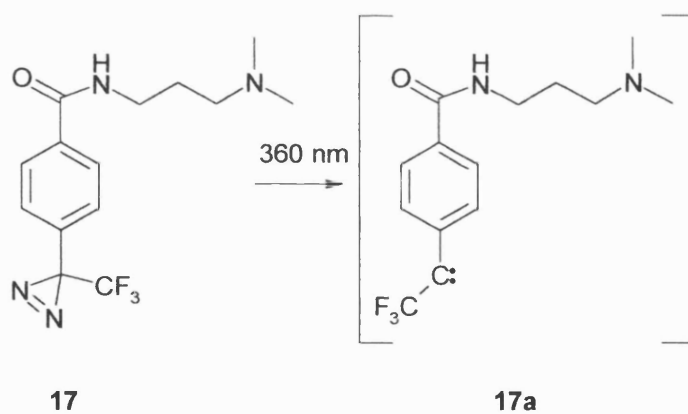
Scheme 15. Photolysis of compound **17**

- **Control experiment**

In order to compare results, a control experiment, in the absence of photolabile ligand, was necessary. This allows a comparative analysis of the masses corresponding to the peaks appearing in the MALDI spectrum in the presence and in the absence of ligand. In this manner, at least theoretically, this would provide the peptides that have been labelled. In addition, a control experiment

gives information about the stability of the enzyme under the experimental conditions.

2.6.4 SDS-PAGE (sodium dodecyl sulphate polyacrylamide gel)

Once photolysis has taken place, and new covalent bonds have been formed in the binding site, the sample is subjected to gel-electrophoresis in order to purify and separated the enzyme into α and β subunits after the labelling. Figure 20 shows a *coomassie-blue* staining gel after the control experiment. It is possible to see two bands of different size; the bigger one corresponds to the α subunit while the smaller one, the most intense in the gel, represents the β subunit. *Coomassie-blue* staining is more convenient than silver staining due to the easy removal of the former prior digestion. Figure 21 shows the corresponding Gel for the experiment, containing the photolabile ligand in the absence (A) and the presence (B) of the parent ligand.
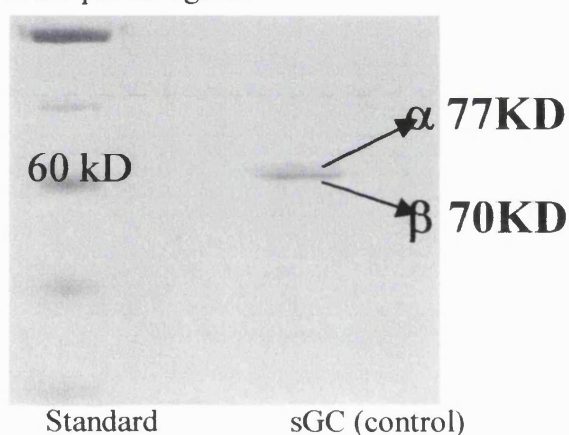
Figure 20. Gel electrophoresis of control experiment
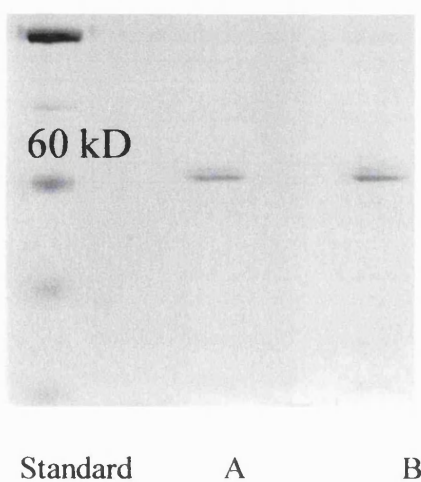
Figure 21. Gel electrophoresis of PAL experiment, containing the photolabile ligand **17** in the absence (A) or presence (B) of the parent ligand **15**.

2.7 Matrix-Assisted Laser Desorption/Ionization Time-Of-Flight (MALDI-TOF)

2.7.1 Trypsin digestion

In order to perform the mass spectroscopic analysis, bands corresponding to the α and β subunits of the protein were excised from the gel and *in gel digested* with trypsin as described in the methods (experimental section). Trypsin is a protease which cleaves at the C-terminus of lysine and arginine residues. Thus, trypsin digestion produces a series of peptide fragments of the protein under study, known as the "peptide fingerprint". These peptides are separated on a mass-to-charge (m/z) ratio basis by mass spectrometry. Each peak in the spectrum represents a separate fragment of the digestion. Therefore we can obtain a peptide mass map of the digest. The masses of all of the peaks from each MALDI-TOF spectrum were entered into an MS-fit table and a nonredundant database was searched as described in materials and methods.

2.7.2 Principle

MALDI-TOF MS is an important analytical tool for identifying proteins in sequence databases. This is due to the ability of MALDI to produce singly charged molecular ions in a mass range up to hundred thousand Daltons without fragmentation. In addition, other advantages associated with this technique are low noise levels, high sensitivity, little sample consumption and short measurement times.

Typically, the sample is mixed with an organic compound which acts as the matrix and allowed to crystallise on a still target. The target is then inserted into the MS and bombarded with a pulsed laser beam. The matrix serves to minimize sample damage from the laser beam by absorbing the incident laser energy. Molecules are desorbed from the surface and ionized (Figure 22, blue square). The analyte ions are then accelerated by an applied high voltage (15-25 kV), separated in a field-free flight tube and detected as an electric signal at the end of the flight tube. Peptide separation is achieved by the fact that the time of flight is proportional to the mass-to-charge ratio. Small ions travel faster

than large ions and therefore reach the detector first. Figure 22 shows a schematic representation of the MALDI-TOF components.
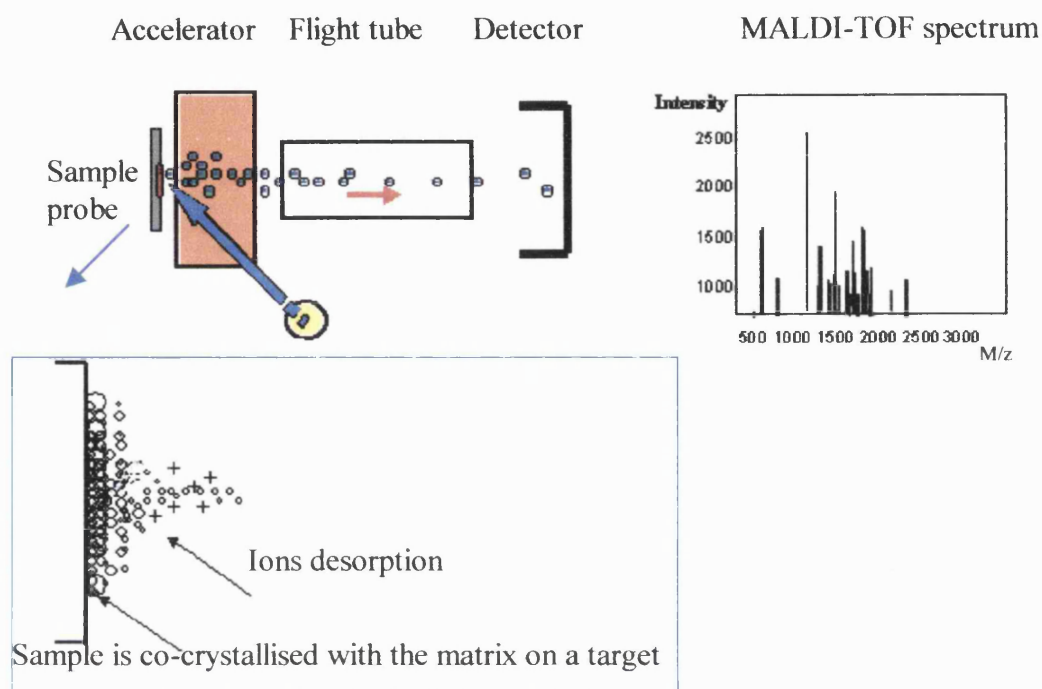
Figure 22. Schematic representation of MALDI-TOF components.

2.7.3 Approach

The methodology we used to elucidate some information about the binding site of the compound under study in sGC is represented in Figure 23. The top half of this figure shows the enzyme alone corresponding to the control experiment, while the picture below represents the complex enzyme-ligand formed after photolysis. Both systems (enzyme alone and enzyme-ligand) are fragmented with trypsin into small peptides and are analysed by MALDI-TOF MS providing a mass peptide map. Comparison of the MALDI-TOF spectra before (control) and after adding the photolabile ligand provides information about which peptide fragments have been modified and consequently labelled. Thus, if a peptide fragment in the enzyme with a mass e, is labelled by the ligand of mass L, then in the spectrum for the labelled protein it is expected to be observed as a peptide fragment with a mass e+L.
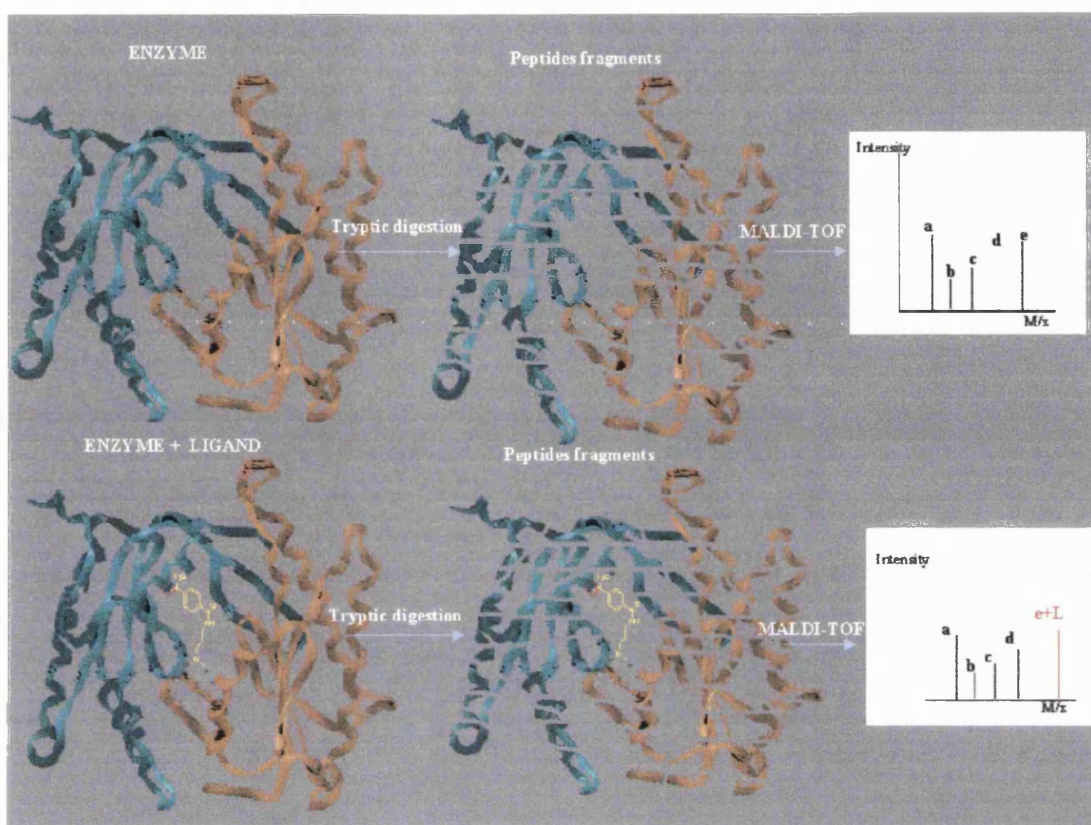
Figure 23. Schematic representation of the method for identifying labelled peptides by MS.

Analysis of the spectrum proceeds as follows:

1. From the observed mass peak list obtained after processing the MALDI-TOF spectrum, the peaks that are common to the labeling experiment and the control experiment are eliminated, as well as those which correspond to Trypsin, matrix and keratin, a possible contaminant.

2. Those masses that are present in the "cold" experiment are removed as we assume that these correspond to unspecific labeling.

3. From each peak in the remaining list (M) is then subtracted the mass corresponding to the reactive carbene species (L) formed after photolysis of the parent ligand. Since it is unknown how many molecules of ligand the enzyme requires for the binding, from each observed peak is subtracted the mass of one (M-L) or two molecules (M-2L) and then the results are compared with predicted peptide sequences from the protein.

4. The experiments are repeated twice in order to compare results and thus the final peptide sequences identified are derived from both experiments.

It is important to make some observations regarding the data processing. In general, not all of the possible predicted peptide fragments are observed in the MALDI spectra. Since not all the peptide fragments are included in the spectrum there is a lack of information about some parts of the protein. This obviously represents a limitation as not all the peptide fragments are analysed. Moreover, the peptide fragments that appear in the spectrum vary from sample to sample and even from the same sample in a different MALDI experiment. Thus, a different percentage of protein coverage is observed in different experiments. Consequently, in order to avoid misleading information and to simplify the analysis we routinely deduct from the sample spectrum both the peaks observed in the control spectrum and those corresponding to the predicted fragments.

2.7.4 Results

Results are presented for each subunit in the presence and in the absence of GTP. Consequently the results are reported as follows:

1. α Subunit with the photolabile ligand **17** in the absence of the substrate GTP

2. α Subunit with the photolabile ligand **17** in the presence of the substrate GTP

3. β Subunit with the photolabile ligand **17** in the absence of the substrate GTP

4. β Subunit with the photolabile ligand **17** in the presence of the substrate GTP
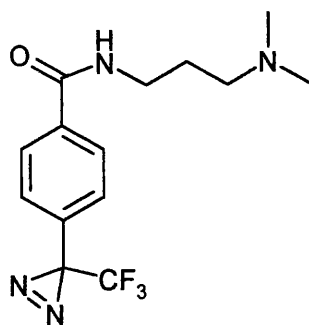
17

In addition, areas of interest in the spectrum are presented for each case. As an example, in the first case the MALDI spectrum of the whole subunit with and without the ligand is presented.

1. α Subunit with the photolabile ligand 17 in the absence of the substrate GTP

Figure 24 represents the MALDI-TOF spectrum for the α subunit after the photoaffinity experiment with the photolabile ligand **17** in the absence of GTP. An initial comparison of this spectrum with the one corresponding to the control experiment (i.e. in the same conditions but in the absence of the photolabile ligand Figure 25) shows the presence of a set of peaks that are absent in the control experiment.
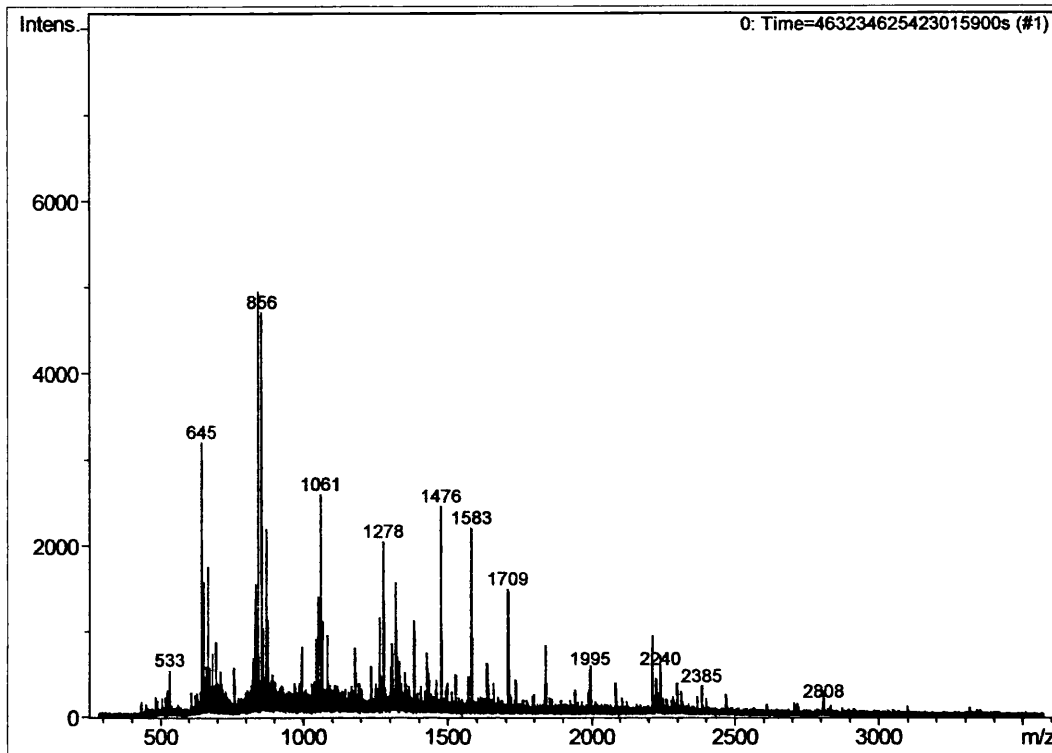
Figure 24. MALDI-TOF spectrum (alpha subunit +L) in the absence of GTP
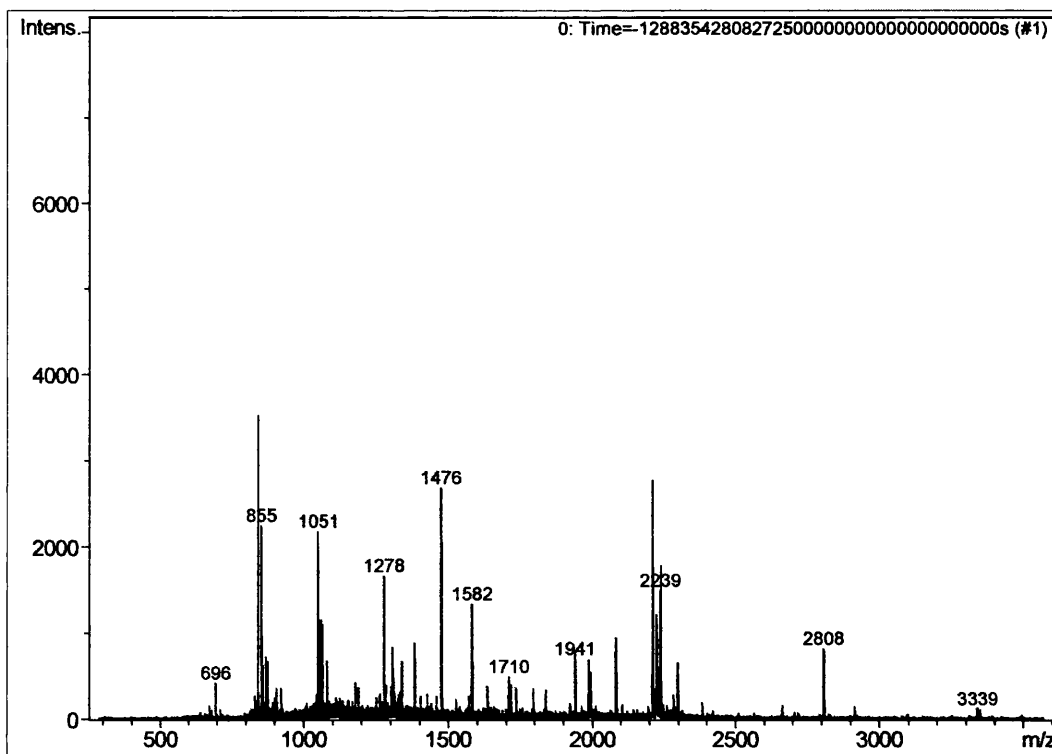
Figure 25. MALDI-TOF spectrum (control alpha subunit) in the absence of GTP

Table 3. Results for α subunit containing photolabile ligand in the absence of the substrate GTP.

First experiment   Second experiment

A	B	C	D	E	F
M	**M-L**	**M-2L**	**M**	**M-L**	**M-2L**
483.2865	197.1572	-88.9721	881.5287	595.3994	309.2701
532.5366	246.4073	-39.722	1924.749	1638.62	1352.49
561.7483	275.619	-10.5103	1963.922	1677.792	1391.663
994.7114	708.5821	422.4528	2010.828	1724.699	1438.569
1334.373	1048.244	762.1147	2026.799	1740.67	1454.541
1352.307	1066.177	780.048	2198.297	1912.167	1626.038
2312.102	2025.973	1739.844	2262.184	1976.054	1689.925
2468.2	2182.07	1895.941	2403.146	2117.017	1830.888
2718.084	2431.954	2145.825	2420.799	2134.67	1848.541
			2566.269	2280.14	1994.011
			2721.186	2435.057	2148.928
			2871.552	2585.423	2299.293
			3396.587	3110.458	2824.328

Table 3 shows the remaining observed masses (**M**) (columns **A** and **D** after analysis as indicated above. The adjacent columns show the masses obtained by subtracting one (**M-L**) (columns **B** and **E**) or two (**M-2L**) (columns **C** and **F**) molecules of ligand from the mass M. Columns **A**, **B** and **C** correspond to the results for the first experiment, while columns **D**, **E** and **F** correspond to the second experiment. The values of M-L, and M-2L that matched with predicted peptide sequences from the protein are marked in blue. Predicted peptide sequences corresponding to those values are shown in Table 4 along with the observed (obs) and predicted masses. Peptide sequences that appear more than once (i.e. in more than one experiment) are marked in bold.

Table 4. Predicted peptide sequences proceeding from M-L values (Panel A) or from M-2L (Panel B) for α subunit containing photolabile ligand in the absence of the substrate GTP.

Panel A

First experiment   Second experiment

M-L obs.	M predicted Peptide sequence	**M-L** obs.	M predicted Peptide sequence
708.582	708.4 ^{2}FCAKLK^7	595.399	598.26 ^{1}MFCAK^5
1048.24	1049.55 ^{82}LIFPEFER^{89} ^{617}INVSPTTYR^{625}	2435.05	2431.16 ^{369}GQMIYMVESSI LFLGSPCVR^{390}
2431.95	2431.16 ^{369}GQMIYMVESSI LFLGSPCVR^{390}		

Panel B

First experiment   Second experiment

M-2L obs.	M predicted Peptide sequence	**M-2L** obs.	M predicted Peptide sequence
780.048	779.33 ^{354}WDNSMK^{359}	1454.541	1455.72 ^{595}YCLFGNNVTLANK^{607}
		1626.038	1625.84 ^{542}ESDTHAVQIALMALK^{556}
		1830.888	1833.87 ^{247}EFVDQPCELYSVHIR^{261}

Finally, Figures 26 and 27 depict parts of MALDI-TOF spectrum lacking (Panel A, control) or containing (Panel B) the peaks (in blue circles) corresponding to the peptide sequences of interest from the first and second experiment, respectively.

Panel A (control)   Panel B (Enzyme +Ligand)
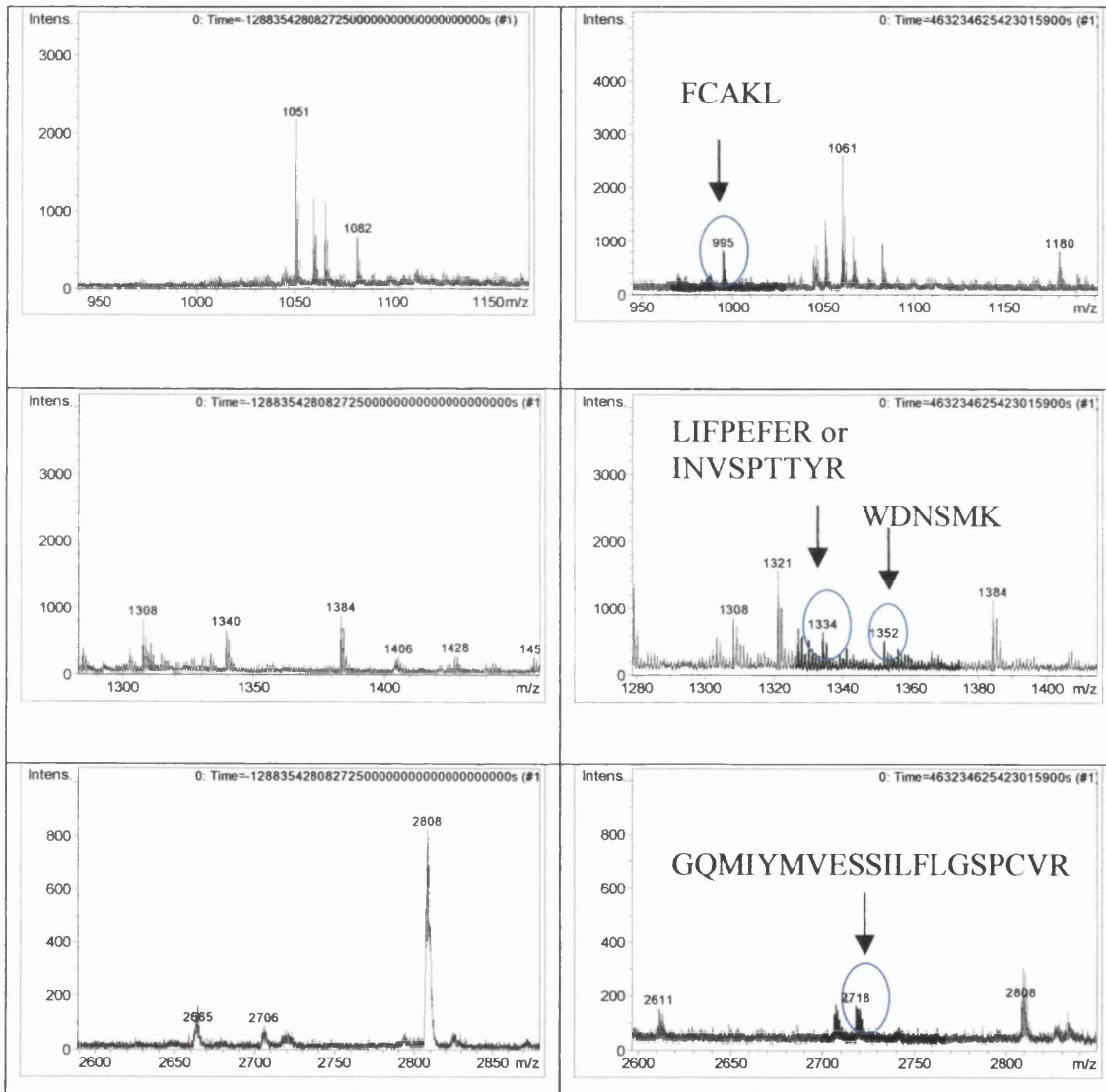
Figure 26. Selective parts of MALDI spectra before (control, Panel A) and after (Panel B) adding the photolabile reagent for α subunit containing photolabile ligand in the absence of the substrate GTP from the first experiment.

Panel A (control)   Panel B (Enzyme +Ligand)
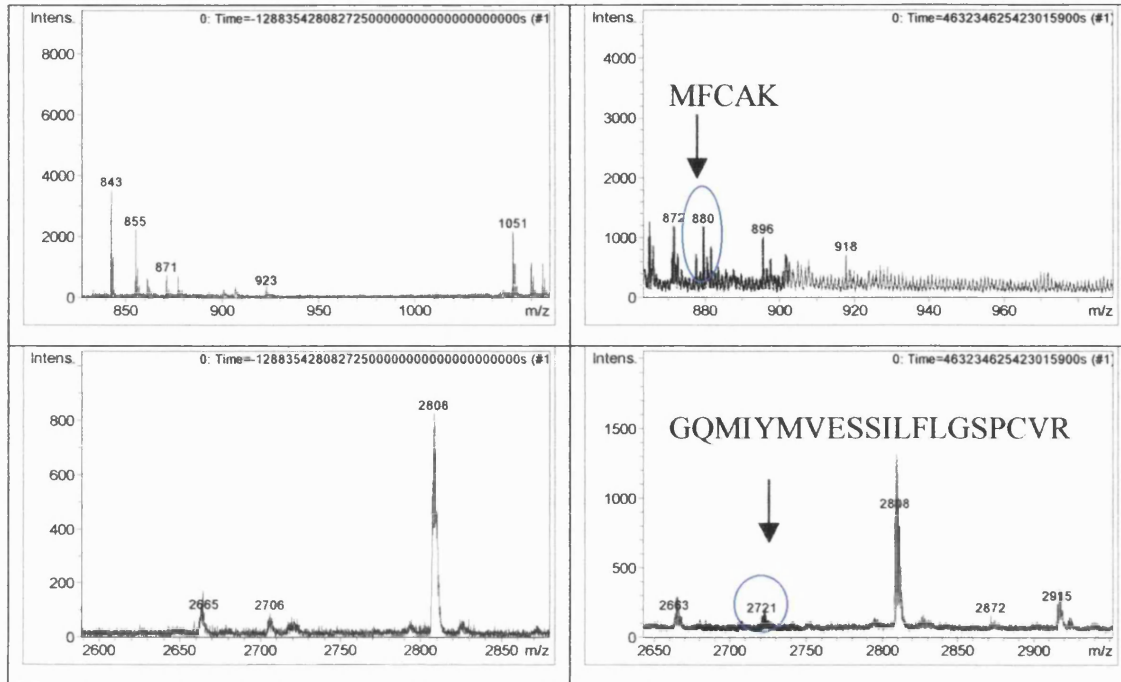
Figure 27. Selective parts of MALDI spectra before (control, Panel A) and after (Panel B) adding the photolabile reagent for α subunit containing photolabile ligand in the absence of the substrate GTP from the second experiment.

- **α Subunit with photolabile ligand 17 in the presence of the substrate GTP**

Table 5. Results for α subunit with photolabile ligand in the presence of the substrate GTP.

First experiment   Second experiment

A	B	C	D	E	F
M	**M-L**	**M-2L**	**M**	**M-L**	**M-2L**
1267.503	981.3738	695.2445	635.683	349.5537	63.4244
1405.491	1119.362	833.2324	735.484	449.3547	163.2254
1497.617	1211.487	925.3579	994.025	707.8957	421.7664
1564.704	1278.575	992.4457	1071.422	785.2922	499.1629
1603.754	1317.625	1031.495	1120.309	834.18	548.0507
1860.901	1574.771	1288.642	1424.654	1138.525	852.3953
1873.889	1587.76	1301.63	1504.589	1218.459	932.33
1875.906	1589.777	1303.648	1621.497	1335.368	1049.238
1905.892	1619.763	1333.634	1687.557	1401.428	1115.299
1968.994	1682.865	1396.736	1922.713	1636.584	1350.455
2010.008	1723.879	1437.75	1968.934	1682.805	1396.676
2083.914	1797.785	1511.656	1978.552	1692.422	1406.293
2260.933	1974.803	1688.674	2002.82	1716.691	1430.562
2335.879	2049.75	1763.62	2104.599	1818.47	1532.341
2564.586	2278.456	1992.327	2196.455	1910.326	1624.196
2717.173	2431.044	2144.915	2313.664	2027.535	1741.406
			2565.648	2279.519	1993.389
			2720.963	2434.834	2148.705
			2825.703	2539.574	2253.445
			2915.014	2628.885	2342.755
			2921.357	2635.227	2349.098

Table 6 (overleaf). Predicted peptide sequences derived from M-L values (Panel A) or from M-2L (Panel B) for α subunit containing photolabile ligand in the presence of the substrate GTP.

Panel A

First experiment   Second experiment

M–L obs.	M predicted Peptide sequences	M–L obs.	M predicted Peptide sequences
1619.76	1618.85 [68]SRVYLHTLAESI CK[81]	349.5537	348.18 [361]SSR[363]
		707.8957	708.4 [2]**FCAK**LK[7]
		834.18	836.4 [391]LEDFTGR[397]
2431.04	2431.16 [369]**GQMIYMVESSI LFLGSPCVR**[390]	1138.525	1137.53 [629]DCPGFVFTPR[638]
		1335.368	1338.71 [296]DMSILQLGHGIR[307]
		1401.428	1403.81 [617]INVSPTTYRLLK[628]
		1910	1910.06 [576]IGHSGSVFAGVVGVKMPR[594]
		2434.834	2431.16 [369]GQMIYMVESSILFLGSPCVR[390]
		2628.885	2630.32 [286]TFPFHFMLDRDMSILQLGHGIR[307]

Panel B

First experiment   Second experiment

M-2L obs.	M predicted Peptide sequence	M-2L obs.	M predicted Peptide sequence
695.244	696.43 [97]TLAKHK[102]	852.3953	855.43 [1]**MFCAK**LK[7]
		1049.238	1049.55 [82]LIFPEFER[89] or [617]INVSPTTYR[625]
		1406.293	1403.81 [617]INVSPTTYRLLK[628]
		1430.562	1433.72 [674]KDVEEANANFLGK[686]
		1532.341	1535.98 [211]ITSLILPGIIKAAAR[225]
		1624.196	1625.84 [542]ESDTHAVQIALMALK[556]
		2253.445	2254.05 [557]MMELSHEVVSPHGEPIKMR[575]

Panel A (control)   Panel B (Enzyme +Ligand)
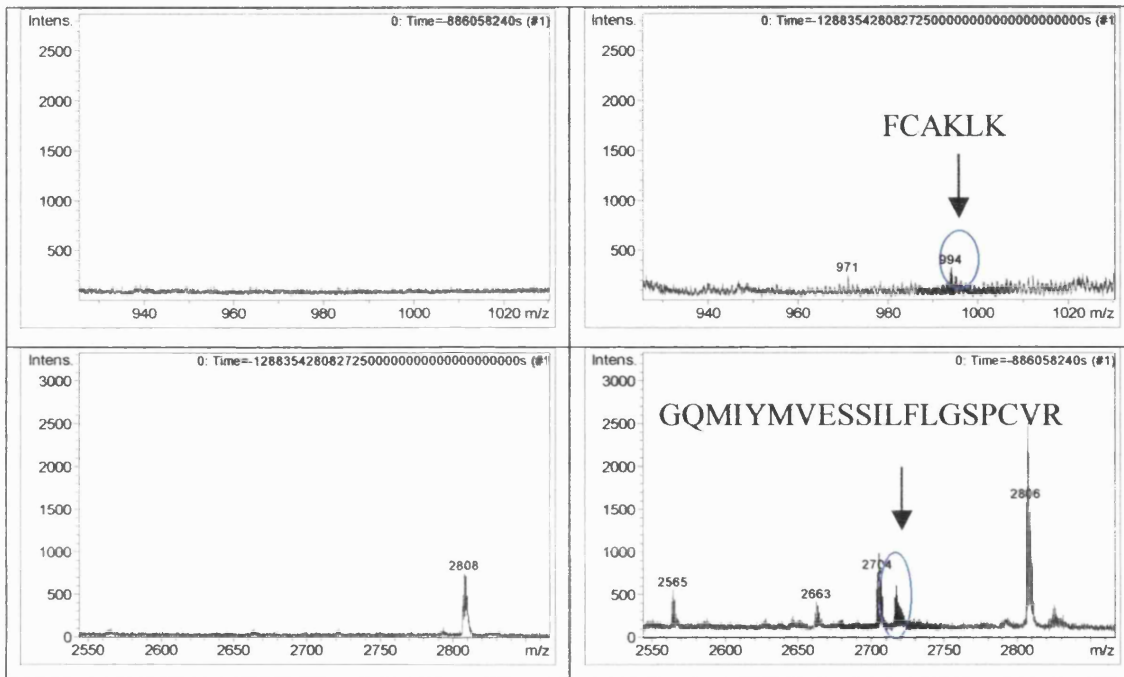
Figure 28. Selective parts of MALDI spectra before (control, Panel A) and after (Panel B) adding the photolabile reagent to the α subunit in the presence of the substrate GTP.

- β **Subunit with photolabile ligand 17 in the absence of the substrate GTP**

Table 7. Predicted peptide sequences proceeding from M-L values (Panel A) or from M-2L (Panel B) for β subunit with photolabile ligand **17** in the absence of the substrate GTP

Panel A

First experiment		Second experiment	
M-L obs.	M predicted Peptide sequence	**M-L** obs.	M predicted Peptide sequence
1955.92	1954.9 [73]MFFVFCQESGYDTILR[88]	835.019	836.37 [122]CTDADKGK[129]
		1987.886	1987.06 [390]TDTLLYSVLPPSVANELR[407]
		2135.062	2134.96 [198]FEENGTQESRISPYTFCK[215]
		3063.251	3062.46 [417]YDNVTILESGIVGFNAFC- SKHASGEGAMK[445]

Panel B

First experiment   Second experiment

M-2L obs.	M predicted Peptide sequence	**M-2L** obs.	M predicted Peptide sequence
887.0947	886.4 [437]HASGEGAMK[445]	887.0947	886.4 [437]HASGEGAMK[445]

Panel A (control)   Panel B (Enzyme +Ligand)
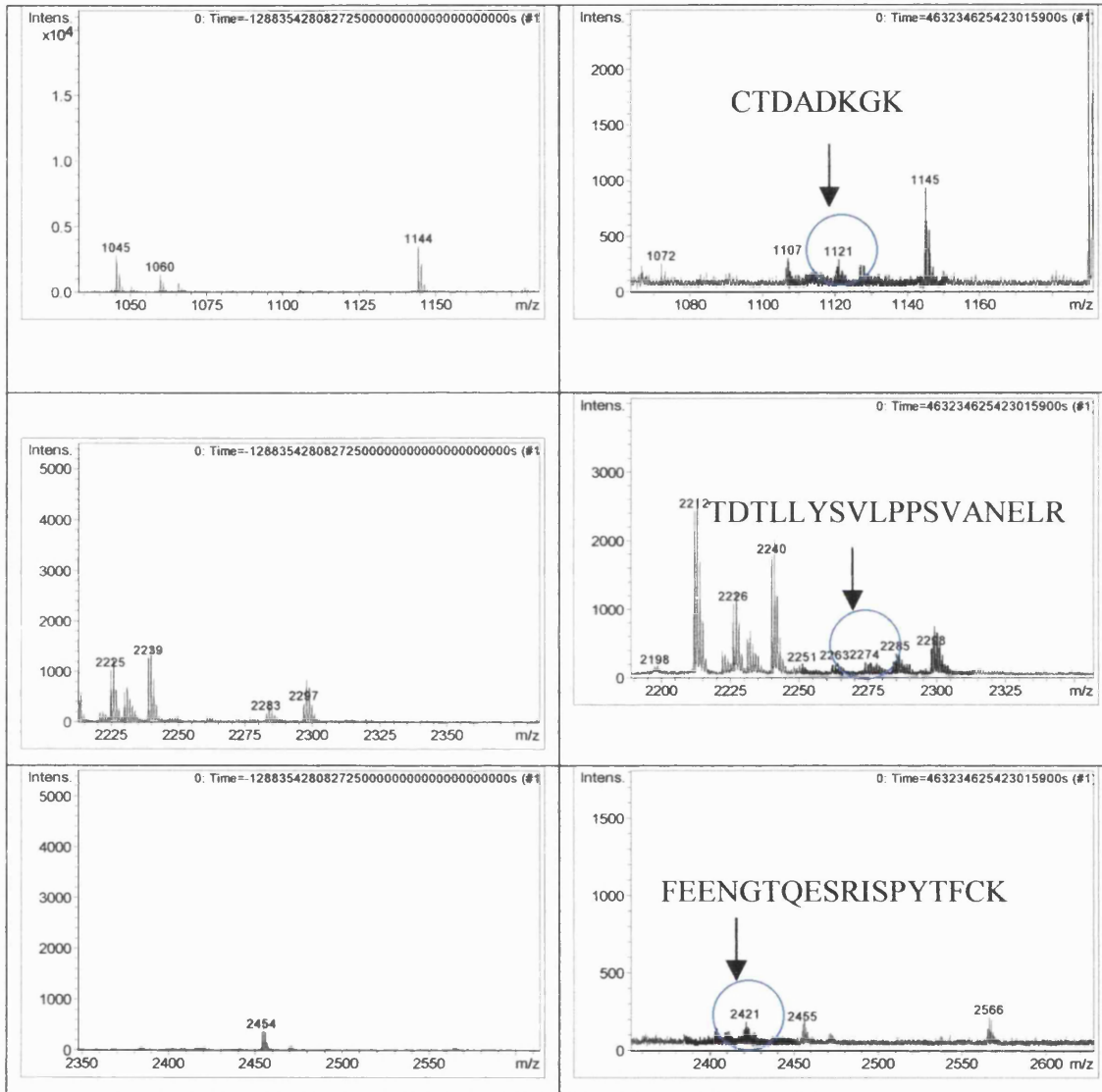
Figure 29. Selective parts of MALDI spectrum before (control, Panel A) and after (Panel B) adding the photolabile reagent to the β subunit in the absence of the substrate GTP

- **β Subunit with photolabile ligand 17 in the presence of the substrate GTP**

Table 8. Results for β subunit containing photolabile ligand in the presence of the substrate GTP.

First experiment   Second experiment

A	B	C	D	E	F
M	**M-L**	**M-2L**	**M**	**M-L**	**M-2L**
938.631	652.5017	366.3724	366.3724	371.3466	85.2173
947.6336	661.5043	375.375	375.375	387.5332	101.4039
970.1401	684.0108	397.8815	397.8815	393.6996	107.5703
1050.125	763.9961	477.8668	477.8668	409.6063	123.477
1406.519	1120.39	834.2608	834.2608	425.6104	139.4811
1497.619	1211.49	925.3605	925.3605	598.7367	312.6074
1839.866	1553.736	1267.607	938.9481	652.8188	366.6895
1994.91	1708.781	1422.652	1097.889	811.7597	525.6304
2261.861	1975.732	1689.602	1317.665	1031.536	745.4064
			2663.202	2377.073	2090.943
			2722.882	2436.753	2150.623

Table 9. Predicted peptide sequences derived from M-L values (Panel A) or from M-2L (Panel B) for the β subunit with photolabile ligand **17** in the presence of the substrate GTP.

M-L obs.	M predicted Peptide sequence	**M-L** obs.	M predicted Peptide sequence
652.5017	651.25 [122]CTDADK[127]	652.819	651.25 [122]CTDADK[127]
763.9961	764.36 [553]TETTGEK[559]		

| **M-2L** obs.	M predicted Peptide sequence	**M-2L** obs.	M predicted Peptide sequence
none		745.4064	746.38 [472]VETVGDK[478]
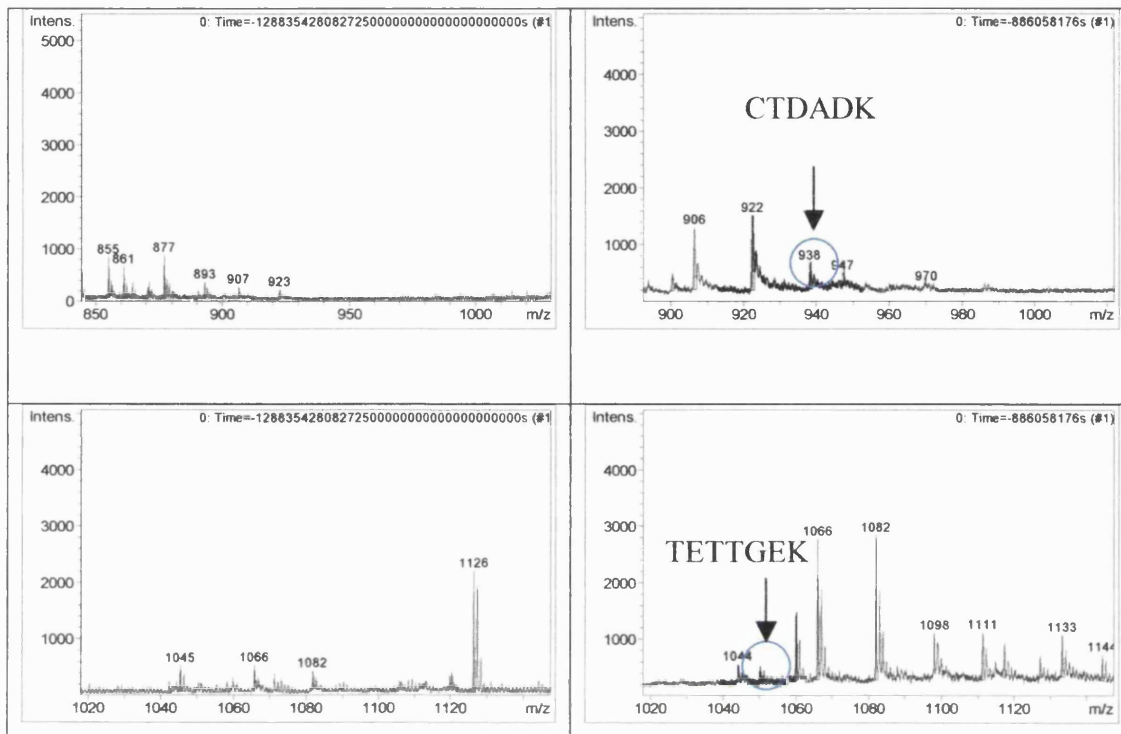
Figure 30. Selective parts of MALDI spectra before (control, Panel A) and after (Panel B) adding the photolabile reagent **17** to the β subunit in the presence of the substrate GTP

A further revision of the remaining peaks was carried out by superposition of the area of interest of the spectra with the corresponding control spectra. By doing this some of the peaks which initially appeared to be a result of labeling were actually found in the control spectra (although at very low intensity). The low intensity of these control peaks meant that they were not identified in the initial processing of the experimental data. After elimination of these peaks, the final peptide sequences are shown in Tables 10-13.

Table 10. Final peptide sequences for α subunit with photolabile ligand in the absence of the substrate GTP

M-L obs.	M predicted Peptide sequence	M-L obs.	M predicted Peptide sequence
708.582	708.4 ^{2}**FCAK**LK^7	595.399	598.26 ^{1}**MFCAK**^{5}
1048.24	1049.55 ^{82}LIFPEFER^{89} or ^{617}INVSPTTYR^{625}	2435.05	2431.16 ^{369}**GQMIYMVESSILFLG SPCVR**^{390}
2431.95	2431.16 ^{369}**GQMIYMVESSI LFLGSPCVR**^{390}		

M-2L obs.	M predicted Peptide sequence	M-2L obs.	M predicted Peptide sequence
780.048	779.33 ^{354}**WDNSMK**^{359}	none	

Table 11. Final peptide sequences for α subunit with photolabile ligand in the presence of the substrate GTP.

First experiment   Second experiment

M-L obs.	M predicted Peptide sequence	M-L obs.	M predicted Peptide sequence
2431.04	2431.16 ^{369}**GQMIYMVESSI LFLGSPCVR**^{390}	707.8957	708.4 ^{2}**FCAK**LK^{7}

M-2L obs.	M predicted Peptide sequence	M-2L obs.	M predicted Peptide sequence
none		1049.238	1049.55 ^{82}**LIFPEFER**^{89} ^{617}**INVSPTTYR**^{625}

Table 12. Final peptide sequences for β subunit with photolabile ligand in the absence of the substrate GTP

First experiment   Second experiment

M-L obs.	M predicted Peptide sequence	**M-L** obs.	M predicted Peptide sequence
none		835.019	836.37 [122]CTDADKGK[129]
		1987.886	1987.06 [390]TDTLLYSVLPPSVANELR[407]
		2135.062	2134.96 [198]FEENGTQESRISPYTFCK[215]

M-2L obs.	M predicted Peptide sequence	**M-2L** obs.	M predicted Peptide sequence
none		none	

Table 13. Final peptide sequences for β subunit with photolabile ligand in the presence of the substrate GTP

First experiment   Second experiment

M-L obs.	M predicted Peptide sequence	**M-L** obs.	M predicted Peptide sequence
652.5017	651.25 [122]CTDADK[127]	652.819	651.25 [122]CTDADK[127]
763.9961	764.36 [553]TETTGEK[559]		

M-2L obs.	M predicted Peptide sequence	**M-2L** obs.	M predicted Peptide sequence
none		none	

2.7.5 Discussion

Activation and photoaffinity labelling of sGC is a difficult task, thus we are dealing with a complex system. Although the analysis has been carried out on what is theoretically expected, it is possible that other more complex reactions, such as ligand rearrangements, are taking place. As mentioned before, based on the homology between sGC and AC we initially hypothesised that the binding of NO-independent ligands could involve the catalytic site of the enzyme. However, as also pointed out, the ligand may bind in other parts of the enzyme. We wanted to address a few questions, although some of them require a combination of experiments to be able to answer.

- Which subunit does the ligand bind to? Does it bind to one or both subunits?

- Does the ligand require the presence of the substrate GTP to bind to the enzyme?

- Has the ligand one or more binding sites?

- How many and which peptide sequences are involved in the binding?

PAL experiments were carried out with the hope of addressing some of the above questions. Based on our results it seems that the ligand under study binds to both the α and the β subunits. Table 14 displays the peptide sequences for each subunit that seem to be involved in the binding of compound **17** in sGC both in the presence and the absence of GTP, where N represents the number of the experiment.

Table 14. Peptide sequences of α and β subunits (summary of the analysis)

Subunit	N	-GTP	+GTP
α	1	^{2}FCAKLK^7 ^{369}GQMIYMVESSILFLGSPCVR^{390} ^{82}LIFPEFER^{89}or^{617}INVSPTTYR^{625}	^{369}GQMIYMVESSILFLGSPCVR^{390}
	2	^{1}MFCAK^5 ^{369}GQMIYMVESSILFLGSPCVR^{390} ^{354}WDNSMK^{359}	^{2}FCAKLK^7
β	1		^{122}CTDADK^{127} ^{553}TETTGEK^{559}
	2	^{122}CTDADKGK^{129} ^{390}TDTLLYSVLPPSVANELR^{407} ^{198}FEENGTQESRISPYTFCK^{215}	^{122}CTDADK^{127}

As we can see there are peptide sequences that appear in the presence and in the absence of GTP. This could imply that the ligand binds to the enzyme independent of the presence or absence of the substrate; this is true if we consider only the peptide sequences that are common in both experiments. Though if we consider all the sequences labelled then it is also possible to observe some sequences which appear when GTP is present but not when it is absent and vice versa.

Considering the peptide sequences that appear in both experiments it seems likely that the sequences of the α subunit involved in the binding are ^{2}FCAK^5 and

[369]GQMIYMVESSILFLGSPCVR[390]. These are not part of the catalytic site. Due to a lack of a crystal structure of sGC is not possible to elucidate the location and distribution of these sequences in the protein. If the ligand interacts with both sequences it may be possible that they are located near with one another in the protein structure.

In this context [122]CTDADK[127] seems to be the most likely peptide sequence in the β subunit involved in the binding. Interestingly, this sequence forms part of the region β(1-385) subunit known as the heme binding domain. In addition, the sequence [198]FEENGTQESRISPYTFCK[215] also belongs to the same region and includes a highly conserved Cys 214. This residue together with Cys 78 have been shown to be involved in the regulation of sGC activity.

It is unkown whether the sequences mentioned above belong to the same binding site or different ones, in other words, if the ligand has one or more binding sites in the enzyme. As we mentioned in the introduction, a recent paper from Murad and co-workers does not exclude the possibility of more than one binding site for YC-1.[55] However, it is unknown whether YC-1 and the ligand under study, as well as other NO-independent ligands share the same binding properties.

During the course of this study a group in Germany reported an interesting finding, in which the binding site of one of the NO-independent ligand (BAY 41-2272) was identified.[100] It seems that this ligand binds to the Cys 238 and Cys 243 of the α subunit. It was also pointed out that this ligand is heme-dependent since ODQ completely inhibited its effect on sGC. This effect is not observed for YC-1 which, in the presence of ODQ, still has some activity as reported by Murad. This could mean that the two ligands do not act in the same way. However, the same group of Germany suggested that YC-1 and BAY 41-2272 have the same binding site since, in their experiments, the presence of YC-1 diminished the covalent binding of the labelled ligand to the α subunit of sGC.

2.7.6 Improvements in the methodology

In order to clarify and simplify the laborious analysis, we decided to synthesise a bromine-containing photolabile analogue. The presence of one bromine atom in the photoprobe produces a distinct isotopic distribution pattern in the mass spectrum. We envisaged that this characteristic peak distribution could facilitate the analysis, on the one hand indicating the peaks that came from the labeling and on the other hand confirming that the chosen peak contains the ligand and is not an artifact. Ideally, we would have carried out PAL experiments with a bromine containing diazirine analogue in order to compare results. However, as the synthesis of the benzophenone containing brominated ligand was more convenient (possible in a two step synthesis), we initially decided to synthesise this ligand, and consequently use it in the PAL experiments in order to prove the idea and to compare results using different photoprobes.

However, as the radioimmunoassay indicated, the presence of the bromine in the molecule unfortunately decreases the activity of the ligand on sGC and therefore it was unsuitable for PAL. Even though we expected significant unspecific labelling we decided to carry out the PAL experiment with this compound. The main reason for this was to establish the approach.

With the purpose of increasing the coverage of the protein in the MALDI spectrum, the protein was treated with iodoacetamide for cysteine modification prior to trypsin digestion. In addition, a tissue-culture hood was used to work up the gels in order to avoid contamination. By doing this the percentage of coverage of the protein increased considerably, thus increasing the map of peptides to be analysed and providing more chance to assure the results. Figure 31 shows the peptide map for the β subunit with and without cysteine modification. As we can see the coverage of the subunit without the modification is 47% (Panel B), while with the modification the coverage is 68% (Panel A). This is a good result for this type of experiment.

Figure 31. Peptides map for the β subunit with (Panel A) and without cystein

modification (Panel B)

Panel A

Top Score: 206 for gi|118056, GUANYLATE CYCLASE SOLUBLE, BETA-1 CHAIN (GCS-BETA-1) (SOLUBLE GUANYLATE CYCLASE SMALL SUBUNIT)

Sequence Coverage: 68%

```
Matched peptides shown in Bold Red

     1  MYGFVNHALE  LLVIRNYGPE  VWEDIKKEAQ  LDEEGQFLVR  IIYDDSKTYD
    51  LVAAASKVLN  LNAGEILQMF  GKMFFVFCQE  SGYDTILRVL  GSNVREFLQN
   101  LDALHDHLAT  IYPGMRAPSF  RCTDADKGKG  LILHYYSERE  GLQDIVIGII
   151  KTVAQQIHGT  EIDMKVIQQR  NEECDHTQFL  IEEKESKEED  FYEDLDRFEE
   201  NGTQESRISP  YTFCKAFPFH  IIFDRDLVVT  QCGNAIYRVL  PQLQPGNCSL
   251  LSVFSLVRPH  IDISFHGILS  HINTVFVLRS  KEGLLDVEKS  ECEDELTGTE
   301  ISCLRLKGQM  IYLPEADSIL  FLCSPSVMNL  DDLTRRGLYL  SDIPLHDATR
   351  DLVLLGEQFR  EEYKLTQELE  ILTDRLQLTL  RALEDEKKKT  DTLLYSVLPP
   401  SVANELRHKR  PVPAKRYDNV  TILFSGIVGF  NAFCSKHASG  EGAMKIVNLL
   451  NDLYTRFDTL  TDSRKNPFVY  KVETVGDKYM  TVSGLPEPCI  HHARSICHLA
   501  LDMMEIAGQV  QVDGESVQIT  IGIHTGEVVT  GVIGQRMPRY  CLFGNTVNLT
   551  SRTETTGEKG  KINVSEYTYR  CLMTPENSDP  QFHLEHRGPV  SMKGKKEPMQ
   601  VWFLSRKNTG  TEETEQDEN
```

Panel B

Top Score: 104 for gi|118056, GUANYLATE CYCLASE SOLUBLE, BETA-1 CHAIN (GCS-BETA-1) (SOLUBLE GUANYLATE CYCLASE SMALL SUBUNIT)

Sequence Coverage: 47%

```
Matched peptides shown in Bold Red

     1  MYGFVNHALE  LLVIRNYGPE  VWEDIKKEAQ  LDEEGQFLVR  IIYDDSKTYD
    51  LVAAASKVLN  LNAGEILQMF  GKMFFVFCQE  SGYDTILRVL  GSNVREFLQN
   101  LDALHDHLAT  IYPGMRAPSF  RCTDADKGKG  LILHYYSERE  GLQDIVIGII
   151  KTVAQQIHGT  EIDMKVIQQR  NEECDHTQFL  IEEKESKEED  FYEDLDRFEE
   201  NGTQESRISP  YTFCKAFPFH  IIFDRDLVVT  QCGNAIYRVL  PQLQPGNCSL
   251  LSVFSLVRPH  IDISFHGILS  HINTVFVLRS  KEGLLDVEKS  ECEDELTGTE
   301  ISCLRLKGQM  IYLPEADSIL  FLCSPSVMNL  DDLTRRGLYL  SDIPLHDATR
   351  DLVLLGEQFR  EEYKLTQELE  ILTDRLQLTL  RALEDEKKKT  DTLLYSVLPP
   401  SVANELRHKR  PVPAKRYDNV  TILFSGIVGF  NAFCSKHASG  EGAMKIVNLL
   451  NDLYTRFDTL  TDSRKNPFVY  KVETVGDKYM  TVSGLPEPCI  HHARSICHLA
   501  LDMMEIAGQV  QVDGESVQIT  IGIHTGEVVT  GVIGQRMPRY  CLFGNTVNLT
   551  SRTETTGEKG  KINVSEYTYR  CLMTPENSDP  QFHLEHRGPV  SMKGKKEPMQ
   601  VWFLSRKNTG  TEETEQDEN
```

2.8 Summary and Conclusion

We have attempted in this work to provide some insight into the mechanism of activation of sGC by NO-independent activators using an amalgamation of ideas in an interdisciplinary manner. The synthesis of activators and their photolabile analogues was carried out. These compounds were tested for activity on sGC using either an ELISA or a radioimmunoassay. Most of the published work on sGC has been performed using YC-1 and therefore more information is available on this compound. We wanted to apply the photoaffinity labeling technique to this compound as well as others in order to compare results and to determine if they share the same binding site. However, the photolabile analogue of YC-1 was found to be inactive on purified sGC, as the radioimmunoassay indicated and therefore was unsuitable for PAL. In contrast, compound 17 was the more active one, and was consequently used for PAL experiments. Photoaffinity labeling coupled to trypsin digestion and mass spectroscopy was used as the methodology to get information about the area of the enzyme where the ligand binds. Results using this approach indicated that the compound under study binds to both the α and the β subunits in sGC. The peptide sequences related to the binding in the β subunit belong to the heme-binding domain. It is not known if the peptide sequences form part of the same binding site in the protein or whether belong to different binding sites.

We also envisaged that the presence of bromine in a photolabile activator would improve and facilitate the analysis of the MALDI spectra. This compound however, was found to be inactive and therefore not a good candidate for PAL experiments. Nevertheless, work recently published confirmed our idea and supported this approach, in this work a photoprobe containing one bromine and two chlorine atoms was used to identify the binding site on the lymphocyte function-associated antigen-1 (LFA-1) of a class of hydantoin-based antagonist of leukocyte cell adhesion. The distinct isotopic distribution pattern in the spectra produced by the halogen atoms confirmed the identity of the specifically labeled tryptic fragment by LC/MS. [101]

In conclusion, despite our effort questions still need to be addressed and work remains to be done to complete our understanding of the mechanism of action of NO-independent activators of sGC. Photoaffinity labeling in combination with MALDI mass spectroscopy represent important tools for studying enzyme-ligand interactions and predicting the region in the protein where ligands bind. However to confirm the binding region and details of the binding at a molecular level a crystal structure of the enzyme-ligand complex is necessary. Mutagenesis studies will also contribute to confirming the amino acids that make up the binding site in the protein. Thus these techniques are complementary to each other sharing the aim of elucidating enzyme-ligand interactions.

Taking into account our results future work could be directed with the aim of improving the methodology herein used. This might start with the synthesis of additional potential activators. Kinetic studies on those will also facilitate the PAL experiments, as a higher affinity of the ligand for the enzyme will lead to less unspecific labelling. To avoid unpleasant surprises it will also be helpful to synthesise a series of photoaffinity ligands with the photophore in multiple position around the pharmacophore, giving a better chance to find active compounds. Making use of the photoaffinity biotinylation approach described in the introduction would be useful and finally introduction of a bromine atom into the molecule will improve the method and facilitate analysis.

A combination of these elements would hopefully provide a good candidate for carrying out PAL-MALDI experiments.

Despite having insufficient time to carry out all the required work we wanted to provide an initial contribution. In order to synthesise a diverse range of compounds as potential activators of sGC we decided to make use of solid-phase organic synthesis, in particular using a traceless linker. Thus, next chapter describes initial work in the synthesis of a traceless linker that we hope would be useful not only for the synthesis of activators of sGC but also for other chemistry purposes.

CHAPTER THREE

Investigation on a benzoisothiazol derivative as a possible traceless linker

3.1 Introduction

3.1.1 Scope of the approach

This chapter deals with initial work on the synthesis of a benzoisothiazol-based traceless linker. As reported in Chapter 1 traceless linkers afford the final molecules with no trace of the point of linkage to the solid phase. We propose that the benzoisothiazol heterocycle should provide a good scaffold as a traceless linker. Scheme 16 illustrates the sequence of reactions that we suggest in order to synthesise a variety of biomolecules (ArR), in solid phase, in a traceless manner. The sequence starts with deprotection of a 6-ester substituted benzoisothiazol **46** to provide the free carboxylic acid derivative **47**. Then, reaction of **47** with a polystyrene resin **48** will form adduct **49**. Introduction of a chlorine as a leaving group at the 3-position (**50**) will supply an attachment point for the molecules of interest by reaction with different phenols forming adduct **51**. Following any synthetic steps that are carried out on the appended aryl group in **51**, the intermediate is activated by oxidation of the sulphur atom to give **52**, which is then ready to undergo cleavage. The cleavage step provides a point of diversity into the molecules as adduct **52** can be cleaved in the presence of palladium and a hydrogen donor to give **53** (R=H) or can undergo cross-coupled reactions to give **54** (R=Ar').
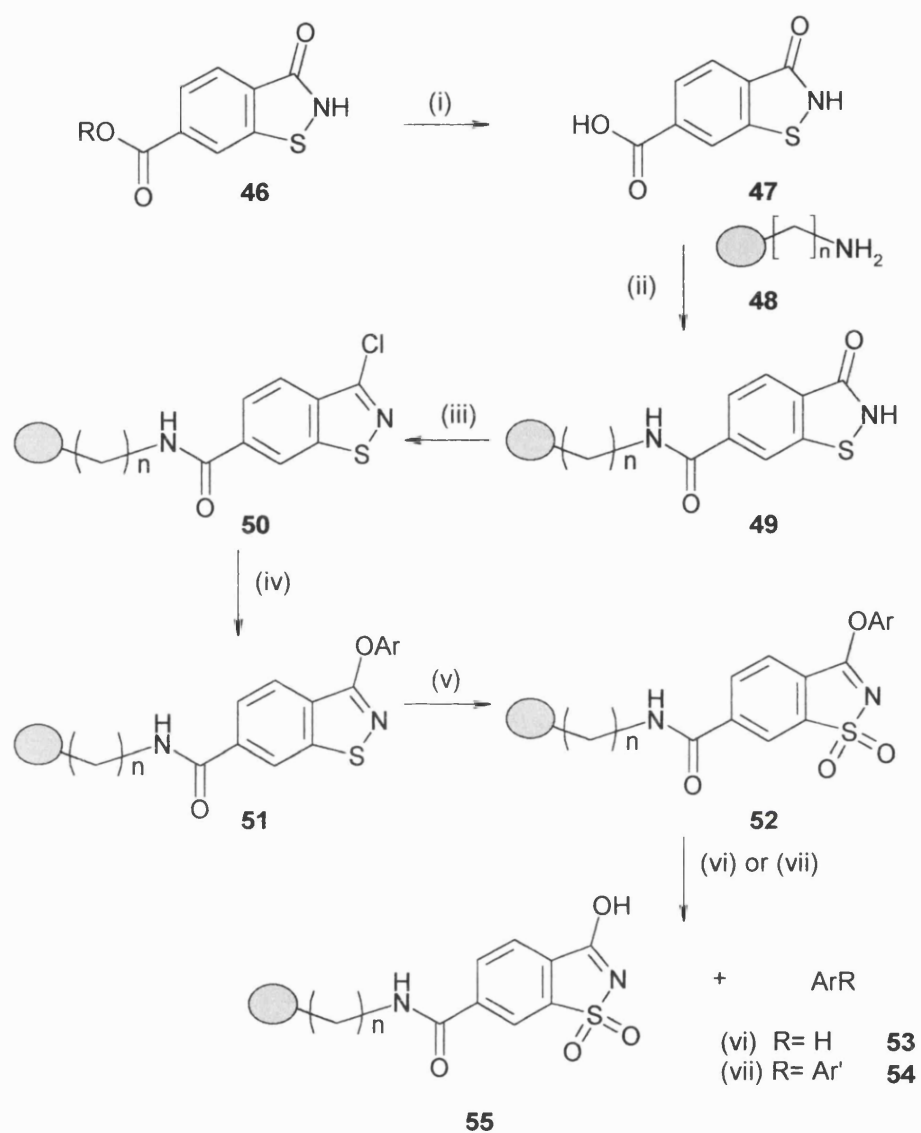
Scheme 16. (i) 10% NaOH (aq.) (ii) DIPEA, HATU, resin **48** (iii) POCl₃ (iv) ArOH (v) H₂O₂, AcOH (vi) H₂/Pd (vii) Ar'Br/Pd

In addition, the phenols introduced can also have functional groups that are subject to chemical transformations which provide another point of diversity. In this regard, Scheme 17 shows an illustrative example for the synthesis of sGC activators **56**.
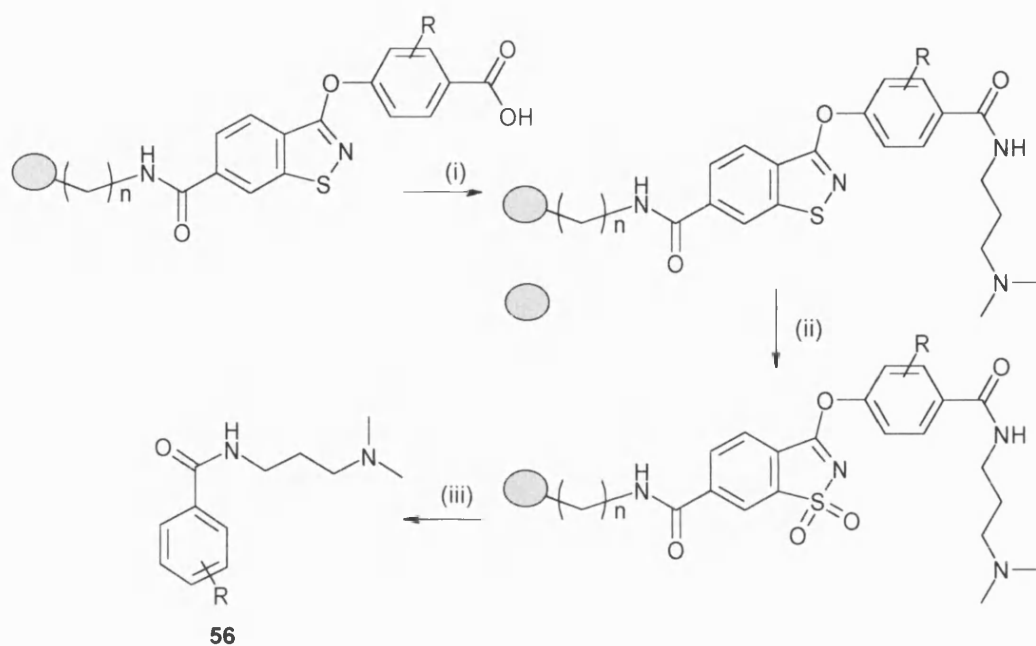
Scheme 17. (i) DIPEA, HATU, amine (ii) H$_2$O$_2$, AcOH (iii) H$_2$/Pd

Schemes 16 and 17 represent a proposal and further investigation is required to confirm it. Herein, we report some background about the benzoisothiazole moiety and our initial research in the synthesis of intermediate **46**.

3.1.2 Background

In 1923 McClelland and collaborators first synthesised 1,2-benzisothiazol-3-one (57),[102] although a member of the same family, 1,2-benzisothiazolone-1,1-dioxide (Saccharin 58), has been known since 1879.
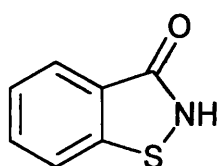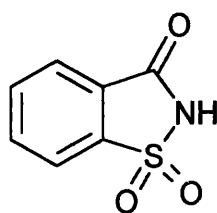
57   **58**

The discovery that this group of compounds had antifungal and antibacterial activity has attracted a great deal of interest and promoted much work in this area.[103]

The fact that the parent compound **57** has pronounced toxicological effects[104] led to an investigation of the pharmacological effects and structure-activity relationship of its derivatives.[105] Consequently a broad spectrum of derivatives of **57** can be found in the literature.

Fisher and Hurni reported a series of substituted derivatives of **57** and showed that the range of bacteriostatic and fungistatic action depends upon the nature and position of the substituents in the nucleus. 6-Chloro-1,2-benzisothiazolone **59** appeared to be the most effective on *Trichomonas*, although substitution in position 7 or introduction of a hydrophilic substituent results in a considerable loss of activity.
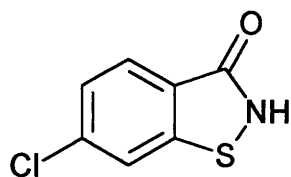
59

Since McClelland's early work, a very large number of derivatives have been synthesised and many variations on the original synthesis have been reported. The chemistry and synthesis of these compounds was reviewed first by Bambas[106] and later by Davis, who included a summary of the reported structures.[107,108]

N-substitution has been extensively investigated using alkyl chains[109] and hydroxyalkyl derivatives.[110] In addition, substitutions at different aromatic ring positions have been described.[111,112,113]

The utility of these compounds as potential antithrombotic agents has also been reported. For example 2-amino-1,2-benzisothiazolin-3-one (**60**) acts as an inhibitor of platelet aggregation both in *in vitro* studies on human platelets and *ex vivo* on rabbit platelets.[114]

60
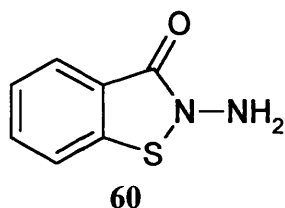
In this field, the structure-activity relationship of a series of substituted compounds of structure **61** has been studied. Several of these (**61a**), (**61b**), (**61c**) (Table 16) were effective inhibitors of adenosine diphosphate induced first-phase aggregation. However, the adverse toxicological effects precluded their use as antithrombotic drugs.[115] Despite this setbacks research in the area continues in order to find a balance between activity and toxicity.

61
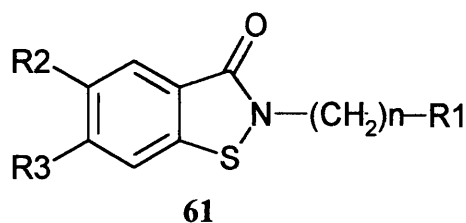
Table 16: Substituents for the active compounds

	61a	**61b**	**61c**
n	3	2	4
R1	1-piperidinyl	3-azabicyclo[3.2.2]non-3-yl	3-azabicyclo[3.2.2]non-3-yl
R2	H	CH_3O	CH_3O
R3	H	CH_3O	CH_3O

Furthermore a 3-(1-piperazinyl)-1,2-benzisothiazole derivative (**62**) has been claimed to be useful in the treatment of schizophrenia, showing minimal side effects.[116]
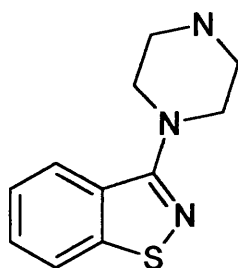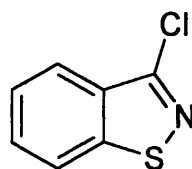
62   **63**

Although the biological properties of compounds in the same family as **57** and **58** are of great interest, it was not the pharmacological activity of these compounds that attracted our attention but their chemical properties.

The nucleophilic displacement of the chlorine atom in 3-chloro-1,2-benzoisothiazol (**63**) provides a method of preparing a variety of substituted derivatives in the 3-position of the molecule.

One particular feature that interested us was the stability of this heterocycle. This allows different chemistry to be applied to various substituted compounds, opening up a range of possibilities for obtaining a large number of biomolecules.

A group at Parma University has reported the synthesis of several 1,2-benzisothiazol-3-ylacetic acid (**64**, R= OEt, OH, NR1R2) and 3-methoxy-1,2-benzisothiazol-5-ylacetic acid derivatives (**65**, X=H, CH_3, C_2H_5; Y=OH,

NHOH, OCH₃, NH₂) in their investigation on the analgesic, antipyretic and anti-inflammatory activity of these compounds.[117]
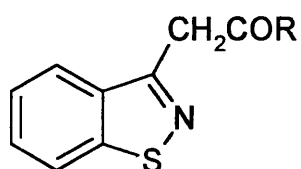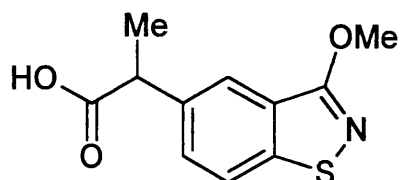
64   **65**

Compounds of structure **64** and **65** have been synthesised following Scheme 18 and 19 respectively.
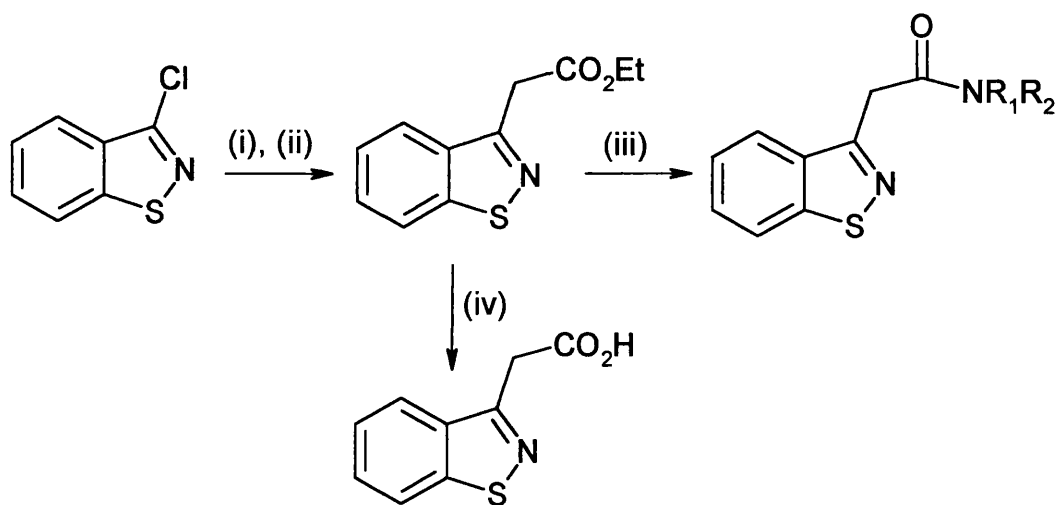
Scheme 18 : (i) CH₂(CO₂Et)₂, (ii) NaOEt, (iii) NHR1R2, (iv) CH₂(CN)CO₂Et.
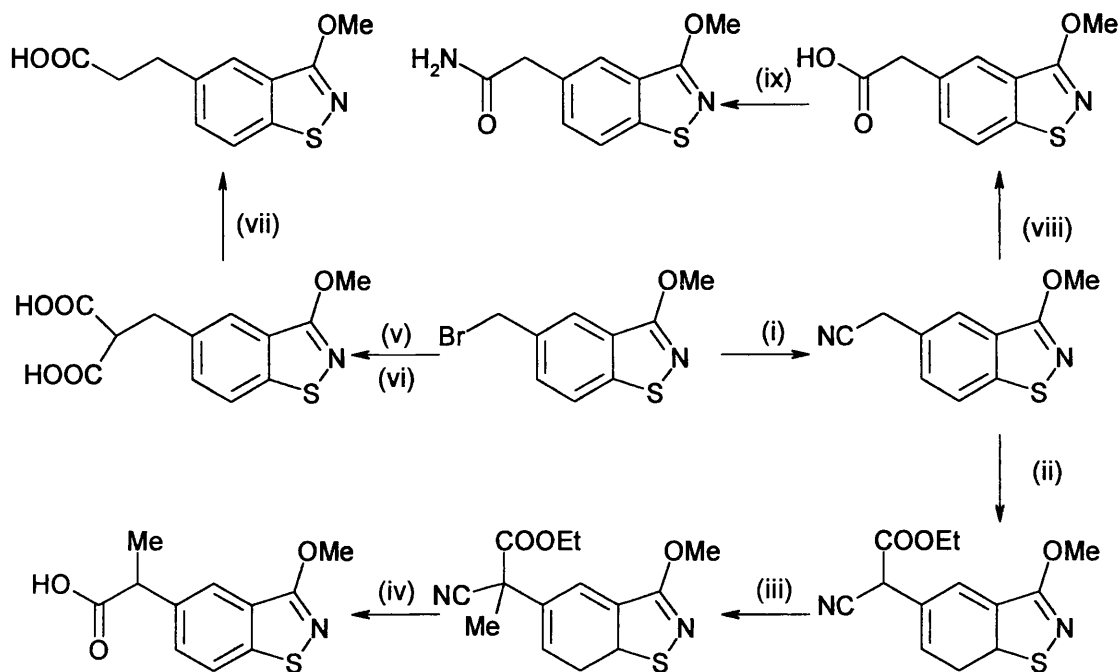
Scheme 19. (i) NaCN, H$_2$O, acetone (ii) NaOEt, CO(OEt)$_2$ (iii) NaOEt, MeI (iv) 10% NaOH, HCl (v) CH$_2$(CO$_2$Et)$_2$, EtONa (vi) 10%NaOH, HCl (vii) 180°C, Na$_2$CO$_3$ (viii) 5% NaOH, HCl (ix) SOCl$_2$, NH$_3$.

This work shows that the heterocycle core remains stable through a series of functional group interconversions, allowing reactions such as nucleophilic displacement, amide formation, saponification, esterification, methylation, and decarboxylation

This stability can be explained by the π-electron delocalization that takes place in these molecules. The short length of both S-N and N-C bonds compared to the single bond values confirms this delocalization, which must involve the empty sulphur 3d-orbitals. ESR Spectroscopic studies on 3-oxo-1,2-benzisothiazolin-2-yls corroborates the electron delocalization from N to C=O indicated by the planar structure that the molecule adopts and by the contribution of the canonical structure **1E**.[118]
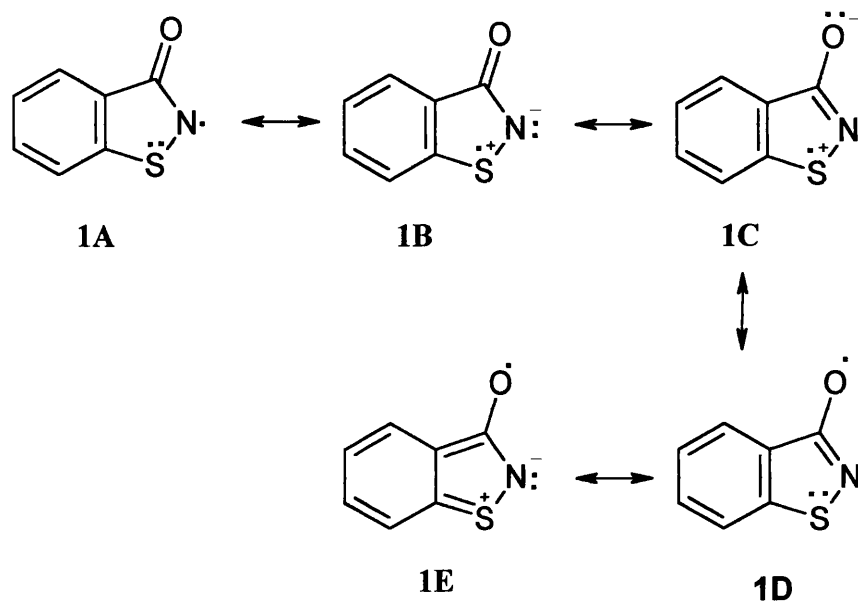
On the other hand, it has been reported that *pseudo*-saccharyl ethers (e.g. **66**) provide an alternative for *ipso* conversion of phenolic ether into arenes in the presence of palladium and a hydrogen donor.[119] Furthermore aryloxypseudosaccharins can also be cross-coupled with diethylzinc in the presence of various nickel or palladium catalysts.[120] Scheme 20 shows catalytic *ipso* substitution of pseudosaccharyl ethers.[121]
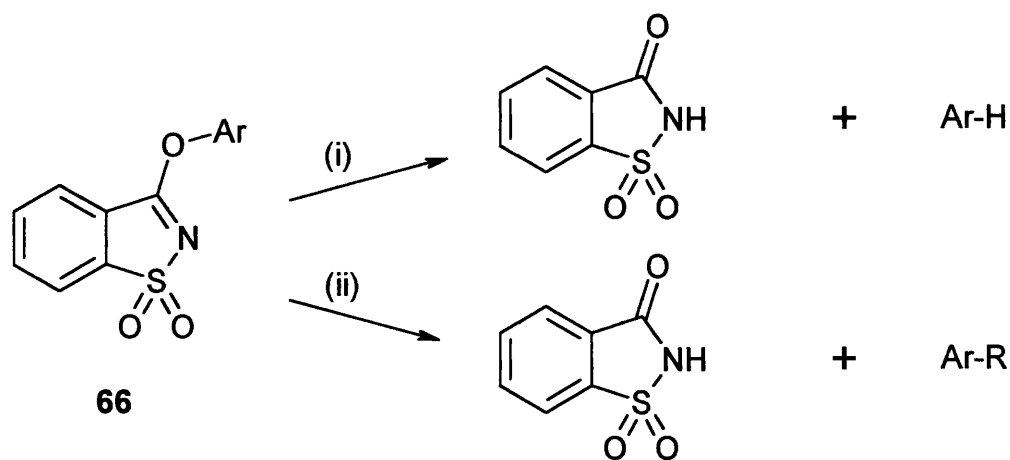
Scheme 20 : (i) Pd/C, NaH_2PO_2, (ii) Ni/RZnX, H2O

X-Ray structure determinations on a variety of these compounds have been reported showing significant differences in length for the C-O bonds of the central C-O-C ether linkages.[19] The ease of this reaction is due to the electron-withdrawing nature of the pseudosaccharyl group, which weakens the original partially double-bonded C-O of the phenol and strengthens the pseudosaccharyl C-O bond, where the oxygen is π-conjugated with the pseudosaccharyl group.

In summary:

- Aryl substituted 1,2-benzoisothiazol-3 ones are stable to a wide range of chemistry.
- The oxidative analogues **52** are readily cleaved to yield the corresponding aryl compound as shown in Scheme 16.

Combining both factors enables the possibility of carrying out different chemistry on the aryl substituted 1,2-benzoisothiazol-3 ones, followed by cleavage of the C-O bond attached to the aryl after activation by the oxidation on the sulphur atom. This combination gives us a potential traceless linker as shown in Scheme 16.
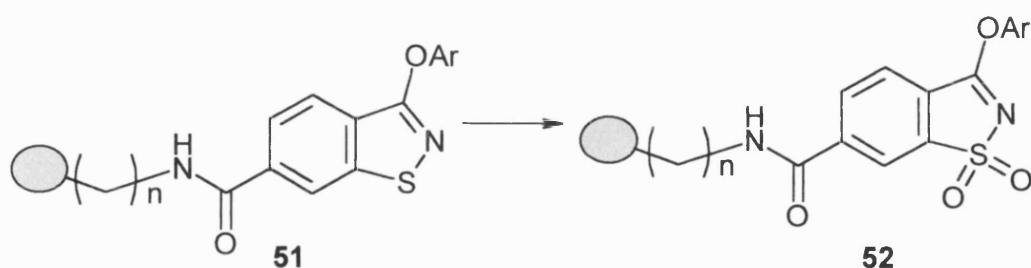
In this chapter we will discuss the chemistry done so far related to the synthesis of the suggested traceless linker. (For a review of traceless linker refer to Chapter one).

3.2 Design of the traceless linker

A linker group tethers the compound being synthesised to the solid phase support. The 3-position on the benzoisothiazol moiety is thus the attachment point for the template where chemical modifications will take place.

We decided to join the resin to the 6-position in the benzoisothiazol skeleton through an amide bond, where the resin provides the amine group and the benzoisothiazol contributes a carboxylic acid. Thus, it was necessary to synthesise compound **46**, where the carboxylic acid is protected as an ester. To our knowledge compound **46** has not been reported in the literature.

46a   R = Me

46b   R = Et
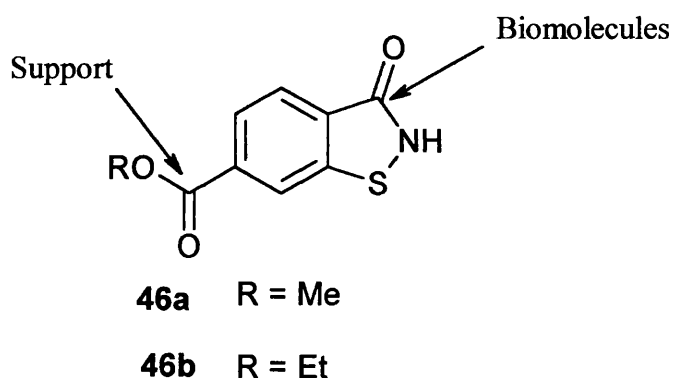
3.3 Chemistry

A number of methods involving variations from the original synthesis of 1,2-benzoisothiazol-3-ones, have been reported.

The method most commonly used involves preparation of 2,2'-dithiosalicylic acid (e.g. **67**) by the Sandmeyer reaction type from substituted anthranilic acids, and transformation of the 2,2'-dithiosalicylic acids into the corresponding bis acid chloride through reaction with thionyl chloride. 2,2'Dithiobis (benzoyl) chlorides are reacted with chlorine or oxalyl chloride and converted into the corresponding 2-chlorocarbonylphenylsulfenyl chlorides. This reacts with dry NH_3 or NH_4OH to give N-unsubstituted, or with primary amines to give N-substituted, 1,2-benzoisothiazol-3-ones.

A combination of the reported methods was suggested for the synthesis of the benzoisothiazol derivative that we are interested in. To prove that the method works well we decided to apply it first to a model system. We decided to synthesise 2-(4-methoxy-benzyl)-1,2-benzoisothiazol-3-one (69) and 2-(2,4-dimethoxy-benzyl)-1,2-benzisothiazol-3-one (70). Both 2,4-dimethoxy-benzyl and 4-methoxy-benzyl substituents were chosen for ease of cleavage by reaction with TFA, giving 1,2-benzoisothiazol-3-one (57).

Compounds 69 and 70 were synthesised following Scheme 21.
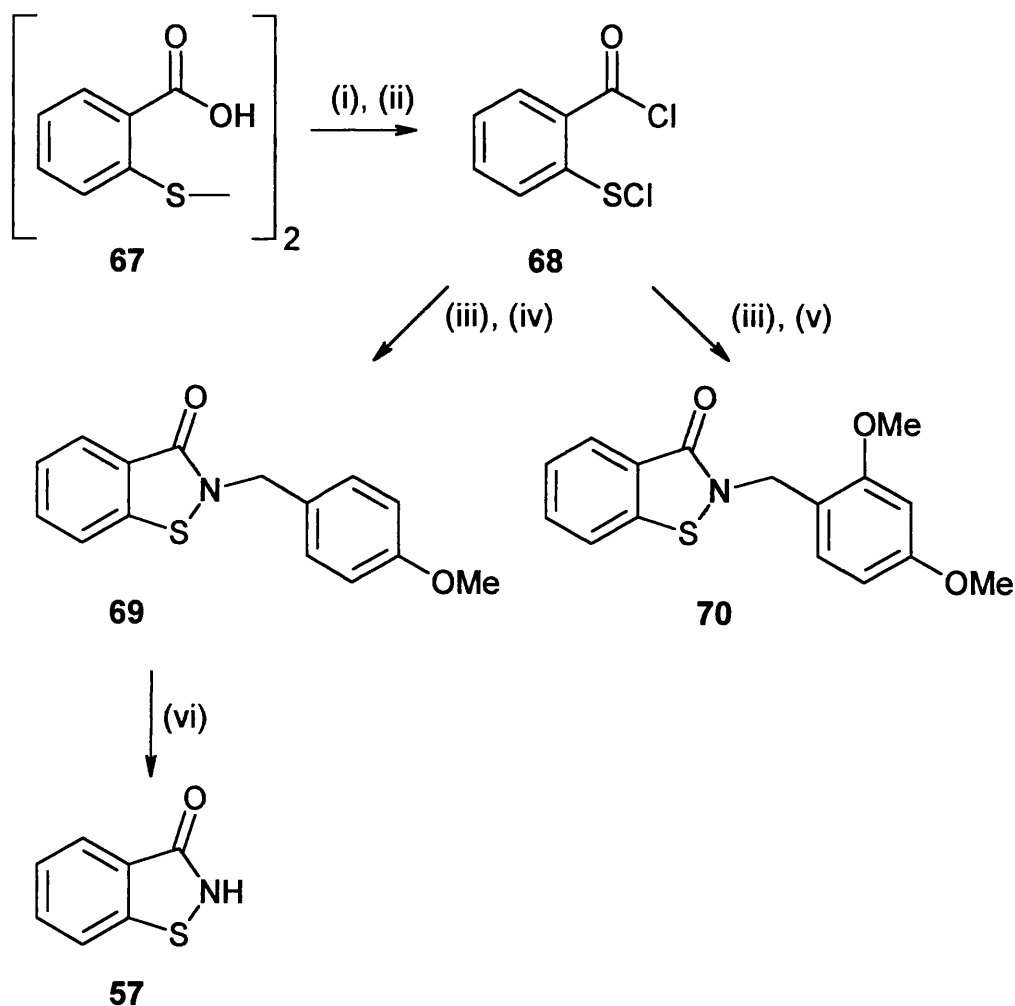
Scheme 21. (i) SOCl₂, 1 drop DMF, (ii) SO₂Cl₂, toluene, (iii) THF, (iv) 4-methoxybenzylamine, (v) 2,4-dimethoxybenzylamine, (vi) TFA, anisole.

Commercially available, 2,2'-dithiosalicylic acid (**67**) reacts with thionyl chloride to give the corresponding bis acid chloride, which by reaction with sulfuryl chloride is converted into 2-chlorocarbonylphenylsulfenyl chloride (**68**). The synthesis of the target compounds **69** and **70** was accomplished by reaction in THF of **68** with 4-methoxybenzylamine or 2,4-dimethoxybenzylamine respectively. Cleavage of the *N*- substituent in **69** with TFA and anisole gave 1,2-benzoisothiazole-3-one (**57**).

With this chemistry established we next examined the synthesis of **46**. In order to obtain compound **46** using the mentioned route, the first objective is to synthesise the intermediate 5,5'-dimethylester-2, 2'-dithiobis(benzoic acid) (**73**), which contains the necessary methyl ester for the introduction of the resin into the core.

Approach 1.

Our first approach to obtain the intermediate **73** was using the Sandmeyer reaction from the corresponding anthranilic acid **71**.
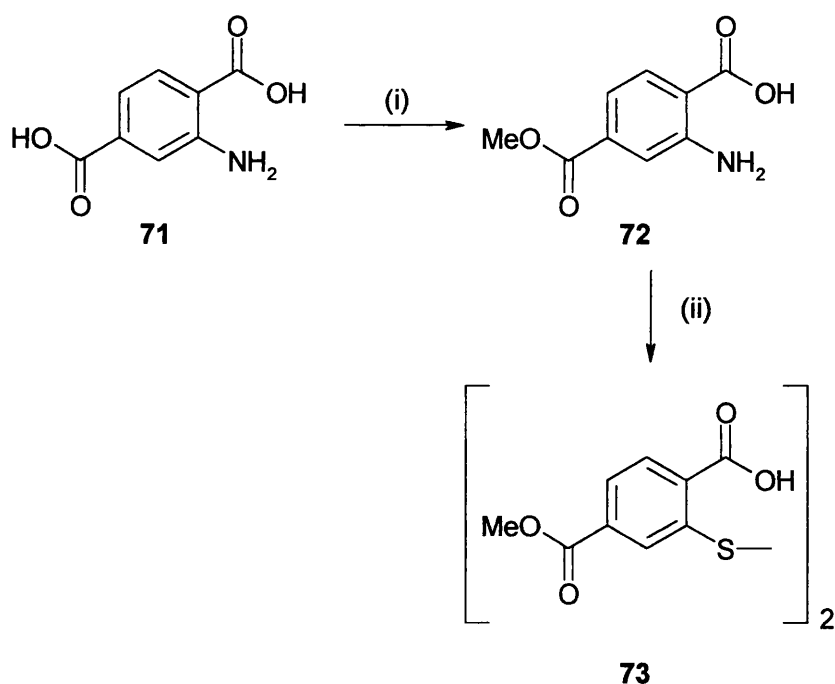
Scheme 22. (i) MeOH anhydrous, H_2SO_4, 60°C, (ii) $NaNO_2$, Na_2S_2, HCl.

Initially, commercially available 2-aminoterephthalic acid (**71**) was esterified to 2-amino-terephthalic acid 4-methyl ester (**72**) (Scheme 22). The selectivity of such a reaction is due to the hydrogen bonds between the amine group in the *ortho* position to the carboxylic acid, which stabilises the acid functionality and prevents its conversion into the methyl ester.

Attempts at the conversion of 2-aminoterephthalic acid 4-methyl ester into the corresponding dithiobis(benzoic acid) through a Sandmeyer reaction failed.[122]

To explain this result we should consider the nature of the reactant and of the reaction. The first step involves the diazotization of the amine into the diazonium salt. A solution of sodium nitrite in concentrated acid (hydrochloric acid or sulphuric acid), which provides a source of the nitrosonium ion (**74**) (Scheme 23), is known as a very effective diazotising medium for even weakly basic amines,[123] which is not the case for the aromatic amine **72**.

$$2NO_2^- + 2H^+ \longrightarrow 2HNO_2 \rightleftharpoons O=N-O-N=O + H_2O$$

$$O=N-O-N=O \rightleftharpoons O=\overset{+}{N} + \overset{-}{O}-N=O$$

74
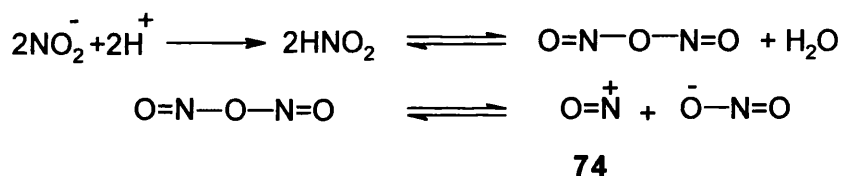
Scheme 23. Formation of the nitrosonium ion

Once the diazonium salt is formed it interacts with a solution of sodium disulphide and the diazo group is replaced, giving rise to the corresponding disulphide.

Since none of the steps involved in the reaction may be affected by the presence of the ester in the molecule, the reason for the negative result may be due to the work up of the reaction. However, due to the explosive nature of the diazonium salts we did not explore that possibility in more detail.

Approach 2.

We thought another strategy to reach the desired 5,5'-dimethylester-2,2'-dithiobis(benzoic acid) (**73**) might be that depicted in Scheme 24.
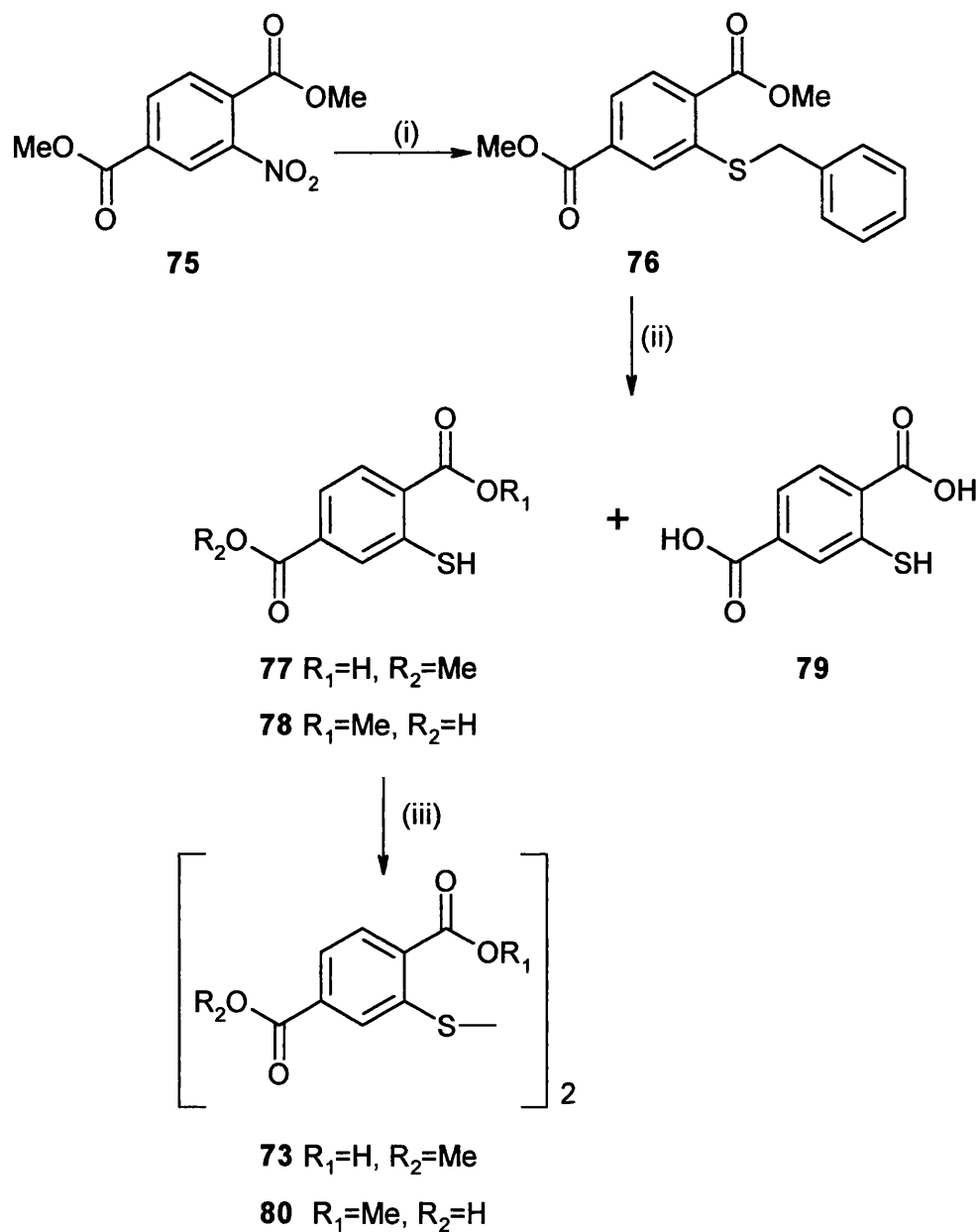
Scheme 24. (i) benzyl mercaptan, DMF, NaH (ii) AlBr$_3$, Toluene (iii) I$_2$, Py

Studies on the aromatic nucleophilic displacement of activated nitro groups, has established this reaction as a valuable synthetic tool.[124, 125, 126]

Initially, commercially available 2-nitroterephthalic acid dimethyl ester (**75**) was considered a good candidate, which by reaction with benzyl mercaptan in

the presence of sodium hydride gave the corresponding 2-benzylsulfonyl-terephthalic acid dimethyl ester (76) in 71% yield. So, by means of a nucleophilic displacement of the nitro group by the benzenesulfonyl group, the sulphur atom is incorporated into the molecule. The nitro group is easily displaced intramolecularly by the sulphur nucleophile due to the effect of the electron withdrawing groups on the aromatic system.[127]

In order to obtain the free thiol, the benzyl group is cleaved from the molecule. Cleavage of the benzyl group is commonly carried out in the presence of aluminium bromide.

Our next aim was to obtain the monoester derivative, 2-mercapto-terephthalic acid 4-methyl ester (77) in order to make subsequent ring closure straightforward.

It has been reported that a compound similar to (76) under the same cleavage conditions, and despite precautions to exclude moisture, always gave a mixture of the diester and the diacid after 3 hours of reaction.[128] Thus, we thought that reaction time could be a critical factor to obtain the monoester. After 12 hours, no traces of diester was observed and monoester (77, 78) and diacid 79 derivatives were isolated.

However, as reported, purification of such a mixture was very difficult, only possible through flash chromatography using polar eluting systems, either 20% MeOH in CHCl$_3$, or 50% EtOAc in cyclohexane. This allowed the isolation, in the best case, of 45% of the monoacid which initially was thought to be 77, where the methyl ester in the *ortho* position to the site where the cleavage takes place is hydrolysed by the Lewis acid. By formation of the monoacid 77, the product can be stabilised by hydrogen bonds between the acid and the thiol. Consideration of the electronic effects driving this reaction makes this result seem quite reasonable. However, when the monoacid was subjected to oxidation and subsequent reactions as shown in Scheme 21, we observed the formation of the corresponding amides instead of the 1,2-benzoisothiazol-3-ones derivatives. This result made us suspect that the isomer from the cleavage reaction was not the desired one. The unhindered 4-carboxylate moiety is susceptible to attack by aluminium bromide, and instead of forming compound

77 the isomer **78** was obtained. Thus, steric and not electronic effects direct the reaction.

In order to distinguish between both compounds and to confirm the structure of compound **78** a NOE experiment was performed. Figure 32 shows the ^{1}H spectrum (in DMSO-d_6), and the alignment is the difference spectrum created after irradiating the sample at the frequency of the protons of interest.

Irradiation at 3.89 ppm, which corresponds to the protons of the methyl ester, shows a positive NOE with the signal of the aromatic proton Hc at 8ppm.

When irradiation at the resonance frequency of the thiol proton (5.7 ppm) was performed, the signal from the proton Ha at 8.2 ppm appeared in the difference spectrum, showing the spatial proximity of both protons. Also, a small signal from the protons of the methyl ester was observed, and no spatial interaction between the thiol proton and the acidic proton was detected. An exchange effect between the proton of the thiol and that corresponding to the acid with the ones of the H_2O present in the solvent was seen.

Finally, irradiation at 7.7 ppm corresponding to the proton Hb showed a NOE effect with the signal at 8 ppm of the proton Hc that confirmed that Hb has got a neighbour-ring relationship with Hc and that it is away from the methyl ester.

Due to the small NOE effect with the protons from the methyl ester when irradiation at 5.7 ppm (SH), HMQC and HMBC experiments were performed to ensure the confirmation of the structure. By HMQC it is possible to assign ^{1}H - ^{13}C correlation for J=1. The proton at 7.7 ppm (Hb) is correlated to carbon at 125.10 ppm (C7), the proton at 8ppm (Hc) is correlated to carbon at 131.32 ppm (C6), and the proton at 8.2 ppm is correlated to carbon at 131.61 ppm (C3). By HMBC it is possible to assign ^{1}H-^{13}C correlation for J=2 and J=3. The spectrum shows that proton Ha is related to C7, C5 and C1 through a J=3; proton Hb is correlated to C3, C5 and C1; and proton Hc is correlated to C4, C2 and C8. These results confirm the structure **78**.
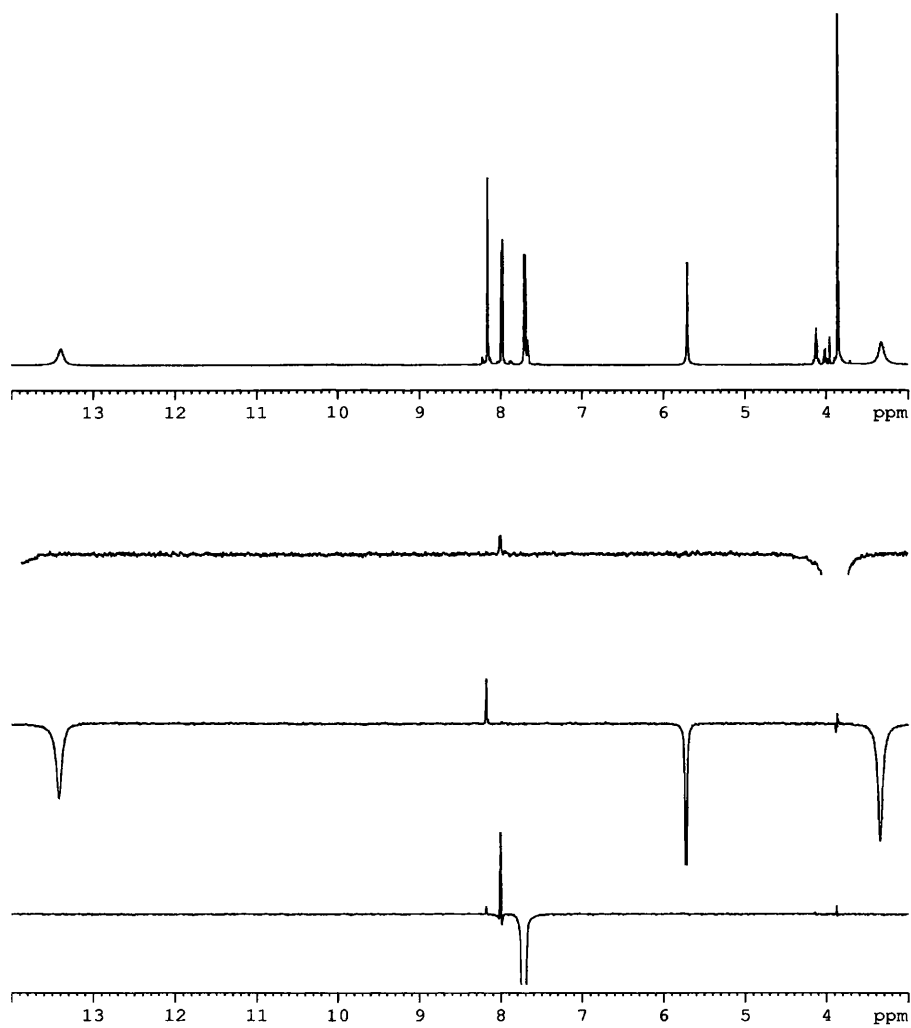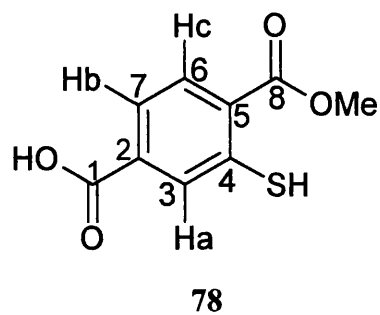
Figure 32. a) H-NMR spectrum for compound **78**. **b, c, d,** NOE spectrum for compound **78**, after irradiation at 3.89 ppm (OMe)(**b**), at 5.7ppm (**c**), at 7.7 ppm (**d**).

Approach 3

In view of these results, we suggested another strategy in which the nucleophilic displacement reaction introduces the sulphur atom into the molecule not as a benzyl sulfuryl but as p-methoxybenzyl sulfuryl. The p-methoxybenzyl group can be cleaved in the presence of TFA and anisole or thioanisol without affecting the ester function. Furthermore, we decided to incorporate the carboxylic acid protected as an ethyl ester, in order to differentiate between the reactivity of the esters. Since the methyl ester is more reactive than the ethyl ester, we thought that under mild conditions the hydrolysis of the methyl ester would take place without affecting the ethyl ester (Scheme 25).
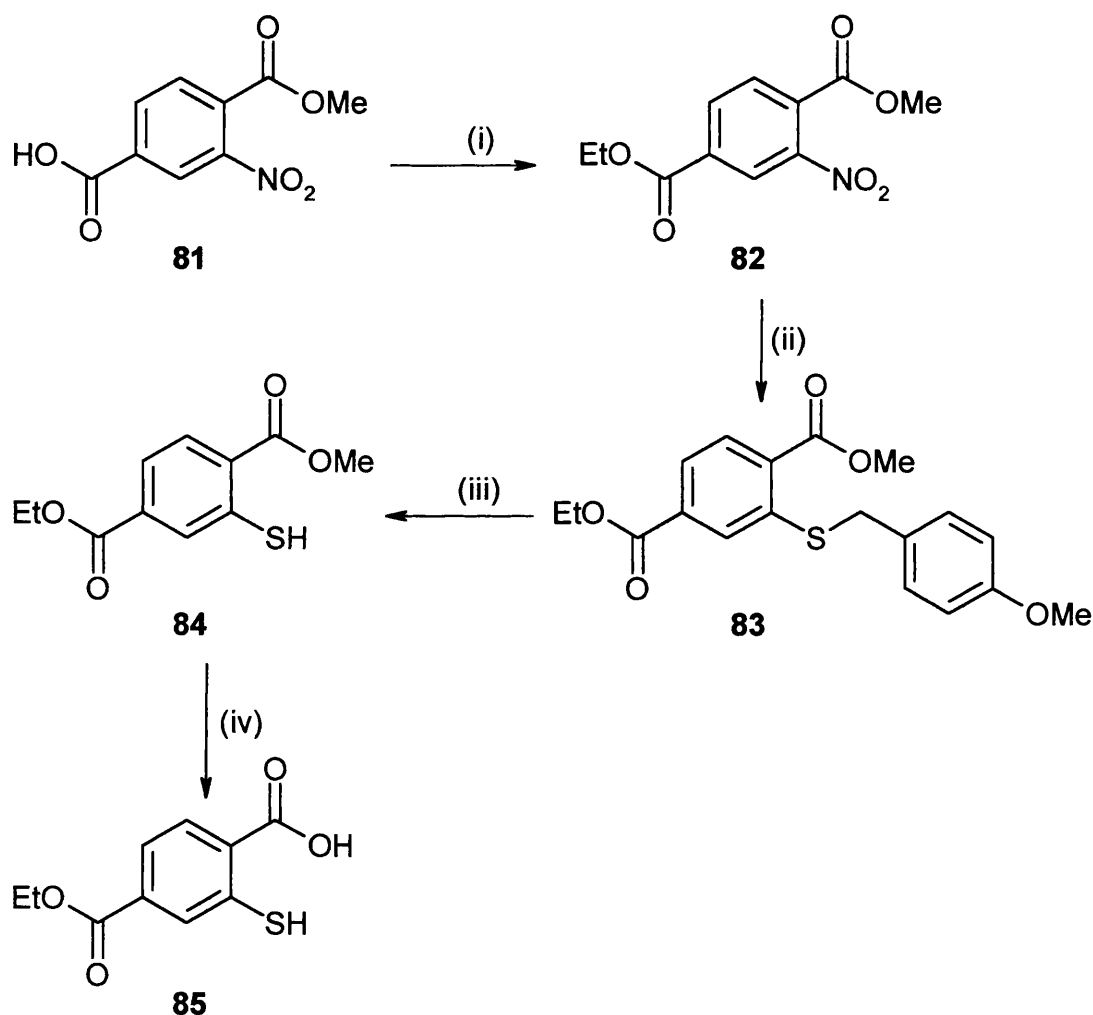
Scheme 25. (i) EtOH anhydrous, H₂SO₄, (ii) 4-methoxy-benzyl mercaptan, DMF, NaH, (iii) TFA, thioanisole, (iv) LiOH, MeOH.

4-(methoxycarbonyl)-3-nitrobenzoic acid (**81**) in dry EtOH in the presence of conc. sulfuric acid undergoes an esterification to give 2-nitro-terephthalic acid 4-ethyl ester 1-methyl ester (**82**), which is converted into compound **83** by a nucleophilic displacement reaction with *p*-methoxybenzyl mercaptan in DMF with NaH as the base. The *p*-methoxybenzyl group is cleaved with TFA and thioanisole to give the thiol derivative (**84**). Compound **84** was subjected to reaction with LiOH (1M) in MeOH in order to obtain selectively the product of saponification of the methyl ester. However, even under such mild conditions none of the desired product was obtained.

Approach 4

Taking these results into account a new procedure was considered. Approach 4 does not involve formation of intermediate **46** but of compound **89** where the ester substituent in the 6-position has been replaced by the amide functionality. The reason for this is to try to avoid competitive reactions in the hydrolysis of the esters. This obviously modifies the reaction that connects the heterocyclic with the resin. The resin now needs to be introduced through a coupling reaction between the double bond of the vinyl group in **89** with an halogen substituted resin such as **90**.

90
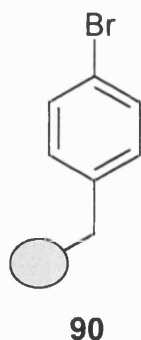
Scheme 26 shows the reactions to synthesise compound **89**. The starting material, 4-(methoxycarbonyl)-3-nitrobenzoic acid **81** is converted into the corresponding amide derivative **86** by reaction with 4-vinylaniline **85**. Again nucleophilic displacement occurs as previously described to introduce the sulphur atom into the molecule to give either **87** by reaction with benzyl

mercaptan or **88** with 4-methoxy-benzyl mercaptan. However, the yield of the nucleophilic displacement reaction of **86** decreases (40% yield) when compared to **75** or **82**. This is due to the presence of the amide instead of the ester making the aromatic system electronically richer and nuchleophilic reactions are thus less favourable. Thus this route was also abandoned and finally the target compound was reached following approach 5.
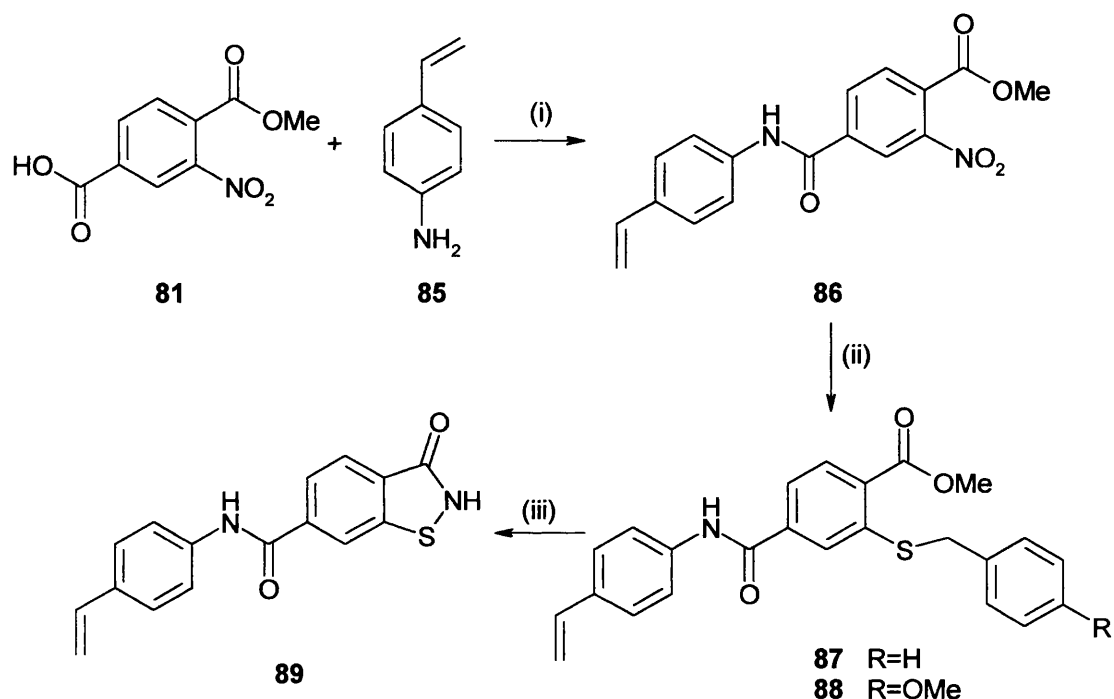
Scheme 26. (i) SOCl₂, DMF (catalytic amount), heat (ii) NaH, DMF, benzyl mercaptan or 4-methoxy-benzyl mercaptan

Scheme 26. (i) $SOCl_2$, DMF (catalytic amount), heat (ii) NaH, DMF, benzyl mercaptan or 4-methoxy-benzyl mercaptan

Approach 5

This approach involves formation of the benzoisothiazole moiety by cyclization of 2-sulfenamoylbenzoate, which is synthesised by amination of the corresponding thiosalicylate (Scheme 27).[129]

As previously described, 2-nitro terephtalic acid dimethyl ester (**82**) underwent nucleophilic displacement with *p*-methoxybenzyl mercaptan followed by cleavage of the *p*-methoxy benzyl group to give the corresponding thiol **84**.

When an aqueous solution of hydroxylamine-*O*-sulfonic acid (HOSA) with an equimolecular amount of potassium hydroxide was added dropwise to an aqueous solution of the thiol **84** and potassium hydroxide on an ice bath the corresponding sulfenamoylbenzoate **93** is formed as a white precipitate. In addition to the required compound, the product of oxidation of the thiol group **95** is also observed as a small peak in MS. In order to minimize this side product water is degassed prior to making up the aqueous solutions. Finally, cyclization of **93** in ethanol with potassium hydroxide at room temperature gives rise the desired product **46b**. In order to obtain compound **46a** starting material 2-nitroterephthalic acid dimethyl ester (**75**) underwent similar reactions. We observed that in this case the amount of the side product **96** increases and purification was required prior to the cyclization. In addition only product **46b** was obtained due to the transesterification reaction as the cyclization step takes place in ethanol.
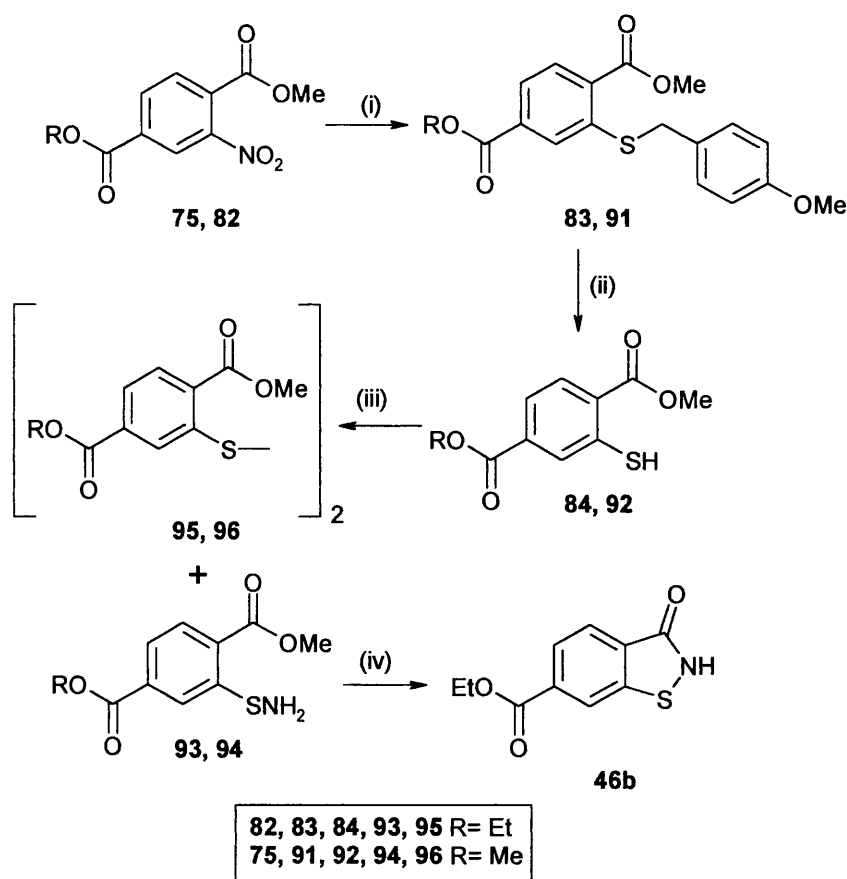
Scheme 27. (i) NaH, DMF, 4-methoxy-benzyl mercaptan (ii) TFA, thioanisole (iii) HOSA, KOH, H_2O (iv) EtOH, KOH

3.4 Summary and Conclusion

A traceless linker based on a benzoisothiazol derivative as the scaffold has been proposed. The aim of the project was to investigate the possibility of applying this chemistry as a method of synthesising a variety of biomolecules in a solid phase manner. This objective is still the subject of investigation as in this Chapter we have reported only our initial work. We have tried several approaches to reach the desired initial intermediate. This was eventually achieved in a 5 step synthesis. However, the method still requires optimisation.

This heterocycle remains to be attached to the resin and the subsequent reactions, as indicated in Scheme 16, need to be completed. This will finally determine the value of this scaffold as a traceless linker.

CHAPTER FOUR

EXPERIMENTAL

4.1 General Information

All starting materials were either commercially available or reported previously in the literature unless noted. Solvents and reagents were used without further purification except THF which was dried over sodium. Reactions were monitored by TLC on precoated silica gel plates (Kieselgel 60 F_{254}, Merck). Purification was performed by flash chromatography using silica gel (particle size 40-63 μm, Merck). ^1H and ^{13}C NMR spectra were recorded on a Bruker AMX-300 spectrometer. Chemical shifts are reported as ppm relative to TMS as internal standard. Mass spectra were recorded on either a VG ZAB SE spectrometer (EI, FAB and APCI) or a Micromass Quattro electrospray LC-mass spectrometer. IR spectra were recorded on a Perkin-Elmer Spectrum One series FT-IR spectrophotometer. Melting points were determined on a Gallenkamp melting point apparatus and are uncorrected. UV-Vis spectra were recorded in a UNICAM Helios α spectrometer. Microanalysis was carried out by the Analytical Services Section, Department of Chemistry, University College London. High-pressure liquid chromatography (HPLC) was performed on an Anachem system, using a HYPERSIL, PEP 100 C-$_{18}$, 5μ, 100x 21.2mm (part no 39105-127) column and 1mL loop size for preparative HPLC or HYPERSIL PEP 100 C-$_{18}$, 5μ, 100 x 2.1mm (part no 39105-088) column and 20μL loop size for analytical HPLC. Irradiation of the photolabile compounds was carried out using a Vilber Lowmart 15 W filtered lamp (VL-215LM) operated at 365 nm and 1350 μw/cm^2.

4.2 Experimental Section for Chapter 2

4.2.1 *Methyl 5-(2-nitrobenzoyl)-2-furoate (26)*
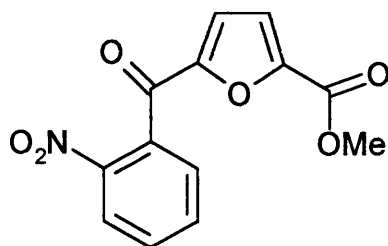
A suspension of 2-nitrobenzoic acid **24** (30.0 g, 0.18 mmol) in thionyl chloride (100 mL) with a catalytic amount of N,N-dimethylformamide (50 μL) was heated at reflux for 2 h. After cooling, the excess thionyl chloride was removed under reduced pressure. The residual oil was dissolved in CH_2Cl_2 (100 mL) and to this solution was added $FeCl_3$ (0.60 g, 3.70 mmol) portion-wise followed by methyl furanoate **25** (22 mL, 0.21 mol). The resultant mixture was heated at reflux for 15 h. A further portion of $FeCl_3$ (0.60 g, 3.70 mmol) was added to the mixture and heating continued for a further 4 h. The mixture was allowed to cool to ambient temperature and then poured onto water (100 mL). The layers were separated and the aqueous layer was extracted with CH_2Cl_2 three times. The combined organic material was washed three times with saturated aqueous $NaHCO_3$, dried ($MgSO_4$) and concentrated under reduced pressure. The crude material was initially purified through a plug of silica using a cyclohexane-EtOAc gradient, then the solid was recrystallised from hexane/CH_2Cl_2 to provide the product as fine yellow needles (14.97 g, 30%). M.p: 137-138°C (from hexane/CH_2Cl_2). (Found: C, 56.48; H, 2.90; N, 4.95. $C_{13}H_9NO_6$ requires C, 56.73; H, 3.30; N, 5.09%); δ_H (CDCl$_3$) 3.90 (3H, s), 7.24 (2H, m), 7.61 (1H, dd, J 7.4, 1.5 Hz), 7.74 (1H, m), 7.82 (1H, m), 8.25 (1H, dd, J 8.1, 1.1 Hz); m/z (EI) 244 (M^+-OCH$_3$).

4.2.2 *Methyl 5-(2-aminobenzoyl)-2-furoate* *(27)*
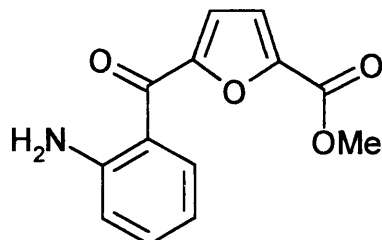
Iron powder (7.7 g, 0.14 mol) was added in three portions to a solution of methyl 5-(2-nitrobenzoyl)-2-furoate **26** (7.0 g, 25.4 mmol) in acetic acid (500 mL) containing water (15 mL) at a temperature of 90°C. The mixture was then heated to reflux for 5h, whereupon TLC analysis indicated the reaction to be complete. The excess acetic acid was removed by rotary evaporation under reduced pressure. Water (400 mL) was added to the residue and the mixture was stirred vigorously for 1 h. The mixture was then basified by the addition of concentrated aqueous ammonia solution and the resultant suspension was filtered through celite. The Celite 'cake' was washed with water followed with copious amounts of CH_2Cl_2. The combined filtrate layers were separated and the aqueous layer extracted five times with CH_2Cl_2. The combined organic material was dried ($MgSO_4$) and concentrated under reduced pressure to give a dark orange solid (5.23 g, 84%). This material was used without further purification in subsequent reactions. A small amount was recrystallised (hexane) to give an orange powder for analysis: M.p: 104-106°C (from hexane). (Found: C, 63.48; H, 4.40; N, 5.66. $C_{13}H_{11}NO_4$ requires C, 63.67; H, 4.52; N, 5.71%); δ_H (CDCl$_3$) 3.96 (3H, s), 6.10 (2H, br s), 6.74 (2H, m), 7.18 (1H, d, J 3.7 Hz), 7.29 (1H, m), 7.34 (1H, m), 8.01 (1H, dd, J 8.1,1.4 Hz); m/z EI (M$^+$) 245.

4.2.3 *Methyl 5-(1H-indazol-3-yl)-2-furoate (19)*
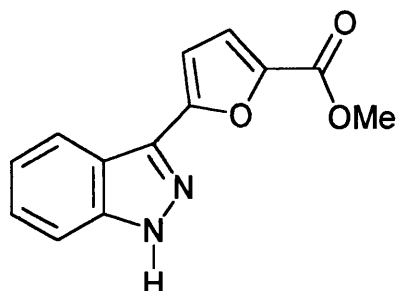
Crude methyl 5-(2-aminobenzoyl)-2-furoate **27** (0.54 g, 1.96 mmol) was dissolved in conc. HCl (15 mL) and cooled to -10°C. A solution of NaNO$_2$ (0.15 g, 2.17 mmol) in water (2 mL) was added and the mixture stirred for 1 h, maintaining a temperature of -10°C. A solution of tin (II) chloride dihydrate (1.10 g, 4.88 mmol) in conc. HCl (2mL) was then added followed by a further 1 h of stirring at -10°C. Ice-water (100 mL) was added and the suspension was extracted three times with EtOAc. The combined extracts was washed with water, dried (MgSO$_4$) and concentrated under reduced pressure. The crude product was purified by passage through a silica plug using a gradient of cyclohexane-EtOAc and then recrystallised (acetone/H$_2$O) to give the product as a yellow solid (0.38 g, 79%): M.p: 157-159°C (from acetone/ H$_2$O); (Found: C, 64.32; H, 4.30; N, 11.13. C$_{13}$H$_{10}$N$_2$O$_3$ requires C, 64.46; H, 4.16; N, 11.56%); δ_H (DMSO-d$_6$) 4.00 (3H, s), 7.31 (1H, d, *J* 3.8 Hz), 7.42 (1H, dd, *J* 7.3, 7.3 Hz), 7.58 (1H, dd, *J* 7.9, 7.9 Hz), 7.61 (1H, d, *J* 3.8 Hz), 7.76 (1H, d, *J* 8.3 Hz), 8.26 (1H, d, *J* 8.3 Hz); δ_C (CDCl$_3$) 159.20 (*C*OOMe), 152.72, 143.75, 141.04, 127.50, 122.34, 121.66, 120.49, 119.72, 109.89, 108.36, 51.90 (Me); *m/z* (EI) 242 (M$^+$).

4.2.4 2,2,2-Trifluoro-1-(4-methylphenyl)ethanone oxime (29) [61]
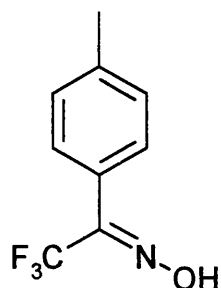
To a stirred mixture of hydroxylamine hydrochloride (11.1g, 159.44 mM), and sodium hydroxide (6.4g, 159.44 mM) in boiling ethanol (500ml) was added a solution of 4-(trifluoroacetyl)toluene (28) (10g, 53.14 mM) in ethanol (80ml). After refluxing for 20 h the solvent was evaporated *in vacuo,* and the residue partitioned between ether and water. The organic layer was washed 3 times with 0.01 N aqueous HCl and 3 times with water, then dried over $MgSO_4$, and purified by chromatography on silica gel, eluting with chloroform. The title compound was isolated as a white solid (8.5g, 79%). M.p: 65- 85°C (lit. 63-86°C). (Found: C, 53.18; H, 3.88; N, 6.79; $C_9H_8F_3NO$ Requires: C, 53.21; H, 3.97; N, 6.89%); δ_H (CDCl$_3$) 2.36 (3H, s, CH$_3$), 7.10-7.39 (4H, m, aromatic H), 8.41 (1H, br s, OH); *m/z* (EI) 203 (M$^+$), 117 (M$^+$-CF$_3$OH), 91, 69.

4.2.5 2,2,2-Trifluoro-1-(4-methylphenyl)-N-{[(4methylphenyl)sulfonyl]oxy} ethanimine (30) [61]
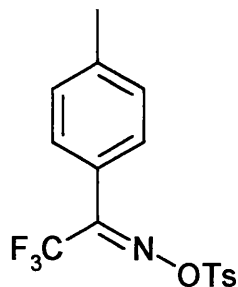
Compound **29** (7.22g, 35.57mM) dissolved in 120 ml of dry pyridine, *p*-toluenesulfonyl chloride (10.17g, 53.34mM) was added and the mixture heated at reflux. After 24 h. the solvent was evaporated *in vacuo,* and the residue subjected to column chromatography eluting with chloroform. The product was

isolated as a white solid, which crystallized from ether-hexane as white needles (11.31g, 89%). M.p: 101°C (from ether-hexane). (Found: C, 53.29; H, 3.59; N, 3.56; $C_{16}H_{14}NO_3S$ Requires: C, 53.78; H, 3.95; N, 3.92%); δ_H (CDCl$_3$) 2.36 (3H, s, CH$_3$), 2.43 (3H, s, CH$_3$), 7.30 (4H, m, aromatic H), 7.4 -7.9 (4H, m, aromatic); m/z (EI) 357.4 (M$^+$) 155, 91, 65.

4.2.6 *3-(4-Methylphenyl)-3-(trifluoromethyl)diaziridine (31)*[61]
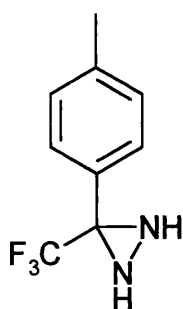
To a solution of **30** (1g, 2.8 mM) in an autoclave was added liquid ammonia (10ml). After heating at 60°C for about 24h the solution was allowed to cool, poured into a beaker, then concentrated under reduced pressure. The residue was partitioned between ether and water and the organic layer dried over Na$_2$SO$_4$. The solvent was removed *in vacuo* and the residue purified by column chromatography on silica eluting with chloroform. Crystallization from n-hexane at -20°C gave the diaziridine as a white solid (0.5g, 88%). M.p: 43-44°C. (Found: C, 53.22; H, 4.32; N, 13.32; $C_9H_9F_3N_2$ Requires: C, 53.44; H, 4.49; N, 13.86%); δ_H (CDCl$_3$) 2.18 and 2.75 (2H, dd, N*H*, AB system), 2.35 (3H, s, CH$_3$), 7.21 and 7.48 (4H, m, aromatic H); m/z (EI) 202(M$^+$), 201, 181, 133, 91.

p-toluenesulfonyl amide was also isolated as a side product :

M.p: 120°C. (Found: C, 48.97; H, 5.06; N, 8.10; (C$_7$H$_9$NSO$_2$) Requires: C, 49.10; H, 5.30; N, 8.10). δ_H (CDCl$_3$) 2.48 (3H, s, Me), 4.79 (2H, br s, NH$_2$), 7.35- 7.85 (4H, m, aromatic); m/z (EI) 171(M$^+$), 155, 107, 91,65.

4.2.7 *3-(4-Methylphenyl)-3-(trifluoromethyl)-3H-diazirene (32)*[88]
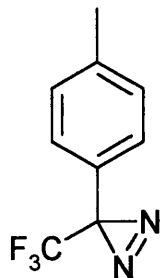
Oxalyl chloride (1.4g, 1ml, 10.9 mM) was added to dichloromethane (30ml) and DMSO (1g, 0.85ml, 11.98 mM) at - 78°C. After 5 min compound **31** (2.02g, 9.99mM) was introduced, followed after a further 15 min by triethylamine (5g, 6.9ml, 49.9mM). The reaction mixture was allowed to warm to room temperature over 2 h, quenched into water, and the organic phase separated and dried over Na₂SO₄. After evaporation the residue was chromatographed on silica eluting with 10% ethyl acetate in light petroleum to give the title compound (1.5g, 75%). The pure diazirine crystallizes upon storage at - 20°C, but melts when warmed to room temperature, (as reported in literature). (Found: C, 53.69; H, 3.71; N, 11.70; $C_9H_7F_3N_2$ Requires: C, 54.00; H, 3.50; N, 14.00%); δ_H (CDCl₃) 2.31 (3H, s, Me), 7.12-7.24 (4H, m, aromatic H); m/z (EI) 200 (M⁺), 172 (M⁺-N₂), 103 (M⁺-CN₂F₃), 91 (M⁺-C₂N₂F₃).

4.2.8 *3-[4-(Bromomethyl)phenyl]-3-(trifluoromethyl)-3H-diazirene (21)*[87]
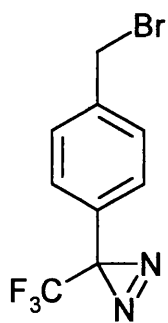
To a stirred solution of **32** (0.13g, 0.65mM) in 3ml of tetrachloromethane, powdered NBS (0.12g, 1 equiv.) was added and the mixture warmed to 70°C.

AIBN (3mg) was then added and the temperature was gradually raised to 77°C. After 40 min, the reaction mixture was cooled, the succinimide separated by filtration, and the filtrate concentrated *in vacuo*. Subsequent column chromatography on silica eluting with petroleum ether/dichloromethane (40:1) yielded the product as an oil, which crystallized at -30°C, but melted when warmed to room temperature. δ_H (CDCl$_3$) 4.51 (2H, s, CH$_2$), 7.15-7.45 (4H, m, aromatic). *m/z* (EI) 278.9 (M$^+$).

4.2.9 *{4-[3-(Trifluoromethyl)-3H-diaziren-3-yl]phenyl}methanol (23)*[130]
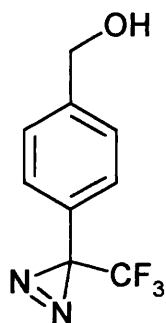
To a solution of 4-[3-(trifluoromethyl)-3H-diazirin-3-yl]benzoic acid (0.136g, 0.59mM) in THF at -20°C was added borane 1M in THF (0.59mL), the reaction mixture was allowed to warm to room temperature overnight. To the reaction mixture was added MeOH (300 μL) and the mixture stirred for 30 min. The solvent was removed *in vacuo*, and the residue was washed twice with ether. Subsequent column chromatography on silica eluting with cyclohexane/ethyl acetate (75:25) gave an oil (0.08g, 63%), which crystallizes at 4°C; δ_H (CDCl$_3$) 1.81 (1H, br s, O*H*), 4.7 (2H, C*H*$_2$OH), 7.17 (2H, dd, AA'BB' system, aromatic H), 7.38 (2H, dd, AA'BB' system, aromatic H); δ_C (CDCl$_3$) 142.99, 128.72, 127.51, 127.11, 124.60, 121.00, 64.85 (CH$_2$OH); δ_F (CDCl$_3$) –65.6.

4.2.10 *Methyl 5-(1-benzyl-1H-indazol-3-yl)-2-furoate (33)*
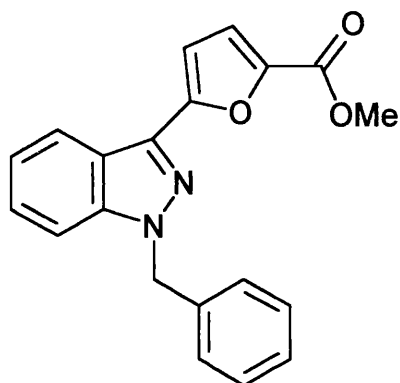
A solution of methyl 5-(1H-indazol-3-yl)-2-furoate **19** (2.0 g, 8.3 mmol) and benzyl bromide **20** (2.5 mL, 21.0 mmol) in THF (100 mL) was added dropwise *via* dropping funnel to a suspension of sodium hydride (60% dispersion in oil: 0.50 g, 12.5 mmol) in THF (200 mL). The resultant mixture was stirred at room temperature for 20 h. The mixture was poured onto brine and the layers separated. The aqueous layer was extracted three times with ether and then the combined organic material was washed with saturated aqueous NaHCO₃ solution, dried (MgSO₄) and concentrated under reduced pressure. The residue was chromatographed on silica (EtOAc:cyclohexane 1:4) and then the product was recrystallised (EtOAc/hexane) to give a yellow solid: M.p: 137-138°C (from EtOAc/hexane); (Found: C, 71.92 ; H, 4.75; N, 8.39. $C_{20}H_{16}N_2O_3$ requires C, 72.28; H, 4.85; N, 8.43%); δ_H (CDCl₃) 3.97 (3H, s), 5.67 (2H, s), 7.03 (1H, d, *J* 3.7 Hz), 7.22-7.43 (9H, m), 8.27 (1H, d, *J* 8.1 Hz); *m/z* (EI) 332 (M⁺).

4.2.11 *Methyl 5-(1-{4-[3-(trifluoromethyl)-3H-diaziren-3-yl]benzyl}-1H-*

indazol-3-yl)-2-furoate (34)
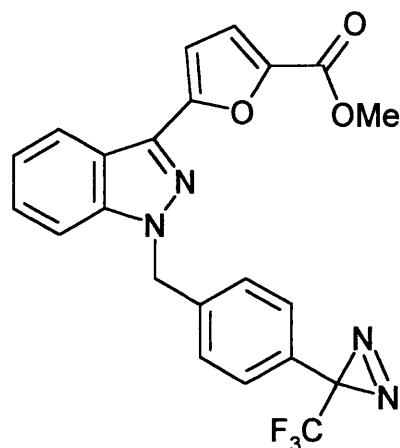
A solution of Methyl 5-(1H-indazol-3-yl)-2-furoate **19** (0.5g, 2.06mM) and 3-

[4-(bromomethyl)phenyl]-3-(trifluoromethyl)-3*H*-diazirene **21** (0.57g,

2.076mM) in THF was added to a suspension of NaH (0.16g, 2.47mM) in THF

at room temperature under N_2 and the mixture allowed to stir overnight. The

reaction mixture was poured onto brine and the layers separated. The aqueous

layer was extracted with ether three times, and the combined organic layers

were washed with a saturated solution of $NaHCO_3$, then water, dried over

$MgSO_4$ and concentrated *in vacuo*. Subsequent column chromatography on

silica eluting with cyclohexane/ethylacetate (80:20) yielded the desired product

(0.5g, 55%). M.p: 101-102 °C (from cyclohexane/ethylacetate). (Found: C,

59.41; H, 3.65; N, 13.17. $C_{22}H_{15}N_4O_3F_3$ requires C, 60.00; H, 3.43; N, 12.73%);

δ_H (CDCl$_3$) 4.00 (3H, s, CO$_2$CH_3), 5.57 (2H, s, CH_2 Ph), 6.89 (1H, d, J 3.5 Hz),

7.29 (1H, d, J 3.5 Hz), 7.09-7.19 (4H, d, Ph), 7.20-7.39 (3H, m, indazole), 8.29

(1H, m); m/z (APCI $^+$) 441(M$^+$+1), 413 (M$^+$-N$_2$).

4.2.12 *[5-(1-Benzyl-1H-indazol-3-yl)-2-furyl]methanol (5)*
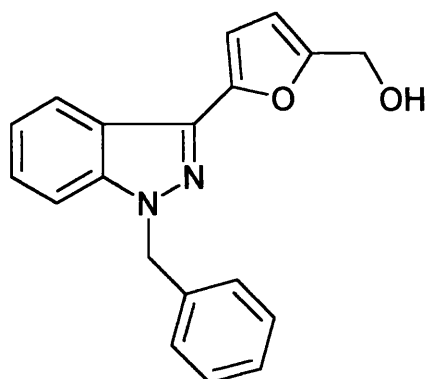
A solution of compound **33** in THF (150 mL) was added dropwise to a suspension of CaBH$_4$.2THF (3.9 g, 18.23 mmol) in THF (150 mL) at room temperature. The resultant mixture was heated to reflux for 15 h. The reaction mixture was allowed to cool, then poured slowly onto brine. The layers were separated and the aqueous layer was extracted three times with ether. The combined organic material was dried (MgSO$_4$) and concentrated under reduced pressure. The crude product was chromatographed on silica (30-40% EtOAc/cyclohexane) and then recrystallised (ethanol/H$_2$O) to give **5** as fine cream needles (1.56 g, 86%). M.p: 112-112.5°C (lit.[48]108-109°C); (Found: C, 74.80; H, 5.28; N, 9.15. C$_{19}$H$_{16}$N$_2$O$_2$ requires C, 74.98; H, 5.30; N, 9.20%); δ_H (CDCl$_3$) 4.76 (2H, s), 5.68 (2H, s), 6.50 (1H, d, *J* 3.3 Hz), 6.90 (1H, d, *J* 3.3 Hz), 7.21-7.40 (8H, m), 8.08 (1H, d, *J* 8.5 Hz); *m/z* (EI) 304 (M$^+$).

4.2.13 *[5-(1-{4-[3-(Trifluoromethyl)-3H-diaziren-3-yl]benzyl}-1H-indazol-3-*

yl)-2-furyl]methanol (16)
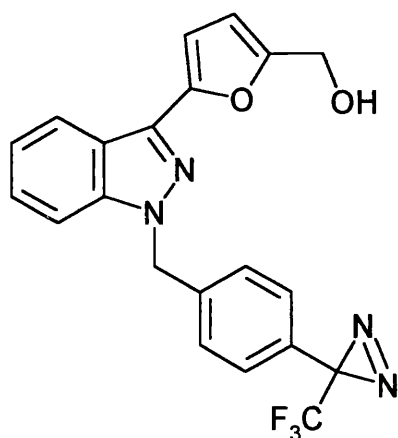
To a solution of **34** (0.16g, 0.363mM) in dichloromethane was added diisobutylaluminum hydride (DIBAL-H) (0.60ml, 0.727mM) at -30°C under N₂. The mixture was stirred and allowed to warm to 0°C. After completion of the reaction, water was added. The resulting solid was removed by filtration and washed with dichloromethane. The filtrate was diluted with water and extracted with dichloromethane. After drying over $MgSO_4$, the combined extracts were evaporated, and the residue was chromatographed on silica eluting with cyclohexane/ethyl acetate (50:50) to yield the required product (0.09g, 60%). M.p: 55-58°C. (Found: C, 61.36; H, 4.01; N, 11.25; $C_{21}H_{15}N_4O_2F_3$ Requires: C, 61.17; H, 3.67; N, 13.59%); δ_H (CDCl₃) 4.7 (2H, s, CH_2OH), 5.6(2H, s, CH_2Ph), 6.42 (1H, d, furyl), 6.81 (1H, d, furyl), 7.15-7.20 (4H, m, Ph), 7.05-7.39, (3H, m, indazole), 7.99 (1H, m, indazole); m/z (FAB⁺) 413(M⁺+ 1), 412(M⁺), 383(M⁺-N₂); m/z (FAB) exact mass 412.1147 $C_{21}H_{15}N_4O_2F_3$ requires 412.1160; Analytical HPLC shows an unique peak with the retention time of 16.38 min using a gradient elution of 3-97% acetonitrile in 0.1% TFA aqueous solution over 20 min at a flow rate of 1 mL/min.

4.2.14 Compounds 33 and 35 from Mitsunobu conditions

To a solution of **19** (0.1g, 0.413mM) in dry toluene was added tributylphosphine (0.2mL, 0.826mM), followed by benzyl alcohol (**22**) (0.085mL, 0.826mM) and 1,1-azobisdimethyl formamide (0.142g, 0.826mM) and the mixture heated at 80°C. After two hours the reaction mixture was allowed to cool. The resulting solid was removed by filtration and washed with toluene, the filtrate concentrated *in vacuo*. Subsequent column chromatography on silica eluting with cyclohexane/ethyl acetate (80:20) gave a yellow oil (0.09g) corresponding to a mixture of compounds **33** and **35**. Both compounds (70 mg) were separated by HPLC using a gradient elution of 40-80% acetonitrile in 0.1% TFA aqueous solution over 20 min at a flow rate of 20 mL/min.

4.2.15 *Methyl 5-(1-benzyl-1H-indazol-3-yl)-2-furoate (33)*
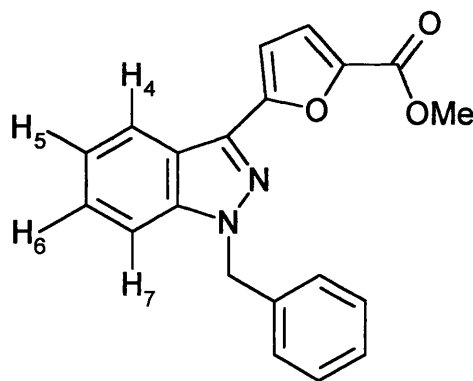
Isolated as a pale yellow solid (16.5mg), M.p.135-137°C (from cyclohexane/EtOAc). δ_H (CDCl$_3$) 3.98 (s, CO$_2$CH_3), 5.71 (2H, s, CH_2Ph), 7.04 (1H, d, J 3.5 Hz, furyl), 7.36 (1H, d, J 3.5 Hz, furyl), 7.30 (1H, m, $J_{5\text{-}4}$ 8.3, $J_{5\text{-}6}$ 6.6, $J_{5\text{-}7}$ 1.1 Hz, indazol), 7.37 (1H, dd, $J_{7\text{-}6}$ 8.45, $J_{7\text{-}5}$ 1.1 Hz, indazol), 7.41(1H, m, $J_{6\text{-}7}$ 8.45 Hz, $J_{6\text{-}5}$ 6.6, $J_{6\text{-}4}$ 1 Hz, indazol), 8.28 (1H, m, $J_{4\text{-}5}$ 8.3, $J_{4\text{-}6}$ 1 Hz, indazol), 7.24 (2H, m, *o*-Ph), 7.32 (2H, m, *m*-Ph), 7.33 (1H, m, *p*-Ph); m/z (FAB) 333 (M$^+$+1), 91; m/z (EI) exact mass 332.11488 C$_{20}$H$_{16}$N$_2$O$_3$ requires 332.1161; analytical HPLC shows an unique peak with the retention time of

5.82 min using a gradient elution of 40-80% acetonitrile in 0.1% TFA aqueous solution over 20 min at a flow rate of 1 mL/min.

4.2.16 Methyl 5-(2-benzyl-2H-indazol-3-yl)-2-furoate (35)
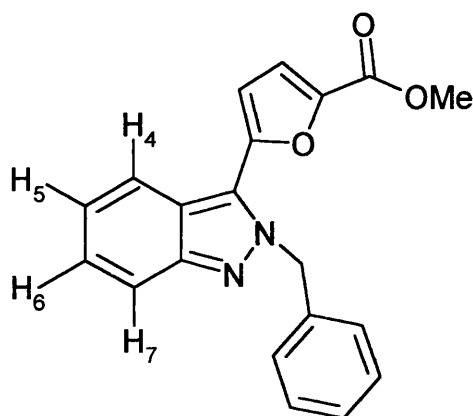
Isolated as a white solid (18.3mg), M.p: 110-115°C (from cyclohexane/EtOAc). δ_H (CDCl$_3$) 3.98 (3H, s, CO$_2$CH_3), 5.98 (2H, s, CH_2Ph), 6.75 (1H, d, J 3.5 Hz, furyl), 7.29 (1H, d, J 3.5 Hz, furyl), 7.31 (1H, m, J_{5-4} 8.3, J_{5-6} 6.6, J_{5-7} 1.1 Hz, indazole), 7.82 (1H, dd, J_{7-6} 8.45, J_{7-5} 1.1 Hz, indazole), 7.41(1H, m, J_{6-7} 8.45, J_{6-5} 6.6, J_{6-4} 1 Hz, indazole), 7.91 (1H, m, J_{4-5} 8.3, J_{4-6} 1 Hz, indazole), 7.24 (2H, m, o-Ph), 7.32 (2H, m, m-Ph), 7.33 (1H, m, p-Ph); m/z (FAB) 333 (M$^+$+1), 91; m/z (EI) exact mass 332.11522 C$_{20}$H$_{16}$N$_2$O$_3$ requires 332.1161; analytical HPLC shows an unique peak with the retention time of 3.39 min using a gradient elution of 40-80% acetonitrile in 0.1% TFA aqueous solution over 20 min at a flow rate of 1 mL/min.

**4.2.17** *[5-(2-Benzyl-2H-indazol-3-yl)-2-furyl]methanol (37)*
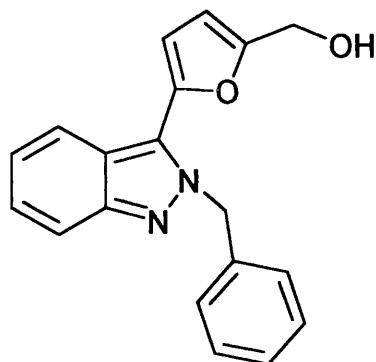
To a solution of **35** (0.04g, 0.12mM) in dichloromethane was added diisobutylaluminum hydride (DIBAL-H, 1.15M) (0.2 mL, 0.24 mM) at -30°C under N_2. The mixture was stirred and allowed to rise to 0°C. After completion of the reaction, water was added. The resulting solid was removed by filtration and washed with dichloromethane. The filtrate was diluted with water and extracted with dichloromethane. After drying over $MgSO_4$, the combined extracts were evaporated, and the residue was chromatographed on silica eluting with 25% ethyl acetate in cyclohexane to yield product **37** (0.015g, 42%); δ_H (CDCl$_3$) 4.61 (2H, s, C*H$_2$*OH), 5.79 (2H, s, C*H$_2$*Ph), 6.36 (1H, d, *J* 3.4 Hz, furyl), 6.50 (1H,d, *J* 3.4 Hz, furyl), 7.15-7.20 (4H, m, Ph), 7.07-7.29, (7H, m, indazol), 7.67 (1H, dd, *J* 9, 1.2 Hz), 7.77 (1H, dd, *J* 8.4, 1.1 Hz); *m/z* (ESP⁺) 305 (M⁺ +1, 100%).

4.2.18 *4-Chloro-N-[3-(dimethylamino)propyl]benzamide (15)*
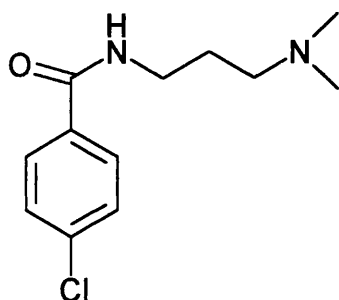
To a solution of 4-chlorobenzoic acid **40** (0.5 g, 3.2 mM) in dry acetonitrile was added *N,N*-dimethylpropane-1,3-diamine (0.4 mL, 3.2 mM), DIPEA (2.73 g, 9.58 mmol) and HATU (1.21 g, 3.2 mM). The reaction mixture was heated at 50°C under nitrogen and stirred very gently for 1 day. The resin was removed by filtration and washed with acetonitrile, the filtrate concentrated *in vacuo*. Subsequent column chromatography on silica eluting with (CHCl₃/MeOH/NH₃; 8.9:1:0.1) gave a pale yellow solid (0.4 g, 52%). M.p: 58-60°C. (Found: C, 59.55; H, 7.44; N, 11.68; C₁₂H₁₇N₂OCl Requires: C, 59.87; H, 7.12; N, 11.64); δ_H (CDCl₃) 1.69 (2H, quintet, *J* 6 Hz, NHCH₂C*H₂*CH₂N(CH₃)₂), 2.23 (6H, s, NHCH₂CH₂CH₂N(C*H₃*)₂), 2.40 (2H, t, NHCH₂CH₂C*H₂*N(CH₃)₂), 3.48 (2H, m, *J* NHC*H₂*CH₂CH₂N(CH₃)₂), 7.30 (2H, dd, aromatic), 7.64 (2H, dd, aromatic), 8.58 (1H, br s, N*H*); δ_C(CDCl₃) 166.34 (CO), 137.62, 133.61, 129.05, 128.67, 59.85 (Me), 45.82 (*C*H₂-NHCO), 41.25 (*C*H₂-NMe₂), 25.38 (-CH₂*C*H₂CH₂-); *m/z* (FAB) 241(M+1), 196 (M+1-NH(CH₃)₂), 139 (M+1-C₅H₁₄N₂), 84 (McLafferty rearrangement).

4.2.19 *N-[3-(Dimethylamino)propyl]-4-[3-(trifluoromethyl)-3H-diaziren-3-yl]benzamide (17)*
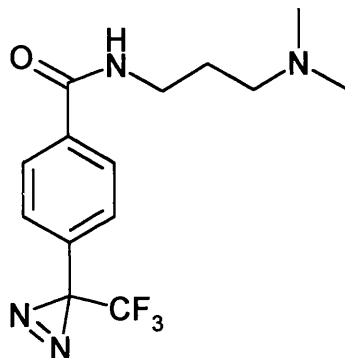
To a solution of 4-[3-(trifluoromethyl)-3H-diaziren-3-yl] benzoic acid **41** (0.1 g, 0.43 mM) in dry acetonitrile was added *N,N*-dimethylpropane-1,3-diamine (0.06 mL, 0.43 mM), DIPEA (0.37 g, 1.3 mmol) and HATU (0.165 g, 0.43 mM). The reaction mixture was heated at 50°C under nitrogen and stirred very gently for 1 day. The resin was removed by filtration and washed with acetonitrile, the filtrate concentrated *in vacuo*. Subsequent column chromatography on silica eluting with (CHCl$_3$/MeOH/NH$_3$; 7.9:2:0.1) gave **17** as a yellow oil (0.07 g, 70%). (Found: C, 53.5; H, 5.45; N, 17.83; C$_{14}$H$_{17}$F$_3$N$_4$O Requires: C, 52.88; H, 5.30; N, 17.15); δ_H (CDCl$_3$) 1.71 (2H, quintet, *J* 6 Hz NHCH$_2$C*H$_2$*CH$_2$N(CH$_3$)$_2$), 2.22 (6H, s, NHCH$_2$CH$_2$CH$_2$N(C*H$_3$*)$_2$), 2.42 (2H, t, NHCH$_2$CH$_2$C*H$_2$*N(CH$_3$)$_2$), 3.52 (2H, m, NHC*H$_2$*CH$_2$CH$_2$N(CH$_3$)$_2$), 7.15 (2H, dd, *J* 8.2, 1.7 Hz), 7.72 (2H, dd, *J* 8.2, 1.7 Hz), 8.73 (1H, br s, N*H*); δ_C (CDCl$_3$) 166.07 (CO), 136.27, 132.24, 127.66, 126.84, 124.16, 120.52, 59.95 (Me), 45.82 (*C*H$_2$-NHCO), 41.42 (*C*H$_2$-NMe$_2$), 25.38 (-*C*H$_2$CH$_2$CH$_2$-); *m/z* (ES$^+$) 315.5 (M+1), 287.4 (M+1-N$_2$); *m/z* (FAB$^+$) exact mass 315.1432 (M+1) C$_{14}$H$_{17}$F$_3$N$_4$O requires 314.1354.

4.2.20 *3-Benzoyl-N-[3-(dimethylamino)propyl]benzamide (18)*

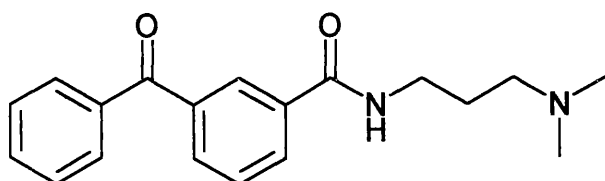To a solution of 3-benzoylbenzoic acid **42** (0.5 g, 2.21 mM) in dry acetonitrile was added *N,N*-dimethylpropane-1,3-diamine (0.28 mL, 2.21 mM), DIPEA (1.89 g, 6.63 mmol) and HATU (0.84 g, 2.21 mM). The reaction mixture was heated at 50°C under nitrogen and stirred very gently for 1 day. The resin was removed by filtration and washed with acetonitrile, the filtrate concentrated *in vacuo*. Subsequent column chromatography on silica eluting with (CHCl₃/MeOH/NH₃; 8.4:1.5:0.1). The product was isolated as a white solid (0.25 g, 42%). M.p: 164-165°C; δH (CDCl₃) 1.73 (2H, quintet, *J* 6 Hz, NHCH₂C*H₂*CH₂N(CH₃)₂), 2.23 (6H, s, CONHCH₂CH₂CH₂N(C*H₃*)₂), 2.49 (2H, t, CONHCH₂CH₂CH₂N(CH₃)₂), 3.58 (2H, m, CONHC*H₂*CH₂CH₂N(CH₃)₂), 7.47-7.65 (4H, m, aromatic), 7.81 (2H, dd, aromatic), 7.90 (1H, m, aromatic), 8.15 (2H, m, aromatic), 9.06 (1H, br s, N*H*); δC (CDCl₃) 196.07 (Ph*C*OPh), 166.27 (*C*ONH), 138.09, 137.69, 135.27, 132.97, 131.74, 130.40, 129.07, 128.89, 128.27, 59.70 (Me), 45.43 (*C*H₂-NHCO), 41.19 (*C*H₂-NMe₂), 25.01 (-*C*H₂CH₂CH₂-); *m/z* (EI) 310, 209, 105, 57.

4.2.21 *4-(4-Bromobenzoyl)benzoic acid (44)*
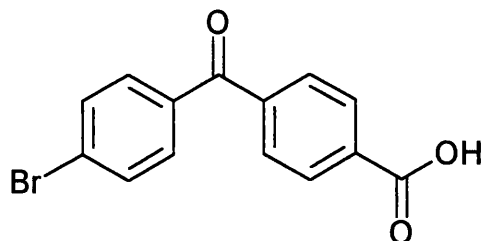
To a solution of ethyl 4-(4-bromobenzoyl)benzoate **43** (0.35 g, 1.05 mM) in THF (3.5 mL) was added 10% NaOH (14.175mL, 35.47 mM). The reaction mixture was stirred under N$_2$ at 50°C overnight. The residue was allowed to cool and dissolved in EtOAc and 4% NaHCO$_3$. The aqueous layer was separated and acidified with conc. HCl to pH 1. Extraction with ether followed by evaporation of the solvent gave **43** as a white product 0.2g, 60%). M.p: higher than 250°C (lit.[131] 273°C). (Found: C, 55.03; H, 2.82; C$_{14}$H$_9$BrO$_3$ Requires: C, 55.11; H, 2.97); δ$_H$ (acetone-d$_6$) 7.64 (4H, m, aromatic H), 7.75 (2H, dd, aromatic H), 8.06 (2H, dd, aromatic H); m/z (EI) 307(M$^+$+2, 8%), 306 (46.5), 305 (M$^+$, 8), 304 (47.5), 186 (8), 185, (95), 184 (8), 183 (100), 149 (97), 121 (16).

4.2.22 *4-(4-Bromobenzoyl)-N-[3-(dimethylamino)propyl]benzamide (45)*
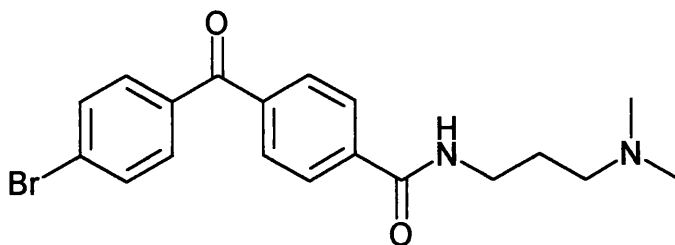
4-(4-bromobenzoyl)benzoic acid **44** (0.1 g, 0.3 mM) was dissolved in $SOCl_2$ (a drop of DMF is added to force the reaction). The reaction mixture was heated at 80°C for 3h. The mixture is allowed to cool and the solvent evaporated. Toluene was added and evaporated. The residue was dissolved in THF and *N,N*-dimethylpropane-1,3-diamine (0.103 mL, 0.82 mM) was added to the solution at 0°C and stirred under N_2 for 20h. The solvent was evaporated and the residue partionated between Et_2O and H_2O, the organic layer was collected, dried and solvent evaporated. The product was purified by HPLC using a gradient elution of 40-80% acetonitrile in 0.1% TFA aqueous solution over 20 min at a flow rate of 20 mL/min. Product **45** was isolated as a white solid (0.045g, 35%). M.p: 115-122°C. Found: C, 46.17; H, 3.69; N, 4.81; $C_{19}H_{22}BrN_2O_2.1.7C_2F_3O_2$ Requires: C, 46.15; H, 3.70; N, 4.81). δ_H (CDCl$_3$) 1.85 (2H, quintet, *J* 6 Hz, NHCH$_2$C*H$_2$*CH$_2$N(CH$_3$)$_2$), 2.40 (6H, s, NHCH$_2$CH$_2$CH$_2$N(C*H$_3$*)$_2$), 2.66 (2H, t, NHCH$_2$CH$_2$C*H$_2$*N(CH$_3$)$_2$), 3.54 (2H, q, NHC*H$_2$*CH$_2$CH$_2$N(CH$_3$)$_2$), 7.58 (4H, m), 7.72 (2H, dd), 7.88 (2H, dd), 8.55 (1H, br s, N*H*); δ_C (CDCl$_3$) 195.35 (Ph*C*OPh), 166.27 (*C*ONH), 139.78, 138.43, 136.29, 132.16, 131.90, 130.30, 128.33, 127.52, 59.70 (Me), 45.43 (*C*H$_2$-NHCO), 41.19 (*C*H$_2$-NMe$_2$), 25.02 (-CH$_2$*C*H$_2$CH$_2$-); *m/z* (APCI) (I%) 391(M$^+$+2, 100), 389 (M$^+$, 85), 346 (70), 344 (67). Analytical HPLC shows an unique peak with the retention time of 8.2 min using a gradient elution of 3-97% acetonitrile in 0.1% TFA aqueous solution over 20 min at a flow rate of 1 mL/min.

4.2.23 ELISA assay

Test compounds (10 mM) were dissolved in DMSO and diluted with tris buffer (40 mM trizma hydrochlorate, 5 mM magnesium chloride 6-hydrate, pH 7.4, 1 M NaOH). Into each well 10 μL of the test compound at 20 × the final concentration was added with 100 μL of reaction buffer (120 μg/mL recombinant soluble guanylate cyclase, 1.1 mg/mL IBMX (Sigma), 2.6 mg/mL GTP (Sigma) in tris buffer). The reaction was started with the addition of 90 μL of 667 nM DEA/NO (RBI) to give a reaction DEA/NO concentration of 300 nM. The plates were then incubated at room temperature for 10 min. To determine the amount of cGMP produced the Biotrak™ cGMP enzyme immunoassay (EIA) system from Amersham was used according to manufacturer's instructions. Briefly the assay was based upon the competition between unlabelled cGMP and a fixed quantity of peroxidase labelled cGMP for a limited amount of cGMP specific antibody. The peroxidase ligand that was bound to the antibody was immobilised on precoated microtitre wells and the amount of labelled cGMP was determined using a one pot stabilised substrate. The concentration of unlabelled cGMP in a sample was subsequently determined by interpolation from a standard curve. The standard curve was prepared in duplicate and each test compound was evaluated in duplicate with at least n=2. The measured cGMP for each compound was expressed as a percentage of the DEA/NO response. Data analysis was performed with Origin software (Microcal Software)

4.2.24 Radioimmunoassay

Purified soluble guanylyl cyclase was obtained commercially (Alexis) and diluted 1 in 500 in buffer containing (mM): 10 Tris-HCl, 1 dithiothreitol and 0.5 % bovine serum albumin, at pH 7.4, and stored on ice. 50 μl of the sGC stock solution was added to 150 μl of reaction buffer at 37 °C, which contained (mM): 50 Tris-HCl, 3 MgCl$_2$, 0.1 EGTA and 0.5 % BSA, at pH 7.4. The final concentration of sGC in the reaction mix was 0.125 μg/ml. Compounds **45** and **37** were dissolved in DMSO, and diluted 1 in 100 to give a final concentration in the reaction mix of 100 μM (1% DMSO). NO was applied from the donor

DEA/NO, which was dissolved in 10 mM NaOH, and diluted 1 in 100, to give a final concentration of 100 μM (a maximal dose for activation of sGC). Aliquots of the reaction mix were quenched after 10 min incubation with compounds and/or DEA/NO in boiling inactivation buffer (10 mM Tris-HCl, 4 mM EDTA). The inactivated samples were assayed for cGMP content by a standard commercially available radioimmunoassay (Amersham).

4.2.25 Photoaffinity experiments

The reaction mixture (35 μL) comprised purified sGC (Alexis) (1.5 μg, with a final concentration of 0.3μM), photolabile ligand **17** (with a final concentration of 0.3μM), and reaction buffer (27.95μL, containing 50mM Trizma Hydrochloride pH 7.4 (with 1M NaOH), 1mM Magnesium chloride 6-hydrate. When the presence of the substrate was required, GTP (3mM) was also included in the reaction buffer. Incubation was carried out for 10 min at 37°C in the dark. After chilling, the reaction mixture was irradiated at 360 nm at a distance of 12 cm for 5 minutes in an ice bath. When parallel experiments were carried out in the presence of unlabelled parent ligand **15**, this was included in the incubation mixture with a final concentration of 300μM.

4.2.26 Sodium dodecyl sulphate polyacrylamide gel electrophoresis (SDS-PAGE)

All SDS-PAGE procedures were done using a mini gel system (Bio-Rad Laboratories, Hemel Hempstead, UK).

Production of the polyacrylamide gels.

The components of stacking and resolving gels used for SDS-PAGE analysis are listed in Table 17. The Acrylamide:Bisacrylamide solution was obtained from Bio-Rad Laboratories, Hemel Hempsted, UK.

Table 17. Components of stacking and resolving gels

Gel components	10% Resolving	Stacking gel
30% solution of 29:1 Acrylamide:Bisacrylamide	6.6mL	1.3mL
0.5M TrisHCl, pH6.8	-	2.5mL
1.5M TrisHCl, pH8.8	5.0mL	-
10% SDS (w/v)	0.2mL	0.1mL
Distilled H_2O	8.2mL	6.1mL
Final volume	20.0mL	10.0mL

Gel mixtures were left open to the air for approximately 20 minutes to de-gas before polymerisation of the resolving gel mixture was initiated by addition of 150μL 20% (w/v) Ammonium Persulphate in distilled water (anhydrous powder-Sigma, Poole, UK) and 20μL N, N, N', N'- Tetramethylethylenediamine (TEMED; Sigma, Poole, UK). After gentle mixing by inversion the mixture was poured into the gel apparatus (Mini-gel system, Bio-Rad Laboratories, Hemel Hempstead, UK) and overlaid with a small amount of distilled water to prevent exposure of the upper portion of the polymerising gel to the air. The gel is poured between two glass plates separated by plastic spacers. Once the gel had polymerised, the water was removed and the polymerisation of the stacking gel was initiated with 75μL 20%Ammonium Persulphate and 13μL TEMED. After gentle mixing, the polymerising mixture was overlaid on the resolving gel and used to fill to the top of the plates. A10 or 15-well plastic comb was then inserted into the plates to create wells where the samples could be loaded. The gel was left to stand for at least 30 minutes before use. If not required the gel apparatus was wrapped in Saran-wrap and stored at 4°C until use. All gels were poured with a thickness of 1.5mm.

Preparation of samples for SDS-PAGE.

Samples to be run on polyacrylamide gels were denatured by addition of an equal volume of 2x Laemmli gel loading buffer (4% (w/v) SDS, 0.02% (w/v) bromophenol blue, 20% (v/v) glycerol, 100mM TrisHCl pH 6.8 all electrophoresis reagents from Sigma, Poole, UK) containing 200 mM

Dithiothreitol (Sigma, Poole, UK) and boiled at 100°C for 3 minutes. If the sample was too viscous to be easily loaded onto the gel it was sonicated for 5 seconds using a Soniprep 150 probe sonicator (MSE) at half power (corresponding to an amplitude of 18 microns on the sonicator).

Loading and running polyacrylamide gels

Before loading, the combs in the gel were removed and the wells washed thoroughly with distilled water. The whole gel apparatus was then immersed into a tank containing fresh running buffer (25mM Tris, 250mM glycine, 0.1% SDS, pH8.3) and samples were loaded into the appropriate wells. 5µL of pre-stained broad range molecular weight markers (Bio-Rad Laboratories, Hemel Hempstead, UK) were loaded into at least one lane of the gel as an aid to estimation of the molecular weights of the protein of interest as well as a visible marker of the efficiency of transfer to nitrocellulose. A maximum of 50 µL of sample was typically loaded into the corresponding well. The rest of the electrophoresis cell was assembled and voltage was applied using a power pack (Powerpac 300; Bio-Rad Laboratories, Hemel Hempstead, UK). The samples were run through the stacking gel at a constant voltage of 40 V and through the resolving gel at 100V. The applied voltage was removed once the dye front had reached the bottom of the glass plates. Gels were stained with coomassie blue for 3h and distained with a solution containing 5% acetic acid/ 40%methanol/ 50%H_2O with stirring.

4.2.27 *In gel tryptic digestion.*

Protein spots corresponding to the α and β subunit of sGC were excised from the gel allowed to de-stain in 50 mM NH_4HCO_3, 40% (v/v) ethanol. The gel pieces were then soaked in 25 mM NH_4HCO_3 twice for 15 minutes, in order to equilibrate the pH to 7-8 (optimal for trypsin activity). In order to dehydrate the gel piece, it was suspended in 100% acetonitrile, three times for 10 minutes each, or until the gel piece turned white. Lyophilisation was done in a Savant Speed Vac Plus centrifuge. At this point when cysteine modification[132] was carried out, a volume of 10 mM dithiotreitol (DTT) in 100 mM NH_4HCO_3

sufficient to cover the gel pieces was added and the protein was reduced for 1h at 56°C. After cooling to room temperature, the DTT solution was replaced with the same volume of 55 mM iodoacetamide in 100 mM NH₄HCO₃. After 45 minutes incubation at ambient temperature in the dark with occasional vortexing, the gel pieces were washed with 50-100 µL of 100 mM NH₄HCO₃ for 10 minutes, dehydrated with net acetonitrile, swelled by rehydration in 100 mM NH₄HCO₃ and shrunk again by addition of the same volume of acetonitrile. The liquid phase was removed, and the gel pieces dried in a Savant Speed Vac Plus centrifuge. Subsequently, the gel pieces were resuspended in 25 mM NH₄HCO₃, 80 ng/µL Trypsin (Promega) and incubated overnight at 37°C.

4.2.28 MALDI-MS

A sample from the digestion (0.5 µL) was spotted on the MALDI target and allowed to air dry. Subsequently 0.5 µL of matrix solution, (1% (w/v) α-cyano-4-hydroxysuccinamic acid in 50% acetonitrile, 0.1% (v/v) trifluoroacetic acid (TFA)), was applied to the dried sample and again allowed to air dry. Spectra were obtained using a Bruker Biflex III Reflectron MALDI time-of- flight mass spectrometer. The apparatus was calibrated using a mixture of six known peptides (angiotensin I, m/z 1046.54, angiotensin II, m/z 1296.68, [Glu1]-fibrinopeptide, m/z 1570.67; resin substrate angiotensinogen, m/z 1758.93, Adrenocorticotropic hormone, fragment 18-30 m/z 2465.7; insulin chain B, m/z 3494.65) (Sigma) dissolved in 50% acetonitrile, (0.1%(v/v) TFA. When possible the spectra were recalibrated using characteristic trypsin peaks at m/z 842.51, m/z 1045.5642 and m/z 2211.1046 as internal markers.

For interpretation of MALDI spectra, a list of mass-to-charge ratio was acquired for each sample and protein fragments were identified using two different browsers (Mascot, Matrix Science; MS-Fit, University of California-San Francisco). Mass tolerance was limited to relative value of ± 200 ppm (parts per million). Analysis of results were done as indicated in section 2.7.3 (chapter 2)

4.3 Experimental Section for Chapter 3

4.3.1 *General procedure for synthesis of N-sustituted 1,2 benzisothiazoles*

To the 2,2'-dithiobis(benzoic acid) derivative **67** (1eq) in a 2-necked-flask fitted with a stirrer and a reflux condenser was added $SOCl_2$ and a drop of DMF. The reaction mixture was heated at 80°C for 3h. The mixture was cooled slightly and the solvent was evaporated off under vacuum. Toluene was added to the mixture and reevaporated. The residue was suspended in toluene and SO_2Cl_2 (3.1 mol) added and the mixture heated under reflux for 2h. The solvent was evaporated off; the residue was suspended in THF and the required amine (3.5eq) was added at 0°C and the mixture stirred overnight. The solution was evaporated and the residue was dissolved in H_2O and extracted with Et_2O. The organic layer was dried and the solvent removed. The crude mixture was purified by flash chromatography (30% EtOAc in cyclohexane)

4.3.2 *2-(4-methoxybenzyl)-1,2-benzisothiazol-3(2H)-one (69)*
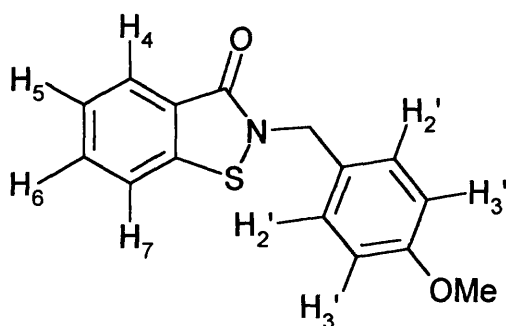
Isolated as a white product (0.3 g, 75%). M.p: 75°C (from ether). (Found: C, 66.75; H, 4.90; N, 5.37;$C_{15}H_{13}NO_2S$ Requires: C, 66.40; H, 4.83; N, 5.16%); δ_H (CDCl$_3$) 3.83 (3H, s, OCH_3), 5.02 (2H, s, CH_2Ph), 6.92 (1H, d, ^3J 8.4 Hz, $H_{3'}$), 7.33 (1H, d, ^3J 8.4 Hz, $H_{2'}$), 7.42 (1H, m, $^3J_{5-4}$ 8.2, $^3J_{5-6}$ 8.2, $^4J_{5-7}$ 1.2 Hz, H_5), 7.50 (1H, dd, $^3J_{7-6}$ 8.2, $^4J_{7-5}$ 1.2 Hz H_7) 7.61 (1H, m, $^3J_{6-7}$ 8.2, $^3J_{6-5}$ 8.2, $^4J_{6-4}$ 1.2 Hz, H_6), 8.10 (1H, dd, $^3J_{4-5}$ 8.2, $^4J_{4-6}$ 1.2 Hz, H$_4$); δ_C (CDCl$_3$) 165.63 (*C*O), 160.09 (*C*OMe), 140.83, 132.11, 130.39, 128.69, 127.15, 125.82, 125.14,

120.76, 114.62, 55.67 (OMe), 47.54 (CH$_2$Ph); m/z (FAB$^+$) 272(M+1, 46%), 164(M-C$_7$H$_7$O, 12), 121(M-C$_7$H$_4$NOS, 100);

4.3.3 *2-(2,4-dimethoxybenzyl)-1,2-benzisothiazol-3(2H)-one (70)*
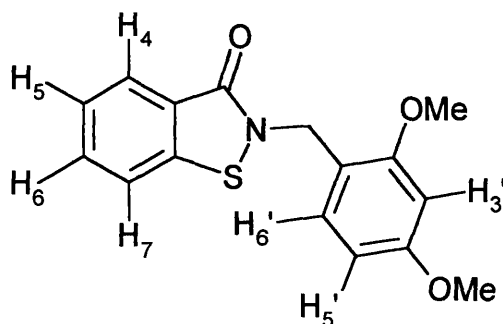
Isolated as a white solid (0.34 g, 69%). M.p: 103°C. (Found: C, 63.67; H, 4.9; N, 4.37; C$_{16}$H$_{15}$NO$_3$S Requires: C, 63.77; H, 5.02; N, 4.65%); δ_H (CDCl$_3$) 4.03 (3H, s, OCH_3), 4.09 (3H, s, OCH_3), 5.02 (2H, s, CH_2Ph), 6.69 (2H, m, $^4J_{3'-5'}$ 2.3 Hz, H_3), 7.51 (1H, m, $^3J_{5'-6'}$ 8.1, $^4J_{5'-3'}$ 2.3 Hz, H_5), 7.57 (1H, d, $^3J_{6'-5'}$ 8.1 Hz, H_6), 7.71 (1H, m, $^3J_{5-4}$ 8.2, $^3J_{5-6}$ 8.2, $^4J_{5-7}$ 1.2 Hz, H_5), 7.79 (1H, m, $^3J_{7-6}$ 8.2, $^4J_{7-5}$ 1.2 Hz H_7), 8.26 (1H, m, $^3J_{6-7}$ 8.2, $^3J_{6-5}$ 8.2, $^4J_{6-4}$ 1.2 Hz, H_6); δ_C (CDCl$_3$) 165.65 (CO), 161.70 (COMe), 159.11 (COMe), 141.19, 131.99, 131.87, 126.95, 125.54, 125.27, 120.58, 117.46, 104.83, 98.98, 55.83 (OMe), 55.76 (OMe), 42.57 (CH$_2$Ph); m/z (APCI) 301(M$^+$), 150.9, 120.9(M$^+$-C$_9$H$_{11}$O$_2$, 100).

4.3.4 *1,2-benzisothiazol-3(2H)-one (57)*
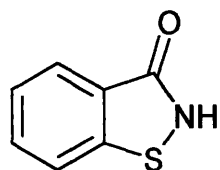
Compound **69** (0.2 g, 0.73 mM), was dissolved in trifluoracetic acid (10 mL). To the solution was added anisole (0.48 mL, 4.43 mM). The reaction mixture was heated at 50°C for 2 days. The acid was evaporated and the residue was partitionated between Et$_2$O and 4% NaHCO$_3$. The aquous layer was acidified with conc. HCl and extracted with EtOAc. The organic fractions were dried,

and the solvent was removed. The crude mixture was subjected to flash chromatography (30% ethyl acetate in cyclohexane). (90 mg, 81%). M.p: 159°C (lit.[102] 158°C); δ_H (CDCl$_3$) 7.34 (1H, m), 7.57 (2H, m), 8.02 (1H, d, J 8.2 Hz); δ_C (CDCl$_3$) 169.21 (CO), 145.20, 132.09, 126.39, 125.66, 125.00, 121.17; m/z (EI) 151(M$^+$, 100 %), 96(36).

4.3.5 *2-amino-4-(methoxycarbonyl)benzoic acid (72)*
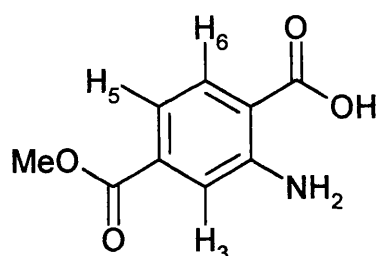
2-Aminoterephthalic acid **71** (2 g, 11.04 mM), dry methanol (36 mL) and conc. H$_2$SO$_4$ (2 mL) were heated at 60 °C for 4 hours; after cooling the reaction mixture was concentrated in vacuum and the residue was diluted with ice-water. The precipitate was filtered and partitioned between chloroform and 5% NaHCO$_3$, the aqueous phase was separated, acidified with 37% HCl and the precipitate was collected by filtration and washed with water until neutral pH to give 2-amino-terephtalic acid 4-methyl ester as a yellow solid (1g, 50%). M.p: 233°C. (Found: C, 55.16; H, 4.50; N, 7.07; C$_9$H$_9$NO$_4$ Requires: C, 55.39; H, 4.65; N, 7.18%). δ_H (DMSO-d_6) 3.32 (2H, br s, NH_2), 3.84 (3H, s, OCH_3), 7.03 (1H, dd, $^3J_{5-6}$ 8.2, $^4J_{5-3}$ 1.6 Hz, H_5), 7.41 (1H, d, $^4J_{3-5}$ 1.6 Hz, H_3), 7.74 (1H, dd, $^3J_{6-5}$ 8.2 Hz, H_6); δ_C (DMSO-d_6) 169.27 (*C*OOH), 166.36 (*C*OOMe), 151.54 (*C*$_2$), 134.25 (*C*$_6$), 131.98 (*C*$_4$), 117.72 (*C*$_5$), 114.66 (*C*$_3$), 113.24 (*C*$_1$), 52.56 (OMe); m/z (EI) 195(M$^+$, 64.34%), 177(M$^+$-H$_2$O, 100), 119(M$^+$-COOMe, 35.01).

4.3.6 *Dimethyl 2-(benzylthio)terephthalate (76)*
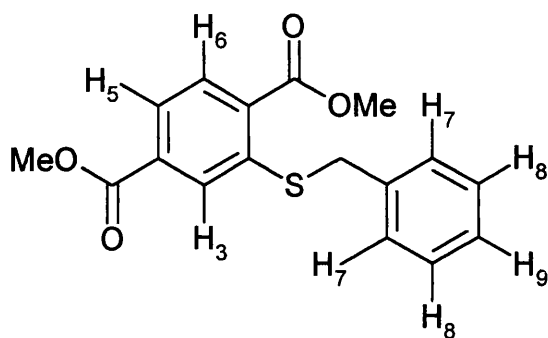
A solution of dimethyl 2-nitroterephthalate **75** (5 g, 21 mM) in dry dimethylformamide was added to a stirred solution of benzyl mercaptan (2.87 mL, 24.5 mM) and sodium hydride (0.56 g, 23.4mM) in DMF maintaining the temperature at -30°C, after 1h at -30°C the solution was allowed to warm to room temperature and after a further 2h. it was poured into water. The organic layer was extracted with ethyl acetate, the solvent dried and removed and the residue was subjected to flash chromatography (5-20% EtOAc/cyclohexane). The product was obtained as a white solid (4.7 g, 71%). M.p: 95-96 °C (from isopropanol). (Found: C, 64.41; H, 5.01; S, 10.11; $C_{17}H_{16}O_4S$ Requires: C, 64.54; H, 5.10; S, 10.13%). δ_H (CDCl$_3$) 3.95 (3H, s, COOCH_3), 3.96 (3H, s, COOCH_3), 4.25 (2H, s, SCH_2Ph), 7.31(1H, m, H_9), 7.35 (2H, m, H_8), 7.47 (2H, m, H_7), 7.81 (1H, dd, $^3J_{5-6}$ 8.2, $^4J_{5-3}$ 1.6 Hz, H_5), 8.03 (1H, dd, $^3J_{6-5}$ 8.2, $^5J_{6-3}$ 0.4 Hz, H_6), 8.09 (1H, dd, $^4J_{3-5}$ 1.6, $^5J_{3-6}$ 0.4 Hz, H_3); δ_C (CDCl$_3$) 166.68 (*C*OOMe), 166.40 (*C*OOMe), 142.67 (C$_2$), 136.18 (C$_4$), 133.62 (C$_1$), 131.62 (C$_6$), 131.53, 129.61, 129.01, 127.87, 127.53, 125.27 (C$_3$), 52.86 (OMe), 52.74 (OMe), 37.89 (SCH$_2$Ph); m/z (EI) 316(M$^+$, 74.9%), 284(M$^+$-S, 47.03), 225(M$^+$-CH$_2$Ph, 67.38), 91(M$^+$-C$_{10}$H$_9$O$_4$S, 100); IR (KBr) ν_{max} 1733.23, 1716.79 cm^{-1}.

4.3.7 *3-mercapto-4-(methoxycarbonyl)benzoic acid (78)*
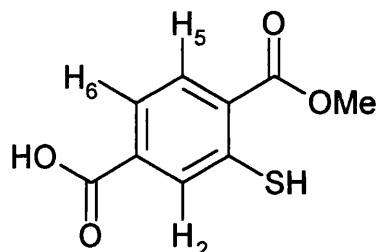
A solution of AlBr$_3$ (2.28 g, 8.6 mM) in dry toluene (45 mL) was placed in a three-necked flask equipped with a drying tube (CaCl$_2$). Addition of dimethyl 2-(benzylthio)terephthalate **76** (1.23 g, 3.9 mM) immediately led to an orange solution. The mixture was heated at 60°C for 12 hours with stirring. Water (3 mL) then was added to the cooled mixture over 30min with stirring. Then more water (5 mL) was added, and the mixture was stirred for 20 min. Et$_2$O was added to dissolve solid, and the solution was extracted with 5% aqueous KOH. The basic extract was acidified with 10% HCl to pH 1 to precipitate a yellow solid, which was subjected to flash chromatography (50% EtOAc in cyclohexane) giving compound **78** as white solid, which became yellow upon exposure to the air (0.36 g, 45%). M.p: 200°C (from MeOH). (Found: C, 49.73; H, 3.65; C$_9$H$_8$O$_4$S Requires: C, 50.90; H, 3.80%); δ_H (DMSO-d_6) 3.89 (3H, s, COOCH_3), 5.71 (1H, s, SH), 7.70 (1H, dd, $^3J_{6-5}$ 8.2, $^4J_{6-2}$ 1.5 Hz, H_6), 7.98 (1H, d, $^3J_{5-6}$ 8.2 Hz, H_5), 8.23 (1H, d, $^4J_{2-6}$ 1.5 Hz, H_2), 13.38 (1H, br s, COOH); δ_C (DMSO-d_6) 166.18 (COOH), 165.57 (COOMe), 138.66 (C$_3$), 134.16 (C$_1$), 131.61 (C$_2$), 131.32 (C$_5$), 128.98 (C$_4$), 125.10 (C$_6$), 52.44 (OMe); m/z (EI) 212(M$^+$, 38.13%), 180(M$^+$-S, 100), 149(M$^+$-OMe, 19.12), 135(M$^+$-CO2, 44.49); IR (KBr) v_{max} 3447.11 (OH), 2542.46 (SH), 1701.43 (CO), 1690 (CO) cm^{-1}.

4.3.8

3-{[5-carboxy-2-(methoxycarbonyl)phenyl]dithio}-4(methoxycarbonyl)benzoic

acid (80)
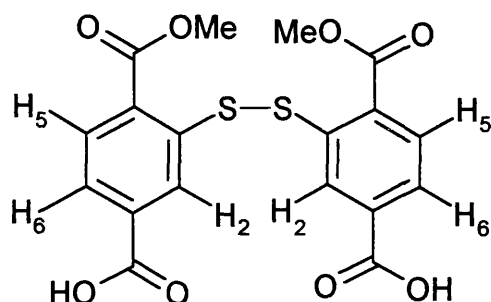
To a solution of 2-mercapto-terephthalic acid 4-methyl ester (0.1 g, 0.47mM) in pyridine (6 mL) was added iodine (0.12 g, 0.47 mM) dissolved in pyridine (2 mL) at room temperature. The reaction mixture was heated at 50°C for 4h. After cooling, the pyridine was removed and the residue was dissolved in HCl (0.5 N) and partitioned between EtOAc and H_2O. The aqueous layer was separated and the precipitate collected (0.1g, 53%). M.p: higher than 250°C; δ_H (DMSO-d_6) 3.95 (6H, s, COOCH_3), 7.88 (2H, dd, $^3J_{6-5}$ 8.2, $^4J_{6-2}$ 1.5 Hz, H_6), 8.13 (2H, dd, $^3J_{5-6}$ 8.2 Hz, H_5), 8.23 (2H, d, $^4J_{2-6}$ 1.6 Hz, H_2), 13.45 (2H, br s, COOH); δ_C (DMSO-d_6) 165.82 (COOH), 165.61 (COOMe), 139.22, 135.04, 131.89, 130.54, 127.17, 126.10, 52.99 (OMe); m/z (EI) 422(M$^+$); IR (KBr) v$_{max}$ 3411.02, 1718.22, 1693.79 cm^{-1}.

4.3.9 *Methyl 4-{[(2,4-dimethoxybenzyl)amino]carbonyl}-3-mercapto-2-methylbenzoate (79)*
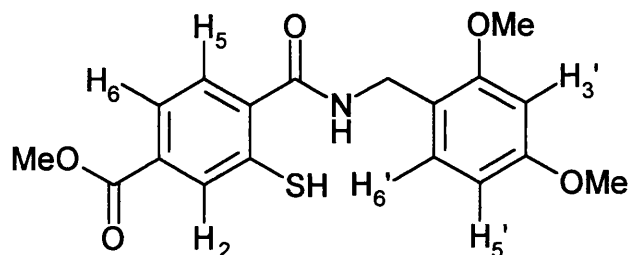
Procedure as indicated in section **4.3.1**, using as starting material compound **80**. Product **79** was isolated as a white solid (0.78 g, 68%). M.p: 138-140°C. (Found: C, 60.07; H, 5.23; N, 3.83; $C_{18}H_{17}NO_5S$ Requires: C, 59.82; H, 5.30; N, 3.88%); δ_H (CDCl$_3$) 3.71-3.80 (6H, 2s, OCH_3), 3.85 (3H, s, COOCH_3), 4.35 (2H, d, ^3J 5.7Hz, CH_2Ph), 6.32 (1H, d, $^4J_{3'-5'}$ 2.4 Hz, $H_{3'}$), 6.35 (1H, d, $^3J_{5'-6'}$ 8, $^4J_{5'-3'}$ 2.4 Hz, $H_{5'}$), 6.45 (1H, br t, ^3J 5.7 Hz, NH), 7.23 (1H, d, $^3J_{6'-5'}$ 8 Hz, $H_{6'}$), 7.45 (1H, dd, $^3J_{6-5}$ 8.1, $^4J_{6-2}$1.5 Hz, H_6), 7.93 (1H, d, $^3J_{5-6}$ 8.1 Hz, H_5), 8.12 (1H, d, $^4J_{2-6}$ 1.5, H_2); *m/z* (FAB$^+$) 360(M$^+$), 301(M$^+$-COOMe), 151(M$^+$-$C_9H_{11}O_2$, 100).

4.3.10 *4-ethyl 1-methyl 2-nitroterephthalate (82)*
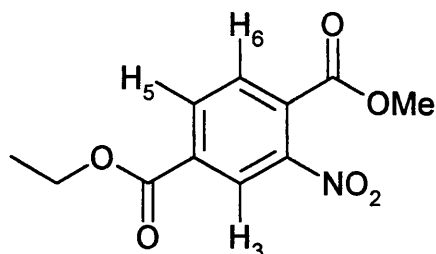
1-Methyl-2-nitroterephthalate (0.5 g, 2.3 mM) was dissolved in dry EtOH (15 mL). To the solution was added conc. H_2SO_4 (500 μL) and stirred under nitrogen overnight at 75°C. The reaction mixture was allowed to cool and the

solvent was removed. Ice-H$_2$O was added and the residue basified drop-wise with 4% NaHCO$_3$ in an ice bath. The product was extracted with EtOAc. The organic layer was dried and the solvent removed to give the product as a white solid. (0.5 g, 93%). 0.2 g was subjected to flash chromatography for analytical purposes using 0-5% EtOAc in cyclohexane as an eluent system obtaining 0.144 g of pure product. M.p: 53°C (from isopropanol) (Found: C, 52.22; H, 4.13; N, 5.37; C$_{11}$H$_{11}$NO$_6$ Requires: C, 52.18; H, 4.38; N, 5.53%). δ$_H$ (CDCl$_3$) 1.30 (3H, t, OCH$_2$C_H_3), 3.88 (3H, s, OCH$_3$), 4.36 (2H, q, OC_H_2CH$_3$), 7.73 (1H, d, $^3J_{6-5}$ 8.2 Hz, H$_6$), 8.25 (1H, dd, $^3J_{5-6}$ 8.2, $^4J_{5-3}$ 1.6 Hz, H$_5$), 8.48 (1H, d, $^4J_{3-5}$ 1.6 Hz, H$_3$); δ$_C$ (CDCl$_3$) 165.59 (_C_OOMe), 164.02 (_C_OOEt), 148.49 (C$_2$), 134.41 (C$_1$), 134.01 (C$_3$), 131.43 (C$_4$), 130.41 (C$_5$), 125.33 (C$_6$), 62.66 (COO_C_H$_2$CH$_3$), 53.86 (COO_C_H$_3$), 14.58 (COOCH$_2$_C_H$_3$); (FAB$^+$) 254(M$^+$+1, 68%), 222(M$^+$-OMe, 100), 208(M$^+$-NO$_2$, 38); IR (KBr) ν$_{max}$ 1737.54, 1712.04 cm^{-1}.

4.3.11 *4-Ethyl 1-methyl 2-[(4-methoxybenzyl)thio]terephthalate (83)*
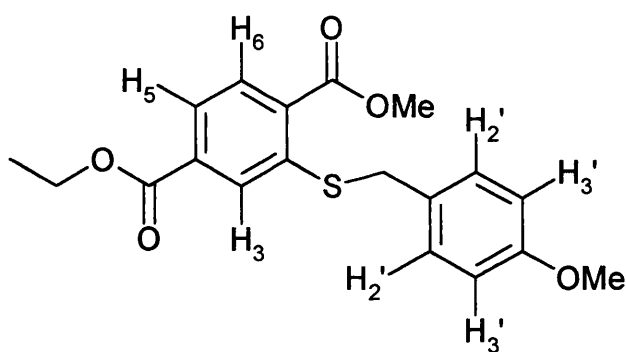
A solution of 2-Nitro-terephthalic acid 4-ethyl ester 1-methyl ester (1.9 g, 7.5 mM) in dry dimethylformamide was added to a stirred solution of 4-methoxybenzyl mercaptan (1.2 mL, 8.7 mM) and sodium hydride (0.2 g, 8.4 mM) in DMF maintaining the temperature at -30°C, after 1h at the temperature -30°C, the solution was allowed to warm to room temperature and after a further 6h. it was poured into water. The organic layer was extracted with ethyl acetate, the solvent dried and removed and the residue was subjected of flash chromatography (5-20% EtOAc/cyclohexane). The product was obtained as white solid (2.2 g, 82%). M.p: 94°C (from isopropanol). (Found: C, 63.09; H,

5.47; S, 8.73; $C_{19}H_{20}O_5S$ Requires: C, 63.32; H, 5.59; S, 8.90%). δ_H (CDCl3)
1.38 (3H, t, OCH2C$\underline{H}$3), 3.77 (3H, s, OCH_3), 3.89 (3H, s, COOCH_3), 4.16 (2H,
s, SCH_2Ph), 4.37 (2H, q, OC$\underline{H}_2$CH$_3$), 6.82 (2H, d,$^3J_{3'-2'}$ 8.2 Hz, $H_{3'}$), 7.36 (2H,
d, $^3J_{2'-3'}$ 8.2 Hz, $H_{2'}$), 7.75 (1H, dd, $^3J_{5-6}$ 8.2, $^4J_{5-3}$ 1.6 Hz, H_5), 7.94 (1H, d, ^3J
$_{6-5}$ 8.2 Hz, H_6), 8.03 (1H, d, $^4J_{3-5}$ 1.6 Hz, H_3); δ_C (CDCl$_3$) 166.71 (COOMe),
165.92 (COOEt), 159.42 (COMe), 142.72 (C$_2$), 133.79 (C$_4$), 131.47 (C$_1$),
131.36 (C$_6$), 130.68 C$_{2'}$), 128.09 (C$_5$), 127.46 (C$_{1'}$), 125.15 (C$_3$), 114.47 (C$_{3'}$),
61.87 (COOCH$_2$CH$_3$), 55.65 (OMe), 52.69 (OMe), 37.22 (SCH$_2$Ph), 14.66
(COOCH$_2$CH$_3$); m/z (EI) 360(M$^+$, 12%), 121(M$^+$-C$_{11}$H$_{11}$O$_4$S, 100); IR (KBr)
ν_{max} 1717.56, 1654.32 cm^{-1}.

### 4.3.12 4-Ethyl 1-methyl 2-mercaptoterephthalate (84)
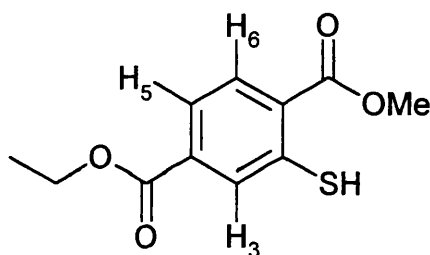
2-Benzylsulfanyl-terephthalic acid 4-ethyl ester 1-methyl ester (1 g, 2.8 mM)
was dissolved in trifluoroaetic acid (30 mL). Thioanisole (2 mL) was added to
the solution, the reaction mixture was stirred under nitrogen at room
temperature for a day. The acid was evaporated and the residue dissolved in
water and neutralized with aq. ammonium. The aqueous layer was extracted
with EtOAc. The organic layer was dried, the solvent removed and the crude
mixture was purified by column chromatography (0-5% EtOAc/ cyclohexne) to
give the product as a white solid (0.3 g, 50%). M.p: 83-85°C. (Found: C,
55.04; H, 5.04; C$_{11}$H$_{12}$O$_4$S Requires: C, 54.99; H, 5.03%). δ_H (CDCl$_3$) 1.33 (3H,
t, COOCH2CH_3), 3.87 (3H, s, COOCH_3), 4.33 (2H, q, COOCH_2CH$_3$), 4.70 (1H,
s, SH), 7.70 (1H, dd, $^3J_{5-6}$ 8.2, $^4J_{5-3}$ 1.6 Hz, H_5), 7.91 (1H, d, $^3J_{6-5}$ 8.2 Hz, H_6),
8.18 (1H, d, $^4J_{3-5}$ 1.6 Hz, H_3); δ_C (CDCl$_3$) 166.89 (COOMe), 165.60 (COOEt),
139.06, 134.12, 132.17, 132.03, 129.61, 125.68, 62.01 (COOCH$_2$CH$_3$), 52.90
(OMe), 14.65 (COOCH$_2$CH$_3$); m/z (EI) 240 (M$^+$, 82%), 195 (M$^+$-OEt, 12), 208
(M$^+$-S, 100), 180 (M$^+$ -COOEt, 32); IR (KBr) ν_{max} 2524.88, 1722.02 cm^{-1}.

4.3.13 *Methyl 2-nitro-4-{[(4-vinylphenyl)amino]carbonyl}benzoate (86)*
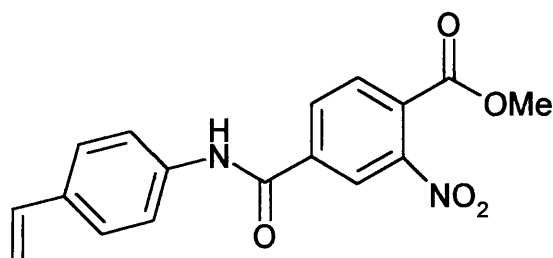
1-Methyl-2-nitroterephthalate **81** (0.4g, 1.78 mM), was dissolved in thionyl chloride. The reaction mixture was heated at 80°C under nitrogen for 3h. The solvent was evaporated and toluene was added and reevaporated. The residue was dissolved in THF and 4-vinylaniline (0.52 mL, 4.44 mM) was added at 0°C and stirred under nitrogen for 1 day. The solvent was evaporated and the residue partitioned between H_2O and CH_2Cl_2. The organic layer was dried, the solvent evaporated and the crude product was purified by column chromatography (5-25% EtOAc/cyclohexane) giving the product as a yellowish solid. (0.4 g, 69%). M.p: 158-162°C (from isopropanol). (Found: C, 62.39; H, 4.18; N, 8.43; $C_{17}H_{14}N_2O_5$ Requires: C, 62.58; H, 4.32; N, 8.58%). δ_H (CDCl$_3$) 4.15 (3H, s, COOCH_3), 5.43 (1H, dd, J 11, 0.6 Hz, H *cis-vinyl*), 5.89 (1H, dd, J 18, 0.6 Hz, H *trans-vinyl*), 6.89 (1H, dd, J 18, 11, Hz), 7.63 (2H, dd, J 8.6, 1.7 Hz), 7.80 (1H, dd, J 8.6, 1.7 Hz), 8.02 (1H, d, J 8.0 Hz), 8.20 (1H, br s, NH), 8.35 (1H, dd, J 8.0, 1.7 Hz), 8.57 (1H, d, J 1.7 Hz); m/z (FAB $^+$) 327(M +1, 100%), 208(M- C$_8$H$_7$NH$_2$, 30.43), 104(M- C$_9$H$_7$N$_2$O$_5$, 22.2); IR (KBr) v_{max} 3386.35, 1724.01, 1674.1 cm^{-1}.

4.3.14 *Methyl 2-(benzylthio)-4-{[(4-vinylphenyl)amino]carbonyl}benzoate (87)*
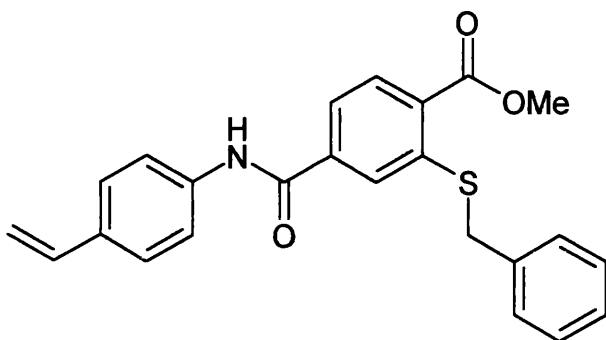
A solution of methyl 2-nitro-4-{[(4-vinylphenyl)amino]carbonyl}benzoate **86** (0.4 g, 1.22 mM) in dry dimethylformamide was added to a stirred solution of benzyl mercaptan (0.17 mL, 1.42 mM) and sodium hydride (0.032 g, 1.425 mM) in DMF maintaining the temperature at -30°C , after 1h at the temperature -30°C, the solution was allowed to rt and stirred under nitrogen for 24h. The solution was poured into water and the organic layer was extracted with ethyl acetate. The solvent was dried and removed, the residue was subjected of flash chromatography (5-20% ethyl acetate/cyclohexane). The product was obtained as white solid (0.095 g, 50%). M.p: 121-125°C (from isopropanol). δ_H (CDCl3) 3.87 (3H, s, COOC*H*₃), 4.17 (2H, s, SC*H*₂Ph), 5.15 (1H, dd, *J* 11, 0.6 Hz, *H* cis-vinyl), 5.64 (1H, dd, *J* 18, 0.6 Hz, *H* trans-vinyl), 6.65 (1H, dd, *J* 18, 11, Hz), 7.22-7.50 (11H, m), 7.70 (1H, d, *J* 1.5 Hz), 7.94 (1H, d, *J* 8.1 Hz); m/z (FAB⁺) 404(M+1, 100%);

4.3.15

Methyl2-[(4-methoxybenzyl)thio]-4-{[(4-vinylphenyl)amino]carbonyl}benzoate

(88)
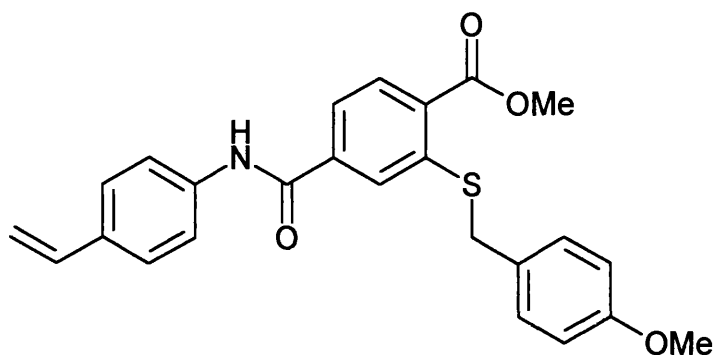
Procedure as for compound **87**, compound **88** was isolated as an orange solid (0.096 g, 45%). M.p: 118-120°C (from isopropanol); δ_H (CDCl$_3$) 3.81 (3H, s, COOCH_3), 3.97 (3H, s, OCH_3), 4.23 (2H, s, SCH_2Ph), 5.27 (1H, dd, J 11, 0.6 Hz, *H cis-vinyl*), 5.75 (1H, dd, J 18, 0.6 Hz, *H trans-vinyl*), 6.73 (1H, dd, J 18, 11, Hz), 6.90 (2H, d, J 8.6 Hz), 7.39 (2H, d, J 8.6 Hz), 7.45 (2H, d, J 8.6 Hz), 7.60 (3H, m), 7.82 (1H, d, J 1.5 Hz) 8.05 (1H, d, J 8 Hz); *m/z* (FAB$^+$) 434(M+1, 15%)

4.3.16 *Dimethyl 2-[(4-methoxybenzyl)thio]terephthalate (91)*
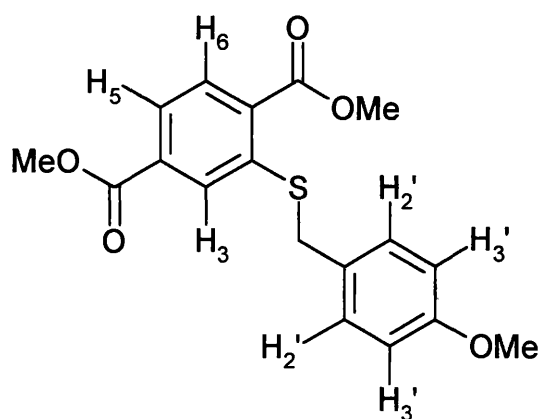
The product was obtained as white needles (3.8 g, 87.5%). M.p: 113-115°C (from cyclohexane/ethyl acetate). (Found: C, 62.27; H, 5.23; S, 9.16; $C_{18}H_{18}O_5S$ Requires: C, 62.41; H, 5.24; S, 9.26%). δ_H (CDCl3) 3.83 (3H, s, OCH_3), 3.96 (3H, s, COOCH_3), 3.98 (3H, s, COOCH_3), 4.22 (2H, s, SCH_2Ph), 6.89 (2H, d, ^3J $_{3'-2'}$ 8.2 Hz, $H_{3'}$), 7.40 (2H, d, ^3J $_{2'-3'}$ 8.2 Hz, $H_{2'}$), 7.81 (1H, dd, ^3J $_{5-6}$ 8.2, ^4J $_{5-3}$ 1.6 Hz, H_5), 8.10 (1H, dd, ^3J $_{6-5}$ 8.2, ^5J $_{6-3}$ 0.4 Hz, H_6), 8.28 (1H, d, ^4J $_{3-5}$ 1.6 Hz, H_3); δ_C (CDCl3) 166.70 (COOMe), 166.45 (COOMe), 159.45 (COMe), 142.84 (C_2), 133.58, 131.58, 131.52, 130.74, 127.98, 127.51, 125.19, 114.49, 55.67 (OMe), 52.86 (COOMe), 52.72 (COOMe), 37.29 (SCH$_2$Ph); m/z (FAB$^+$) 347 (M+ 1, 10.39%), 121(M-$C_{10}H_9O_4S$, 100); IR (KBr) v_{max} 1720.86, 1709.59 cm^{-1}.

4.3.17 *Dimethyl 2-mercaptoterephthalate (92)*
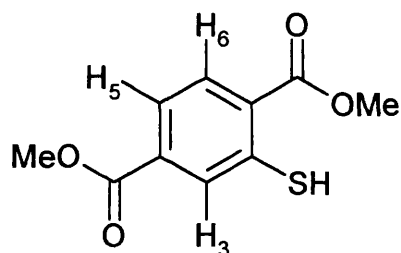
Procedure as for compound **83**, using as starting material compound **91**. Product **92** was isolated as a white solid (0.3 g, 50%). M.p: 104-106 °C. (Found: C, 53.09; H, 4.18; S, 14.01; $C_{10}H_{10}O_4S$ Requires: C, 53.09; H, 4.46; S, 14.17%). δ_H (CDCl3) 3.96 (3H, s, COOCH_3), 3.98 (3H, s, COOCH_3), 4.81 (1H, s, SH), 7.80 (1H, dd, ^3J $_{5-6}$ 8.2, ^4J $_{5-3}$ 1.6 Hz, H_5), 8.02 (1H, d, ^3J $_{6-5}$ 8.2 Hz, H_6), 8.09 (1H, dd, ^4J $_{3-5}$ 1.6 Hz, H_3); δ_C (CDCl3) 166.91 (COOMe), 166.05 (COOMe), 139.11 (C_2), 133.75 (C_4), 132.21 (C_6), 132.06 (C_5), 129.73 (C_1), 125.67 (C3), 52.91 (OMe), 52.87 (OMe); m/z (FAB$^+$) 227 (M+1, 100%), 195 (M-OMe, 91.96), 121 (M-$C_3H_4O_3S$, 13.13); IR (KBr) v_{max} 2545.68, 1721.53 cm^{-1}.

4.3.18 *4-Ethyl 1-methyl 2-(aminothio)terephthalate (94)*
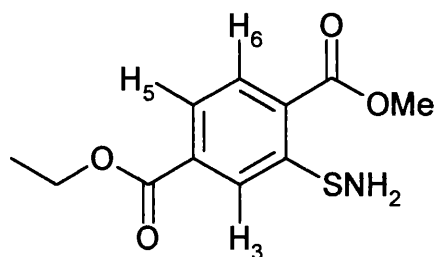
Hydroxylamine-*O*-sulfonic acid (HOSA) (0.07 g, 0.6 mM) was dissolved in water (4.2 mL) in which potassium hydroxide (0.035 g, 0.6 mM) was dissolved. This solution was added dropwise to a solution of thiosalicylate (0.1 g, 0.42 mM) in water (4.1 mL) in the presence of potassium hydroxide (0.023 g, 0.42 mM) on an ice bath under N_2. After 30 minutes, the precipitated white solid was filtered and dried under reduce pressure. The product was isolated as a white solid (0.04g, 40 %). M.p: 65-70°C. δ_H (CDCl3) 1.4 (3H, t, OCH$_2$C*H$_3$*) 2.73 (2H, br s, N*H$_2$*), 3.99 (3H, s, OC*H$_3$*), 4.45 (2H, q, OC*H$_2$*CH$_3$), 7.80 (1H, dd, $^3J_{5\text{-}6}$ 8.1, $^4J_{5\text{-}3}$ 1.5 Hz, *H$_5$*), 8.05 (1H, d, $^3J_{6\text{-}5}$ 8.2 Hz, *H$_6$*), 8.62 (1H, d, $^4J_{3\text{-}5}$ 1.6 Hz, *H$_3$*); δ_C (CDCl3) 166.57 (*C*OOMe), 166.06 (*C*OOEt), 141.38 (C$_2$), 134.50, 131.84, 131.84, 127.84, 127.84, 62.05 (O*C*H$_2$CH$_3$), 52.58 (OMe), 14.52 (COOCH$_2$*C*H$_3$); m/z (FAB$^+$) 256 (M+1, 14%), 255(M$^+$, 63), 239 (M$^+$-NH$_2$, 100).

4.3.19 *Ethyl 3-oxo-2,3-dihydro-1,2-benzisothiazole-6-carboxylate (46b)*
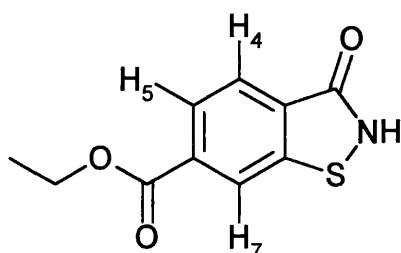
Compound **94** (0.04 g, 0.16 mM) was dissolved in the solution of potassium hydroxide (8.8 mg, 0.16 mM) in ethanol (3 mL). After the solution was stirred for 40 minutes at room temperature, the solvent was evaporated under reduced pressure. The product was purified by HPLC using a gradient elution of 40-80% acetonitrile in 0.1% TFA aqueous solution over 20 min at a flow rate of 20 mL/min. Compound is isolated as a white solid (20 mg, 56%). M.p: higher than 240°C; δ_H (methanol-d$_4$) 1.4 (3H, t, OCH$_2$CH_3), 4.4 (2H, q, OCH_2CH$_3$), 7.85 (1H, dd, $^3J_{5-6}$ 8.2, $^4J_{5-3}$ 1.3 Hz, H$_5$), 7.96 (1H, d, $^3J_{4-5}$ 8.2 Hz, H$_4$), 8.3 (1H, d, $^4J_{7-5}$ 1.3 Hz, H$_7$); δ_C (CDCl$_3$) 165.36 (CO), 127.67, 125.00, 123.16, 61.28 (OCH$_2$CH$_3$), 14.13 (OCH$_2$CH$_3$). IR (KBr) ν_{max} 1723.98, 1645.9 cm^{-1}; m/z (ES⁻) 222 (M-1, 100%), 194 (M-Et, 50).

References-Chapters 2 and 3

1   Ignarro, L.; Murad, F. *Nitric oxide biochemistry, molecular biology, and therapeutic implications.* Academic press. **1995**. 263-275.

2   Yuen. P. S. T.; Garbers. D.L. *Annu. Rev. Neurosci.* **1995**, *15*, 193-225.

3   Marletta, M. A. *J. Biol. Chem.* **1993**, *268*, 12231-12234.

4   Schmidt, H. H. H. W.; Lohmann, S. M.; Walter, L U. *Biochim. Biophys. Acta.* **1993**, *1178*, 143-175.

5   Palmer, R. M.; Ferrige, A. G.; Moncada, S. *Nature* **1987**, *327*, 524-526.

6   Waldman, S. A.; Murad, F. *Pharmacol. Rev.* **1987**, *39*, 163-196.

7   Koesling, D.; Harteneck, C.; Humbert, P.; Bosserhoff, A.; Frank, R.; Schultz,G.; Bohme. *FEBS Lett.* **1990**, *266*, 128-132.

8   Nakane, N.; Arai, K.; Saheki, S.; Kuno, T.; Buechler, W.; Murad, F. *J. Biol. Chem.* **1990**, *265*, 16841-16845.

9   Koesling, D.; Herz, J.; Gausepohl, H.; Niroomand, F.; Hinsch, K. D.; Mulsch, A.; Bohme, E.; Schultz, G.; Frank, R. *FEBS Lett.* **1988**, *239*, 29-34.

10 Nakane, N.; Saheki, S.; Kuno, T.; Ishii, K.; Murad, F. *Biochem. Biophys. Res. Commun.* **1988**, *157*, 1139-1147.

11 Buechler, W. A.; Nakane, M.; Murad, F. *Biochem. Biophys. Res. Commun.* **1991**, *174*, 351-357.

12 Harteneck, C.; Wedel, B.; Koesling, D.; Malkewitz, J.; Bohme, E.; Schultz, G. *FEBS Lett.* **1991**, *292*, 217-222.

13 Russwurm, M.; Behrends, S.; Harteneck, C.; Koesling, D. *Biochem. J.* **1998**, *335*, 125-130.

14 Gupta, G.; Azam, M.; Yang, L.; Danziger, R. *J. Clin. Invest.* **1997**. *100*. 1488-1492.

15 Yuen, P. S.; Potter, L. R.; Garbers, D. L. *Biochemistry* **1990**, *29*, 10872-10878.

16 Zabel, U.; Weegner, M.; La, M.; Schmidt, H. *Biochem. J.* **1998**, *335*, 51-57.

17 Hobbs, A. J. *Trends. Pharmacol. Sci.* **1997**, *18*, 484-491.

18 Liu, Y.; Ruoho, A. E.; Rao, V. D.; Hurley, J. H. *Proc. Natl. Acad. Sci. USA.* **1997**, *94*, 13414-13419.

19 Wedel, B.; Harteneck, C.; Foerster, J.; Friebe, A.; Schultz, G.; Koesling D. *J. Biol. Chem.* **1995**, *270*, 24871-24875.

20 Yuen, P. S.; Doolittle, L. K.; Garbers, D. L. *J. Biol. Chem.* **1994**, *269*, 791-793.

21 Foster, D.; Wedel, B.; Robinson, S.; Garbers, D. *Physiol. Biochem. Pharmacol.* **1999**, *135*, 1-41.

22 Stone, J. R.; Marletta, M. A. *Biochemistry* **1995**, *34*, 14668-14674.

23 Brandish, P. E.; Buechler, W.; Marletta, M. A. *Biochemistry* **1998**, *83*, 721-729.

24 Ignarro, L.; Adams, J.; Horwitz, P.; Wood, K. *J. Biol. Chem.* **1986**, *261*, 4997-5002.

25 Zhao, Y.; Marletta, M. A. *Biochemistry* **1997**, *36*, 15959-15964.

26 Zhao, Y.; Schelvis, J. P.M.; Babcock, G. T. *Biochemistry* **1998**, *37*, 4502-4509.

27 Stone, J. R.; Marletta, M.A. *Biochemistry* 1994,33,5636-5640

28 Baochen, F.; Gupta, G.; Danziger, R. S.; Friedman, J. M.; Rousseau, D. L. *Biochemistry* **1998**, *37*, 1178-1184.

29 Stone, J. R.; Marletta, M.A. *Biochemistry* **1996**, *35*, 1093-1099.

30 Friebe, A.; Wedel, B.; Foerster, J.; Harteneck, C.; Malkewitz, J.; Schultz, G.; Koesling, D. *Biochemistry* **1997**, *36*, 1194-1198.

31 Saburo, N.; Hori, H.; Imai, K.; Kawamura-Konishi, Y.; Suzuki, H. *J. Biochem.* **1997**, *121*, 654-660.

32 Tsai, A. *FEBS Lett.* **1994**, *341*, 141-145.

33 Moncada, S.; Palmer, R. M.; Higgs, E. A. *Pharmacol. Rev.* **1991**, *43*, 109-142.

34 Garthwaite, J.; Boulton, C. L.; *Annu. Rev. Physiol.* **1995**, *57*, 683-706.

35 Ignarro, L. J.; Degnan, J. N.; Baricos, W. H.; Kadowitz, P. J.; Wolin, M. S. *Biochim. Biophys. Acta.* **1982**, *718*, 49-59.

36 Craven, P. A.; DeRubertis, F. R. *Biochim. Biophys. Acta.* **1983**, *745*, 310-321.

37 Traylor, T. G.; Sharma, V. S. *Biochemistry* **1992**, *31*, 2847-2849.

38 Dierks, E. A.; Hu S.; Vogel, K. M.; Yu, A. E.; Spiro, T. G.; Burstyn, J. N. *J. Am. Chem. Soc.* **1997**, *119*, 7316-7323.

39 Yu, A. E.; Hu, S.; Spiro, T. G.; Burstyn, J. N. *J. Am. Chem. Soc.* **1994**, *116*, 4117-4118.

40 Denium, G.; Stone, J. R.; Babcock, G. T.; Marletta, M. A. *Biochemistry* **1996**, *35*, 1540-1547.

41 Schelvis, J. P. M.; Zhao, Y.; Marletta, M. A.; Babcock, G. T. *Biochemistry* **1998**, *37*, 16289-16297.

42 Stone, J. R.; Marletta, M.A. *Biochemistry* **1994**, *33*, 5636-5640.

43 Stone, J. R.; Sands, R. H.; Dunham, W. R.; Marletta, M. A. *Biochem. Biophys. Res. Comm.* **1995**, *207*, 572-577.

44 Bussygina, O. G.; Belushkina, N. N.; Grigoryev, N.B.; Severina, I.S. *Biochemistry* (Moscow) **1995**, *60*, 1111-1116.

45 Kharitonov, V. G.; Sharma, V. S.; Pilz, R. B.; Madge, D.; Koesling, D. *Proc. Natl. Acad. Sci. USA.* **1995**, *92*, 2568-2571.

46 Stone, J. R.; Marletta, M.A. *Biochemistry* **1995**, *34*, 16397-16403.

47 Burstyn, J. N.; Yu, A. E.; Dierks, E. A.; Hawkins, B. K.; Dawson, J. H. *Biochemistry* **1995**, *34*, 5896-5903.

48 Kuo, S-C.; Lee, F-Y.; Teng, C-M. EP667345/1995 (*Chem. Abstr.*, **1995**, *123*, 340113)

49 Wu, C. C.; Ko, F. N.; Kuo, S. C.; Lee, F. Y.; Teng, C. M. *Br. J. Pharmacol.* **1995**, *116*, 1973-1978.

50 Friebe, A.; Schultz, G.; Koesling, D. *EMBO J.* **1996**. *15*, 6863-6868.

51 Friebe, A.; Koesling, D. *Mol. Pharmacol.* **1997**, *53*, 123-127.

52 Stone, J. R.; Marletta, M. A. *Chem. Biol.* **1998**, *5*, 255-261.

53 Sharma, V. S.; Magde, D.; Kharitonov, V. G.; Koesling, D. *Biochem. Biophys. Res. Comm.* **1999**, *254*, 188-191.

54 Denninger, J. W.; Schelvis, J. P. M.; Brandish, P. E.; Zhao, Y.; Babcock, G. T.; Marletta, M. A. *Biochemistry* **2000**, *39*, 4191-4198.

55 Martin, E.; Lee, Y-C.; Murad, F. *PNAS.* **2001**, *98*, 12938-12942.

56 Bayley, H.; *Photogenerated Reagents in Biochemistry and Molecular Biology*, (Eds) T. S. Work and H. R. Burdon, Elsevier, Amsterdam, **1983**.

57 Hatanaka, Y.; Hashimoto, M.; Kurihara, H.; Nakayama, H.; Kanaoka, Y. *J. Org. Chem.* **1994**, *59*, 383-387.

58 Fleming, S.A. *Tetrahedron* **1995**, *51*, 12479-12520.

59 Hotanoka, Y.; Nakayama, H.; Kanaoka, Y. *Rev.Heteroatom Chem.* **1996**, *14*, 213-243.

60 Brunner, J.; Senn, H.; Richards, F.M. *J. Biol. Chem.* **1980**, *255*, 3313-3318.

61 Nassal, M. *Liebigs. Ann. Chem.* **1983**, 1510-1523.

62 Saul Patai. *The Chemistry of the hydrazo, azo and azoxy groups* (part 1).

63 Carey, F.A.; Sundeberg, R. J; *Advanced organic chemistry* (part B), Plenum Press, New York and London.

64 Delfino, J.; Schreiber, S. L.; Richards, F. M. *J. Am. Chem. Soc.* **1993**, *115*,

65 Smith R. A. G.; Knowles, J. R. *J. C. S. Perkin* II 686-694.

66 Smith R. A. G.; Knowles, J. R. *J. Am. Chem. Soc*, **1973**, *95*, 5072-5073.

67 Brunner, J.; Richards, F. M. *J. Biol. Chem.* **1980**, *255*, (8) 3319-3329.

68 Nakayama, T. A.; Khorama, H. G. *J. Org. Chem.* **1990**, *55*, 4953-4956.

69 Yamaguchi, T.; Saneyoshi, M. *Nucleic Acids Res.* **1996**, *24*, 3364-3369.

70 Hatanaka, Y.; Hashimoto, M.; Kanaoka, Y. *Bioorg. Med. Chem.* **1994**, *2*, 1367

71 Hatanaka, Y.; Hashimoto, M.; Kanaoka, Y. *J. Am. Chem. Soc.* **1998**, *120*, 453-454.

72 Fang, K.; Hashimoto, M.; Jockusch, S.; Turro, N. J.; Nakanishi, K. *J. Am. Chem. Soc.* **1998**, *120*, 8543-8544.

73 Hashimoto, M.; Hatanaka, Y.; Yang, J.; Dhesi, J.; Holman G. D. *Carbohydr. Res.* **2001**, *331*, 119-127.

74 Hashimoto, M.; Yang, J.; Holman G. D. *Chembiochem.* **2001**, *2*, 52-59.

75 Lin, S.; Fang, K.; Hashimoto, M.; Nakanishi, K.; Ojima, I. *Tetrahedron Lett.* **2000**, *42*, 4287-4290.

76 Dorman, G.; Prestwich, G. D. *TIBTECH*, **2000**, *18*, 64-77.

77 Dorman, G. *Topics in current chemistry.* **2000**, *211*, 171-225.

78 Pellicena, P.; Scholten, J. D. Zimmerman, K.; Creswell, M.; Huang, C. C.; Miller, W. T, *Biochemistry* **1996**, *35*, 13494-13500.

79 Wang, J.; Bauman, S.; Colman, R. F. *Biochemistry* **1998**, *37*, 15671-15679.

80 Madhusoodanan, K. S.; Colman, R. F. *Biochemistry* **2001**, *40*, 1577-1586.

81 Liu, Y.; Ruoho, A. E.; Rao, V. D.; Hurley, J. H. *Proc. Natl. Acad. Sci. USA.* **1997**, *94*, 13414-13419.

82 Zhang, G.; Liu, Y.; Ruoho, A. E.; Hurley, J. H. *Nature* **1997**, *386*, 247-253.

83 Galle, J.; Zabel, U.; Hubner, U.; Hatzelmann, A.; Wagner, B.; Wanner, C.;
    Schmidt, H. H. H. W. *Br. J. Pharmacol.* **1999**, *127*, 195-203.

84 Selwood, D. L.; Brummell, D. G.; Budworth, J.; Burtin, G. E.; Campbell, R.
    O.; Chana, S. S.; Charles, I. G.; Fernandez, P. A.; Glen, R. C.; Goggin, M.
    C; Hobbs, A. J.; Kling, M. R.; Liu, Q.; Madge, D, J.; Meillerais, S.; Powell,
    K, L.; Reynolds, K.; Spacey, G. D.; Stables, J. N.; Tatlock, M. A.; Wheeler,
    K. A.; Whisar, G.; Woo, C-K. *J. Med. Chem.* **2001**, *44*, 78-99.

85 Gordon, D. W. *Synlett.* **1998**, 1065.

86 Collot, V.; Dallemagne, P.; Bovy, P. R.; Rault, S. *Tetrahedron* **1999**, *55*,
    6917-6922.

87 Nassal, M. *J. Am. Chem. Soc.* **1984**. *106*, 7540-7545.

88 Richardson, S. K.; Ife, R. J. *J. Chem. Soc. Perkin Trans.* I. **1989**, 1172-1174.

89 Yoon, N. M.; Pak, C. S. *J. Org. Chem.* **1973**, *38*, 2786-

90 O. Mitsunobu, O.; Yamada, M. *Bull. Chem. Soc. Jpn.* **1967**, *40*, 2380

91 Tsunoda, T.; Nagaku, M.; Nagino, C. *Tetrahedron Lett.***1995**, 36, (14), 2531
    -2534.

92 Monnet, M.; Prevost, P. *Tetrahedron* **1993**, *49*, No. 26, 5831-5844

93 Walker, M. A. *J. Org. Chem.* **1995**, *60*, 5352-5355.

94 Tsunoda, T.; Ozaki, F. *Tetrahedron Lett.* **1996**, *37*, (14), 2463-2466.

95 Shull, B. K.; Sakai, T. *J. Org. Chem.* **1997**, *62*, 8294-8303.

96 Tunoori, A. R.; Dutta, D. *Tetrahedron Lett.* **1998**, *39*, 8751-8754.

97 T. Tsunoda, J. Otaka, Y. Yamamamiya and S. Ito, *Chem. Lett.* **1994**, 539.

98 cGMP enzymeimmunoassay. Amersham pharmacia biotech code RPN 226.

99 Straub, A.; Stasch, J-P.; Alonso-Alija, C.; Benet-Buchholz, J.; Ducke, B.;
    Feurer, A.; Furstner, C. *Bioorg. Med. Chem. Lett.* **2001**, *11*, 781-784.

100 Stasch, J-P.; Becker, E. M.; Alonso-Alija, C.; Apeler, H.; Dembowaky, K.;
    Feurer, A.; Gerzer, R.; Minuth, T.; Perzborn, E.; Pleiβ, U.; Schroder, H.;
    Schroeder, W.; Stahl, E.; Steinke, W.; Straub, A.; Schramm, M. *Nature*
    2001, *410*, 212-215.

101 Last-Barney, K.; Davidson, W.; Cardozo, M.; Frey, L.L.; Grygon, C. A.;
    Hopkins, J. L.; Jeanfavre, D. D.; Pav, S.; Qian, C.; Stevenson, J. M.; Tong,
    L.; Zindell, R.; Kelly, T. A. *J. Am. Chem. Soc.* **2001**, *123*, 5643-5650.

102 McClelland.; McKibben. *J. Chem. Soc.* **1923**, *123*, 170.

103 De A. *"Progress in medicinal chemistry"* (Ellis GP. West GB. Eds) Elsevier/North-Holland Biomedical Press. **1981**, *18*,117-133.

104 Andersen, K. E,; Hamann, K. *Fd Chem. Toxic.* **1984**, *22*, 655-660.

105 Fisher, R,; Hurni, H. *Arzneimittel-Forsch.* **1964**, *14*, 1301-1306.

106 Bambas, L.L. *The Chemistry of Heterocycles Compounds*; Weissburger, A., Ed.; Wiley-interscience: New York, **1952**; *4*, 253-270.

107 Davis M. *Advances in heterocyclic chemistry*; Katritzky AR. Boulton AJ, Ed.; Academic Press. New York, **1972**; *14*, 58-63.

108 Davis M. "Advances in heterocyclic chemistry"; Katritzky AR. Boulton AJ, Ed.; Academic Press. New York, **1985**; vol. 38, pp 114-116.

109 Ponci, R,; Vitali T,; Mossini F,; Amoretti L. *Il Farmaco Ed Sc.* **1967**, *22*, 999-1010.

110 Borgna, P,; Carmellino, ML,; Natangelo, M,; Pagani, G,; Patori, F,; Pregnolato, M,; Tereni, M. *Eur. J. Med. Chem.* **1996**, *31*, 919-925.

111 Ponci, R,; Baruffini, A,; Gialdi. *Il Farmaco Ed Sc.* **1964**, *19*, 121-136.

112 Ponci, R,; Baruffini, A,; Gialdi. *Il Farmaco Ed Sc.* **1964**, *19*, 254-268.

113 Carmellino, ML,; Pagani, G,; Pregnolato, M,; Terreni, M,; Pastoni, F. *Eur. J. Med. Chem.* **1994**, *29*, 743-751.

114 Vicini, P,; Manotti, C,; Caretta, A,; Amoretti, L. *Arzneim.-Forsch/Drug Res.* **1997**. *47(11)*, 1218-1221.

115 Baggaley, K.H,; English, P.D,; Jennings, J.A,; Morgan, B,; Nunn, B,; William, A,; Tyrrell, R. *J. Med. Chem.* **1985**, *28*, 1661-1667.

116 Yevich, J. P,; New, J. S,; Smith, D. W,; Lobeck, W.G,; Catt, J. D,; Minielli, J. L,; Elison, M. S, Taylor, D.P,; Riblet, L.A,; Temple, D. L, Jr. *J. Med. Chem.* **1986**, *29*, 359-369

117 Vicini, P.; Amoretti, L,;Morini, G,; Impicciatore. *Farmaco Ed.Sci*, **1984**, 39 (10), 817-829.

118 Miura, Y. *J. Org. Chem.* **1988**, *53*, 2850-2852.

119 Brigas, A. F,; Johnstone, R. A. W. *Tetrahedron Lett.* **1990**, *31*, 5789.

120 Brigas, A. F,; Johnstone, R. A. W. *J. Chem. Soc., Chem. Commun.* **1994**, 1923-1924

121 Alves, J. A.C,; Barkley, J. V,; Brigas, A.F,; Johnstone, R. A. W. *J. Chem., Perkin Trans.* **1997**, *2*, 669-677.